

**An Experimental Study of Wave Generated Dynamic Load on
Coastal Embankment**

A Thesis

Submitted by

Moyen Uddin Ahmmmed

In partial fulfillment of the requirement for the degree of
MASTER OF SCIENCE IN WATER RESOURCES ENGINEERING



Department of Water Resources Engineering
BANGLADESH UNIVERSITY OF ENGINEERING AND TECHNOLOGY
DHAKA
2010

CERTIFICATE OF APPROVAL

The thesis titled “AN EXPERIMENTAL STUDY OF WAVE GENERATED DYNAMIC LOAD ON COASTAL EMBANKMENT”, Submitted by Moyen Uddin Ahmmed, Roll No: 100516002(P), Session- October, 2005 has been accepted as satisfactory in partial fulfillment of the requirement for the degree of Master of Science in Water Resources Engineering on 13 December 2010.

BOARD OF EXAMINERS

Dr. Umme Kulsum Navera
Professor
Department of Water Resources Engineering
BUET, Dhaka-1000, Bangladesh

Chairman

Dr. M. A. Matin
Professor and Head
Department of Water Resources Engineering
BUET, Dhaka-1000, Bangladesh

Member
(Ex-officio)

Dr. M. Mirjahan
Professor
Department of Water Resources Engineering
BUET, Dhaka-1000, Bangladesh

Member

Mr. Zahirul Haque Khan
Director
Coast, Port and Estuary Management Division
Institute of Water Modeling (IWM), Dhaka, Bangladesh

Member
(External)

13 DECEMBER, 2010

CANDIDATE'S DECLARATION

It is hereby declared that this thesis or any part of it has not been submitted elsewhere for the award of any degree or diploma.

Signature of the supervisor

Signature of the Candidate

Dr. Umme Kulsum Navera
Professor
Department of Water Resources Engineering
BUET, Dhaka-1000, Bangladesh

Moyen Uddin Ahmmed

TABLE OF CONTENT

	Page No.
<i>Acknowledgement</i>	i
<i>Abstract</i>	ii
<i>Table of Contents</i>	iii
<i>List of Figures</i>	vii
<i>List of Tables</i>	xv
<i>List of Photographs</i>	xvii
<i>List of Notations</i>	xviii
<i>Acronyms and Abbreviations</i>	xx
CHAPTER 1	
INTRODUCTION	
1.1 Background of the study	1
1.2 Geography and physiography of the coastal area of Bangladesh	4
1.3 Rationale of the study	6
1.4 Objectives with specific aims of the study	9
1.5 Organization of the thesis	10
CHAPTER 2	
LITERATURE REVIEW	
2.1 General	12
2.2 Coastal problems	12
2.3 Structural measures for the reduction of Coastal problems	14
2.4 Basic physics of wave pressures on sea faced sloping side of structures	24
2.5 Design consideration for a coastal embankment	25
2.6 Case study in Bangladesh	32
2.7 Summary	34

CHAPTER 3**THEORY AND METHODOLOGY**

3.1 General	35
3.2 Theory	35
3.2.1 Theory of Coastal embankment	35
3.2.2 Wave	36
3.2.3 Characteristics of wave field	41
3.2.4 Wave run-up	43
3.2.5 Overtopping	45
3.2.6 Wave reflection	45
3.2.7 Hydraulic loads on embankment	47
3.2.7.1 Hydraulic loads due to flows	48
3.2.7.2 Hydraulic load due to water level	48
3.2.7.3 Hydraulic load due to waves	48
3.2.7.4 Factors affecting hydraulic load	49
3.2.7.5 Wave loads	49
3.2.8 Structural responses	53
3.2.9 Theoretical analysis of wave forces	53
3.2.10 Break water	57
3.2.11 Monolithic sunken Cassion breakwater	59
3.3 Basis for laboratory Experiment	61
3.4 Methodology	61
3.4.1 Physical model components	62
3.4.2 Laboratory flume	63
3.4.3 Wave generator	64
3.4.4 Reservoir	66
3.4.5 Wire screen to reduce wave reflection	66
3.4.6 Bank slope preparation	67
3.4.7 Velocity meter	69
3.4.8 Breakwater used in the experiment	73
3.4.9 Pipes	73

	Page No.
3.5 Measurement technique	74
3.5.1 Wave period measurement	76
3.5.2 Wave length measurement	76
3.5.3 Wave height measurement	77
3.5.4 Run-up height measurement	77
3.5.5 Velocity component measurement	77
3.6 Test procedure of Experiment	78
3.7 Test scenarios	79
3.9 Summary	81

CHAPTER 4

RESULTS AND DISCUSSION

4.1 General	83
4.2 Comparisons between theoretical and experimental data	83
4.3 Relation graph between wave length and wave period	91
4.4 Relation between wave period and wave height	95
4.5 Relation between wave length and wave height	99
4.6 Relation graph between run-up height with wave period	102
4.7 Run-up height and wave length relationship	107
4.8 Run-up height and wave height relationship	111
4.9 Change in velocity for different loading condition	115
4.10 Analysis of force on embankment	126
4.11 Relation to dynamic and static load	138
4.12 Dynamic load effect on embankment height	145
4.13 Comparison with Miche-Rundgren curve	150
4.14 Summary	153

CHAPTER 5

CONCLUSIONS AND RECOMMENDATIONS

5.1 General	154
5.2 Conclusions	154

5.3 Recommendations for the further study	Page No. 155
REFERENCES	157
APPENDIX A	A1-A7
APPENDIX B	B1-B12
APPENDIX C	C1-C4
APPENDIX D	D1-D2

LIST OF FIGURES

		Page No.
Figure 1.2.1	Map representing Coastal zone of Bangladesh	7
Figure 1.5.1	Flow chart showing outline of this research work	11
Figure 2.3.1	A brief account of major embankment of Bangladesh.	17
Figure 2.4.1	Definition sketch to explain the predicted wave pressure on coastal structure	25
Figure 2.5.1	Schematization of an embankment	26
Figure 3.2.1	Wave height change after breaking	39
Figure 3.2.2	Classification of ocean waves according to wave period	41
Figure 3.2.3	Water conditions and wave motion on the breakwater slope	43
Figure 3.2.4	Definition sketch of slope	45
Figure 3.2.5	Wave reflection mechanism	46
Figure 3.2.6	Main causes of hydraulic load	47
Figure 3.2.7	Wave impact on slope	49
Figure 3.2.8	Process affecting hydraulic load at a structure	50
Figure 3.2.9	Loading zones on a coastal structure	52
Figure 3.2.10	Classification of wave force problems by type of wave action and structure type	54
Figure 3.2.11	(a) Pressure diagram without wave loading (b) Pressure diagram with wave loading (water level at crest). (c) Pressure diagram with wave loading (water level at trough)	55
Figure 3.2.12	Sloping wall	57
Figure 3.2.13	Various types of breakwater (a) A bubble type breakwater, (b) Composite rubble Mound Front breakwater, (c) Floating flexible breakwater, (d) Floating Rigid breakwater, (e) Monolithic floating, (f) Composite vertical monolithic top breakwater	60
Figure 3.4.1	Plan and longitudinal section of the laboratory flume.	63

	Page No	
Figure 3.4.2	E-30 Probe	70
Figure 3.4.3	Diagram, showing voltage components versus velocity vectors	71
Figure 4.2.1	Comparison of wave length for different experimental setup (for bed slope = 1:2 and water depth = 40 cm)	84
Figure 4.2.2	Comparison of wave length for different experimental setup (for bed slope = 1:2 and water depth = 30 cm)	85
Figure 4.2.3	Comparison of wave length for different experimental setup (for bed slope = 1:3 and water depth = 40 cm)	85
Figure 4.2.4	Comparison of wave length for different experimental setup (for bed slope = 1:3 and water depth = 30 cm)	86
Figure 4.2.5	Comparison of wave length for different experimental setup (bed slope = 1:2 and water depth = 40 cm)	87
Figure 4.2.6	Comparison of wave length for different experimental setup (bed slope = 1:2 and water depth = 30 cm)	87
Figure 4.2.7	Comparison of wave length for different experimental setup (bed slope = 1:3 and water depth = 40 cm)	88
Figure 4.2.8	Comparison of wave length for different experimental setup (bed slope = 1:3 and water depth = 30 cm)	88
Figure 4.2.9	Comparison of wave length for different experimental setup (for slope = 1:2 and water depth = 40 cm)	89
Figure 4.2.10	Comparison of wave length for different experimental setup (for slope = 1:2 and water depth = 30 cm)	89
Figure 4.2.11	Comparison of wave length for different experimental setup (for slope = 1:3 and water depth = 40 cm)	90
Figure 4.2.12	Comparison of wave length for different experimental setup (for slope = 1:3 and water depth = 30 cm)	90
Figure 4.3.1	Wave parameter relationship for 1:2 bank slopes and 40 cm water depth	92
Figure 4.3.2	Wave parameter relationship for 1:3 bank slopes and 40 cm water depth	92

		Page No.
Figure 4.3.3	Wave parameter relationship for 1:2 bank slopes and 30 cm water depth	93
Figure 4.3.4	Wave parameter relationship for 1:3 bank slopes and 30 cm water depth	93
Figure 4.3.5	Wave parameter relationship for CC block at various slopes and water depth	94
Figure 4.3.6	Wave parameter relationship for submerged breakwater condition at various slopes and water depth	94
Figure 4.3.7	Wave parameter relationship for Floating breakwater condition at various slopes and water depth	95
Figure 4.4.1	Comparison of wave height and wave period at 1:2 slope and 40 cm water depth	96
Figure 4.4.2	Comparison of wave height and wave period at 1:3 slope and 40 cm water depth	96
Figure 4.4.3	Comparison of wave height and wave period at 1:2 slope and 30 cm water depth	97
Figure 4.4.4	Comparison of wave height and wave period at 1:2 slope and 30 cm water depth	97
Figure 4.4.5	Comparison of wave parameters for CC block condition	98
Figure 4.4.6	Comparison of wave parameters for submerged breakwater condition	98
Figure 4.4.7	Comparison of wave parameters for floating breakwater condition	99
Figure 4.5.1	Relation between wave length and wave height at 1:2 slope and 40 cm water depth	99
Figure 4.5.2	Relation between wave length and wave height at 1:3 slope and 40 cm water depth	100
Figure 4.5.3	Relation between wave length and wave height at 1:2 slope and 30 cm water depth	100
Figure 4.5.4	Relation between wave length and wave height at 1:3 slope and 40 cm water depth	101

		Page No.
Figure 4.5.5	Comparison of wave parameters for CC block in various slopes and water depth	101
Figure 4.5.6	Comparison of wave parameters for submerged breakwater in various slopes and water depth	102
Figure 4.5.7	Comparison of wave parameters for Floating breakwater in various slopes and water depth	102
Figure 4.6.1	Run-up height changes with wave period for 1:2 slope and 40 cm water depth	103
Figure 4.6.2	Run-up height changes with wave period for 1:3 slope and 40 cm water depth	103
Figure 4.6.3	Run-up height changes with wave period for 1:2 slope and 30 cm water depth	104
Figure 4.6.4	Run-up height changes with wave period for 1:3 slope and 30 cm water depth	104
Figure 4.6.5	Run-up height changes with wave period for CC block at different slope and water depth	105
Figure 4.6.6	Run-up height changes with wave period for submerged breakwater condition at different slope and water depth	106
Figure 4.6.7	Run-up height changes with wave period for floating breakwater condition at different slope and water depth	106
Figure 4.7.1	Wave length and run-up height relationship for 1:2 slope and 40 cm water depth	108
Figure 4.7.2	Wave length and run-up height relationship for 1:3 slope and 40 cm water depth	108
Figure 4.7.3	Wave length and run-up height relationship for 1:2 slope and 30 cm water depth	109
Figure 4.7.4	Wave length and run-up height relationship for 1:3 slope and 30 cm water depth	109
Figure 4.7.5	Variation in run-up height for CC block condition at different slope and water depth	110

		Page No.
Figure 4.7.6	Variation in run-up height for submerged breakwater condition at different slope and water depth	110
Figure 4.7.7	Variation in run-up height for submerged breakwater condition at different slope and water depth	111
Figure 4.8.1	Comparisons between wave height and run-up height for 1:2 slope and 40 cm water depth	111
Figure 4.8.2	Comparisons between wave height and run-up height for 1:3 slope and 40 cm water depth	112
Figure 4.8.3	Comparisons between wave height and run-up height for 1:2 slope and 30 cm water depth	112
Figure 4.8.4	Comparisons between wave height and run-up height for 1:3 slope and 30 cm water depth	113
Figure 4.8.5	Comparisons between wave height and run-up height for CC block condition at various slope and water depth	114
Figure 4.8.6	Comparisons between wave height and run-up height for submerged breakwater condition at various slope and water depth	114
Figure 4.8.7	Comparisons between wave height and run-up height for floating breakwater condition at various slope and water depth	115
Figure 4.9.1	Velocity vector for 1:2 slope, 1 sec wave period and 40 cm water depth at 3R, 6R and 9R distance from the toe	116
Figure 4.9.2	Velocity vector for 1:2 slope, 2 sec wave period and 40 cm water depth at 3R, 6R and 9R distance from the toe	117
Figure 4.9.3	Velocity vector for 1:2 slope, 2.5 sec wave period and 40 cm water depth at 3R, 6R and 9R distance from the toe	117
Figure 4.9.4	Velocity vector for 1:2 slope, 1 sec wave period and 30 cm water depth at 3R, 6R and 9R distance from the toe	118
Figure 4.9.5	Velocity vector for 1:2 slope, 2 sec wave period and 30 cm water depth at 3R, 6R and 9R distance from the toe	118

		Page No.
Figure 4.9.6	Velocity vector for 1:2 slope, 2.5 sec wave period and 30 cm water depth at 3R, 6R and 9R distance from the toe	119
Figure 4.9.7	Velocity vector for 1:3 slope, 1 sec wave period and 40 cm water depth at 3R, 6R and 9R distance from the toe	119
Figure 4.9.8	Velocity vector for 1:3 slope, 2 sec wave period and 40 cm water depth at 3R, 6R and 9R distance from the toe	120
Figure 4.9.9	Velocity vector for 1:3 slope, 2.5 sec wave period and 40 cm water depth at 3R, 6R and 9R distance from the toe	120
Figure 4.9.10	Velocity vector for 1:3 slope, 1 sec wave period and 30 cm water depth at 3R, 6R and 9R distance from the toe	121
Figure 4.9.11	Velocity vector for 1:3 slope, 2 sec wave period and 30 cm water depth at 3R, 6R and 9R distance from the toe	121
Figure 4.9.12	Velocity vector for 1:3 slope, 2.5 sec wave period and 30 cm water depth at 3R, 6R and 9R distance from the toe	122
Figure 4.10.1	Variation of loads for 1:2 slope and 40 cm water depth, when $\lambda = 1$	131
Figure 4.10.2	Variation of loads for 1:2 slope and 30 cm water depth, when $\lambda = 1$	131
Figure 4.10.3	Variation of loads for 1:3 slope and 40 cm water depth, when $\lambda = 1$	132
Figure 4.10.4	Variation of loads for 1:3 slope and 30 cm water depth, when $\lambda = 1$	132
Figure 4.10.5	Variation of loads for 1:2 slope and 40 cm water depth, when $\lambda = 0.9$	133
Figure 4.10.6	Variation of loads for 1:2 slope and 30 cm water depth, when $\lambda = 0.9$	133
Figure 4.10.7	Variation of loads for 1:3 slope and 40 cm water depth, when $\lambda = 0.9$	134

		Page No.
Figure 4.10.8	Variation of loads for 1:3 slope and 30 cm water depth, when $\lambda = 0.9$	134
Figure 4.10.9	Comparison of wave load reduction for CC block with various slops and water depth condition, when $\lambda = 1$	135
Figure 4.10.10	Comparison of wave load reduction for submerged breakwater with various slops and water depth condition, when $\lambda = 1$	135
Figure 4.10.11	Comparison of wave load reduction for submerged breakwater with various slops and water depth condition, when $\lambda = 1$	136
Figure 4.10.12	Comparison of wave load reduction for CC block with various slops and water depth condition, when $\lambda = 0.9$	136
Figure 4.10.13	Comparison of wave load reduction for submerged breakwater with various slops and water depth condition, when $\lambda = 0.9$	137
Figure 4.10.14	Comparison of wave load reduction for floating breakwater with various slops and water depth condition, when $\lambda = 0.9$	137
Figure 4.11.1	Dynamic load change with wave height for 1:2 slope and 40 cm water depth, when $\lambda = 1$	140
Figure 4.11.2	Dynamic load change with wave height for 1:2 slope and 30 cm water depth, when $\lambda = 1$	140
Figure 4.11.3	Dynamic load change with wave height for 1:3 slope and 40 cm water depth, when $\lambda = 1$	141
Figure 4.11.4	Dynamic load change with wave height for 1:3 slope and 30 cm water depth, when $\lambda = 1$	141
Figure 4.11.5	Dynamic load change with wave height for 1:2 slope and 40 cm water depth, when $\lambda = 0.9$	144
Figure 4.11.6	Dynamic load change with wave height for 1:2 slope and 30 cm water depth, when $\lambda = 0.9$	144
Figure 4.11.7	Dynamic load change with wave height for 1:3 slope and 40 cm water depth, when $\lambda = 0.9$	145

		Page No.
Figure 4.11.8	Dynamic load change with wave height for 1:3 slope and 30 cm water depth, when $\lambda = 0.9$	145
Figure 4.12.1	Settlement as function of time	146
Figure 4.12.2	Run-up height reduction for different load condition on 1:2 slope and 40 cm water depth	147
Figure 4.12.3	Run-up height reduction for different load condition on 1:2 slope and 30 cm water depth	148
Figure 4.12.4	Run-up height reduction for different load condition on 1:3 slope and 40 cm water depth	148
Figure 4.12.5	Run-up height reduction for different load condition on 1:3 slope and 30 cm water depth	149
Figure 4.12.6	Run-up height reduction for CC block condition on different slope and water depth	149
Figure 4.12.7	Run-up height reduction for submerged breakwater condition on different slope and water depth	150
Figure 4.12.8	Run-up height reduction for floating breakwater condition on different slope and water depth	150
Figure 4.13.1	Comparison with Miche-Rundgren curve for $\chi = 1$	151
Figure 4.13.2	Comparison with Miche-Rundgren curve for $\chi = 0.9$	151

LIST OF TABLES

		Page No.
Table 2.3.1	Dimension of embankments used in Bangladesh.	18
Table 2.3.2	Features of design of shown protection works along Marine drive	18
Table 2.6.1	Embankments and their characteristics	33
Table 3.2.1	An overview of types of structures with different H/ Δ D values	37
Table 3.4.1	Sign correction for velocity meter	72
Table 3.5.1	Wave generator setup for experimental runs	75
Table 3.7.1	Test scenarios for 1:2 bank slope	80
Table 3.7.2	Test scenarios for 1:3 bank slope	81
Table 4.2.1	Rate of change in wave parameters for different conditions	91
Table 4.6.1	Changes of run-up height due to breakwater with respect to CC condition	107
Table 4.9.1	The velocities (m/s) measured for various conditions for 1:2 slope and 40 cm water depth.	123
Table 4.9.2	The velocities (m/s) measured for various conditions for 1:2 slope and 30 cm water depth	124
Table 4.9.3	The velocities (m/s) measured for various conditions for 1:3 slope and 40 cm water depth	125
Table 4.9.4	The velocities (m/s) measured for various conditions for 1:3 slope and 30 cm water depth	126
Table 4.10.1	Magnitude of loads for 1:2 bank slope, when $\lambda = 1$	127
Table 4.10.2	Magnitude of loads for 1:3 bank slope when, $\lambda = 1$	128
Table 4.10.3	Magnitude of loads for 1:2 bank slope, when $\lambda = 0.9$	129
Table 4.10.4	Magnitude of loads for 1:3 bank slope, when $\lambda = 0.9$	130
Table 4.11.1	Relation with Total force, static force and dynamic force, when $\lambda = 1$	138

	Page No.
Table 4.11.2 Relation with Total force, static force and dynamic force, when $\lambda = 1$	139
Table 4.11.3 Relation with Total force, static force and dynamic force, when $\lambda = 0.9$	142
Table 4.11.4 Relation with Total force, static force and dynamic force, when $\lambda = 0.9$	143
Table 4.13.1 Meaning of four cases	152

LIST OF PHOTOGRAPHS

	Page No.	
Photograph 3.4.1	Laboratory flume	62
Photograph 3.4.2	Wave generator	63
Photograph 3.4.3	Laboratory flume with bank slope	64
Photograph 3.4.4	Wave generator labeling with main parts	65
Photograph 3.4.5	RPM adjustment	66
Photograph 3.4.6	Weir screen in the flume	67
Photograph 3.4.7	Preparing a bank slope	68
Photograph 3.4.8	Sand layer over the acrylic plate	68
Photograph 3.4.9	Detail of a bank slope	69
Photograph 3.4.10	A complete bank slope	69
Photograph 3.4.11	Photographical representations for Programmable electromagnetic liquid velocity meter (P.-e.m.s.); (a) various parts of P. EMS; (b) Actual velocity reading display	72
Photograph 3.4.12	Rectangular breakwater	73
Photograph 3.4.13	Two types of breakwater used in experiment (a) Submerged breakwater in still water (b) Floating breakwater	74

LIST OF NOTATIONS

B	The berm width
C_n	Constant depending on the type of wave spectrum and exceedance percentage
c	Wave celerity
D_n	Characteristic diameter of structure, armour unit, stone, gravel or sand
d	Water depth
f	Wave frequency
F_c	Load of wave crest
F_t	Load of wave trough
F_d	Dynamic load of wave
F_{net}	Net wave load
F'	Dynamic component of force
F''	Horizontal component of the dynamic force due to waves
F_s	Static load of wave
F	Total wave load
g	Acceleration gravity
H	Wave height
H_s	Significant wave height
H_i	Incident wave height
L	Wave length
L_s	Slope length
L_{slope}	The horizontal length between the two points on the slope
R	Run-up height
R_u	Run-up
R_d	Run-down
S	Wave steepness
T	Wave period
t	Elapse time
T_p	Top period

V_x	Velocity component of stream wise velocity
V_y	Velocity component of transverse velocity
w	Unit weight of water
ρ_w	Density of water
α	Direction of wave propagation
χ	Wave reflection coefficient
ξ	Breaker index
θ	Slope angle of embankment made with horizontal
γ_R	Reduction factor due to slope roughness and permeability
γ_B	Reduction factor due to berm
γ_β	Reduction factor due to oblique wave attack
Δ	Relative mass density
ϕ_b	Maximum piezometric head

ACRONYMS AND ABBREVIATIONS

AD	Anno Domino
BUET	Bangladesh University of Engineering and Technology
CEP	Coastal Embankment Project
CC	Cement Concrete
cm	Centimeter
DWRE	Department of Water Resources Engineering
D/S or d/s	Downstream
EPWAPDA	East Pakistan Water and power Development Board
HRZ	High Risk Zone
HRA	High Risk Area
kN	Kilo Newton
MHW	Mean High Water
MLW	Mean Low Water
SPM	Shore Protection Manual
Sec	Second
U/S or u/s	Upstream

ACKNOWLEDGEMENT

All praises are due to Almighty ALLAH, Who enables the author to complete this thesis work and report.

The author expresses his deep sense of gratitude and respect to his honorable supervisor, Dr. Umme Kulsum Navera, Professor, Department of Water Resources Engineering, BUET, Dhaka for her constant supervision, scholastic guidance and patience help throughout the thesis work and preparation of the report. She makes the author interested to the field of coastal engineering. Her continuous directions, advices and help encouraged the author all through.

The author wishes to express his sincere appreciation to Dr. M. A. Matin, Professor and Head, Department of Water Resources Engineering, BUET, for his timely co-operation and guidance.

The author wants to express his sincere thanks to Dr. M. Mirjahan, Professor, Department of Water Resources Engineering, BUET, for his valuable comments and co-operation. The author is very much grateful to Dr. Sabbir Mostafa Khan, Professor, Department of Water Resources Engineering, BUET for his valuable suggestions to improve the quality of presentation. The author is grateful to Mr. Zahirul Haque Khan, Director, Coast, Port and Estuary Management Division, Institute of Water Modeling (IWM) for his kind consent to be a member of the examination board and for sparing valuable time to evaluate the thesis paper and putting precious comment and suggestion.

Acknowledgements are also due to all laboratory staff of Hydraulics and River Engineering Laboratory, DWRE, BUET, Md. Nazimuddin, laboratory assistant; Md. Golam Mostafa and Md. Abdullah Al Mamun for their cordial help during the time of laboratory experiment. Thanks are also due to his friends and classmates for their encouragement especially to Mr. Debjit Roy.

Finally, the author would like to dedicate this dissertation to his parents who were the source of his constant encouragement.

ABSTRACT

Coastal embankment is a structural measure usually taken near coastline to protect inland habitat and crops. This research work considers only those embankments which are located along the coast line directly facing the sea. The general practices in Bangladesh for the design of coastal embankment normally consider high tide level as the design high water. Based on the design criteria it can be said that, the consideration of periodicity of small waves while designing an embankment is one of the most important parameter. For accurate design consideration, the main parameters are wave height, wave direction, current and soil properties. The effects of the above considerations might result in changes in the alignment, crest level, slope or drainage system of the embankment. The study analyzes the effect of dynamic loading due to wave associated with submerged, floating breakwater and CC block condition on coastal embankment.

An experimental investigation was conducted to study the behaviour of wave parameters with different loading conditions in the laboratory flumes of Hydraulics and River Engineering Laboratory of the Department of Water Resources Engineering, BUET. Test runs were conducted for different wave periods, water depths with loading conditions such as by providing CC block, submerged breakwater and floating breakwater. Before the test runs, instrumental setup of wave generator had been done and pointed for individual condition runs. Total 36 test runs were conducted. All the above performances have been done by two different slopes of 1:2 and 1:3 against the wave action by changing the wave period, water depth and protection work.

Wave loads, especially dynamic loads were calculated from the experimental values of wave parameters by using Sainflou's formulae (1928). The study shows that presence of breakwater in front of the coastal embankment resulted in a change in the loading distribution. Breakwater position (submerged or floating) individually affect the wave loads further more.

CHAPTER 1

INTRODUCTION

1.1 Background of the Study

The coastal zone has been recognized as natural resources for the activities of human beings, particularly in those countries which are greatly depend on the coast for cultural as well as economic activities. The ocean, especially the nearshore ocean, has been utilized for various purposes, such as harvesting, transportation and recreation. In addition, the land behind the coast has been developed to support agriculture, industry, living spaces and recreational usage. In order to safeguard these multifaceted activities, numerous engineering works have been emplaced in the coastal zone, with particular intensity during the last half a century. In the beginning, the appropriate design to ensure structural integrity was the main concern of coastal engineers. Soon, the disruptive impact of these structures on the coastal environment became the object of serious concern, to not only coastal engineers, but also to the coastal residents and users and eventually the national government. It is also true that adverse beach changes have been occurring all over the world, which were variously attributed to sea level rise, unusually severe storms, reduction in sediment supply from rivers, as well as to man's direct interference in the natural littoral system through the creation of coastal facilities (Horikawa, 1988).

The coastal communities world-wide are facing enormous difficulty to reduce mitigate shoreline erosion. The most significant natural erosive forces along the open shore lines are wind driven wave action with water level changes which results from tide, wind set-up, sea-level rise and storm surges. Various measures can be used for coastal protection. Direct measures include the coastal structures such as seawall, dyke, groynes, breakwater, embankment etc., which are used for many purposes such as water inundation, coastal-defense, wave-attenuation, flow-guidance, inland protection etc (Pilarczyk, 1990).

There are two basic types of wave erosion control methods. These are vegetative and structural measures (Nandi, 2002). Vegetative method involves plantation of trees

and woody shrub and the mechanism to check wave erosion is the soil binding properties with large root systems and the damping of wave energy along its propagation. It is widely used in shore, stream bank and around human settlement. Sometimes rocks and boulders are also used to make the system more effective. This method is environment friendly, but needs a certain time to be functional. It is suitable when land is cheap and available for reasonable width and length.

Structural measures are immediate measures and they include sea wall, gravity wall, bulkheads, groins, jetties, revetments and breakwaters. Seawall, groins, jetties are massive structure that dissipate full force of waves and are adopted for shoreline protection. Bulkheads and gravity wall are next in size that retains the fill. Breakwaters are the front line defense structure to protect shorelines against wave actions. Revetments are used as a direct protective structure against moderate waves (SPM, 1984). There are various types of revetments such as loose stones and boulders, gunny bags, cement concrete (CC) blocks, articulated mattress etc. Now a days, in all over the world the use of CC blocks have become very popular due to durability, easy construction and ease in quality control. Designers choose CC blocks considering cost and function of revetments also.

The main force acting on the sea side face of a coastal embankment is wave which are generated and developed in deep seas, very wide rivers, lakes, haors, beels or any other large mass of water mainly due to wind action. It may also be produced due to movement of marine vessels, explosion due to earthquakes etc. Worldwide erosion due to waves is a problem in the conservation of beaches and shoreline, maintenance of dock and harbor, reclamation of land from sea for airport and industry, roads and dams, human settlements etc.

In Bangladesh the areas prone to wave erosion are the coastal areas and wetland areas adjacent to haor and beels. Coastal area lies in the southern part of Bangladesh and is open to Bay of Bengal. Besides storm surges produced by cyclonic wind and tides, the coastal area is continuously attacked by waves. The storm surges have been noted to be some 3 m to 6 m in height (ESCAP, 1988). Haor areas are located in

northwest part of the country whereas beel areas lie in the southeast part of the country. They are flooded in monsoon. Wind generated waves in haor and beel areas have been reported to vary between 1 m and 1.5 m. Since last decade wave erosion in these wetlands are causing severe damages of villages and human settlements, roads and embankments (Nandi, 2002).

Bank protection structures are subjected to waves and currents. In many occasions, wave forces causes failure of structures. Therefore, proper knowledge regarding wave action and related failure mechanisms of protection measures is of utmost importance. Engineers have been assessing the performance of different design options undertaken at existing protection works and determining the need for betterment of the structures. Coastal embankments are used for various purposes and their failure mechanisms are different with respect to the condition it is in.

The possible causes of failure can be summarized as follows: (i) normally the embankments are designed to be behind the swash zone having both breaking and non –breaking wave attacking its seaward side. In this case the embankment is under severe risk due to breaker zone consideration. (ii) Crest level consideration of dynamic load is of prime importance. The embankments are constantly in change of water level and pressure within the wave height region. The same material is under both tensile stress and compressive stress during one wave period and which must be considered in the design. If the effect of dynamic load ignored during design and construction period there might be possible failure in the embankment. (iii) The seaward slope should be far milder than land ward slope. It may occupy more space in the embankment site along the sea side but this will provide adequate safety under repeated wave action. (iv) Coastal embankments are subjected to saline water, so adequate drainage facilities are must in both sea side and country side to avoid damage. Due to heavy rain water logging can happen in country side and without proper drainage it might become a harmful cause for the embankment, and (v) the height of wave has a significant influence on the resultant force acting on the embankment slope. The direction of incident wave causes this force to change so,

during different time of year an embankment can face change in forces (Navera and Nandi, 2007).

The dynamic loading has an important role on the embankment due to direct wave loading, which should be a vital consideration while designing an embankment. In this research work, the effects of dynamic load on the seaward side of a coastal embankment have been thoroughly investigated in a laboratory setup where many relations have been investigated.

1.2 Geography and Physiography of the Coastal Area of Bangladesh

The coastline, the boundary between land and sea, is moving. It changes its shape and position continuously. The time scale of this change ranges from geological time to the single period of wind waves; the spatial scale ranges from the size of a continent to the wave length of a sand ripple. In the geological time scale, the change in the position of the coastline is governed by the crustal movement of the earth and by the change in sea level associated with long-term variations in climate. The sea level over the last tens of thousands of years is considered to have varied. It is still rising during the present interglacial stage, and will continue to do so until the next glacial age reverses the trend. Although the process related to the geological time scale is responsible for the fundamental geological structure of the coastline, the main concern of the coastal engineers is on the coastline variations of much shorter-term caused by the small-scale forces such as waves and currents. The time scale of these shorter-term variations is comparable to the life-time of human beings and the expected useful life of most man-made coastal structures (Horikawa, 1978).

The coastal area of Bangladesh represents an area of 47,211 square kilometer, 32 percent of the country's geographical area, where about one fourth of the population lives in the coastal area depending on agriculture, fishery, forestry, near shore transport, solar salt mining etc. i.e. 28 percent of the country's total population lives at 6.85 million households (Population census, 2001). In terms administrative consideration, 19 districts out of 64 are considered as coastal district. A study of

IPPC (Inter Governmental Panel of Climate Change) in 2001 reveals that 20 percent and 40 percent of the world population lives within 30 kilometers and 100 kilometers of the coast respectively, which is very true in terms of Bangladesh's perspective. Most of the country lies within 10 m above mean sea level and the coastline extends for some 710 km (excluding major indentations) from the Indian border in the west to the border with Myanmar in the southeast. The coastal area encompasses the regions of Cox's Bazar, Chittagong, Noakhali, Barisal, Patuakhali and Khulna and includes some 2.5 million ha of coastal tidal lands (Bashirdlah *et al.*, 1989).

Bangladesh is one of the coastal marginal countries of the Bay of Bengal. The southern most part of Bangladesh is bordered by about 710 kilometer long coastal belt, which has the continental shelf up to 50 meter deep with an area of about 37,000 square kilometer. The coastal zone of Bangladesh includes coastal plain islands, tidal flats and estuaries near and offshore waters. It extends to the edge of a wide (about 20 km.) continental shelf. The northern part of the Bay of Bengal is narrow and funnel shaped serving to concentrate wave energy from storm centre to the south. The continental shelf has an area of about 69,000 km² (Sivasubramaniam, 1985) partially bisected by the Swatch of No Ground, a submarine canyon, 100-100 m deep, which lies 24 km off Hanninghata and runs away from the coast in a southwesterly direction. The Burma Trench, a more extensive submarine canyon extends northwards from the Sunda Trench, parallel to the coast (ESCAP, 1988). From the point of view, the genetic classification of Bangladesh coast can be considered as the coast of emergence or advancing coast. From the morphological point of view, it is of type irregular or cliff coast and from another geomorphologic basis it is sandy soft type coast. A vast river network, a dynamic estuarine system and a drainage basin intersect the coastal zone, which made coastal ecosystem as a potential source of natural resources, diversified fauna and floral composition, though there also have immense risk of natural disasters. Due to its diversified nature, the coast of Bangladesh broadly divided into three geo-morphological regions:

- a) The western region includes the numerous low-lying islands and vast mangrove swamps of the Sundarbans.

- b) The central region runs from the Tetulia to the Big Feni River estuary and includes the mouth of the Meghna river. The older, inland sections of the delta, in the north, are comparatively high with sandy soils; the lower central parts are subject to extensive flooding every rainy season; and, the accreting coastal zone is subject to regular tidal inundation.
- c) The eastern region comprises the much smaller estuarine systems of the Chittagong-Cox's Bazar Coast (Chakaria Sundarbans and Naaf Estuary, Karnaphuli, Sangu, Matarnuhuri) from the Big Feni River to Badar Mokam. The coast is regular, unbroken and protected by mud flats and submerged sands. A continuous sand beach runs from Cox's Bazar to Badar Mokam, for about 145 km. There is a single coral island, Jinjiradwip, off the extreme southern tip of the country and several larger islands to the north. In this region the coastline runs parallel to a series of low forested hill ranges and valleys running north to south.

In this research work the embankments which are situated at the eastern region are taken into consideration as these are wave dominated coast. Here intensive investigation is required to formulate the design parameters which are needed to construct a coastal embankment.

1.3 Rationale of the Study

The coastal zone is essentially a multi resource system which provides space, living and non-living resources for human activities and it has a regulatory function for the natural and manmade environment. Private and public bodies use the resources for subsistence (water and food), economic activities (space, living and non-living resources, energy) and recreation. Industrialization, commercial development and steadily growing population pressure in many places have resulted in an increase of erosion flooding, loss of wetlands, pollution and over population of land and water resources in the coastal zone. Coastal areas are increasingly threatened by natural processes such as storm surges that cause severe coastal erosion. They are also threatened by human activities that increase erosion and pollution and degrade

valuable habitats that serve as a source of food and livelihood for many coastal residents (SPM, 1984).

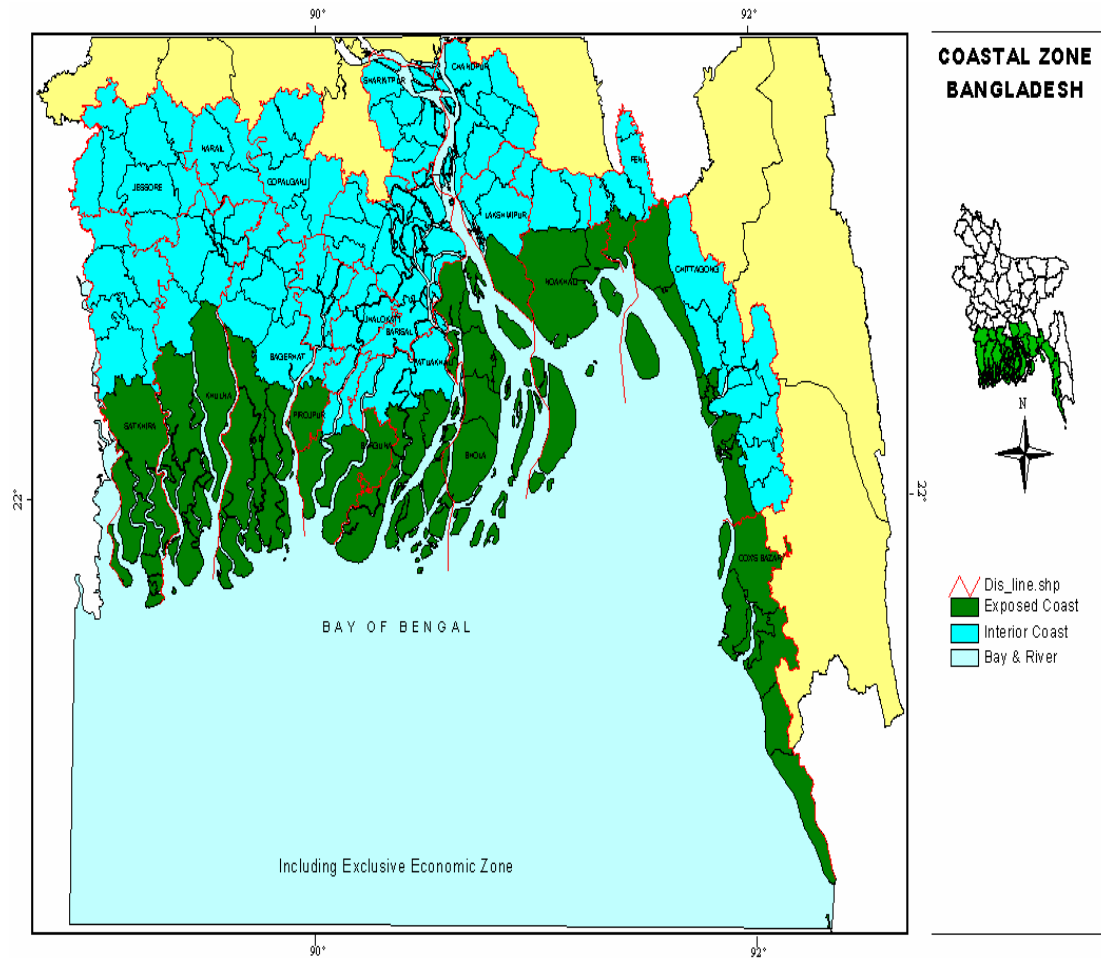


Figure 1.2.1: Map representing Coastal zone of Bangladesh (Source: Islam, 2004)

Sometimes cyclone associated with tidal waves caused great loss of lives and property. Nearly one million people have been killed in Bangladesh by cyclones since 1820 due to cyclone they are being estimated 10% of the world's developing in the Indian Ocean (Gray, 1968). Approximately 45 damaging cyclones were reported in the coastal areas of Bangladesh from 1793 to May, 1997 thus cyclone frequency during this period averred once in every 4.5 years. Among which the largest cyclones occurred in 1961, 1963, 1965, 1966, 1970, 1985 and 1991 and in 1996. The last devastation cyclone to hit Bangladesh occurred on 29 April, 1991. An estimated 131,000 to 139,000 people died, with the majority of those dying being below the age of 10, and a third of them below the age of five; also more women than men died

(Talukder and Ahmed, 1992). The total economic impact of the cyclone was US\$2.4 to 4.0 billion (Kausher et al., 1996).

To minimize the impact of natural disasters as well as to achieve the aim of agricultural production, construction of earth embankments and dykes, their repairing and rebuilding for irrigation, flood control and drainage have been the history of Bangladesh since time immemorial. Earth embankments in Bangladesh are beset with multi-faceted problems. The design and construction methods used to build the embankments, the nature and extent of erosive forces to destabilize them and above all the attitude of the local people for whom they are built altogether determine the magnitude and degree of instability. In the coastal belt and offshore islands also, severe bank erosion problems occur frequently. New accretion and shifting of the bank line due to erosion happen almost in the same way as those observed in the inland rivers. However, the nature and extent of erosive forces damaging the seashore and successively the dykes differ in certain aspects from those of the inland riverbanks.

The marine drive of Bangladesh which had been built from Cox's bazar to Teknaf is an appropriate example of coastal embankment directly subjected to the wave attack. Wave loads are the main cause of its damage as it hammered by the continuous dynamic loads of wave which is clearly differs from the embankments that are at the inland river banks.

The present study deals with an investigation of the effect of wave load on structure under normal condition and using breakwater protection before it. The Performance of a hydraulic structure can be examined from hydraulic and geotechnical viewpoint. From hydraulic viewpoint, the wave action is taken into account in the present study. This is accounted in two different bank slope condition, different loading condition by dissipating wave load under submerged and floating breakwater action. Effect of geotechnical aspects, was not taken in account. However, the scope of this study does not include the geotechnical performance of the structure. Two different bank slope with sea side sloping face of 1:2 (45°) and 1:3 (30°) were used in the laboratory

setup. Normally coastal embankments are constructed with a sea side slope of 1:5 to 1:7 in Bangladesh. The wave run-up height and the dynamic load decreases as the slope become milder. The experiment for this research work has been carried out in the steeper slope to observe the effect of dynamic load as the main parameter. The effect of dynamic load on the milder slopes will be less than that of the steeper slopes. Effect of wave velocity of different wave period (1, 2 and 2.5 second) on the structure with three different conditions (in this thesis work these are termed as different loading condition) are observed which are,

- using plane beach with CC block on the slope (expressed as CC block condition)
- using plane beach with CC block and submerged breakwater (expressed as submerged breakwater condition)
- using plane beach with CC block and floating breakwater (expressed as floating breakwater condition)

A lot of work has been carried out by different researchers to improve the coastal problems worldwide whereas in Bangladesh these are very limited in number. This situation might be improve by proper understanding and relevant researches on this subject as we have rich and proliferate coastal resources.

1.4 Objectives with Specific Aims of the Study

As the force exerted by the wind generated wave is one of the most important parameter for coastal embankment design, concentrated investigation and ample works are mandatory in this field to evaluate the design parameters needed for constructing a sustainable coastal embankment. To fulfill the above requirement this research work has been designed such that some relations among the wave parameters may develop.

Based on aforesaid discussion the study has undertaken some laboratory investigations with the following specific objectives:

1. To compare run-up height with different wave parameters
2. To compare the change in velocity with different loading conditions
3. To calculate the force on embankment for different test scenarios
4. To develop a relationship between dynamic and static loads
5. To observe the effect of dynamic load on embankment height.

The possible outcomes of the present study are as follows:

1. The expected outcome of the present study will be beneficial to understand the behavior of dynamic load on coastal embankment.
2. The effect of breakwater will play an important role on embankment height reduction.

1.5 Organization of the Thesis

The whole research work has been stated step by step through six chapters. The flow chart shown in the Figure 1.5.1 illustrates the outline of these chapters.

Apart from this first chapter the thesis has been divided into five chapters. The chapters possess what are shortly stated below:

Chapter 2 focuses on the review of the literature relevant and related to the theme of the study. Here some previous formulae, our coastal problems and previous work have been discussed.

Chapter 3 deals with the general theory, detail description of the laboratory experimental set up and data collection techniques.

Chapter 4 presents the analysis of data with graphical presentation of results.

Chapter 5 discusses major findings of the study and recommendations for further study are also discussed in this chapter.

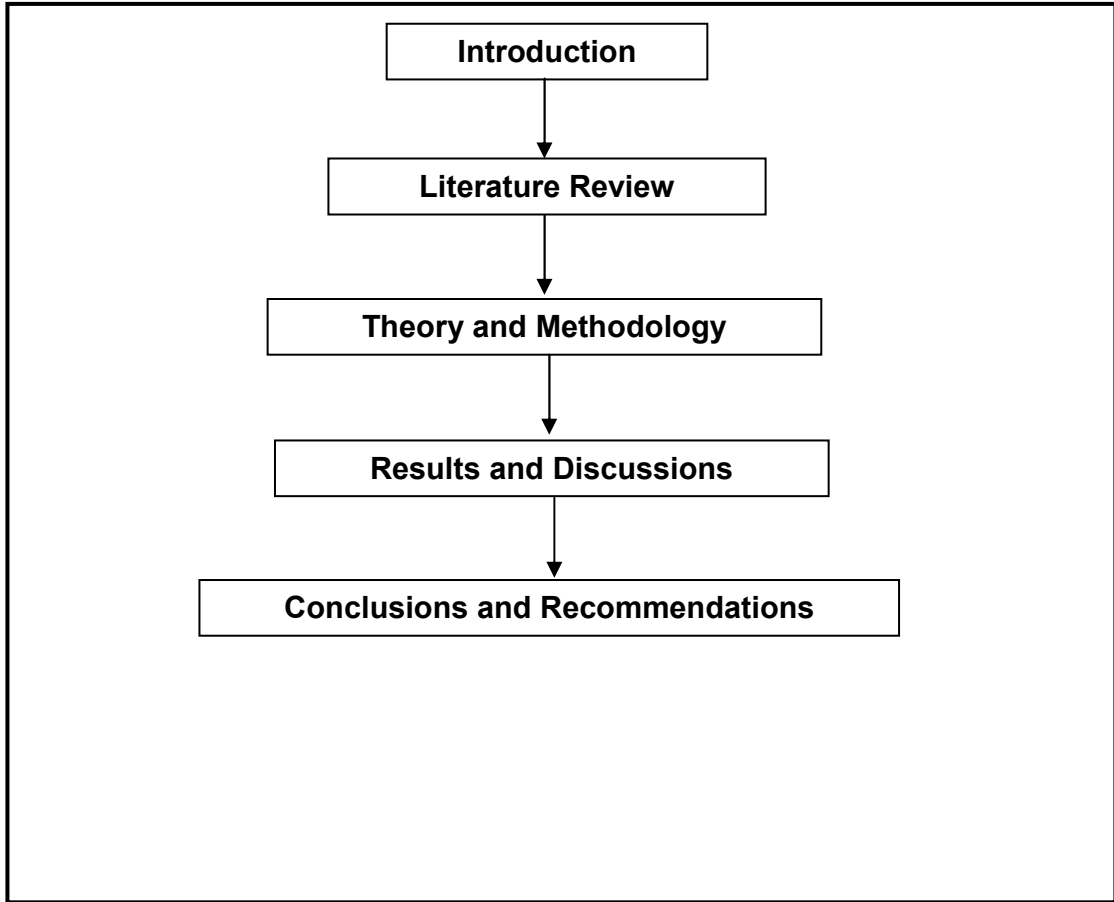


Figure 1.5.1: Flow chart showing outline of this research work.

CHAPTER 2

LITERATURE REVIEW

2.1 General

Generally in Bangladesh, coastal embankment is a structural measure usually located behind the swash zone near coastline to protect inland habitat and crops. The coastal embankments are subjected to direct wave loading. Whenever the embankment is under loading by water body, it will be under dynamic load exerted by wave (Navera and Nandi, 2007). These dynamic loads are very much important to coastal embankment design. This chapter describes our coastal problems, history of embankment building (including coastal embankment) in Bangladesh and review of several works done for the coastal embankment.

2.2 Coastal problems

Bangladesh is one of the severe cyclonic disaster prone countries in the world. Chittagong, the second important city in Bangladesh, is situated along the Bay of Bengal and the Karnafully River and suffered severest from cyclonic disaster in the past several cyclones. In 1991 cyclone, a large part of the city was flooded with surge water and the city was experienced with a human death of approximately 1071. More than 90% of the deaths are caused by surge water. The then only Export Processing Zone (EPZ) of the country, very close to the Bay of Bengal was damaged to an extreme (approximately US\$ 16.77 million) due to cyclonic winds and storm surges in 1991 cyclone. So, it is essential to protect the city from cyclonic storm surge inundation (Ali, 1997).

Another coastal problem is sea level rise. Intergovernmental Panel Climate Change (IPCC) estimated a 3.3°C rise in the global temperature under business-as-usual conditions by 2100 with a range of uncertainty of 2.2 to 4.9°C. IPCC's estimation of global sea level rise was 1.0 to 2.0 mm/ year over the last century (IPCC, 2001a). IPCC estimated that sea level rise would be 66 cm under business-as-usual

conditions by 2100 with a range of uncertainty of 13 to 110 cm (IPCC, 2001b). With the high increasing rate of global temperature, sea level will rise at a faster rate of 2-6 times than the present rate (Kausher, 1993). Wigley and Raper (1987) estimated that the greenhouse-gas-induced thermal expansion contribution to sea-level rise between 1880 and 1985 was 2-5 cm and for the period 1985-2025 the estimate of greenhouse-gas-induced warming was estimated to 0.6-1.0°C. The resulting concomitant oceanic thermal expansion would raise sea level by 4-8 cm. Over the last 100 years Bangladesh has warmed up by about 0.5°C and 0.5 m rise of sea level in the Bay of Bengal (BUP, 1993). In the southwestern Khulna region 5.18 mm/year sea level rises is recorded which may goes up to 85 cm by 2050. World Bank's study on the impact of sea level rise in Bangladesh reveals that, 15 to 17 percent land areas of i.e. 22135 to 26562 square kilometers will be inundated within next 100 years by 100 cm. sea level rise, which will make 2 crore people environmental refugee and a country like Bangladesh may will not be able to accommodate such huge uprooted people (Sarwar, 2005).

The coastal embankments were constructed in 1970's to protect the agricultural lands from saline water inundation during normal high tides. The embankments receive periodical damage due to wave actions during monsoon and occasional severe damage by surge water during cyclone. The periodical damage progress towards the severe damage and the embankments could not work under even moderate intensity of cyclone (Ali, 1997).

In looking at the sea surface, it is typically irregular and three-dimensional (3-D). The sea surface change in time and thus, it is unsteady. At this time, this complex, time varying 3-D surface cannot be adequately described in its full complexity; neither can the velocities, pressures, and accelerations of the underlying water required for engineering calculations. In order to arrive at estimates of the required parameters, a number of simplifying assumptions must be made to make the problems tractable, reliable and helpful through comparison to experiments and observations. Some of the assumptions and approximations that are made to describe

the 3-D, time-dependent complex sea surface in a simpler fashion for engineering works may be unrealistic, but necessary for mathematical reasons (CEM, 2003).

Wind generated wave produces the most powerful forces to which coastal embankment are subjected. This wind generated waves are another important problem which may not considered previous coastal structure works (Navera and Nandi, 2007). The result is the catastrophic failure of the embankments which are along the sea beach. This study considers several cases of coastal embankment in Bangladesh and has obtained necessity of dynamic effect significantly in designing of coastal embankment.

2.3 Structural Measures for the Reduction of Coastal Problems

In reducing the damages to human lives and cattle heads which is caused by storm surge flooding during cyclones, cyclone shelters and killas (raised earthen place) are constructed in the most likely surge prone areas. The areas suffering major damages due to surge flooding are termed as High Risk Area (HRA). After the severe cyclonic catastrophe in 1970, World Bank agreed to donate US \$ 25 million with the then Pakistan Government aimed at constructing shelters in HRZ. But this project was suspended due to liberation war of Bangladesh (the then East Pakistan) in 1970. After liberation, Bangladesh Government started the ‘Coastal Area Rehabilitation and Cyclone Shelter Project’ (Ali, 1997).

The earliest recorded embankment in this subcontinent was built during the Sultani period (1213-1519 AD). Sultan Ghiyasuddin Iwaz Khilji built a series of embankments to protect his capital, Lakhnauti from floods. The Grand Trunk Road, which has a length of about 150 miles (240 km) and built during his time, also acted as a flood control embankment. The Mughal emperors constructed embankments along different large rivers (www.banglapedia.org).

The history of coastal embankments in Bangladesh traces back as early as during the British Emperor in India. In Bangladesh coastal embankments were constructed as

early as the 17th century on private initiative under the patronage of zamindars. Systematic development of large-scale embankments for flood control started in the 1960s. Since then hundreds of kilometers of embankments have been built along rivers and in the coastal areas of Bangladesh. These embankments provide a protected environment for agricultural and other economic activities (www.banglapedia.org).

After the abolishment of Zaminder systems in 1950, the then East Pakistan Water and power Development Board (EPWAPDA) launched a project named 'Coastal Embankment Project', aimed at increasing crop production through protection of agricultural lands from saline water inundation during normal high tides. This project covered 13765 sq. km area of which 71% were agricultural lands. A maximum normal flood of 20 year return period was considered as the design flood. The project extended from the Haribanga river near India border to the border Makam south tip of Bangladesh stretching along the 710 km shoreline (EPWAPDA, 1968). The project area was divided to three regions. Eastern region covers 1133 sq. km extending from Chittagong to Arakan Hill Tracts. Central region or estuary which is funneled apex shape of Bay of Bengal covering 3360 sq. km and the western region is formed by deltaic action of Ganges-Brahmaputra-Meghna with an area of 9271 sq. km (Ali, 1997). Under this project a total 4037 km. earthen embankment, 1039 drainage sluices were constructed for 108 polders (closed earthen embankment) (Ali, 1997).

During the last few decades, under the program of flood control and drainage improvement, about 7,555 km of embankment (including coastal embankments of about 4,000 km), 7,907 hydraulic structures including sluices, and around one thousand river regulators, 1,082 river closures and 3,204 km of drainage channels have been built spending a thousand crore taka. A brief account of major embankments in Bangladesh is shown in the Figure 2.3.1 (www.banglapedia.org).

The Coastal Embankment Project (CEP) covers the coastal districts of Bangladesh and includes Cox's Bazar, Chittagong, Feni, Noakhali, Lakshmipur, Bhola, Barisal,

Patuakhali, Jhalokati, Barguna, Pirojpur, Khulna, Satkhira and Bagerhat districts. The CEP comprises a complex network of dikes and drainage sluices and was the first comprehensive plan for providing protection against flood and saline water intrusion in the coastal area. The project was implemented between 1961 and 1978 by the Bangladesh water development board in two phases. Phase I comprises some 92 polders providing protection to one million ha of land. Phase II consists of 16 polders covering another 0.40 million ha. Polder is a Dutch word meaning an area enclosed by dikes. Within the CEP more than 4,000 km of embankment and 1,039 drainage sluices have been constructed. Embankments include sea dikes at locations facing the Bay of Bengal where high waves occur; interior dikes along rivers where wave action is less severe; and marginal dikes are along channels where current and wave action is mild. Typical dimensions of three types of embankments are shown in the Table 2.3.1 (www.banglapedia.org).

The first category embankments of the Table 2.3.1 are that types of embankment where wave load is the dominant factor to the sea side slope. These type embankments have been shown in the Figure 2.3.1 through box. These embankments are facing continuous loads striking by waves which are sometimes more than the static loads (www.banglapedia.org). Marine drive of Bangladesh in Cox's bazar is the one of the embankment facing continuous wave loads. Features of the existing design of Marine Drive are shown in Table 2.3.2. The marine drive was constructed from kalatoli to Inani in Cox's Bazar district. Part of the marine drive which is about 1 (one) kilometer in length was completely washed out near Kalatoli, Cox's bazar due to severe wave attack. The pictorial representation of present condition of the marine drive is shown in appendix-C.

As a wind wave passes from deep water to the beach its speed and length are first only a function of its period (or frequency); then as the depth becomes shallower relative to its length, the length and speed are dependent upon both depth and period; and finally the wave reaches a point where its length and speed are dependent only on depth (and not frequency) (CEM, 2003).

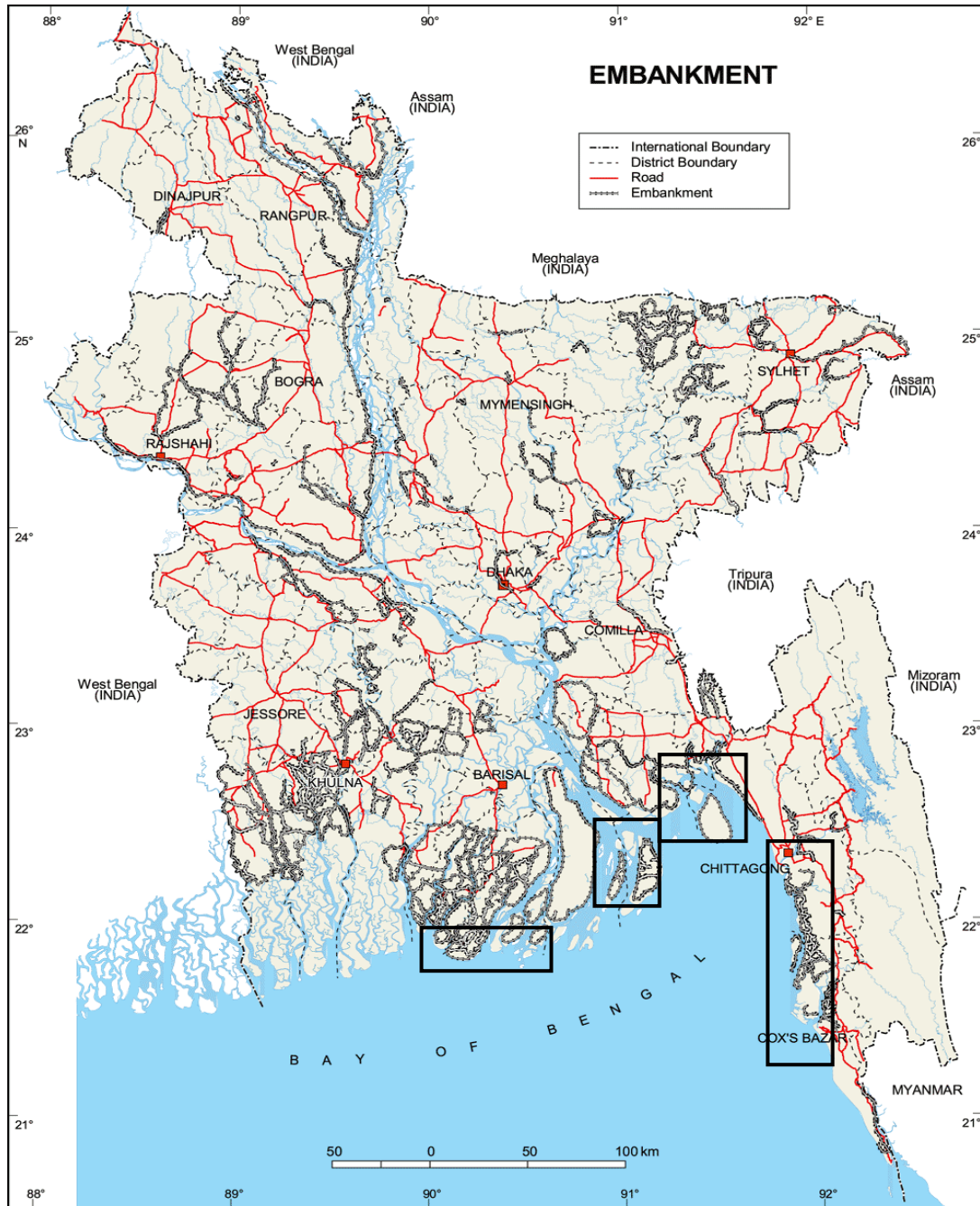


Figure 2.3.1: A brief account of major embankment of Bangladesh
 (Source: http://www.banglapedia.org/httpdocs/HT/E_0049.HTM)

The history of wind wave research is relatively short. Although there were basic developments last century (Airy, 1845; Stockes, 1847), a concerted effort really only began as a result of the military imperative of the Second World War. The work of Sverdrup, Munk and Bretschneides (Sverdrup and Munk, 1944 a, b; Bretschneides, 1952a) provided the first observational data base, upon which, to base theories for

the evolution of wind generated waves. This work was, however, largely empirical. A theoretical framework began to develop with the studies of wind wave generation by Miles and Phillips (Miles, 1957; Phillips 1957). A more complete understanding of the full evolution process, however, awaited the insight into nonlinear interactions provided by Hasselmann (Hasselmann, 1962).

Table 2.3.1: Dimension of embankments used in Bangladesh
(Source: www.banglapedia.org).

Embankment type	Side slope		Crest width (m)	Free board (m)	Set back distance (m)
	Country side	Sea side			
Sea dike	2:1	7:1	4.2	1.5	75
Interior dike	2:1	3:1	4.2	0.9	50
Marginal dike	2:1	2:1	2.4	0.9	40

Table 2.3.2: Features of design of shown protection works along Marine drive

Particulars	Description
Block Dimensions	600 x 600 x 600 mm ³ Keys 600 x 600 x 400 mm ³ Normal
Geotextile	Thickness >3.00 mm Mass > 350 gm/m ² Strip tensile Strength > 25 kN/m ² Effective Opening < 0.08 mm
Sand Below Geotextile	150 mm Thick sand of FM > 1.50
Slope of the Protection	1V : 4H
Slope of the Bathymetry	About 1V : 3H in 4.00 km point About 1V : 3.75H in 17.50 km point About 1V : 6H in 10.00 km point
Soil size (d ₅₀) under layer	d ₅₀ = 0.37 mm
Wind speed	30 m/s
Wave height	2 m

Literatures on detailed studies of wave pressures on sloped seawalls are scarce. But studies on wave induced pressures due to non breaking and breaking waves on vertical walls are well documented. For example, Sainflou (1928) proposed a theoretical method for calculating the dynamic pressures due to non breaking waves

on vertical walls. Experimental observations by Rundgren (1958) have indicated that Sainflou's method may significantly overestimate the non breaking wave force particularly for steep waves. The higher order theory by Miche (1944), as modified by Rundgren (1958), to consider the wave reflection coefficient of the structure, appears to best fit experimentally measured forces on vertical walls for steep waves. Minikin (1963) has developed a design procedure based on observations of full scale breakwaters and the results of Bagnold's theory to determine the breaking wave pressures on vertical walls. The method gives extremely high pressure values, as much as 15 to 18 times those calculated for non breaking waves. Goda (1974) has developed an empirical formula to estimate the non breaking and breaking pressures on vertical walls and is widely used in Japan for the design of vertical caisson type breakwaters. A large number of studies were carried out further on breaking wave forces on caisson type breakwaters throughout the world (Oumeraci et al., 1994; Takahashi et al., 1993, etc.).

The physics of wave transformations and the resulting wave pressures on sloped structures are quite different compared to vertical walls. Some studies on impact pressures on sloped structures are reported. Model and prototype tests for wave impact and run-up on a uniform 1:4 slope were carried out by Fuhrboter (1986) mainly to investigate the scale effects of small scale experiments. The study was concentrated on impact pressures closer to free water surface. The probability distribution of the wave impact pressures as log-normal functions were found to be the same in the model and in the prototype. With respect to scale effects, it was found that the pressures from small waves scaled up towards prototype according to Froude law are relatively higher than those measured at prototype scale. Grune and Bergmann (1994) have carried out experimental investigations on wave induced shock pressures on composite slopes and berms. Again the main attention was given on impact pressures closer to free water surface. It was concluded that for a slope with berm in the front, the peak pressures may decrease due to breaking effect or increase due to shoaling effect depending on the water depth on the berm (Neelamani et al., 1999).

Shuto (1972) has developed an approximate theory of two-dimensional long waves on sloping dikes in the Lagrangian description. The theory is applicable for the case of either no reflection or for full reflection and does not provide information on phase shift due to the reflection by sloping structures, which are essential for wave pressure prediction (Neelamani et al., 1999).

Numerous studies were carried out on wave reflection, run-up and run-down aspects on seawalls and dikes, which are related to wave pressures. Notable examples are: Madsen and White (1976), Ahrens and Titus (1981) and Ahrens et al. (1993) on wave reflection, Hunt (1959) on wave run up due to regular waves on impermeable seawalls, Van der Meer and Janssen (1995) on irregular wave run-up and overtopping and Schuttrumpf et al., 1994, on wave run-up, wave set-up and wave run-down (Neelamani et al., 1999).

These studies can be divided into three groups based on the particular range of dimensionless parameters and the applications that were examined. The first group, which includes the first four studies, was concerned with the wave elevation distribution around large circular islands and lighthouses. The tests conducted were for a rather limited range of wave interaction parameters with a scatter parameter, ka , greater than 0.6. All three investigations showed good agreement with linear diffraction theory. Isaacson (1978) proposed a cnoidal wave theory approach to estimating the run-up on large circular cylinders in shallow water and showed that, though the cnoidal theory underestimated the experimentally measured wave run-up, it provided better estimates than linear diffraction theory.

The second group of studies were conducted by Galvin and Hallermeier (1972), Hallermeier (1976), and Haney and Herbich (1982). They examined the wave elevation distribution around thin piles where the scatter parameters were small and the separated flow effects were dominant. Galvin and Hallermeier (1972) studied the run-up phenomena around piles of various cross sections and noted that the wave elevation distribution around circular cylinders was symmetric. Haney and Herbich (1982) studied the wave run-up around vertical and inclined piles and pile groups. In

that study, wave run-up data were presented as a function of the velocity head estimated using the crest velocity under a nonlinear regular-wave form. From a hydraulics perspective, the interpretation of wave run-up in terms of elevation and velocity heads was quite attractive. However, the results were for a very limited range of dimensionless parameter values outside the diffraction regime and surprisingly very little scatter was observed.

The third group includes the experimental studies by Chakrabarti and Tam (1975) and Niedzwecki and Duggal (1990). The Keulegan-Carpenter numbers indicate that the tests were mainly in the diffraction regime. Chakrabarti and Tam (1975) correlated the wave elevations around the cylinder to pressure profiles measured at the same points around the cylinder. They found that the pressure profiles around the cylinder at the still-water level matched the wave elevations at the corresponding points. In the study by Niedzwecki and Duggal (1990), regular-wave profiles around a test cylinder were presented to illustrate the degree of wave-structure interaction for two very different wavelengths. Wave run-up and wave-force results for truncated and full-length cylinders subjected to both regular and random waves were presented. Experimentally based transfer functions relating incident- and enhanced-wave conditions were presented. The results clearly showed increases in run-up when either the incident-wave steepness or scatter parameters were increased (Niedzwecki et. al., 1992).

Neelamani et al., (1998) has investigated on wave pressure at different levels on a seawall with wide ranges of the hydrodynamic and structure parameters. He predicted wave induced pressures based on wave reflection, run-up and run-down and wave phase shift due to reflection in the run-up zone and in the run-down zone.

Iribarren (1965) developed a theoretical model for the stability of stone on a slope under wave attack. Iribarren continued his efforts throughout the years until his final publication on the subject at the PIANC conference of 1965 in Stockholm. Iribarren assumed a set of simple relations between F_{wave} , D_n , H , ρ and g as follows.

It must be expected that the shape of the block and the period of the wave play a role. Furthermore, the relation between the wave force (F_{wave}) and the wave height (H) and stone size (D_n) indicate the dominance of drag forces, whereas acceleration forces (g) are neglected. Considering the equilibrium for down rush along the slope, this leads to a requirement for the block weight.

Since 1942, systematic investigations into the stability of rubble slopes have been performed at the Waterways Experiment Station in Vicksburg, USA. On the basis of these experiments, Hudson (1961a, 1961b) proposed another expression as the best fit for the complete set of experiments.

When comparing the formulae of Iribarren and Hudson, the difference appears to be large. The influences of wave-height, rock density and relative density are equal. The coefficients are different, but can easily be compared. The main difference occurs in the influence of the slope. A comparison of the two expressions within the validity area of the Hudson formula ($1.5 < \cot \alpha < 4$) reveals that the correct choice of coefficients leads to a minor difference between the two formulae only. It is evident that for very steep slopes (close to the angle of natural repose) Hudson cannot give a reliable result. It is also likely that for very gentle slopes waves will tend to transport material up the slope, a factor that was not considered by Hudson at all. This becomes clearer when one takes the third root from both formulae. In 1988 Van Der Meer (1988) presented his PhD thesis on "Rock slopes and Gravel Beaches under Wave Attack". In the first place, he used a clear and measurable definition of damage.

Recently Masoom (2002) has studied the riprap protective structure with soil reinforcement. The study has observed the influence of riprap placement type such as uniformly placed riprap and randomly placed riprap on the performance of bank protection work subject to wave action. In the study it is shown that randomly placed riprap on geotextiles shows for progressive failure which provides time for repairing. But uniformly placed riprap shows sudden failure.

Kobayashi and Wurjanto (1990) developed a numerical model to predict the flow and armor response on a rough permeable slope as well as the flow in a thin permeable under layer for a normally incident wave train. Computation was made for six test runs to examine the accuracy and capability of the numerical model for simulating the fairly detailed hydrodynamics and armor response under the action of regular waves. The computed results with and without a permeable under layer indicated that the permeability effects would increase the hydraulic stability of armor units noticeably and decrease wave run up and reflection slightly.

Norton and Holmes (1992) developed a numerical model for the reshaping of dynamically stable breakwaters under normally incident monochromatic waves. The armor layer was numerically represented by a random assembly of interacting spherical particles. The numerical model of Kobayashi and Wurjanto (1990) was used to predict wave induced velocities on the seaward slope. A force model was used to assess armor stability on the slope and an empirical procedure was adopted to estimate the displacement distance of unstable armor units. The preliminary comparison of the numerical model with experimental tests on a berm breakwater was promising. It should be stated that the particle dynamics method (e.g., Haff 1991) has been used to simulate the dynamic behavior of a number of particles over a short duration time for cases where fluid forces may be neglected or simplified considerably.

Mitwally et. al., 1989 concluded in his study that it is common practice to assume a constant value of the water particle velocity along the tributary lengths of the members. This simplification gives good results for long wavelengths but may entail a marked overestimation for short wavelengths. For strength design, the line structure approximation holds as most of the wave energy is contained in longer waves. However, for fatigue consideration, the line structure approximation loses accuracy, since the peak wave energy is contained in shorter waves and spatial correlation of wave forces becomes important. For real offshore structures, these separation to wavelength ratios are only achieved by shorter waves. This is an important consideration for fatigue design.

2.4 Basic physics of wave pressure on sea faced sloping side of structures

The present development of the predictive methods on wave pressures on a sloped coastal structure is based on the fundamental principles of wave transformation on such structures. The sea bed is considered horizontal, the wave is considered traveling perpendicular to the slope and hence the wave is assumed propagating without any transformation till the toe of the wall. The waves undergo significant transformation during its propagation on the sloped structure. Its height increases and length reduces and consequently the waves become unstable and either spilling or plunging or surging type breaking occurs on the structure (depends upon the structure slope and the incident wave steepness) along with significant turbulence and energy dissipation. The remaining energy in the incident wave is used for carrying certain amount of water and results in the run-up of water mass. The pressures in the run-up zone are caused mainly by the thickness of the flowing water mass. Hence from the physics of wave transformations on the sloped walls, one can consider three zones of pressures during run-up process (Figure 2.4.1). (Neelamani et al., 1999)

Zone 1 ($0 < z < d - H_i/2$), where the waves are in general non-breaking and the resulting pressures are governed by the partial reflection and phase shift during reflection from the sloped structures; Zone 2 ($d - H_i/2 < z < d$), where the type of wave breaking and turbulence is significant and the resulting pressures are highly stochastic; Zone 3 ($d < z < \text{Run-up height}$), where the pressure is induced by the run-up water.

During the run-down process, the potential energy of the water present in the run-up zone is converted into kinetic energy and a part of this energy is dissipated due to turbulence and the remaining part of the energy is used for the wave reflection and hence resulting in a partial standing wave envelope in front of the structure.

Since the wave reflection takes place from the sloped face, it causes phase shift which is quite different from that of a vertical wall. This physics of wave run-down

is used to consider two different zones of wave pressures (Zones 4 and 5 as shown in Figure 2.4.1). During run-down, the seawall below the still water surface is exposed to atmosphere. The structure in these run-down regions is initially loaded with hydrostatic pressures. During run-down, the dynamic pressure varies with reference to this static pressure and results in pressures, which are less than the initial static pressures. This region on the seawall is considered as Zone 4 ($d - \text{Run-down} < z < d$). Zone 5 ($0 < z < d - \text{Run-down}$) is the region, where the negative wave pressures occur due to the effect of partial reflection and phase shift. (Neelamani et al., 1999)

These physics of waves on sloped structures are useful for theoretical investigation and empirical predictions.

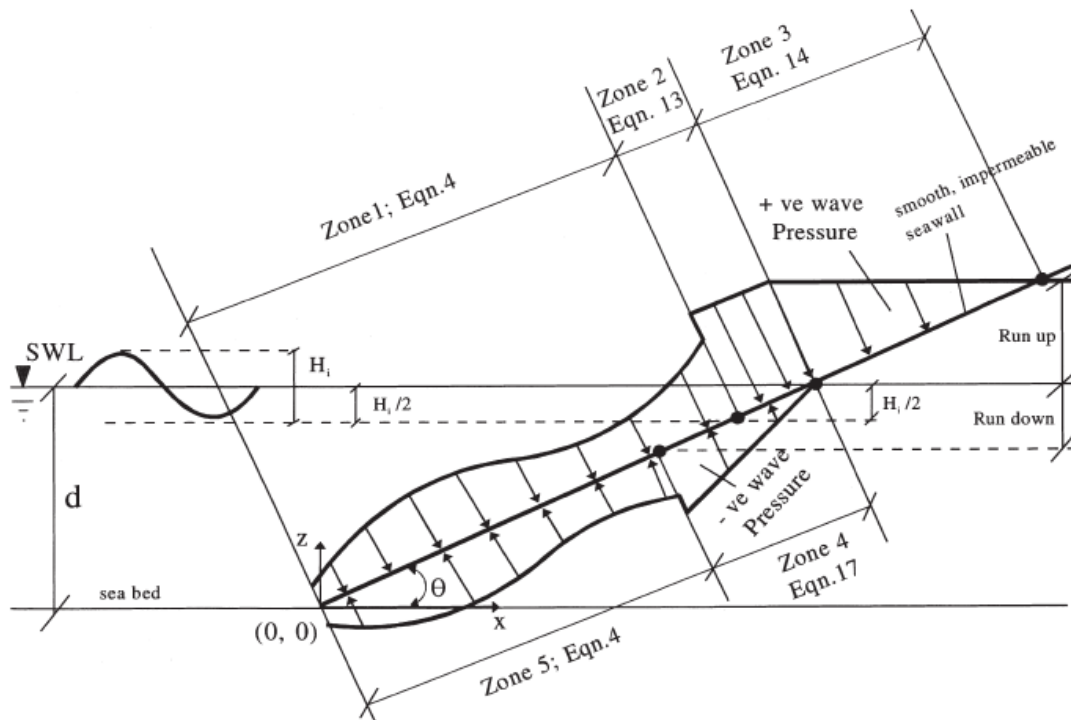


Figure 2.4.1: Definition sketch to explain the predicted wave pressure on coastal structure (Source: Neelamani et al., 1999)

2.5 Design consideration for a coastal embankment

In Bangladesh River training work has passed a several time whereas the coastal work is a new sector. A number of river protection works have done and upgraded which have come to success. There is some difference in river structure design and coastal structure design which should be identified and implemented in coastal

embankment design. Though this study deals with the dynamic load impact and wave action on the embankment side, here is some detail design considerations and a schematization (Figure 2.5.1) for a coastal embankment, which will help to differ from the design of a river embankment.

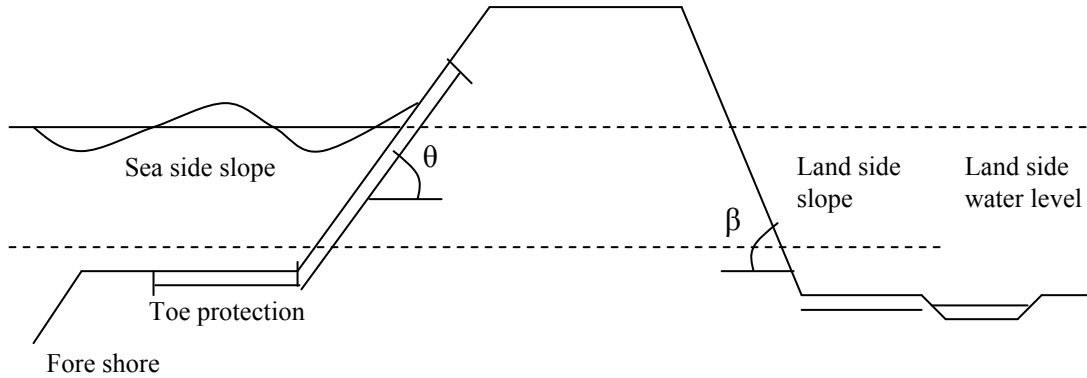


Figure 2.5.1: Schematization of an embankment (Source: Pilarczyk, 1990)

(A) Steeper or milder slope gradient: (Pilarczyk et. al., 1995)

- Steeper slope makes the protective length (revetment) shorter; as a first approximation, the slope length (L_s) is related to the height of the slope (h_s) to be protected by, $L_s = h_s / \sin \alpha$.
- For breaking waves ($\xi_{op} < 2.5$) the run-up ($R_{u2\%}$) on the steeper slope will increase proportionally to $\tan \alpha$, namely: $R_{u2\%} \approx 8H_s \tan \alpha$; this yields a higher crest position and eventually, a larger volume of the structure.
- The run-down on the steeper slope also increases, possibly leading to higher over pressures and thus, thicker protective elements.
- For steeper slopes of loosely placed blocks, the friction between the blocks increases with $\sin \alpha$. However, it is difficult to quantify the consequences of this effect exactly.
- For steeper slopes the internal gradients increase, leading to more severe requirements concerning the sub layers.

- A steeper slope imposes more severe requirements for the support by a toe-protection.
- The damage progress after an initial damage is more rapid for the steep slopes, thus providing more dangers of scouring.
- Steep slopes are more easily damaged by ice, especially when using slopes steeper than 1 on 3, the above considerations should be taken into account for a proper design.
- For steeper slopes the risk of geotechnical instability increases.

(B) Berm or no berm

- Application of a berm reduces the run-up, making possible a lower crest elevation.
- A berm can serve as a maintenance road.
- A berm creates a discontinuity in a protection (weak point).
- A berm reduces the phreatic level in a dike with a positive effect in case of low permeable or impermeable revetments.
- A berm reduces ice ride-up.

(C) High or low permeability of the cover layer

- High permeability, in combination with a proper sub layer, reduces the uplift pressure and leads to thinner units. It is however important that the permeability does not decrease during the life time (aging).
- When the high permeability is created by large openings in or between blocks, washing out of the sub layers can take place; to avoid this the following measures can be taken:
 - (a) coarser filter, however this sometimes leads to increase of the hydraulic gradients across the cover layer and thus to thicker units,
 - (b) geotextiles underneath the cover layer elements. Attention should be paid to a sufficiently low hydraulic resistance

normal to the slope, which should not increase the uplift pressure again.

(c) another solution can be the use of bounded filters (sand-bitumen, sand-cement, etc.). To reduce these disadvantages the permeability should be distributed over the units instead of being concentrated (e.g. in one big hole).

- High permeability of the cover layer may increase the hydraulic gradients at the sub layer-subsoil interface or in the subsoil; proper care should be exercised in adequate sub layer design.
- High permeability of cover layer reduces the run-up somewhat.
- In the case of a very high permeability of block revetments created by large holes the drag forces along the slope may increase considerably, leading to large forces on the units and thus larger dimensions.

(D) Rough or smooth surface

- A rough surface (can also be obtained by using blocks of various height) reduces the run-up and thus it reduces the crest elevation and eventually the volume of dike. This effect is evident mainly when the whole run-up zone is equipped with roughness elements. When the upper slope is protected by a grass-mat the application of the roughness elements on the lower part of a slope will have a limited effect.
- High roughness elements introduce high drag-forces which should be incorporated in the stability calculations.
- Rough surface is unfavorable under ice condition.

(E) High or low permeability of sub layers (filter)

- Decreasing of sub layer-permeability reduces the uplift forces on the cover layer. In the case of a cover layer of low permeability this may lead to reduction of the thickness of the cover layer. However, it should be checked whether this lower permeability of the sub layer and the corresponding reduction of weight is acceptable with respect to the stability of the sub layers.
- For non-cohesive (granular materials a decrease of the permeability can be obtained by: a) finer granular material (however, washing out through the cover layer should be avoided and the geotechnical (in-) stability should be checked); b) wide-graded material (the internal stability should be examined).
- Applying clay as a cohesive sub layer needs formulation of proper specifications on clay properties to avoid erosion, piping or shrinkage. However, it should be checked whether an impermeable sub layer might cause other problems, e.g. malfunctioning of the toe.
- Lower permeability of sub layer/filter increases the hydraulic gradients at the interface with the subsoil or inside it. This can be coped with by increasing the thickness of the sub layer/filter or by applying a geotextiles on top of the subsoil. Besides, the geotechnical stability should be evaluated.

(F) Shape of sub layer/filter-material

- Rounded material is often cheaper than broken material; however, in the case of insufficiently compacted grains, a slightly lower angle of internal friction may lead to geotechnical instability, more settlement and forces on the toe-structure.

(G) Thick or thin sub layer/filter

- In the case of block revetments of low permeability, reduction of the thickness of sub layer/filter leads to reduction of the up-lift forces but simultaneously it leads to increase of the hydraulic gradients along the interface with the sub-soil or inside it.

(H) Concrete (or other artificial material) or natural stone

- Natural stone, if available in respect to the required quality and quantity can often be a favorite solution.
- Concrete blocks (or asphalted revetments) can often be a good alternative (especially when the natural stone is not locally available) because of, a) often lower cost, b) good/constant quality, c) uniform size, d) mechanical execution, e) more choice regarding composition, size etc.

(I) Effect of ageing and /or wearing/fatigue

During the lifetime of revetment structures their original specifications can change due to climatologically effects (wind, rain, frost, abrasion, sedimentation due to waves, marine growth etc.). As far as possible the course of time should be taken into account in the design process.

Ageing of the cover layer:

- Due to the wave attack at various water levels the permeability and the interlocking may change with time. For small interspaces between the blocks the permeability can decrease due to siltation of sediment while the friction between the blocks may increase.
- Vegetation in the interspaces may also increase the friction/interlocking; however, it is possible that in the case of a heavy wave attack, the silted and/or vegetated interspaces will be cleaned up again, thus providing no additional strength at the moment of design

loading on the protective units.

Ageing of the sub layers:

- In the case of alternative materials used as sub layers (minestone, slags, silex etc.) special attention should be paid to the changes of the physical properties of these materials under influence of air, wave shocks, varying humidity, frost etc.
- In the case of geotextiles special attention should be paid to the possibility of clogging and/or blocking (leading to drastic change of permeability and thus increase of uplift pressure).
- The siltation of the sub layers/filter has in general a positive effect; due to the decrease of permeability the up-lift forces decrease.

(J) Residual strength of revetments

Revetments should be designed in such a way that the chance of failure is acceptably low. The quantification of a risk is related to the type of revetment, especially regarding the progress of damage, for example:

- a very rough surface is more sensitive to damage than a smooth surface;
- application of a strong geotextiles retards the extension of damage to the subsoil;
- cohesive-(clay) or bounded-sub layers are primary measures to increase the secondary strength of revetment-structures if the permeability of those materials is not a disadvantage for the total stability and if the cohesive material is of sufficient strength.

(K) Wave load (SPM, 1984)

- Forces due to non-breaking wave forces are primarily hydrostatic which later come under dynamic effects of turbulent water. Dynamic forces are much greater than the hydrostatic forces. Wave conditions

at an embankment on the seaward side are affected by incident and reflected wave. Wave height at the embankment is given by, $H_w = H_i + H_r = (1 + \chi)H_i$, where H_i = incident wave height and χ is the reflection coefficient. If reflection is complete and reflected wave has the same amplitude as the incident wave then $\chi = 1$. A lower value of χ may be assumed when the embankment is built on a rubble base but value of χ less than 0.9 should not be used for design purposes.

- When the wave crest is at the wall, pressure increases and from zero at the free surface to $(\gamma h + p_1)$ at the bottom, when the trough is at the wall, pressure increases from zero at the water surface to $(\gamma h - p_1)$ at the bottom. Where p_1 is approximated as, $p_1 = \left(\frac{1 + \lambda}{2}\right) \frac{\gamma H_i}{\cosh(2\pi h/L)}$.

It is clear that the design of open sea embankment should be different from river embankment in consideration of wave dynamic load which is the most dominant factor for coastal embankment.

2.6 Case study in Bangladesh

The first project to build coastal embankments along the coastal belt was taken four decades ago. The project was divided into three regions. Eastern region covers 1133 sq. km. extending from Chittagong to Arakan Hill Tracts. Central region or estuary which is funneled apex shape of Bay of Bengal covering 3360 sq. km and the western region is formed by deltaic action of Ganges-Brahmaputra-Meghna with an area of 9271 sq. km (Ali, 1997). To cover this areas three types of embankments exists in this area. Larger embankments or sea dykes are situated along the Bay of Bengal and major rivers. Interior embankments are along the bank of rivers and marginal embankments are provided along the bank of small rivers. Among these three embankments the sea dykes along the Bay of Bengal can come under wave action. The embankments along the rivers are not considered in this study according to the definition of this study. This study has selected three cases of analysis which

are (A) Sea dykes at Kutubdia island, (B) Sea dykes at Maheshkhali and (C) Marine drive at Cox's Bazar.

Islam (1999) stated that, in many cases the embankments are designed with insufficient setback, resulting in increased exposure to waves and current action. This may be due to the high costs involved in land acquisition. Sometimes the setback area is also eroded. Furthermore, insufficient supervision during construction results in poor-quality earthworks with the use of inappropriate soil materials, insufficient or no clod breaking, inadequate compaction and no or insufficient lying of topsoil layers. Scouring holes and rills appear in no time after completion of the construction.

Table 2.6.1: Embankments of these types have the following characteristics.

(Source: Navera and Nandi, 2007)

Sea dyke	Crest height (m)	C/S slope	S/S slope	Location
A	5.1	1:2	1:7	Behind swash zone
B	4.88	1:2	1:7	Behind swash zone
C	4.88	1:1.5	1:2	In swash zone

The study checked the causes of failure for each type of embankment of the above table. (i) Location of an embankment: The embankment of type A and B are located 300 m from the coastline and maximum swash zone width is found in this study as 16 m so these structures are located far behind the action of wave. For embankment C which is located near the coastline which is definitely inside the swash zone. (ii) Crest level: Type A and type B embankments are located far from the action of wave, so the crest heights are adequate. Type C is under wave action repeatedly. The maximum wave height it can sustain is 1.02 m. (iii) Slope of the sea side and country side: Type A and B shows that in the sea side the slope of the embankments are 1:7 which can protect them for possible shear failure. In the other hand Type C has the slope of 1:2 which is definitely not enough to sustain periodic loading where pressure changes continuously. (iv) Drainage facilities: There is no possibility of drainage

congestion for type A and B which is found by analyzing the detail cross sections. The country side of Type C is frequently get rain water from hills nearby. The sea side also gets periodic loading which needs proper drainage. (v) Wave direction: The seasonal variation of wave direction should be considered in the design. The incident wave angle changes the magnitude of force for constant wave height Type A and B need not to worry about this failure as both the structures are not under direct action of wave. But for type C embankment incident wave angle can be a critical factor for design purpose. Wave from 45 degree angle perpendicular to the shoreline came as vulnerable from this study (Navera and Nandi, 2007).

2.7 Summary

Mainly three types of embankments exist in Bangladesh. Larger embankments or sea dykes are situated along the Bay of Bengal. Interior embankments are along the bank of rivers and marginal embankments are provided along the bank of small rivers. Among these three embankments the sea dykes along the Bay of Bengal can come under wave action. In Bangladesh, basically no embankment has yet been constructed for wave dynamic load protection and the existing embankment has a very poor performance against storm surge, wind generated wave. So, it has been observed some embankments have catastrophic failure under wave loading. It has raised a question about the effectiveness of the embankment against wave attack and requires an evaluation of its effectiveness before raising or constructing a new embankment. Marine drive of Bangladesh at Cox's bazaar is the example of the above case. These are reasons which are based for this research work. Where wave loads on sloping embankment were calculated through an experimental setup.

CHAPTER 3

THEORY AND METHODOLOGY

3.1 General

For this research work many terms come forward which are treated as the theory of this study. This chapter involves with those terms and definition and the equations used for the work are discussed in this chapter. Methodology or experimental descriptions are also stated in this chapter.

3.2 Theory

Coastal embankments have to resist direct wave load than the general embankments built in the rivers thus it is simply different from the river embankment. So, the wave characteristics and its impact on the embankment slope, magnitude of wave loads are the significant factors which are related to the coastal embankment stability. The general discussion of these wave characteristics and other related factors have discussed in the section.

3.2.1 Theory of Coastal embankment

Coastal embankment is a structural measure usually taken near coastline to protect inland habitat and crops. Characteristics of coastal embankment are (i) located behind the swash zone, (ii) when loaded it will be under dynamic loading, (iii) when under load it may go inside the swash zone, (iv) it may be over topped during extreme wave height, (v) apron may be visible, (vi) material would be selected in such a way that it may prevent saline water impact and (vii) adequate drainage should be provided. Again the purposes of Coastal embankments are (i) to protect inland from saline water, (ii) to protect human habitat/settlement from extreme weather condition and (iii) to promote access to coastal areas (Navera and Nandi, 2007).

According to Van der Meer (1990), only two types of structures have to be distinguished if the response of the various structures is concerned. They are,

1. Statically stable structures are structures where no or minor damage is allowed under design conditions. Traditionally designed breakwaters belong to the group of statically stable structures. It is roughly be classified by $H/\Delta D = 1-4$. Where, H = wave height, Δ = relative mass density and D = characteristic diameter of structure, armour unit (rock or concrete), stone, gravel or sand and
2. Dynamically stable structures are structures where profile development is concerned. Units (stones, gravel or sand) are displaced by wave action until a profile is reached where the transport capacity along the profile is reduced to a very low level. Material around the still water level is continuously moving during each run-up and rundown of file has reached to equilibrium. Dynamic stability is characterized by the design parameter profile, and can roughly be classified by $H/\Delta D > 6$.

3.2.2 Wave

A wave is the generic terms for any periodic fluctuation in water height, velocity or pressure. The effect of water waves are of paramount importance in the field of coastal embankment. Surface waves generally derive their energy from the winds. Waves have potential energy in the form of their surface displacement and kinetic energy in the motion of the water particles. Waves transmit this energy as they propagate. There is a relatively small mass transport in the direction of wave propagation (SPM, 1984). When directly being generated and affected by the local winds, a wind wave system is called a wind sea. After the wind ceases to blow, wind waves are called swell, or, more generally, a swell consists of wind generated waves that are not - or hardly- affected by the local wind at the same moment. Wind waves in the ocean are called ocean surface waves.

Table 3.2.1: An overview of types of structures with different $H/\Delta D$ values
 (Source: Van der Meer, 1990)

$H/\Delta D < 1$	Caissons or seawalls. No damage is allowed for these fixed structures. The diameter, D , can be the height or width of the structure.
$H/\Delta D = 1-4$	Stable breakwaters. Generally uniform slopes are applied with heavy artificial armour units or natural rock. Only little damage (displacement) is allowed under severe design conditions. The diameter is a characteristic diameter of the unit, such as the nominal diameter.
$H/\Delta D = 3-6$	S-shaped and berm breakwaters. These structures are characterized by more or less steep slopes above and below the still water level with a more gentle slope in between. This gentle part reduces the wave forces on the armour units. Berm breakwaters are designed with a very steep seaward slope and a horizontal berm just above the still water. The first storms develop a more gentle profile which is stable further on. The profile changes to be expected are important.
$H/\Delta D = 6-20$	Rock slopes/beaches. The diameter of the rock is relatively small and can not withstand severe wave attack without displacement of material. The profile which is being developed under different wave boundary conditions is the design parameter.
$H/\Delta D = 15-500$	Gravel beaches. Grain sizes, roughly between ten centimeters and four millimeters, can be classified as gravel. Gravel beaches will change continuously under varying wave conditions and water levels (tide). Again the development of the profile is one of the design parameters.
$H/\Delta D > 500$	Sand beaches (during storm surges). Also material with very small diameters can withstand severe wave attack. The Dutch coast is partly protected by sand dunes. The dune erosion and profile development during storm surges is one of the main design parameters. Extensive basic research has been performed on this topic (Vellinga, 1986). Sand beaches are treated somewhere else in this short course.

Wind waves are mechanical waves that propagate along the interface between water and air; the restoring force is provided by gravity, and so they are often referred to as surface gravity waves. As the wind blows, pressure and friction forces perturb the equilibrium of the water surface. These forces transfer energy from the air to the water, forming waves. In the case of monochromatic linear plane waves in deep water, particles near the surface move in circular paths, making wind waves a combination of longitudinal (back and forth) and transverse (up and down) wave motions. When waves propagate in shallow water (where the depth is less than half the wavelength) the particle trajectories are compressed into ellipses. As the wave amplitude (height) increases, the particle paths no longer form closed orbits; rather, after the passage of each crest, particles are displaced slightly from their previous positions, a phenomenon known as Stokes drift (wikipedia.org).

Five factors influence the formation of wave,

- wind speed
- distance of open water that the wind has blown over (called the fetch)
- width of area effected by fetch
- time duration the wind has blown over a given area
- water depth

The greater each of the variables, the larger the waves.

Waves are characterized by:

- wave height (H)
- wave length (L)
- wave period (T)
- direction of wave propagation (α)

Wave height (H) is the vertical distance from the crest of a wave (the highest portion of a wave) to the trough of the wave (the lowest portion of the wave). For a given wind speed, many different wave lengths are produced and for each wave length many different wave heights are developed. The general relationship is that higher waves tend to have longer wave length (lower frequencies).

Waves height decrease in the surf zone as to lose energy due to wave breaking. The decrease in height of the broken waves is mainly controlled by the bottom slope. Various investigations have been conducted, among which Horikawa and Kuo presented the diagram shown in Fig. 3.2.1 to emphasize the influence of the bottom slope on the wave height changes.

Wave length (L) is the horizontal distance from one wave crest to the next wave crest or the distance from one wave trough to the next wave trough. Although difficult to measure at sea, this parameter may be measured on aerial photograph. It is directly related to wave period by $L = 5.12T$, where L is wave length in feet and T is wave period in second.

Wave period (T) is the time, usually measured in seconds, that it takes for a complete wave cycle (crest to crest or trough to trough) to pass a given fixed point. It depends upon the speed of movement of the wave across the surface. It is the one characteristics of a wave that remains constant at all times, no matter what changes occur in height or length. With shorter wave length waves moving slower and longer wave length waves moving faster.

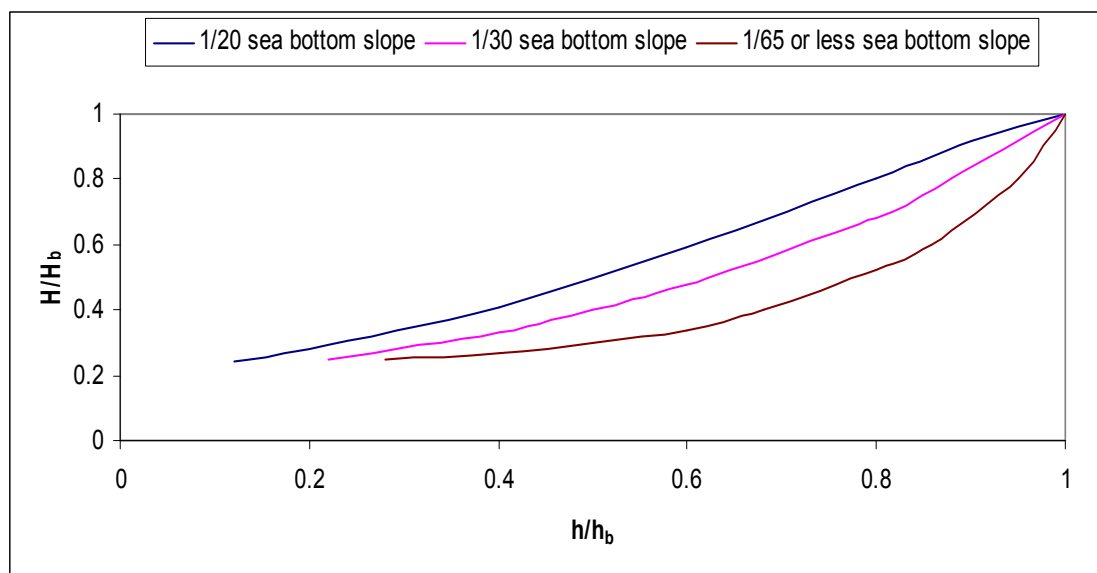


Figure 3.2.1 Wave height change after breaking (Source: Horikawa et. al., 1996)

Wave frequency (f) is the number of wave cycles passing a fixed point in 1 second and it is inversely proportional to wave period. It is measured by, $f = \frac{1}{T}$.

Wave direction is the direction in true degrees of a azimuth that the majority of the waves in a group are coming from. Wave direction is best determined during observation by sighting along the wave crests and troughs and either adding 90^0 to or subtracting it from the direction obtained. Add or subtract 90^0 to/from the true bearing thus obtained to determine the wave direction.

Waves are classified in various ways. Ocean waves have a very wide range of periods. The energy of waves of fixed period is proportional to H^2 , as shown in the following section. Figure 3.2.2 is a diagram originally drawn by Munk in 1951 which displays the predominant types of waves in the ocean, the names of the various waves for each period range, and the agents generating these waves.

Figure 3.2.2 shows that waves of the greatest energy concentration are wind waves. Wind waves are generated and developed by wind action stated above and their wave period is normally less than 10 to 15 sec, while heights of as much as 34 m have been reported. Swells consist of wind-generated waves that have traveled out of their generating area.

Water depth has an important influence which creates two type of waves. The wave length being very large compared to the water depth, $kd \rightarrow \alpha$, is called a deep water wave (or surface wave). The wave length being very small compared to the water depth $kd \rightarrow 0$ is called shallow water wave (long wave). Again the ratio between water depth and wave length is called the relative water depth. In general, waves in the ranges of $d/L > 1/2$ and $d/L < 1/20 \approx 1/25$ are considered to be deep water waves and long waves, respectively.

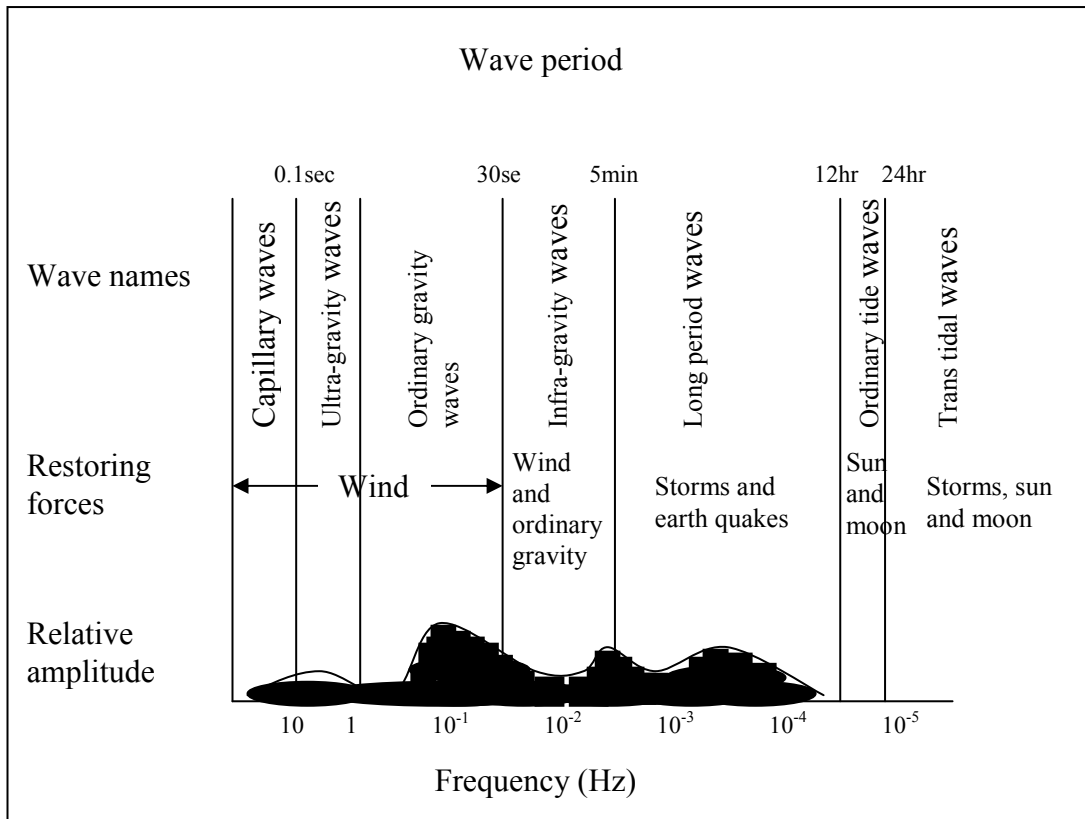


Figure 3.2.2: Classification of ocean waves according to wave period (Source: Munk, 1951).

3.2.3 Characteristics of Wave Field

In the laboratory regular waves are generated. But the characteristics of wave field in the real life are irregular. Wave height of irregular waves is usually characterized by the value of significant wave height (H_s), which is the average height of the one third of the highest waves. For weather reporting and for scientific analysis of wind wave statistics, their characteristic height over a period of time is usually expressed as significant wave height. In a given sea condition, many different size waves are present. Observers determine significant wave height, or the average wave height of the highest 1/3 of all the waves present. Ideally, the heights of 50 to 100 waves should be recorded on a piece of paper, and then the highest 1/3 of the recorded heights should be averaged to obtain significant wave height for the seas. The important factor in determining both the average height and the average period for

sea waves is that only the highest 1/3 of the waves, the significant waves, is evaluated.

In general $H_{x\%}$ is a characteristics wave in irregular wave field and it can be stated as $H_{x\%}$ = wave height exceeded by x% of the waves. Therefore other characteristics waves are defined as in the following way:

$$H_{1\%} = 1.52H_s$$

$$H_{2\%} = 1.4H_s$$

$$H_{5\%} = 1.22H_s$$

$$H_{13.5\%} = H_s$$

$$H_{50\%} = 0.59H_s \text{ (Median wave height).}$$

Other characteristics of waves are peak wave period, T_p . Wave period at peak of the spectrum is called peak wave period, which is 1.1 to 1.3 times of average wave period.

Wave steepness is another important characteristic of wave field. It is defined as

$S = \frac{H_s}{L_o}$. Again Iribarren number of surf parameter is of crucial importance in all

kinds of problems in shore protective works. It is defined as $\xi = \frac{\tan \alpha}{\sqrt{H_s/L_o}}$, where α is

the angle of the slope and $\frac{H_s}{L_o}$ is already defined as the wave steepness.

For breaking waves water depth is greater than three times of significant wave height ($d \geq 3H_s$).

3.2.4 Wave Run-up

Run-up is defined as the maximum water level on a slope height during a wave period. This is defined relative to still water. The run-up height R describes the vertical distance between highest run-up level R_u and deepest run-down R_d (which is similar to the definition of wave height) (Muttray, et al., 2006).

The maximum wave run-up level R_u on the slope is of more practical importance than the wave run-up height R . The highest wave run-up depends on wave run-up height R and on the asymmetry of the wave run-up R_u/R . The latter was determined from experimental data.

Prediction of wave run-up may be based on simple empirical equations. Those equations are developed by model test results or numerical models of wave structure interaction (Nandi, 2002).

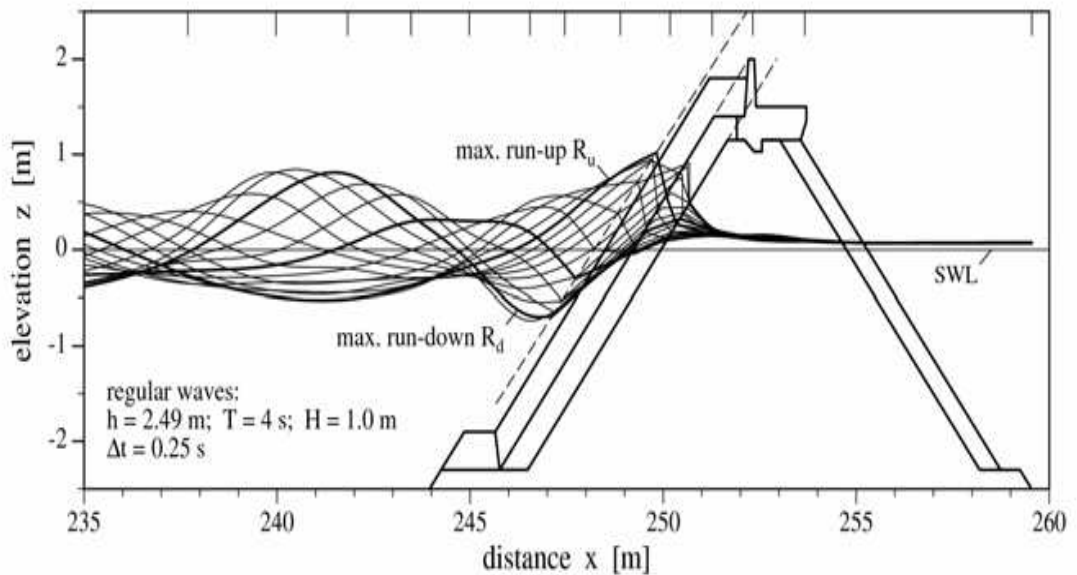


Figure 3.2.3: Water conditions and wave motion on the breakwater slope

(Source: Muttray, et al., 2006)

The effective run-up (R), on an inclined structure can be defined as,

$$R = R_n \gamma_R \gamma_B \gamma_\beta$$

where,

R_n = run-up on smooth plane slopes, defined as the vertical height above still water level, and n = index of exceedance percentage.

γ_R = reduction factor due to slope roughness and permeability,

γ_B = reduction factor due to berm,

γ_β = reduction factor due to oblique wave attack, and

ξ^β = breaker index.

Wave run-up is reduced by three reduction factors, namely: berms, roughness on the slope and oblique wave attack.

Definition of the average slope angle:

Research is very often performed with nice straight slopes and the definition of $\tan\alpha$ is then obvious. In practice, however, a dike slope may consist of various more or less straight parts and the definition of the slope angle needs to be more precisely defined. The slope angle becomes average slope angle. Figure 2.4 gives the definition of slope (Pilarczyk et.al., 1998).

The wave action is concentrated on a certain part of the slope around the water level. Examination of many tests showed that the part $1.5 H_s$ above and below the water line is the governing part (Pilarczyk et.al., 1998). As berms are treated separately the berm width should be omitted from the definition of the average slope. The average slope is then defined as:

$$\tan \alpha = 3H_s / (L_{slope} - B)$$

Where, L_{slope} = the horizontal length between the two points on the slope $1.5 H_s$ above and below the water line, and B = the berm width.

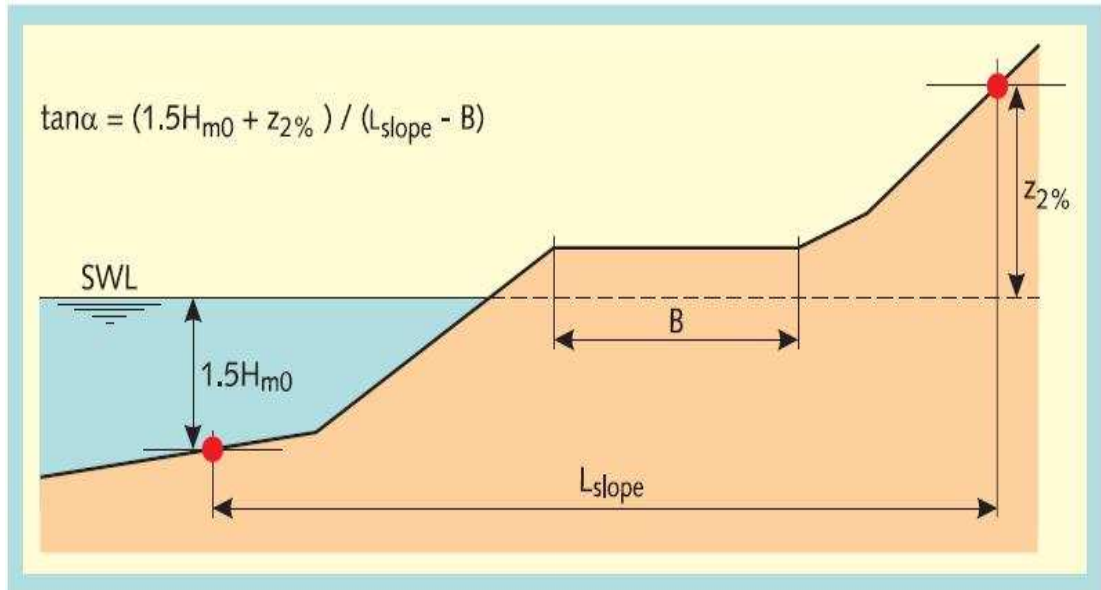


Figure 3.2.4: Definition sketch of slope (Source: Pilarczyk et.al., 1998)

3.2.5 Overtopping

If extreme run-up levels exceed the crest level of the structure it will result in overtopping. This may occur for relatively few waves under the design event and a low overtopping rate may often be accepted without severe consequences for the structure or the area protected by it. Seawalls and breakwaters are often designed on the basis that some (small) overtopping discharge is to be expected under extreme wave conditions (Masoom, 2002).

3.2.6 Wave reflection

Like sound waves, surface waves can be bent (refracted) or bounced back (reflected) by solid objects. Waves do not propagate in a strict line but tend to spread outward while becoming smaller. Where a wave front is large, such spreading cancels out and the parallel wave fronts are seen traveling in the same direction. Where a lee shore exists, such as inside a harbor or behind an island, waves can be seen to bend towards where no waves are. When approaching a gently sloping shore, waves are slowed down and bent towards the shore. When approaching a steep rocky shore, waves are bounced back, creating a 'confused sea' of interfering waves with twice the

height and steepness. Such places may become hazardous to shipping in otherwise acceptable sea conditions (Anthoni, 2000).

Wave reflections are of importance on the open coast and at commercial and small harbors. Reflected waves can also propagate into areas of a harbor previously sheltered from wave action. They will lead to greater peak orbital velocities, increasing the likelihood of movement of beach material (Masoom, 2002).

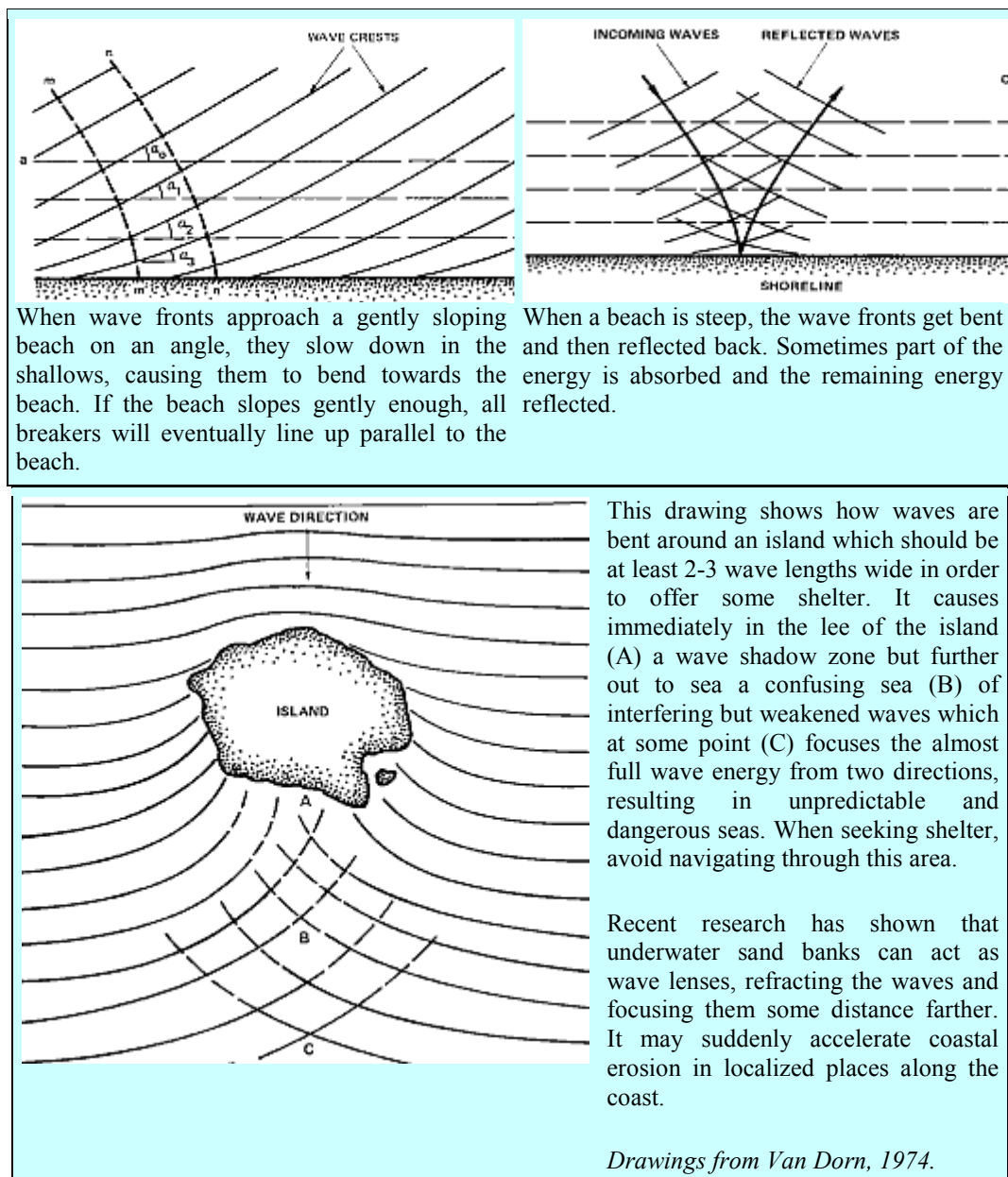


Figure 3.2.5: Wave reflection mechanism
(Source: www.seafriends.org.nz/oceano/waves.htm).

3.2.7. Hydraulic loads on embankment

River and canal banks and embankments generally consist of easily erodible materials requiring protection against hydraulic loads. Main causes of hydraulic loads are shown in the Figure 3.2.6.

The hydraulic loads on coastal embankment are due to the following causes.

- i) Flows
- ii) Water level and
- iii) Waves.

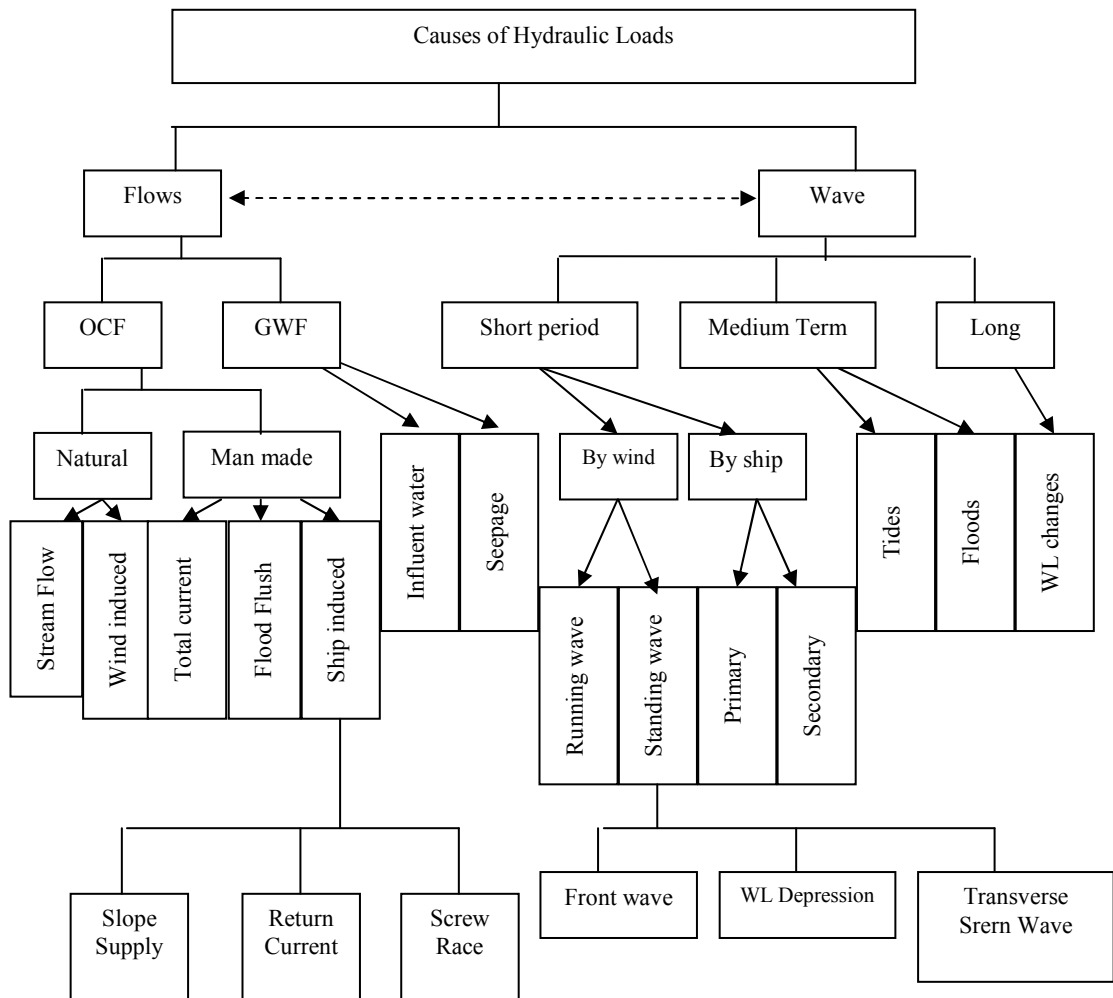


Figure 3.2.6 Main causes of Hydraulic Load

3.2.7.1 Hydraulic loads due to flows

It is an important load on coastal structure. But the study does not allow this load on the structure. Therefore, the hydraulic loads due to flows are not considered here.

3.2.7.2 Hydraulic load due to water level

Water level in front of the structure may cause seepage pressure if other side has differential water level. Water becomes as an imposed load on the structure. During design of hydraulic structure this load must be considered. In this study this loads had not been calculated but its effect on various wave parameters, velocities and loads have been discussed at the Result and Discussion chapter.

3.2.7.3 Hydraulic load due to waves

Wave is an important and dominating force in design of coastal structures. Waves are generated in large mass of water body like in sea. Among other causes of wave generation wind, earthquake, ship etc are important. This research work has been conducted with this type of load through a laboratory experiment to characterize this load with various wave parameters.

It is very complex to define a wave load on structure. The behaviour of wave load is not static. It imposes somewhere dynamic load and other where quasi-static load. It is well known that the pressure under a wave increase and decreases with the wave cycle as long as the water keeps in touch with the point where the pressure is considered. This is often called the quasi-static wave load, as shown point 1 in Figure 3.2.7.

When water from the wave collides with the surface, a very short, very high, impact pressure will occur. This is called the dynamic wave load, wave impact or wave shock, shown in point 2 of Figure 3.2.7. In this figure the shape of the impact pressure distribution is assumed to be a triangle with H as base length. Here, P is

impact pressure and H is wave height. The conclusion is that wave height is the dominating characteristic to determine wave load on the structure

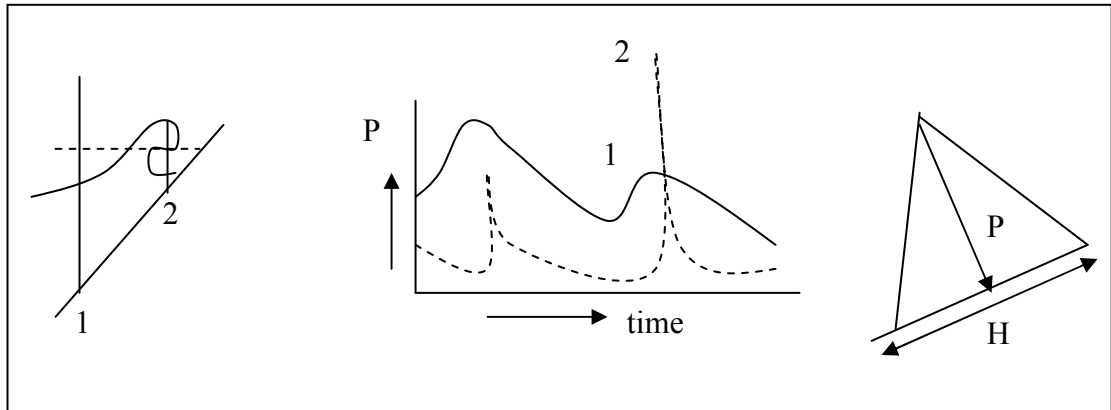


Figure 3.2.7: Wave impact on slope (Source: Schiereck, 2001)

3.2.7.4 Factors affecting hydraulic load

Wind generated waves, tides and wave setup cause rise in water level. The water level cause force on the structure. Besides forces due to water level waves act as dynamic force on structure. However there are several causes that affect hydraulic loads on the structure. These are shoaling, refraction, diffraction and breaking; which are shown in Figure 3.2.8

3.2.7.5 Wave loads

The wave load on a structure can be expressed as,

- External loads and
- Internal loads

Upon breaking on a slope the regular waves exert cyclic hydraulic loads. The external loads can be quantified by way of physical model tests and with numerical methods (Petit et al., 1994; Van Gent et al., 1994). The practical use of the numerical simulations is still very limited, especially regarding the wave-induced pressure distribution on a slope (in space and time). A much simpler approach towards a

computation of the relevant wave loads is to abandon a full description of time and place dependent wave pressures on slope, and to concentrate only on the instant of critical wave loads. For placed block revetments the most critical load situation occurs at the moment of maximum wave run-down. The strength against external

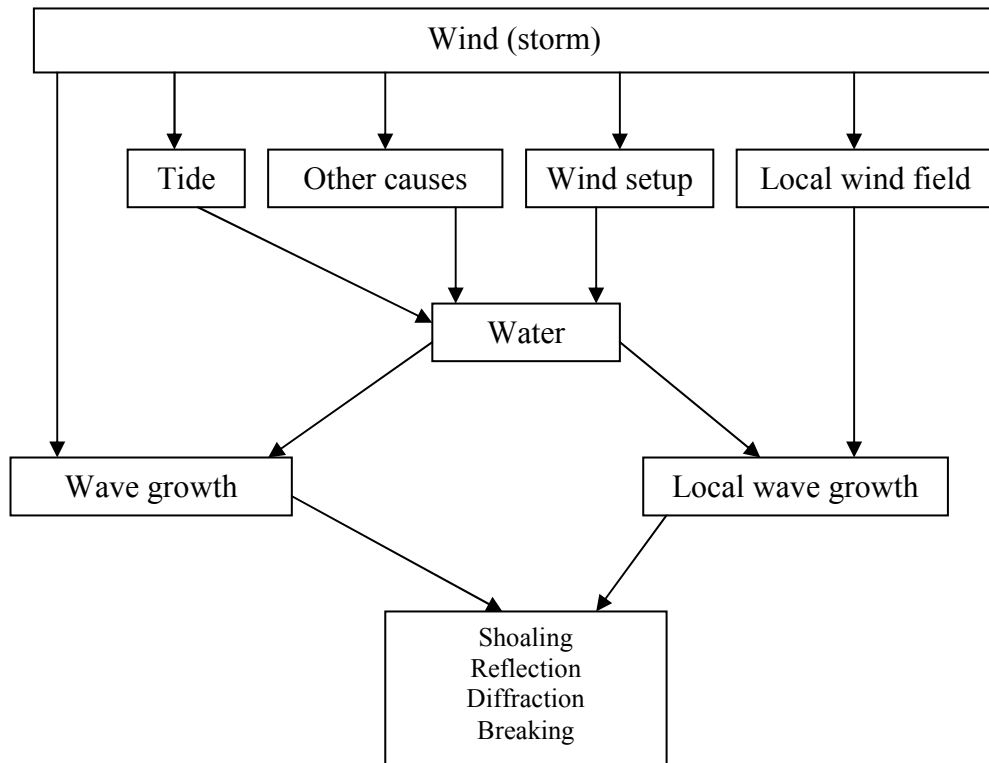


Figure 3.2.8 Process affecting hydraulic load at a structure (Nandi, 2002)

loadings can primarily be provided for by a sufficient weight of the armour elements. Empirical formulas for ϕ_b (maximum piezometric head) and β , based on wave pressure measurements in a small-scale model with slopes between $\frac{1}{2} < \tan \alpha < \frac{1}{4}$ and wave steepness between $0.01 < H/L_o < 0.07$ (regular waves), are given in (Burger et al., 1990):

$$\frac{\phi_b}{H} = \min\left(\frac{\xi_0}{\sqrt{\tan \alpha}}; 2.2\right)$$

$$\tan \theta = \cot \beta = \frac{5.9 \tan \alpha}{\xi_0}$$

$$\frac{d_s}{H} = \min\left(\frac{0.11 \tan \alpha}{(H/L_o)^{0.8}}; 1.5\right)$$

Model tests have shown that the same formulas can be applied with reasonable accuracy for oblique wave attack up to 45° as for perpendicular wave attack.

The internal hydraulic loading on the revetment can be split up into two items:

- 1) The pressure under the cover layer, relative to the pressure on top of the cover layer, causing uplift of the blocks.
- 2) The hydraulic gradients under the cover layer (mainly parallel along the slope), which can cause the migration of subsoil particles.

The internal loading of revetments without granular filter has to be described with more sophisticated solution methods. For example, the STEENZET/2 program of the Delft Geotechnics, a finite element program specially developed to calculate the pore pressure response in the filter layer(s) and subsoil below a placed block revetment. This program can use measured wave pressures as a boundary condition and it can handle laminar as well as turbulent flow (Hjortnaes Pedersen et al., 1987). The internal loadings depend to a large extent on the permeability ratio of cover and filter layer.

(a) Loading zones (CUR/TAW, 1984)

The degree of a wave attack on a dike or other defense structure during a storm surge depends on the orientation in relation to the direction of the storm, the duration and strength of the wind, the extend of the water surface fronting the sea-wall and the bottom topography of the area involved. For a coastal structure the following approximate zones can be distinguished (Figure-3.2.9):

- I. The zone permanently submerged (not present in the case of a high level “foreshore”)
- II. The zone between mean low water (MLW) and mean high water (MHW), the ever-present wave loading of low intensity is of importance for the long-term behavior of structure

- III. The zone between MHW and the design level, this zone can heavily attacked by waves but the frequency of such reduces as one goes higher up the slope
- IV. The zone above design level, where there should only be wave run-up.

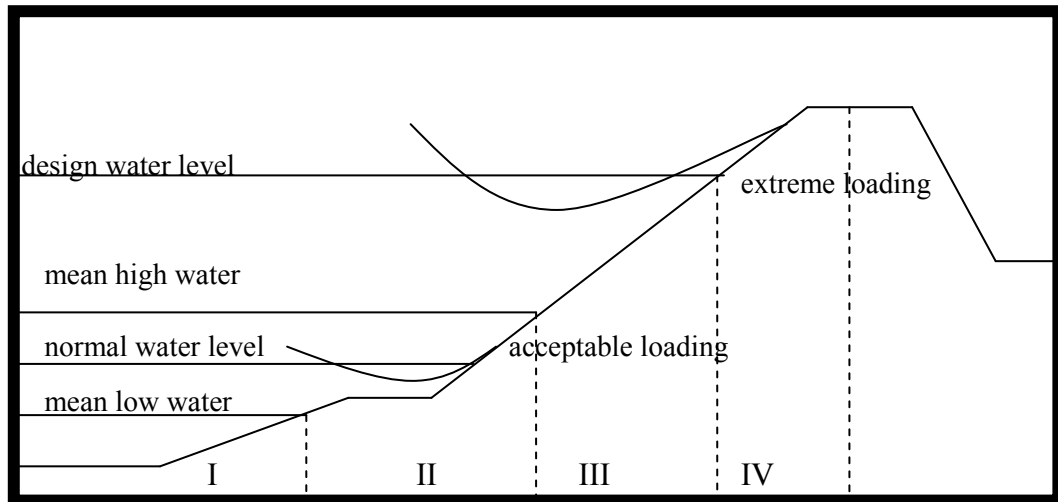


Figure 3.2.9: Loading zones on a coastal embankment (Source: Pilarezyk, 1990)

(b) Wave structure interaction:

The function of a vertical structure is to reflect incoming waves, while that of a mound structure constructed is to dissipate wave energy. When wave attack and break on the slope of a structure, a certain mass of water falls on the slope and induces a negative pressure inside the mound.

The interaction between waves and slopes is dependent on the local wave height and period, the external structure geometry (water depth at the toe), slope with/without berm, the crest elevation and the internal structural geometry (type, size and grading of revetments and secondary layers). The type of structure wave interaction is defined by,

$$\xi = \frac{\tan \alpha}{\sqrt{\frac{H_s}{L_0}}} = \frac{1.25}{\sqrt{H_s}} T \tan \theta$$

where, ξ = Breaker index

H_s = Incident wave height

L_0 = Wave length at deep water (= $1.56 T^2$ in metric units)

T = Wave period

θ = Slope angle of the front face

3.2.8 Structural Responses

The main hydraulic responses of a bank protection structure which experiences wave action are wave run-up and run-down, overtopping, transmission and reflections. They are discussed above.

3.2.9 Theoretical analysis of wave forces

The study of wave forces on coastal structures can be classified in two ways: (a) by the type of structure on which the forces act and (b) by the type of wave action against the structure. The types of wave that can act on the structure are nonbreaking, breaking and broken waves. Figure 3.2.10 illustrates the subdivision of wave force problems by structure type and the type of wave action and indicates nine types of force determination problems encountered in design.

At the experiment which was conducted in flume, the waves generated by wave generator were generally non-breaking. So, the total study was arranged for non-breaking wave forces. Forces due to non-breaking waves are primarily hydrostatic which later come under dynamic effects of turbulent water. Dynamic forces are much greater than the hydrostatic forces.

Sainflou (1928) proposed a method for determining the pressure due to nonbreaking waves. The advantage of his method has been ease of application, since the resulting pressure distribution may be reasonably approximated by a straight line. Experimental observations by Rudgren (1958) have indicated Sainflou's method overestimates the nonbreaking wave force for steep waves. The higher order theory

by Miche (1944), as modified by Rudgren (1958), to consider the wave reflection coefficient of the structure, appears to best fit experimentally measured forces on vertical walls for steep waves, while Sainflou's theory gives better results for long waves of low steepness (SPM-II).

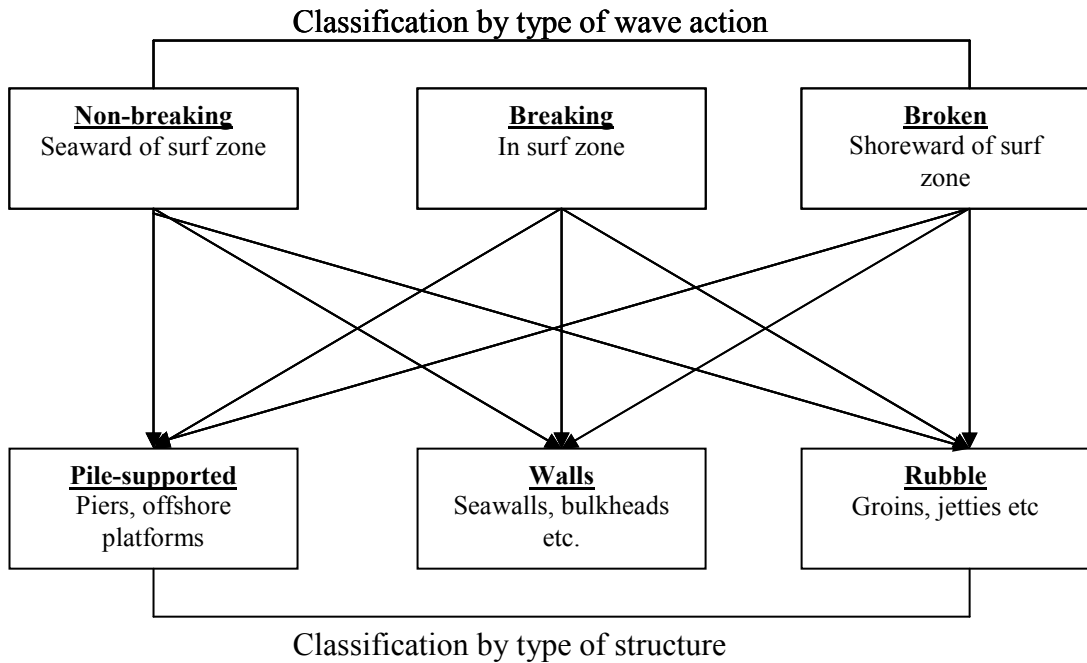


Figure 3.2.10: Classification of wave force problems by type of wave action and structure type (SPM-II).

Wave conditions at an embankment on the seaward side are affected by incident and reflected wave. Wave height at the embankment is given by $H_w = H_i + H_r = (1 + \chi)H_i$, where H_i = incident wave height and χ is the reflection coefficient. If reflection is complete and reflected wave has the same amplitude as the incident wave then $\chi = 1$. A lower value of χ may be assumed when the embankment is built on a rubble base but value of χ less than 0.9 should not be used for design purposes.

Pressure distribution without wave loading and also for the crest and trough of clapoits at a vertical wall are shown in Figure 3.2.11. When the wave crest is at the wall, pressure increases and from zero at the free surface to $(\gamma h + p_1)$ at the bottom,

when the trough is at the wall, pressure increases from zero at the water surface to $(\gamma h - p_1)$ at the bottom. Where p_1 is approximated as, $p_1 = \left(\frac{1+\lambda}{2}\right) \frac{\gamma H_i}{\cosh(2\pi h/L)}$.

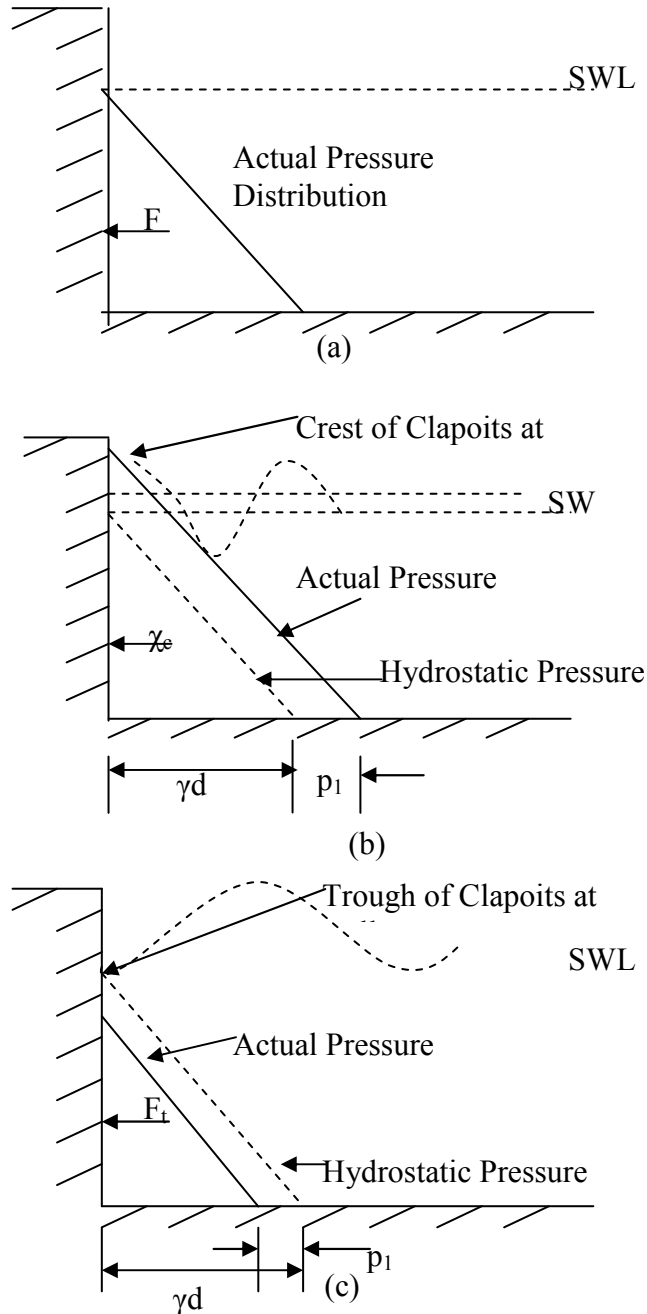


Figure 3.2.11: (a) Pressure diagram without wave loading
 (b) Pressure diagram with wave loading (water level at crest).
 (c) Pressure diagram with wave loading (water level at trough) (SPM, 1984)

Figure D1 and Figure D2 (Shown in Appendix D) permit a more accurate determination of forces from a nonbreaking wave at a wall. Figure D1 is for a reflection coefficient $\chi = 1$ and Figure D2 identical dimensionless parameter for $\chi = 0.9$. The forces found by using these curves do not include the force due to the hydrostatic pressure at still water level. The horizontal wave forces may be evaluated using the figures with the computed values of H_i / gT^2 , the value of F / wd^2 can be determined from curves of constant H_i / d . The upper family of curves (above $F / wd^2 = 0$) will give the dimensionless force when the wave crest is at the wall: F_c / wd^2 ; the lower family of curves (below $F / wd^2 = 0$) will give the dimensionless force when the trough is at the wall: F_t / wd^2 .

The dynamic load can be measured by,

$$F_d = F_c - F_t \text{ ----- (3.2.1)}$$

Values found for F_c and F_t do not include the force due to the hydrostatic pressure distribution below the still-water level. The design problems require calculation of the total force including a hydrostatic contribution. In these cases the hydrostatic force is found by the following equation:

$$F_s = \frac{wd^2}{2} \text{ ----- (3.2.2)}$$

Where $F_s = \text{Staticload}$, $w = \text{unit weight of water} = 10 \text{ kN/m}^3$ for sea water and $d = \text{water depth}$.

The total force, F , when strike the vertical face of a structure at an oblique angle, the dynamic component of the pressure or force will be less than for the waves that strike perpendicular to the structure face. The Force may reduce by the equation,

$$F_d' = F_d \sin^2 \alpha \text{ ----- (3.2.3)}$$

where, α is the angle between the axis of the structure and the direction of wave advance, F_d' is the reduced dynamic component of force and F_d is the dynamic load that would occur if the wave hit perpendicular to the structure.

Formulas previously presented for wave forces may be used for structures with nearly vertical faces. If the face is sloped backward, the horizontal component of the dynamic force due to waves should be reduced to

$$F_d'' = F_d' \sin^2 \theta \text{ ----- (3.2.4)}$$

where θ is defined in the figure 3.2.12. The vertical component of the dynamic force may be neglected in stability computations.

So, the total load strike on the sloping face of the embankment at a wave period duration can be measured by, the following equation,

$$F = F_d'' + F_s \text{ ----- (3.2.5)}$$

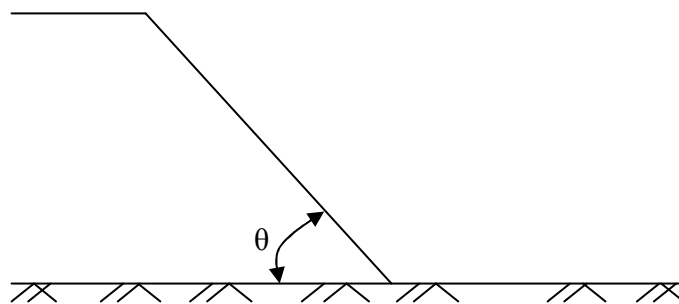


Figure 3.2.12: Sloping wall

3.2.10 Break Water

Breakwater is an offshore structure to protect a harbor from wave energy or deflect currents. When it also serves as a pier, it is called a quay, when covered by a

roadway it is called a mole. In the United States a breakwater commonly consists of a long mound of stone rubble and of cheaper materials like rubber tires and oil drums. The flow of waves up its slope, and the formation of swirls by its rough surface dissipate wave energy. A pneumatic breakwater consists of perforated pipes discharging air bubbles; another type has underwater pipes that direct streams of water against approaching waves to cause them to break. Breakwaters are also used to promote sedimentation, which depending on the breakwater's alignment, will infill to produce a stable beach. The Chesapeake breakwater was the first built in the United States.

There are twenty different breakwater types (Massie, 1976) are listed in alphabetical order-

- a) Air Bubble Curtains.
- b) Beaches.
- c) Composite- Rubble Mound Front.
- d) Composite- Vertical Monolithic Top.
- e) Floating Flexible.
- f) Floating Rigid.
- g) Monolithic "Floating".
- h) Monolithic- Porous Front.
- i) Monolithic- Sloping Front.
- j) Monolithic Sunken Caisson.
- k) Monolithic Vertical- Constructed In Place.
- l) Oil Slick.
- m) Pile Row.
- n) Resonant Breakwater.
- o) Rubble Mound-Pell-Mell Artificial Armor Units.
- p) Rubble Mound- Placed Units.
- q) Rubble Mound- Stone.
- r) Rubble Mound- Stone with Asphalt Spotting.
- s) Submerged- Vertical or Rubble Mound.
- t) Vertical Sheet Pile Cells.

No one type of breakwater is always best. Further, the choice of a breakwater for a given situation is dependent upon so many factors that are nearly impossible to give specific rules of thumb for determining the “best” type. A few general rules can be given, however:

- Rubble mound structures are the most durable and as such are best suited to extremely heavy wave attack.
- Monolithic structures use less space and material; this is especially true in deeper water.
- Special types of breakwaters are usually best suited to specific special applications.

In this experiment a Monolithic Sunken Caisson type breakwater has been used according to the flume size.

3.2.11 Monolithic Sunken Caisson Breakwater

Monolithic Sunken Caisson Breakwater is a temporary structure floated into place and sunk and ballasted to form an initial breakwater. It is often used to cut off currents so that it can then be buried in a natural beach or other more permanent breakwater.

It can be placed on the site very quickly; can provide quay facilities on lee side, occupies little space, uses little material, provides promenade, provides work road for later construction phases. But its size is limited by towing limitations; easily damaged- often by only a moderate storm, foundation difficulties on fine sand bed, requires smooth bed e.g. Normandy beach head- World War II (Massie, 1976).



(a)



(b)



(c)



(d)



(e)



(f)

Figure 3.2.13: Various types of breakwater (a) A bubble type breakwater, (b) Composite rubble Mound Front breakwater, (c) Floating flexible breakwater, (d) Floating Rigid breakwater, (e) Monolithic floating, (f) Composite vertical monolithic top breakwater (Source: web site).

3.3 Basis for laboratory Experiment

Wave parameters such as wave period, wave length and run-up height have significant effect on the wave loads which are the prime importance for coastal embankment design. Again, breakwater at the front of an embankment will dissipate the wave energy by reducing wave velocity. This condition will also change the wave parameters. These changes in parameters and velocities shall finally minimize the wave loads impact on the embankment face. An experiment was conducted to calculate wave parameters and their behavioral change on loads. Embankment slope plays an important role to those parameters and loads, so the experiment was run through two different slope of embankment are, 1:2 and 1:3. Wave loads also changes with water depth. This is why, two different water depths (30 cm and 40 cm) were used for various conditions in the experiment. Next the question comes that, in what position of breakwater settings will minimize the more energy. To compare the situation two positions were choose in the experiment. One is submerged condition and the other is floating condition. Thus, all the above performances have been done by two different slopes against the wave action by changing,

- Bed slope
- Wave Period and
- Water depth

3.4 Methodology

The experimental runs had been conducted in the large tilting flume under the Hydraulic and River Engineering Laboratory of the Department of Water Resources Engineering, BUET. A brief description of experimental setup and its various components and modification of existing physical model facilities is described below.

3.4.1 Physical model components

For collection of the necessary data the following main components were divided into two parts:

- a) The permanent part
- b) The temporary part

The permanent part of the experimental setup is permanently set in the laboratory which consist of,

- i) Laboratory flume
- ii) Wave generator
- iii) Water reservoir.



Photograph 3.4.1: Laboratory flume

The temporary part consists of the following components:

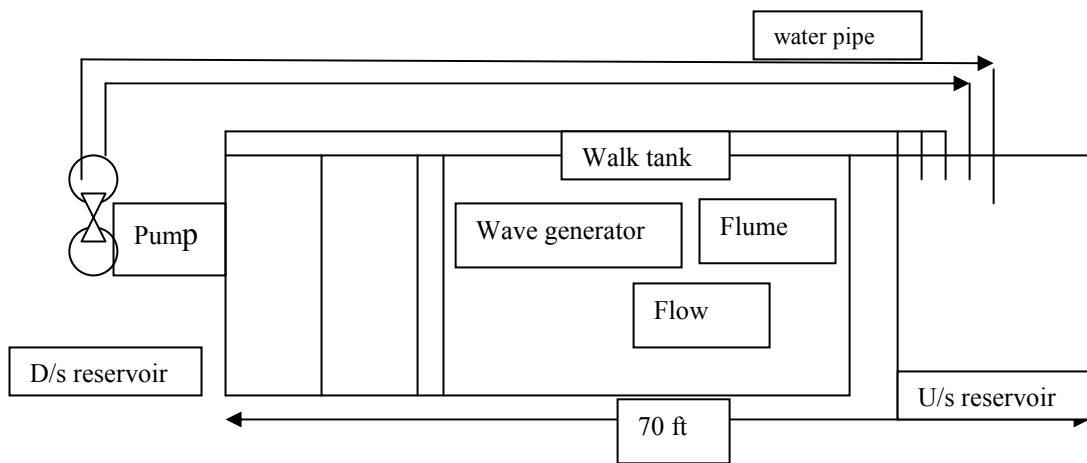
- i) Artificial embankment (bank slope)
- ii) Break water and
- iii) Pipes for water supply.

Other necessary accessories used were, wire screen, concrete blocks etc. Overviews of physical model components of physical model facility are described in brief.

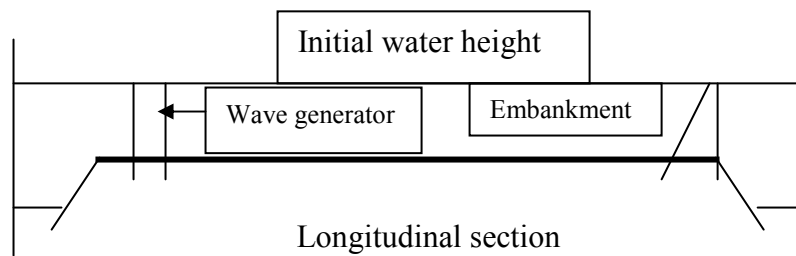


Photograph 3.4.2: Wave generator

3.4.2 Laboratory flume



Plan view



Longitudinal section

Figure 3.4.1: Plan and longitudinal section of the laboratory flume.

The flume used for the study is 21.34 m (70 ft.) long, 0.76 m (2.5 ft.) width and 0.76 m (2.5 ft.) deep. The side walls are vertical and made of glasses placed in steel frames and bed is painted water resistance colour. The flume is generally used for flowing water from the upstream to the downstream reservoir. A wave generator is located at the downstream end just ahead of the tail gate. It consists of a reservoir and stilling chamber. The stilling chamber is located behind the wave generator. This chamber is approximately 3.0 m (9.8 ft.) length of the flume. For the present study water is stored up to two certain levels by constructing two bank slopes at the upstream end and raising tailgate at the downstream end of the flume. Water is supplied in the flume through an external pipe. Flume was set and ensured in such a condition that there was no leakage.



Photograph 3.4.3: Laboratory flume with bank slope

3.4.3 Wave generator

Wave generator consists of a motor and paddle with two vertical limbs as shown in photograph 3.4.4.

The wave paddle is kept hanging from the top through hinge joints. Displacement of wave paddle is controlled by a crank which is connected to the wave paddle by a

connecting rod. Radius of rotation of the crank can be controlled by screw adjustment.



Photograph 3.4.4: Wave generator labeling with main parts

The wave paddle is allowed to move horizontally to a distance equal to the radius of rotation of the rotating crank. Therefore, the displacement of the wave paddle can be adjusted by changing the radius of rotation of the crank. Frequency of rotation can also be controlled by a motor. Wave period of generated waves can be altered by rotating its rotational speed (Photograph 3.4.5) and wave height can be altered by changing the arm of paddle. Rotational speed can be altered from 20 rpm to 120 rpm and paddle arm can be altered from 25 mm to 320 mm. Horizontal movement of wave paddle in the flume containing water generates waves of different amplitude depending on the depth of water stored.

During movement of paddle two displacements were observed. One is rotational displacement and another is vertical displacement. By adjusting vertical limbs these two types of displacements were adjusted.



Photograph 3.4.5: RPM adjustment

3.4.4 Reservoir

It is a steel structure. Water is stored in the reservoir. There is a facility to control water supply.

3.4.5 Wire Screens to reduce wave reflections

Several screens were set to reduce wave reflections. Screens were made of coarse wire mesh. They were placed in front of wave generator as shown in photograph 3.4.6. Numbers of screens and spacing have been determined by trial and error method. Screens were kept at approximately 5 cm. apart from each other. In this study finally 20 screens have been used to reduce reflections. When the crests of waves generated were seen in a straight line from side view reflection of the wave was considered to be reduced at the minimum.



Photograph 3.4.6: Wire screens in the flume

3.4.6 Bank slope preparation

Steel frame used as wave damper has been taken as a base on which the experimental bank slope was set. First the damper was turned over and flat surface was used as a base of slope. Then an acrylic sheet of 1.5 cm thickness was set over it. Then cotton net was used (Photograph 3.4.7) as representative of geotextiles and was glued over it to make sufficient friction between blocks and sheet. Sheets were screwed so that it is easy to alter slope. The wooden frame was kept fixed so that it could not be moved.

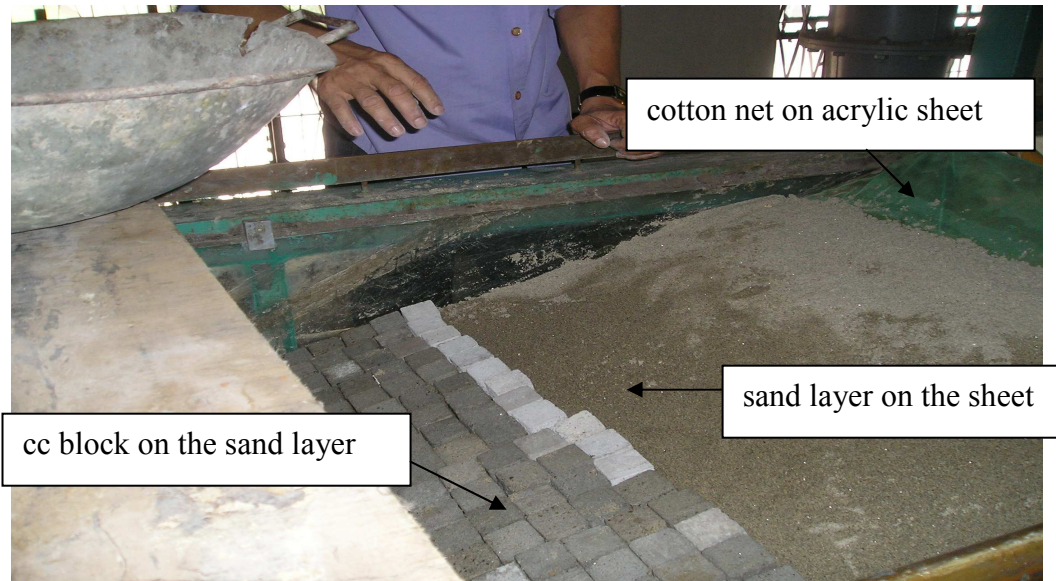
Sand layer is set over the net (Photograph 3.4.8 and Photograph 3.4.9) then blocks have been placed on the bank slope with close block system for wave run up observations as shown in Photograph 3.4.10. To check the stability of blocks for particular set up free block system has been used. In this system blocks were made frictionless at the sides by gluing a separator (a piece of wire) on side surface. The system was considered to represent free blocks system of the prototype situation. In the free block system only line contracts between blocks were achieved.



Photograph 3.4.7: Preparing a bank slope



Photograph 3.4.8: Sand layer over the acrylic plate



Phototograph 3.4.9: Detail of a bank slope



Phototograph 3.4.10: A complete bank slope

3.4.7 Velocity meter

In the laboratory actual velocity of wave was measured by the equipment named Electro magnetic liquid velocity meter (P. – e.m.s). The Programmable E.M.S. can be generally applied for flow monitoring purpose in open channels and fully or partially filled pipes. In general, the instrument consists of the following basic parts:

- a) the probe, with built in pre-amplifier
- b) the Control Unit in the U.C.C. (Universal Carrying Case) with display screen
- c) connection cables.

The Programmable E.M.S. is in fact the inside-out version of the well known pipe flow meter employing Faraday's Induction Law for measurement of the velocity (V) of a conductive liquid moving through a magnetic field. The magnetic field is induced by a pulsed current through a small coil inside the body of the sensor. Two pairs of diametrically opposed platinum electrodes (e) sense the Faraday induced voltages produced by the flow past the sensor. It is capable of measuring velocity components in a 2D plane. The measured flow velocities were transported for display from the probe to the control unit. It is important that the generated electromagnetic field should not be disturbed.

Dimensions of the probe are shown in Fig. 3.4.2. For accurate measurement, the probe is to be cleaned regularly and immersed in water for a couple hours prior to taking any measurement.

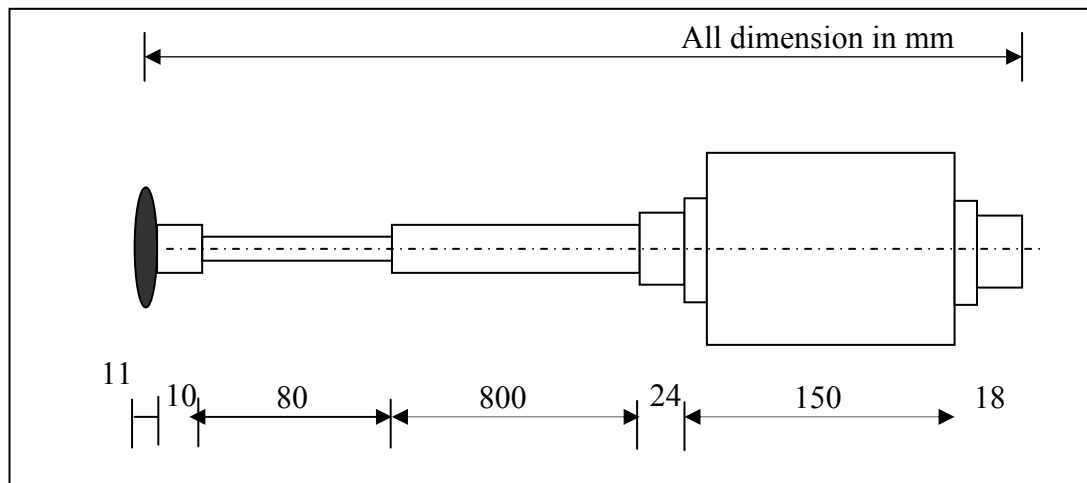


Figure 3.4.2: E-30 Probe.

The sensor has been designed in such a way that these voltages are proportional to the sine (V_y) and cosine (V_x) of the magnitude of the liquid-velocity (V_e) parallel to the plane of the electrodes (Figure 3.4.3).

It shows the horizontal and vertical velocities (V_x and V_y) in the component form of X and Y. X axis is parallel to the flow direction and Y axis is perpendicular with X axis. The actual velocity can be calculated from the measured velocities V_x and V_y by:

$$V_e = \sqrt{(V_x^2 + V_y^2)}$$

And the angle α by:

$$\text{Arctan } \alpha = (V_y \div V_x)$$

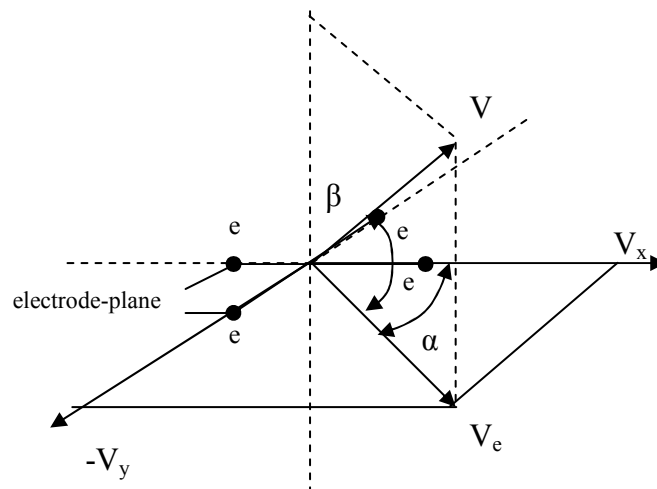


Figure 3.4.3: Diagram, showing voltage components versus velocity vectors

Source: (Manual PEMS, August 1993)

For flow passing this reference plane at an angle β the magnitude of V_e shall equal $V \cos \beta$. In order to meet the different tilt response requirements for various applications, sensors of ellipsoidal and spherical geometry were designed. By means of advanced electronic the low level output signals of the probe are converted to high level output signals from which the magnitude of the velocity and its direction (referred to a reference) can be derived by application of common trigonometry.

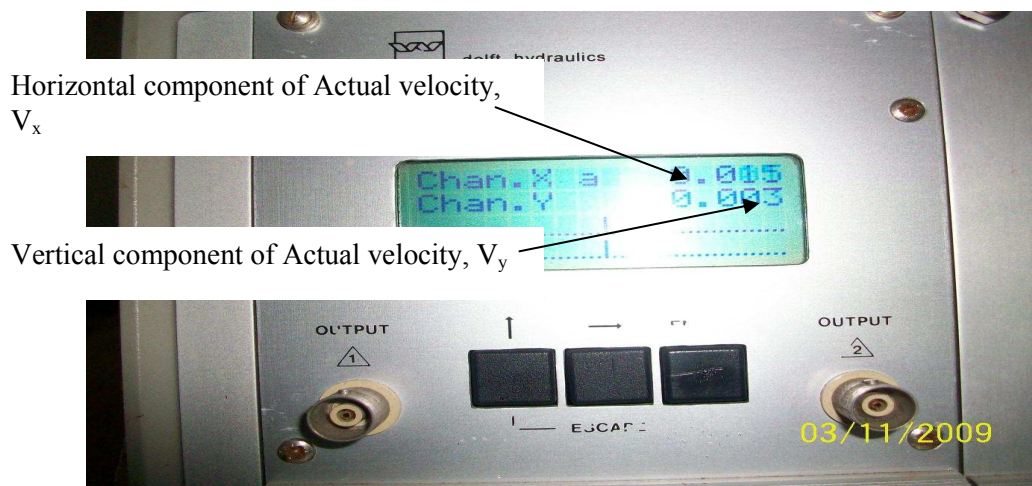
For the last calculation a sign correction has to be applied which are shown in the Table 3.4.1.

Table 3.4.1: Sign correction for velocity meter (Manual PEMS, August 1993)

V-out X (m/s)	V-out Y (m/s)	α
+	+	0^0-90^0
-	+	90^0-180^0
-	-	180^0-270^0
+	-	270^0-360^0



(a)



(b)

Photograph 3.4.11 Photographical representations for Programmable electromagnetic liquid velocity meter (P.-e.m.s.); (a) various parts of P. EMS; (b) Actual velocity reading display.

3.4.8 Breakwater used in the experiment

Breakwater used for the experiment was rectangular and 75 cm x 35 cm x 16 cm in dimension (Photograph 3.4.12). It had three equal hollow parts to resist the vertical and horizontal pressure of water in the flume. It is made of plastic and has been used both as floating and submerged condition. It was about 10 pounds in weight.



Photograph 3.4.12: Rectangular breakwater

It was placed at the toe of the bank slope. The breakwater was placed as fully submerged condition and as floating condition at a fixed place. At submersible condition it occupied 23 cm with the wooden platform. The distance of its placement was taken for the study was 100 cm.

3.4.9 Pipes

Two pipes were used for water supplying (50 cm) in the flume from outside. Reservoir supply water was not in use. Because it could disturb the complete embankment set up by supplying heavy water at a time from the reservoir (because regulator was not so much smooth). That's why two flexible pipes were used for instant water supply from regular water supply lines.



(a) Submerged Breakwater in still water



(b) Floating breakwater

Photograph 3.4.13: Two types of breakwater used in the experiment.

3.5 Measurement Techniques

In this study three wave period (1 second, 2 second and 2.5 second) were fixed for two different water depths (40 cm and 30 cm). Then ω , dimensionless parameter $(\frac{f+e}{f})$ and rpm were calculated for experimental set-up.

In this way different setup for different water depth (40 cm and 30 cm) for different wave period (1 sec, 2 sec and 2.5 sec) has been obtained which are given below as tabulated form. These wave period values and wave length values are named here theoretical values.

Table 3.5.1: Wave generator setup for experimental runs

h (cm)	T (sec)	$\omega = \frac{2\pi}{T}$	$\frac{\omega^2 h}{g}$	From figure A.2		$\frac{f+e}{f}$	From Laboratory			rpm
				f	e		f	e+f	$\frac{f+e}{f}$	
40	1	6.28	1.61	0.19	0.74	4.8	1.4	6.7	4.7	8
	2	3.14	0.40	0.63	0.42	1.67	3.9	6.7	1.72	9
	2.5	2.51	0.26	0.5	0.59	2.18	3.6	7.8	2.17	15
30	1	6.28	1.21	0.25	0.72	3.88	1.3	5	3.8	12
	2	3.14	0.30	0.46	0.6	2.30	3.1	6.4	2.06	16
	2.5	2.51	0.19	0.51	0.58	6.8	0.8	5.3	6.63	15

Then experiment was done and following experimental values were measured:

- i) Wave period (T sec)
- ii) Wave length (L cm)
- iii) Run-up height (R cm)
- iv) Wave height (H cm)
- v) Actual velocity component (V_x and V_y in m/sec)

These values were measured in three different statuses,

- using plane beach and CC block (expressed in this thesis paper as CC block condition)
- using plane beach CC block and submerged breakwater (expressed as submerged breakwater condition) and
- using plane beach CC block and floating breakwater (expressed as floating breakwater condition).

All the study was done for two different bank slope- 1:2 and 1:3.

3.5.1 Run-up height measurement

Run-up height (R) is the measurement of the maximum vertical height on a slope above the still water level during a wave period. It is done by visual observation and measured by marking points on the slope made of CC blocks. The uppermost point was marked finally and vertical reading of that point with point gauge gave wave run-up for that particular setup. Several data were taken. Average of these data represents the run-up height (R).

In most cases, where the toe of the embankment lies, which is where the slope changes into the foreshore. A foreshore is a part in front of the embankment and attached to the structure, and can be horizontal or up to a maximum slope of 1:10. It is actually possible that this foreshore has a changing bottom. In such a case the position of the toe is not constant. During design of an embankment, we have to estimate where the foreshore lies or will lie under the design conditions and this also determines the position of the toe of the embankment. This same situation applies for a safety assessment of an embankment. For measuring wave run-up, the foreshore profile available at that moment must be used for verification, and the wave height at the position of the toe of the embankment (Van der meer, 2002). This is why, all the experimental measurements were taken at 3R (3 x Run-up height of that particular experimental set-up), 6R (6 x Run-up height of that particular experimental set-up) and 9R (9 x Run-up height of that particular experimental set-up) distance from the toe of that particular slope.

3.5.2 Wave period measurement

Wave period is the time, usually measured in seconds, that it takes for a complete wave cycle (crest to crest or trough to trough) to pass a given fixed point. First a point on the flume side glass was marked; number of wave crests passing the point was counted for a minutes. Thus the wave period was measured by dividing the number with 60. This is experimental wave periods (T) which are less than the pre

calculated wave period. Wave periods were measured at 3R, 6R and 9R position from toe stated in art 3.5.1.

3.5.3 Wave length measurement

Wave length was measured by marking two adjacent wave peaks on the glass and then taking its length by scale or measuring tape. Five measures were taken by this way and then the average value of these five was taken as wave length (L). Wave lengths were measured at 3R, 6R and 9R position from toe where wave periods were measured.

3.5.4 Wave height measurement

Wave height measurement was a significant part of the study. Wave height measurement was conducted by scale. Taking still water level as reference level, crest of the wave was measured and the trough of wave by another scale. Several values were taken and then the average heights (H) were taken for the study. Wave heights were measured at 3R, 6R and 9R position from toe where wave periods were measured.

3.5.5 Velocity component measurement

Velocities are measured with a programmable electromagnetic velocity meter (P-EMS). Total velocity measurement procedure required two to three hours. Each velocity reading has been taken as actual velocity. Once wave period was measured; velocity reading was counted each wave period interval or its n times interval. It gives the water partials actual velocity as it comes every wave period interval. P-EMS probe is placed at a constant (wave height + 3 cm) cm below the static water level. Areas selected for velocity measurement are 3, 6, 9 and 18 times of wave run-up height. 20 (twenty) readings of actual velocity component (V_x and V_y) were taken. When breakwater is installed, one reading at the front of the breakwater (18 times of wave run-up) was taken.

3.6 Test procedure of experiment

A specific sequence of test procedure has been followed for every experimental run. These includes flume cleaning, wave generator set-up for maintaining a wave period, slope preparation, breakwater installation, water depth maintain, different data collection during and after experimental run and preparation for the next run. Methodology has been discussed briefly here:

Step-1

Straight flume was cleaned to make free from debris, moss and floating dirt before starting each experimental run. Cleaning has been done with bleaching powder to prevent moss and fungi infestation.

Step-2

Selecting a slope using one type of material, an embankment was made at the U/s reservoir end of flume (Figure 3.4.1). Slope of the embankment was marked along the flume wall.

Step-3

Before operating wave generator, some adjustment was done between rotational and transitional movement that produced the required wave period and wave height. Appendix- A gives rotational, e parameter and f parameter to develop non-breaking harmonic waves. The stepwise procedure to generate regular waves without breaking at the paddle of wave generator has been presented in Appendix- A. This process was repeated before every wave period settlement when the flume is empty.

Step-4

Water was supplied to maintain 40 cm and 30 cm water depth by the pipes to the flume according to the run condition.

Step-5

For a particular set of slope, material and wave height, wave was generated by using wave generator at a particular frequency.

Step-6

The wave generator was continued to develop non-breaking waves for 1 hour and 30 minutes.

Step-7

Wave height, run-up height, wave period and wave length were measured. These are measured data based on which the calculation are presented in Chapter 4.

Step-8

During this period velocity components were taken from velocity meter for different intervals of wave period and noted on a data sheet.

Step-9

All the readings were taken at 3 different positions related to the wave run-up height (R). Such as at the distance of 3R, 6R and 9R from the toe for every particular condition.

Step-10

During the test runs for submerged and floating breakwaters an additional step has been added for the installation of it. For each case breakwater is set 100 cm. apart from the toe of the bank slope. An additional velocity reading was taken at 15R or 18R distance from the toe.

3.7 Test Scenarios

Thirty six runs were conducted for the present study. Test program contents information with respect to run no, bank slope (1:2 and 1:3), water depth (40 cm and 30 cm), wave period, run-up height, effect of breakwater (submersed or floating) and velocity in which experiment was done. Same type of blocks (1 inch x 1 inch x 1

inch) was used in these run. First wave period and water depths were fixed. Then wave generator was set according to measurement techniques stated earlier. Water was poured and waves were applied in water. A summary of experimental runs conducted in present study is summarized in Table 3.7.1 and 3.7.2 as test scenarios.

Table 3.7.1: Test scenarios for 1:2 bank slope

Slope	Water depth (cm)	Wave period (sec)	Run no.	Material used for slope protection
1:2	40	1	1	C.C block
			2	C.C Block and Submerged break water
			3	C.C Block and Floating break water
		2	4	C.C block
			5	C.C Block and Submerged break water
			6	C.C Block and Floating break water
		2.5	7	C.C block
			8	C.C Block and Submerged break water
			9	C.C Block and Floating break water
	30	1	10	C.C block
			11	C.C Block and Submerged break water
			12	C.C Block and Floating break water
		2	13	C.C block
			14	C.C Block and Submerged break water
			15	C.C Block and Floating break water
		2.5	16	C.C block
			17	C.C Block and Submerged break water
			18	C.C Block and Floating break water

Table 3.7.2: Test scenarios for 1:3 bank slope

Slope	Water depth (cm)	Wave period (sec)	Run no.	Material used for slope protection
1:3	40	1	19	C.C block
			20	C.C Block and Submerged break water
			21	C.C Block and Floating break water
		2	22	C.C block
			23	C.C Block and Submerged break water
			24	C.C Block and Floating break water
		2.5	25	C.C block
			26	C.C Block and Submerged break water
			27	C.C Block and Floating break water
	30	1	28	C.C block
			29	C.C Block and Submerged break water
			30	C.C Block and Floating break water
		2	31	C.C block
			32	C.C Block and Submerged break water
			33	C.C Block and Floating break water
		2.5	34	C.C block
			35	C.C Block and Submerged break water
			36	C.C Block and Floating break water

3.8 Summary

To design a coastal structure properly, one must consider wave–structure interactions. Because of the appearance of a coastal structure, wave motions are altered. Moreover, the turbulence intensity might be increased in the vicinity of the structure due to flow separation (Losada et al., 1995). The enhanced turbulence could have significant impacts on wave force, on the scouring process at the toe of a structure and on other mixing processes. Most of existing experimental studies of

wave–structure interaction have been mainly focused on the estimations of wave reflection and transmission. While this information is useful in characterizing the effectiveness of the structure, the detailed velocity measurements are essential for the understanding of the physical process involved. Furthermore, the detailed velocity measurements are essential for validating any mathematical/numerical models that are to be used for designing a coastal structure.

CHAPTER 4

RESULTS AND DISCUSSION

4.1 General

In coastal water, waves and structural interaction create a complex loading conditions and damage the structure. Sufficient knowledge on wave pressure on the seaside face is mandatory to design a coastal protection structure. The mild slope sandy beach is more erodible by wave forces and also by wind action. In such sandy beaches, morphological behaviour is an important issue for construction of coastal structures. So bed material of this kind of beach is also a considerable matter for coastal structure design.

Researches based on dynamic load impact on coastal embankment are limited in Bangladesh because researches were mostly done to study protection work and very small works were done for load on vertical seawall. Practically, studies of dynamic load on coastal structures in coastal region of Bangladesh are very few in numbers.

In this present study, an experimental investigation has been carried out with various wave parameters for different loading conditions by using CC blocks, submergible breakwater and floating breakwater and actual velocity were measured. For this purpose, 36 nos. of experimental runs have been conducted with variable depth, bank slope and wave period.

4.2 Comparisons between Theoretical and Experimental data

The theoretical part of the study was prepared to analyze loading conditions for three different wave periods like 1 sec, 2 sec and 2.5 sec. Practically in the flume this values would not be completely obtained due to limitations such as wave reflection, wall friction etc. Thus, experimental values of wave length and wave height were changed due to changing wave periods. Observed velocity were also changes because of different loading conditions.

Wave length changes and measured values were compared with theoretical values. Values of wave length in different loading conditions for different slopes and water depths are shown in the Figure 4.2.1 to Figure 4.2.4. The figures were drawn on the basis of experimental setup discussed in the article 3.7. It can be seen from the figures that the measured values are smaller than the theoretically computed values. Measured values were changed nearly in uniform shape. Coastal engineering considers problems near the shoreline normally in water depths of less than 20 m. Structure designs usually require knowledge of the wave field over an area of 1-10 km² in which the depth may vary significantly. Again, wave breaking and transformation of wave height through the surf zone. The transformation of wave height through the surf zone impacts wave setup, run-up, nearshore currents and sediment transport (CEM, 2003). This is why, to set the breakwater at surf zone it was set 100 cm apart from the toe of the embankment in the experimental setup. Further study is needed to verify the appropriate location for breakwater setup. From the observation which came out was that, wave length had been reduced due to breakwater effect and at floating breakwater effect this reduction rate were more than that of CC blocks.

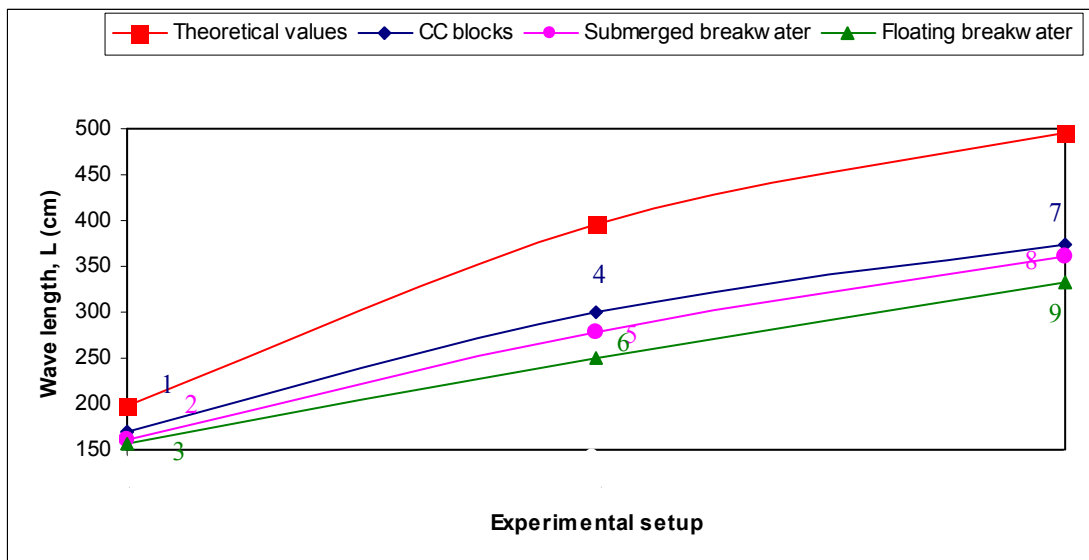


Figure 4.2.1: Comparison of wave length for different experimental setup (for bed slope = 1:2 and water depth = 40 cm).

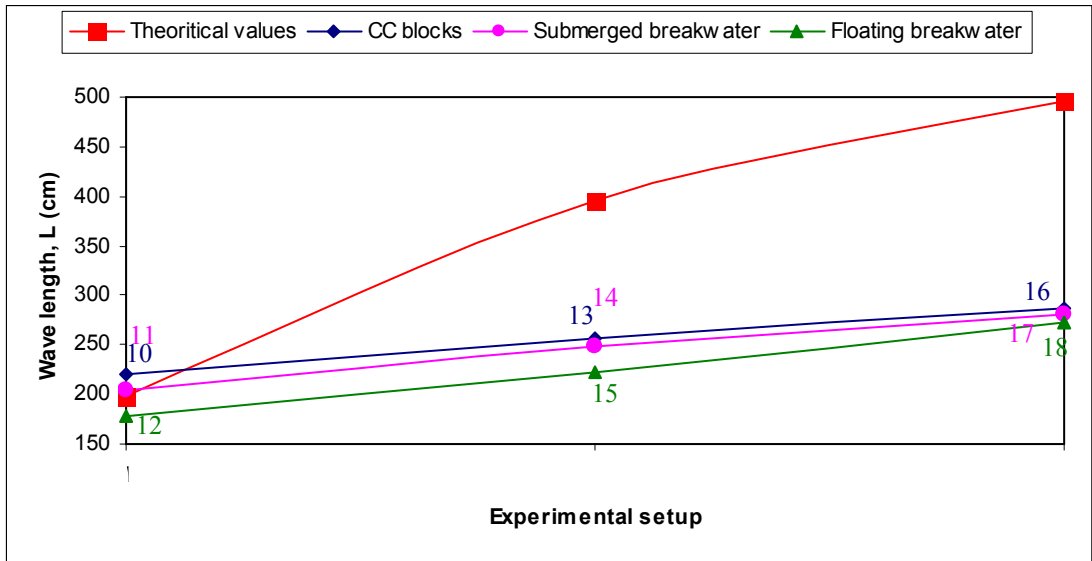


Figure 4.2.2: Comparison of wave length for different experimental setup (for bed slope = 1:2 and water depth = 30 cm).

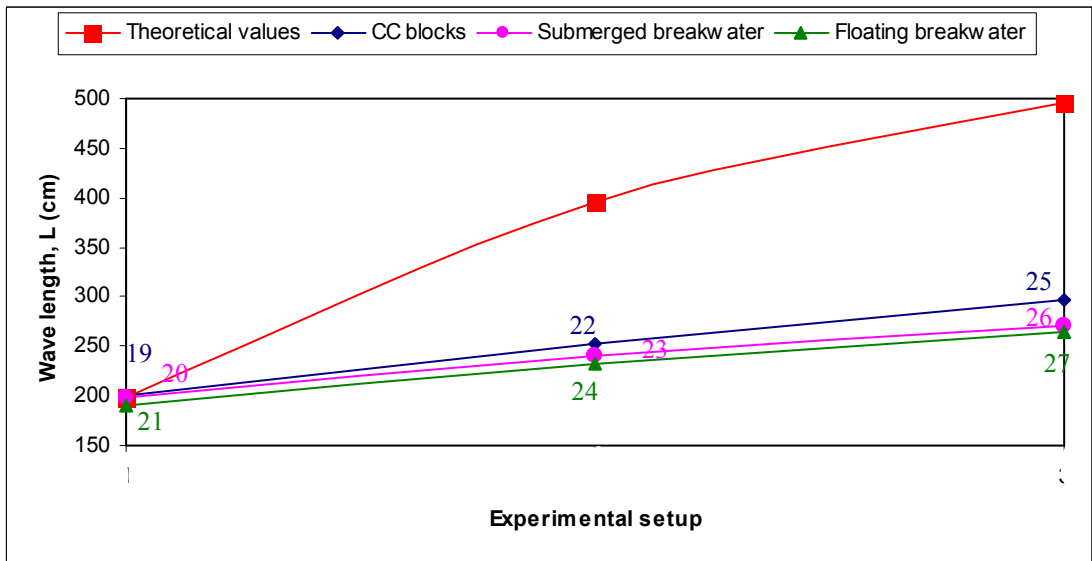


Figure 4.2.3: Comparison of wave length for different experimental setup (for bed slope = 1:3 and water depth = 40 cm).

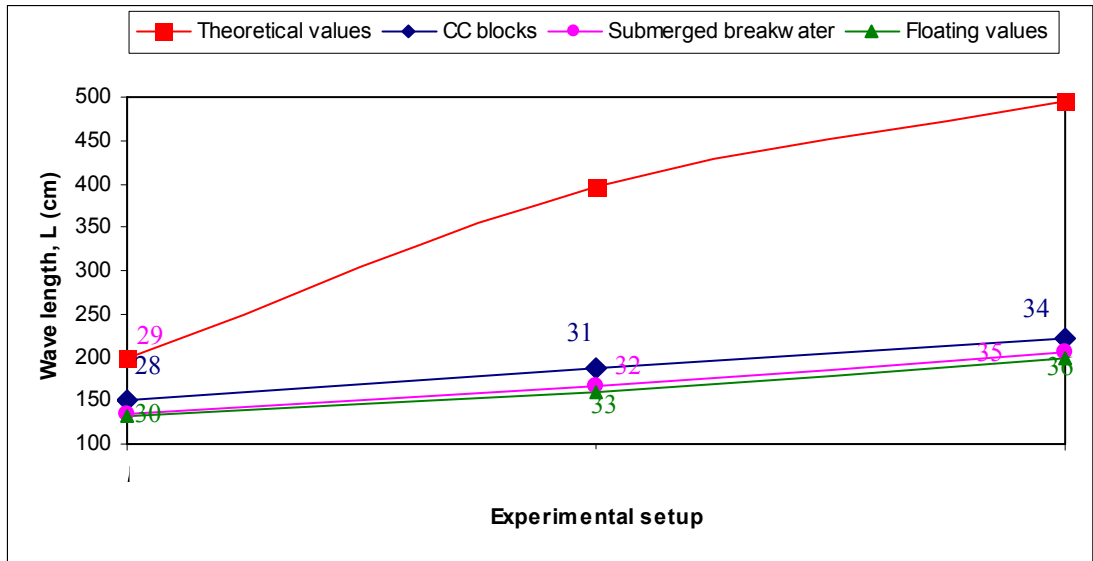


Figure 4.2.4: Comparison of wave length for different experimental setup (for bed slope = 1:3 and water depth = 30 cm).

Wave periods were also seen to be decreasing for submerged breakwater condition than that of CC block condition. Also wave periods for floating breakwater condition were less than the submerged breakwater condition. All the values were less from the theoretical values (Figure 4.2.5 to Figure 4.2.6). These figures also show that, wave periods are lower in magnitude for lower water depth. When water depth was 40 cm, the values are higher and for 30 cm water depth the values are lower. So, water depth (d) has an effect to these wave parameters.

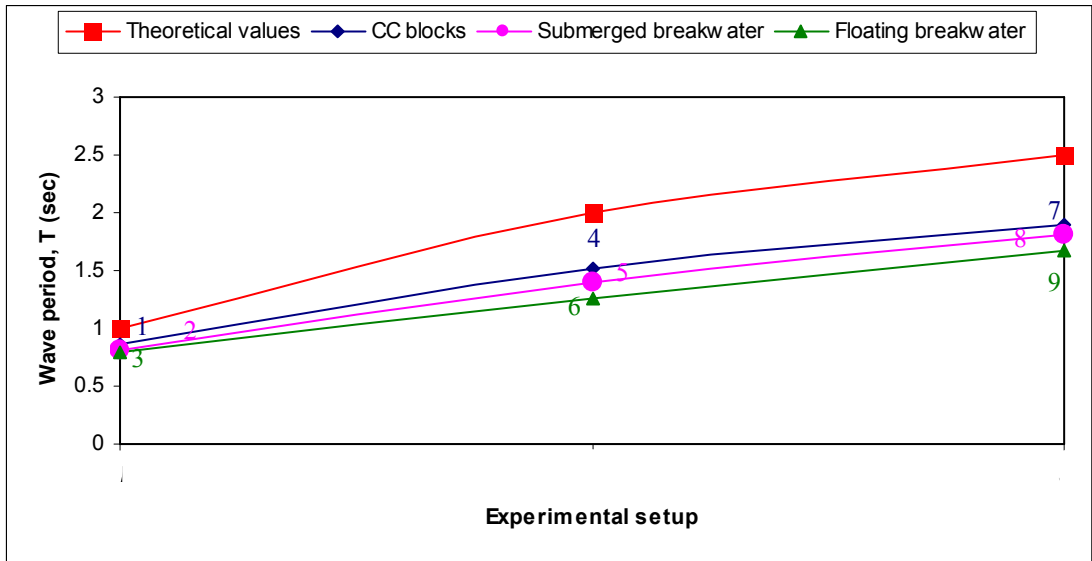


Figure 4.2.5: Comparison of wave length for different experimental setup (bed slope = 1:2 and water depth = 40 cm).

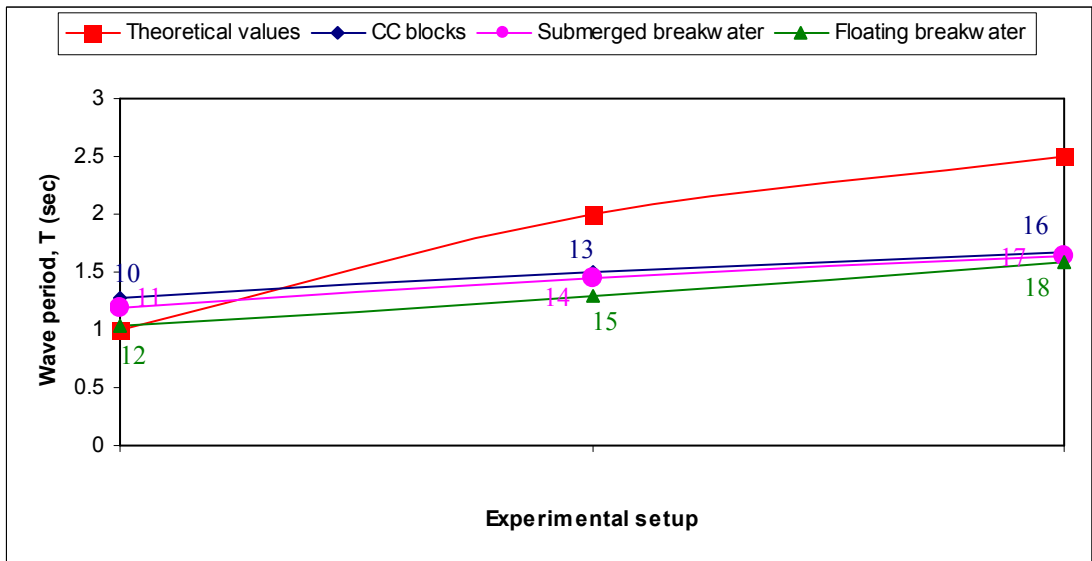


Figure 4.2.6: Comparison of wave length for different experimental setup (bed slope = 1:2 and water depth = 30 cm).

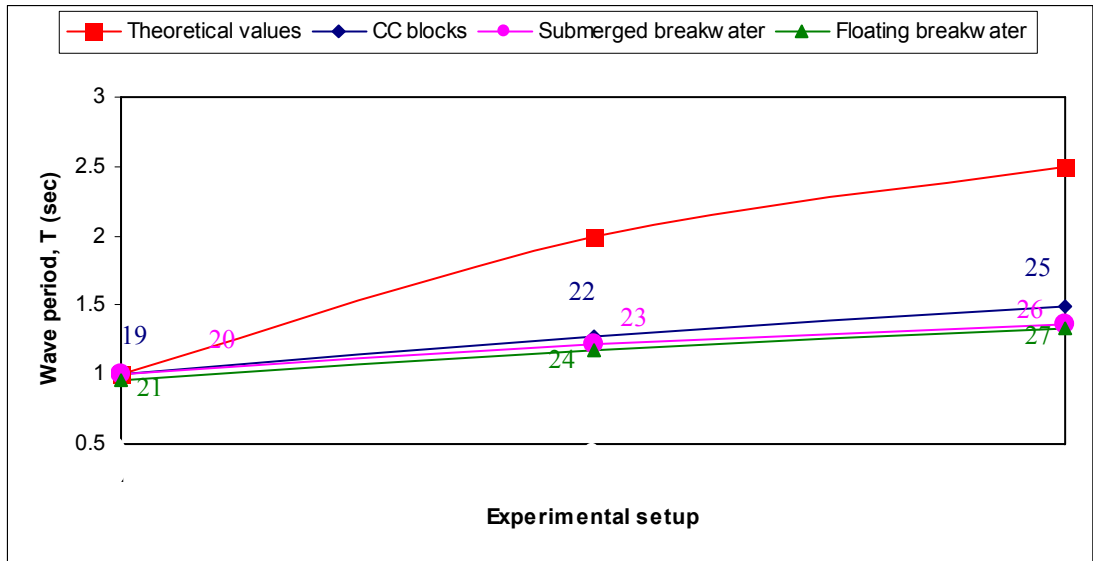


Figure 4.2.7: Comparison of wave length for different experimental setup (bed slope = 1:3 and water depth = 40 cm).

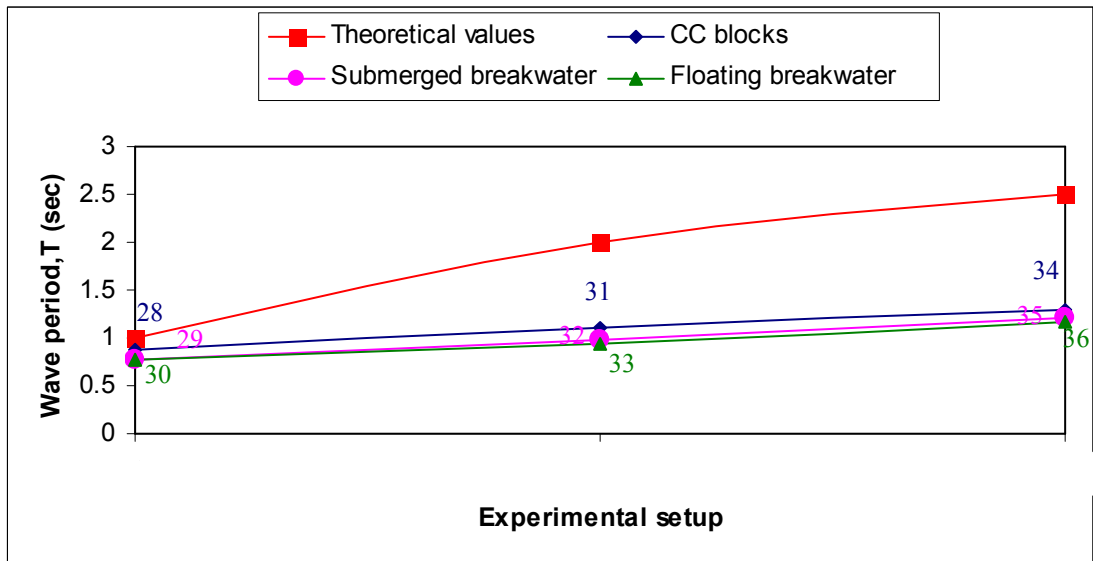


Figure 4.2.8: Comparison of wave length for different experimental setup (bed slope = 1:3 and water depth = 30 cm).

Wave heights were also changing for wave period changes with near about a constant manner. Wave heights were different for different loading conditions and different slopes. For one fixed condition (assuming the CC block condition) there were three wave height values for three different wave periods. Figure 4.2.9 to Figure 4.2.12

showed this phenomenon. Wave height values were seen to be least for floating breakwater condition and less for submerged breakwater condition than that of the CC block condition. But it can be also seen that theoretical values of wave heights were greater than the measured values.

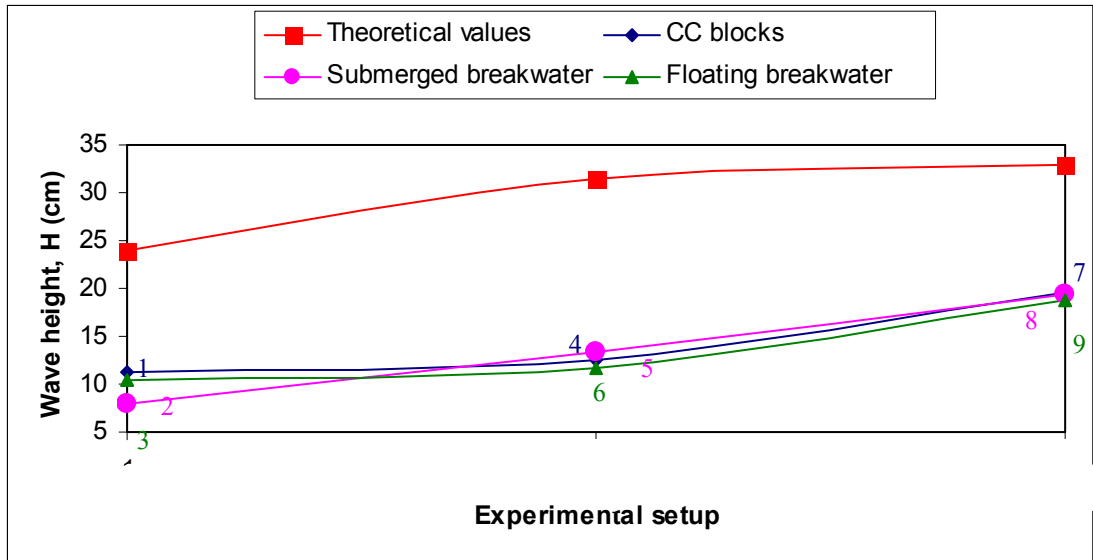


Figure 4.2.9: Comparison of wave length for different experimental setup (for slope = 1:2 and water depth = 40 cm).

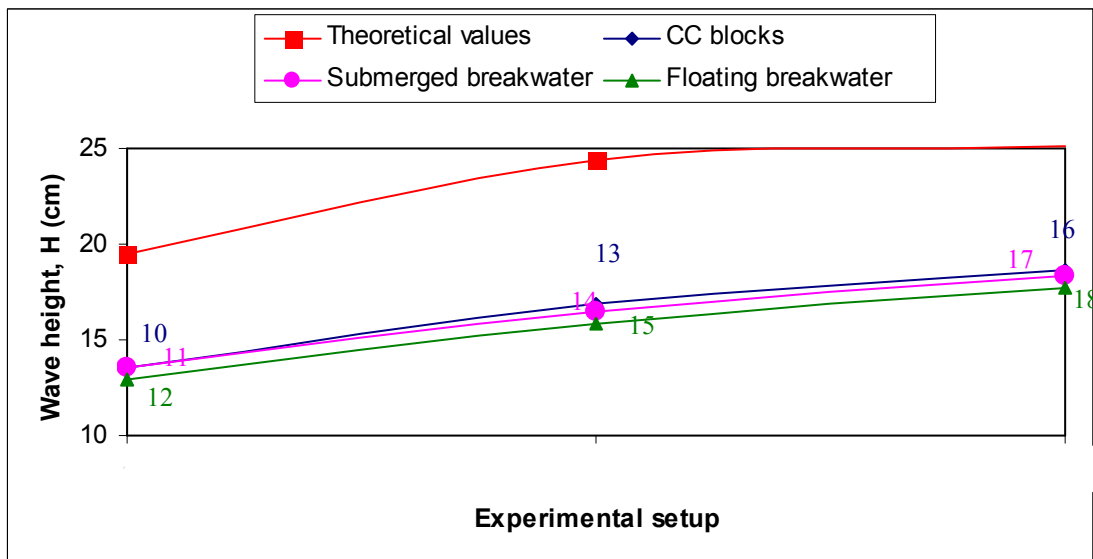


Figure 4.2.10: Comparison of wave length for different experimental setup (for slope = 1:2 and water depth = 30 cm).

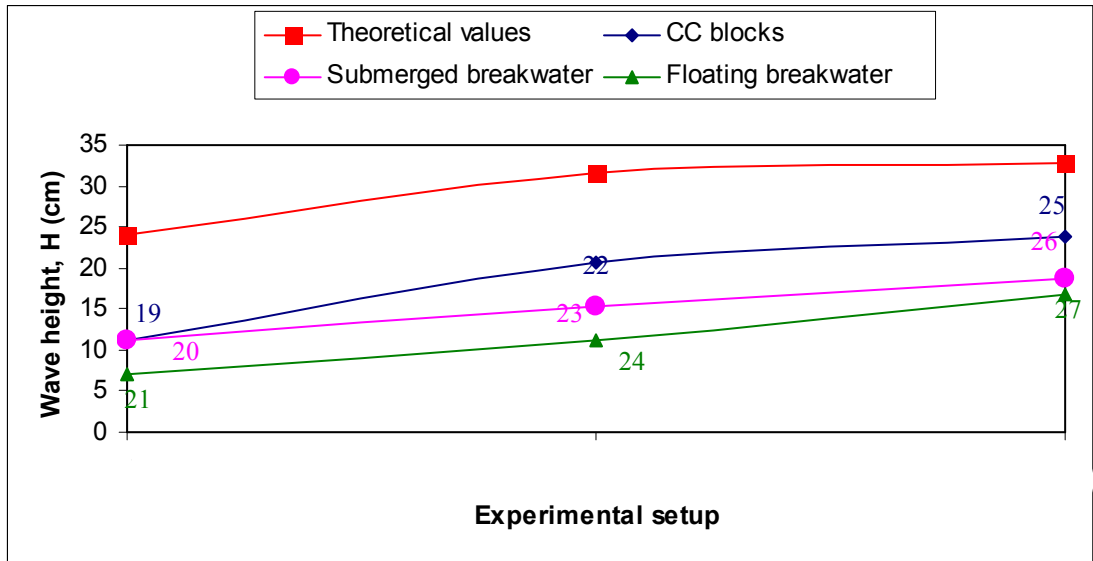


Figure 4.2.11: Comparison of wave length for different experimental setup (for slope = 1:3 and water depth = 40 cm).

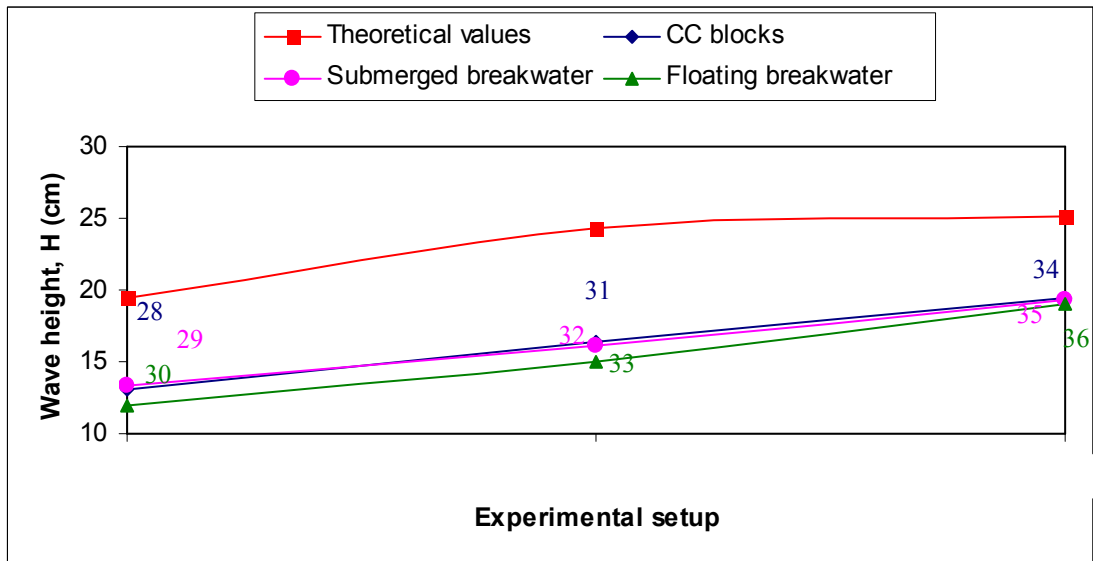


Figure 4.2.12: Comparison of wave length for different experimental setup (for slope = 1:3 and water depth = 30 cm).

Wave length, wave period and wave height were reduced by using breakwater in the laboratory setup. The rate of reduction based on CC block condition with various parameters were calculated and shown in the Table 4.2.1.

Table 4.2.1: Rate of change in wave parameters for different conditions

Parameters			Change in wave length (%)			Change in wave Height (%)			Change in wave Period (%)		
			1	2	2.5	1	2	2.5	1	2	2.5
Theoretical wave period, T sec			1	2	2.5	1	2	2.5	1	2	2.5
1:2	40	Submerged breakwater	5.88	7.33	4.00	29.77	-6.35	1.06	30.00	-6.67	1.35
		Floating breakwater	8.24	16.67	11.47	7.37	6.45	4.31	7.50	6.67	5.41
	30	Submerged breakwater	7.27	3.13	2.10	0.00	2.61	1.87	0.00	3.85	3.26
		Floating breakwater	19.09	13.28	4.90	4.37	6.29	5.19	5.17	8.97	8.70
1:3	40	Submerged breakwater	1.00	4.76	8.78	0.00	25.49	21.28	0.00	30.00	28.57
		Floating breakwater	4.50	7.94	10.81	37.28	45.81	28.87	37.50	50.00	36.73
	30	Submerged breakwater	10.67	11.17	6.79	-1.50	1.86	0.52	-1.79	2.67	1.01
		Floating breakwater	12.00	14.89	9.50	9.38	8.84	2.14	10.71	12.00	4.04

Note: Positive (+ve) sign indicate reduction and Negative (-ve) sign indicate increment.

4.3 Relation graph between wave length (L) and wave period (T)

While analyzing the relation, firstly the theoretical data were plotted for different loading condition. Then experimental data were plotted on the same graph. These data seemed such that they were on a straight line. The slope of the lines is same which shows that the experimental data were acceptable. Figure 4.3.1 to Figure 4.3.4 represented this relation. The figures showed that, at the same bank slope and water depth, the values were least for floating breakwater and values were less for submerged breakwater than CC block.

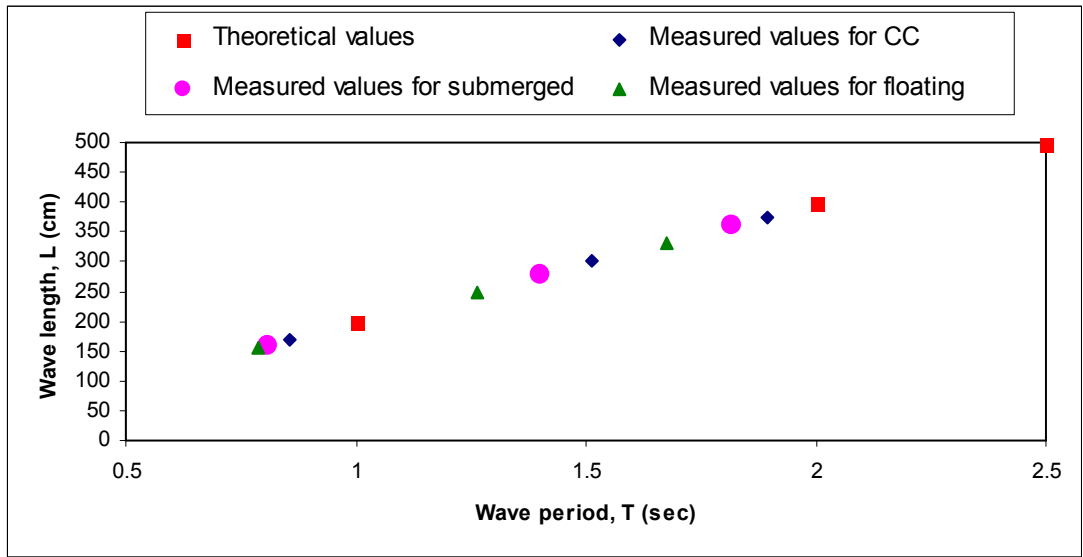


Figure 4.3.1: Wave parameter relationship for 1:2 bank slope and 40 cm water depth

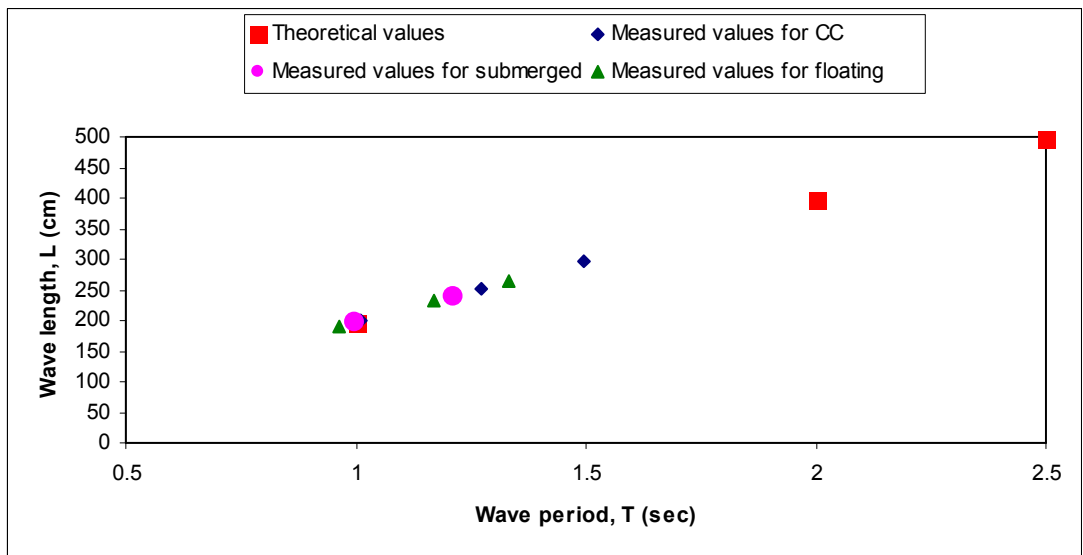


Figure 4.3.2: Wave parameter relationship for 1:3 bank slope and 40 cm water depth

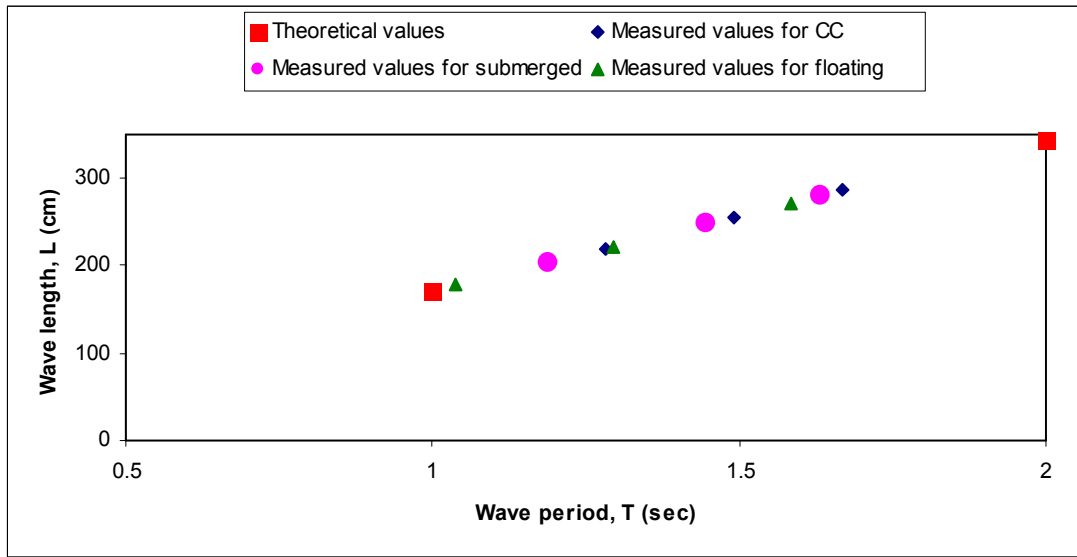


Figure 4.3.3: Wave parameter relationship for 1:2 bank slope and 30 cm water depth

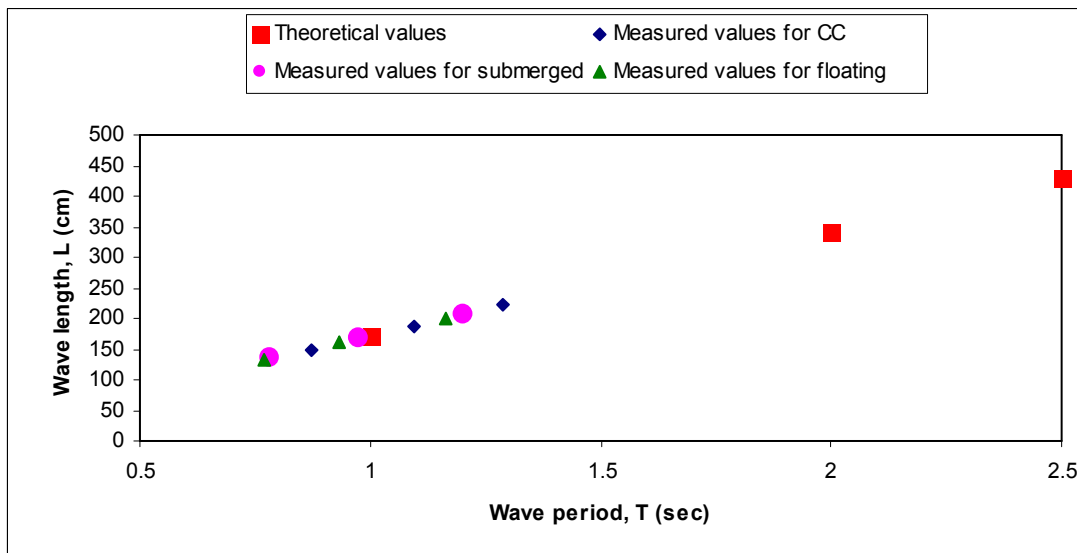


Figure 4.3.4: Wave parameter relationship for 1:3 bank slope and 30 cm water depth

This experiment was done through three different loading conditions. For all these three conditions (CC block condition, submerged condition and floating condition) data were taken separately. The wave length and wave period data were seen to be reduced for using breakwater. This reduction is more when the floating breakwater was used. Figure 4.3.5, Figure 4.3.6 and Figure 4.3.7 showed the relation graph between the wave length and wave period for different loading condition.

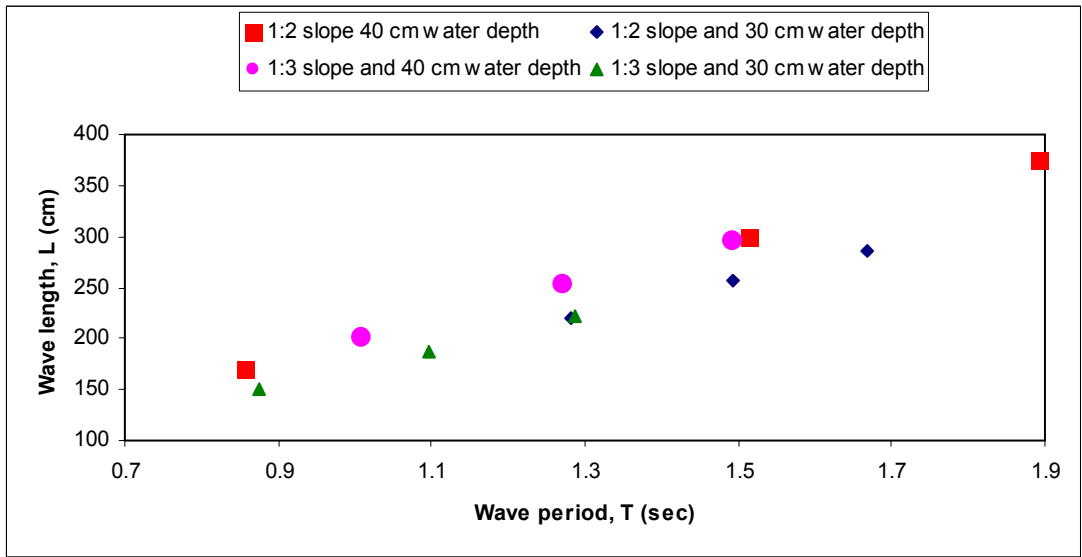


Figure 4.3.5: Wave parameter relationship for CC block at various slope and water depth.

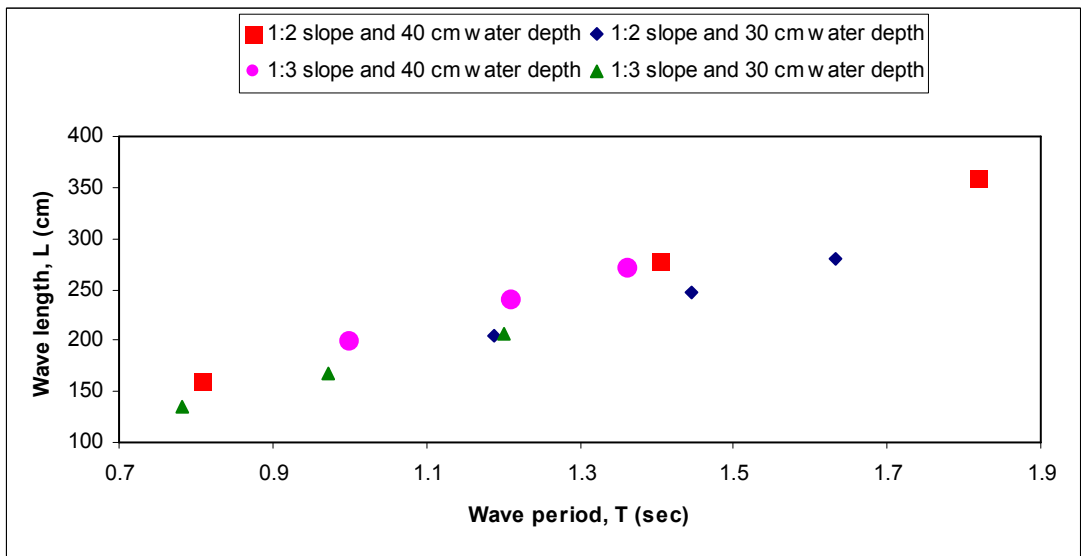


Figure 4.3.6: Wave parameter relationship for submerged breakwater condition at various slope and water depth.

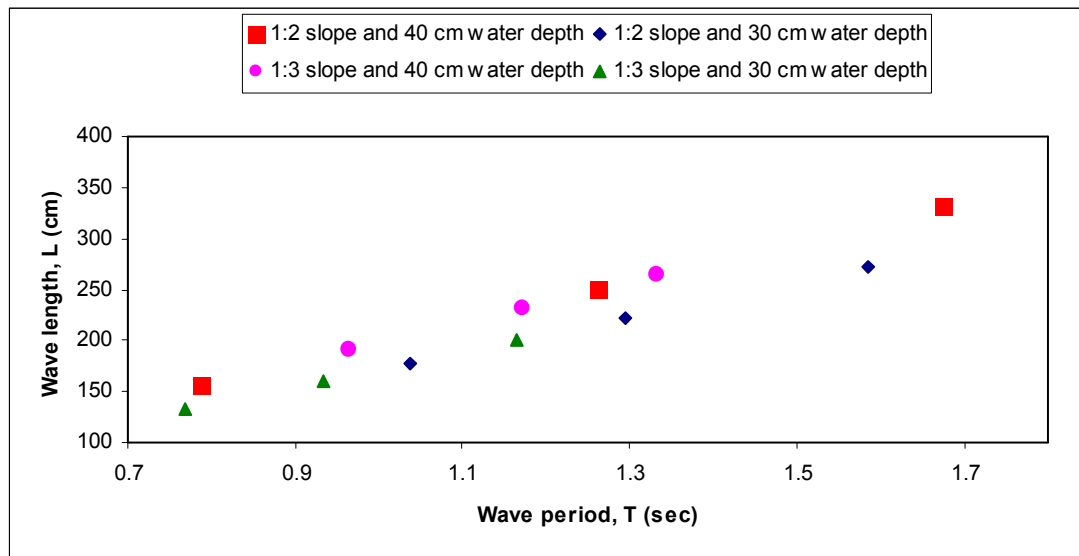


Figure 4.3.7: Wave parameter relationship for Floating breakwater condition at various slope and water depth.

Figure 4.3.5 showed that, wave length and wave period were reduced linearly with slope reduction. That is, milder slope (1:3 slope) reduced the wave parameters (wave length and wave period) more than steeper slope (1:2 slope). The effect of water depth on wave length and wave period was also came to clear from above figures, as it was seen that at the same slope the values were reduced due to water depth reduction (Figure 4.3.5 to Figure 4.3.7). These figures showed that the values of wave lengths and wave periods were large in higher water depth (40 cm) and less in low water depth (30 cm). If we plot wave length versus wave period in a graph using linear wave theory for a constant water depth, it shows a straight line with a slope. The above graphs were plotted using the experimental values which are showing also straight line. So, they agree with linear wave theory.

4.4 Relation between wave period (T) and wave height (H)

It has been stated in section-4.2 that, wave periods have been changed at a definite shape where as wave heights did not. Now these two type values were plotted on the graph and the relation of wave period and wave heights were shown (Figure 4.4.1 to 4.4.4). These figures showed that the wave heights were smaller for smaller wave period. At same water depth the values of wave heights were reduced at a high rate

with reduced wave period for milder slope (1:3) than steeper slope (1:2). The wave height values were also seen to be changed because of three different loading conditions. The values of wave heights were found smaller at floating breakwater condition than submerged breakwater condition. At CC block condition the values were largest than that of other two loading conditions.

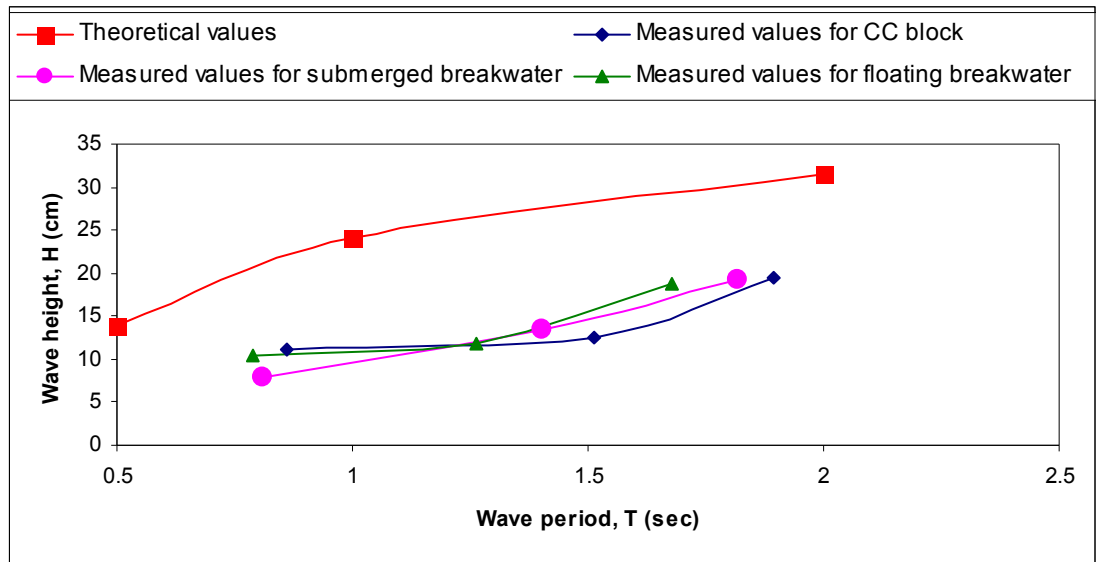


Figure 4.4.1: Comparison of wave height and wave period at 1:2 slope and 40 cm water depth.

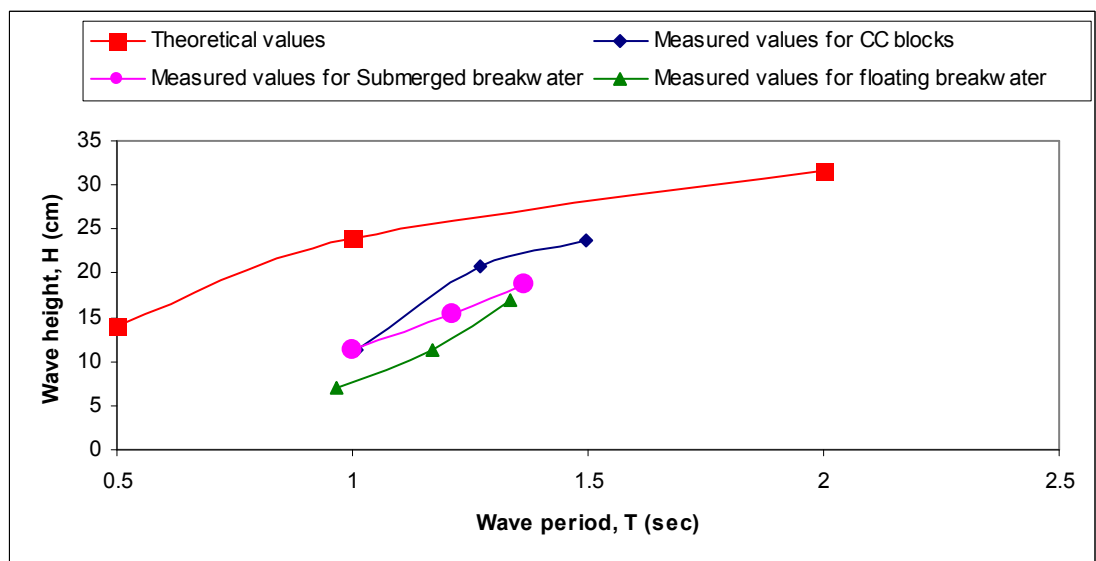


Figure 4.4.2: Comparison of wave height and wave period at 1:3 slope and 40 cm water depth.

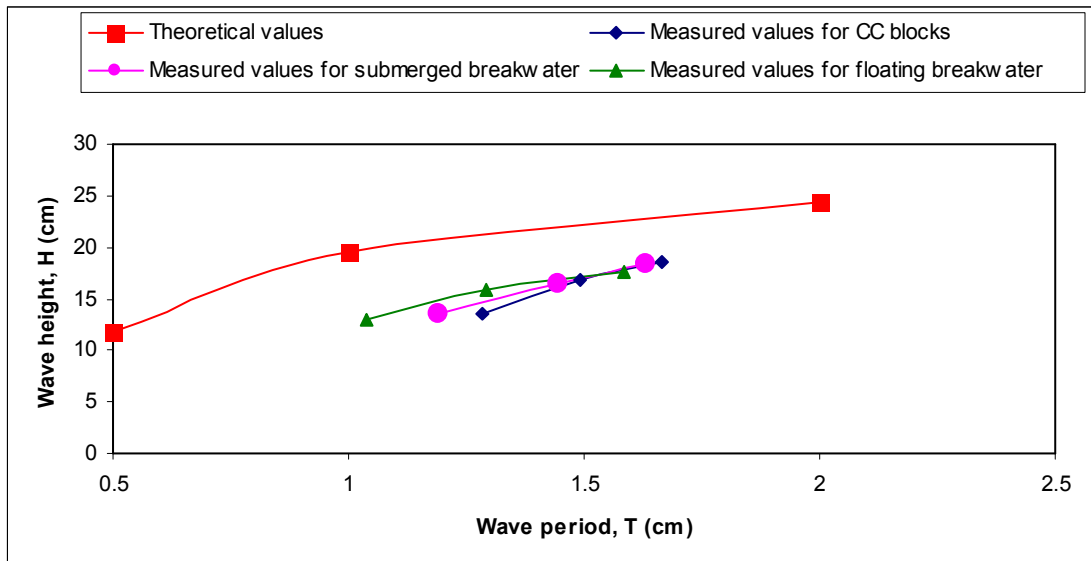


Figure 4.4.3: Comparison of wave height and wave period at 1:2 slope and 30 cm water depth.

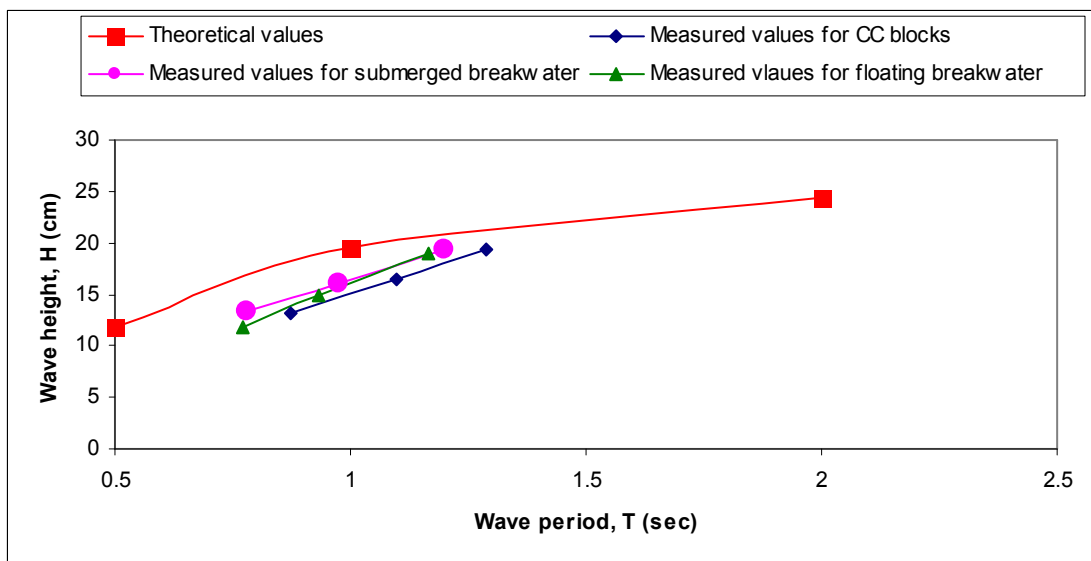


Figure 4.4.4: Comparison of wave height and wave period at 1:3 slope and 30 cm water depth

Figure 4.4.5, Figure 4.4.6 and Figure 4.4.7 showed the wave height changes for constant loading conditions. Every figure showed that the wave heights were increased with wave period increment. When slopes were unchanged, the values

were decreased because of the water depth reduction. Again, from these figures it was clear that for milder slope values were smaller and for steeper slope they were large.

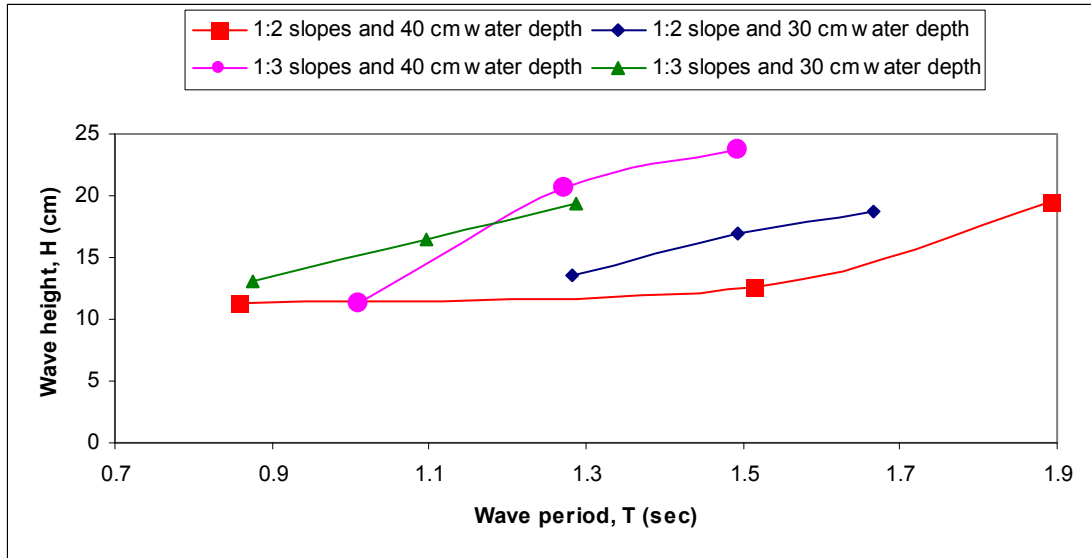


Figure 4.4.5: Comparison of wave parameters for CC block condition

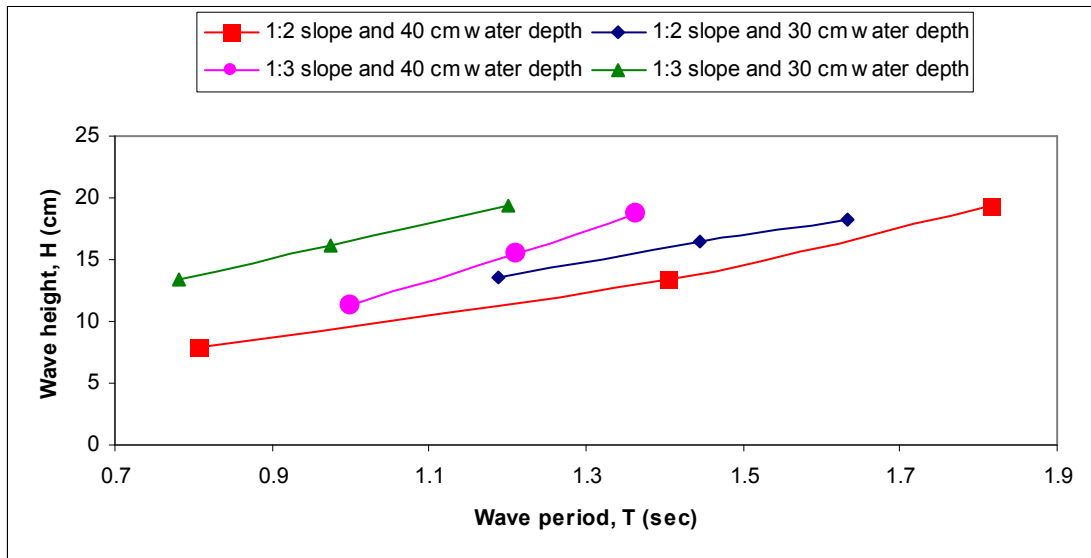


Figure 4.4.6: Comparison of wave parameters for submerged breakwater condition

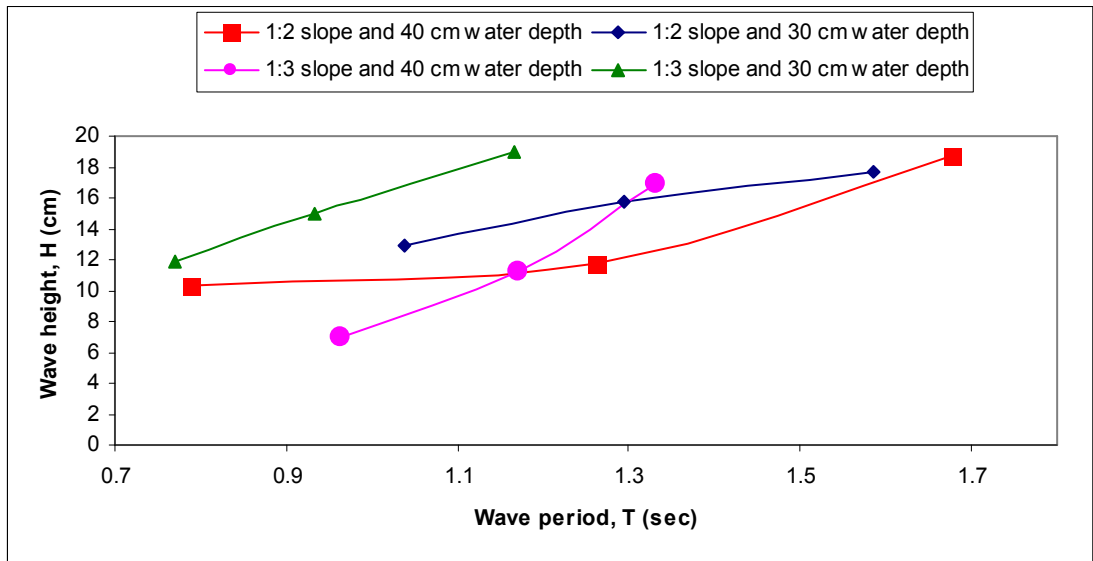


Figure 4.4.7: Comparison of wave parameters for floating breakwater condition

4.5 Relation between Wave length (L) and Wave height (H)

Values of wave heights were increased with the increasing values of wave length. Figure 4.5.1, Figure 4.5.2, Figure 4.5.3 and Figure 4.5.4 showed the wave height changes with wave length for two types of slope (1:2 and 1:3) and water depth (40 cm and 30 cm).

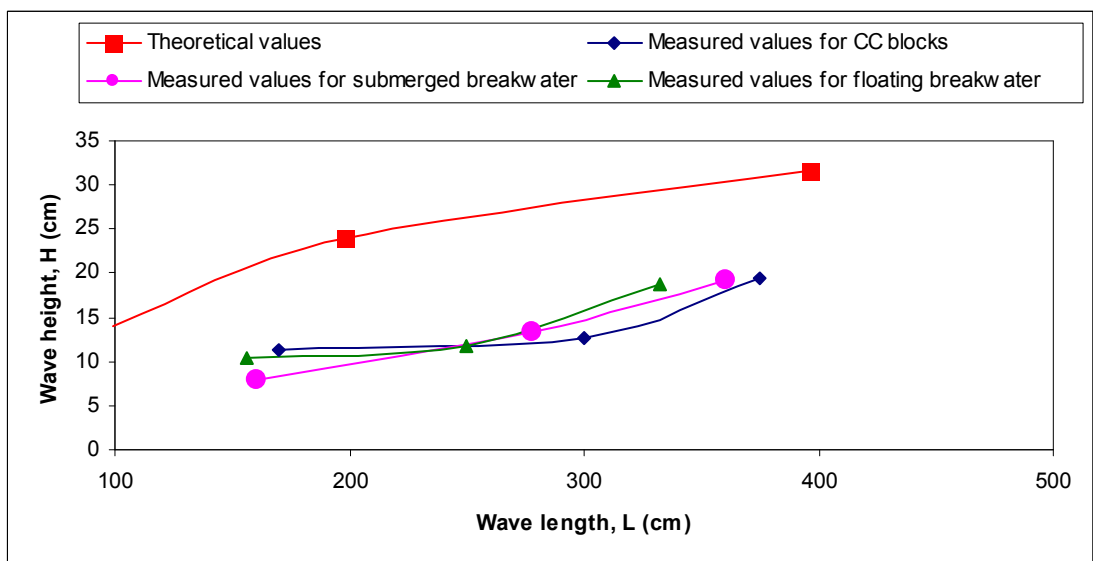


Figure 4.5.1: Relation between wave length and wave height at 1:2 slope and 40 cm water depth.

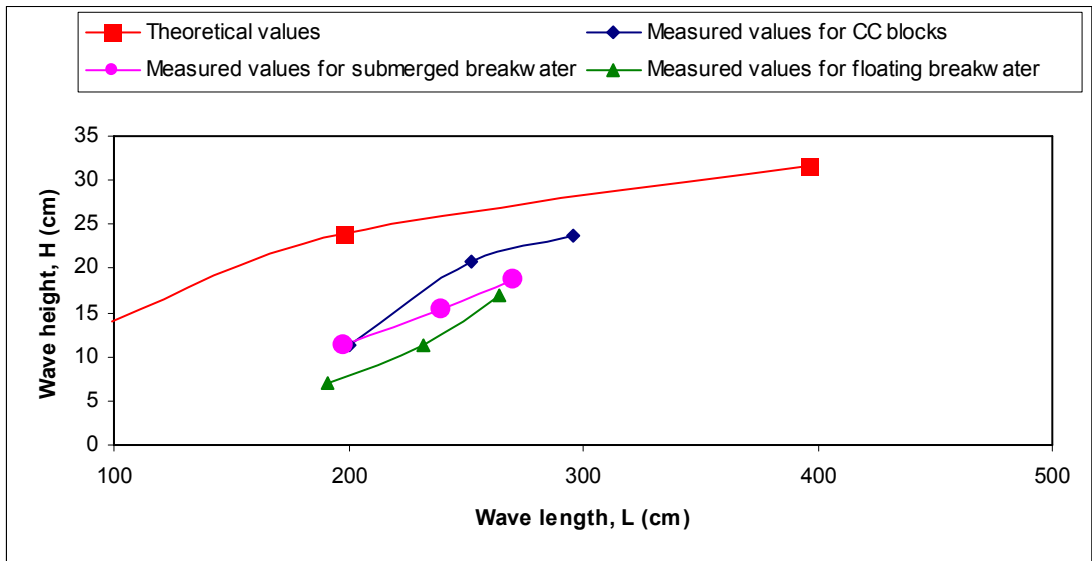


Figure 4.5.2: Relation between wave length and wave height at 1:3 slope and 40 cm water depth.

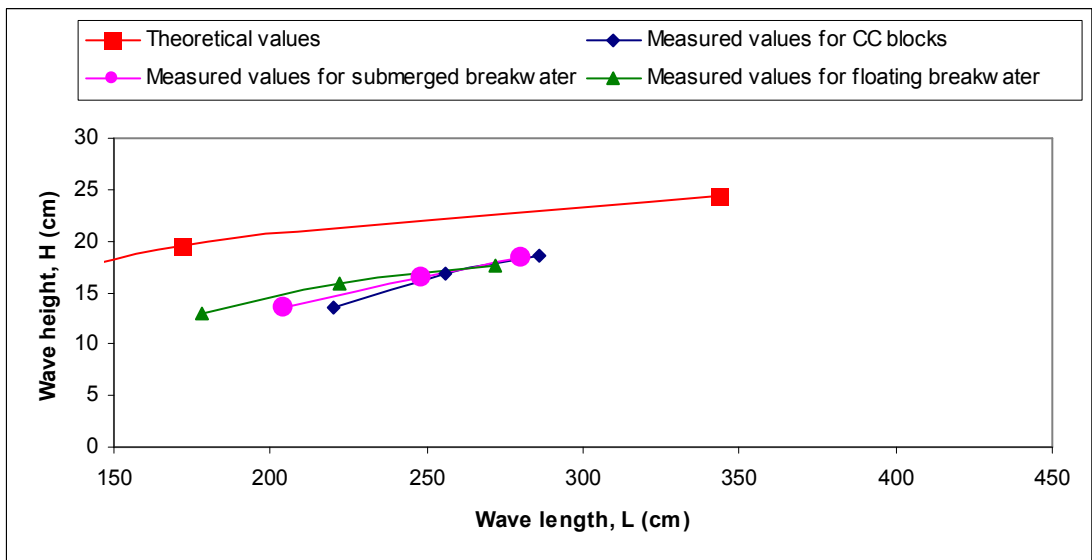


Figure 4.5.3: Relation between wave length and wave height at 1:2 slope and 30 cm water depth.

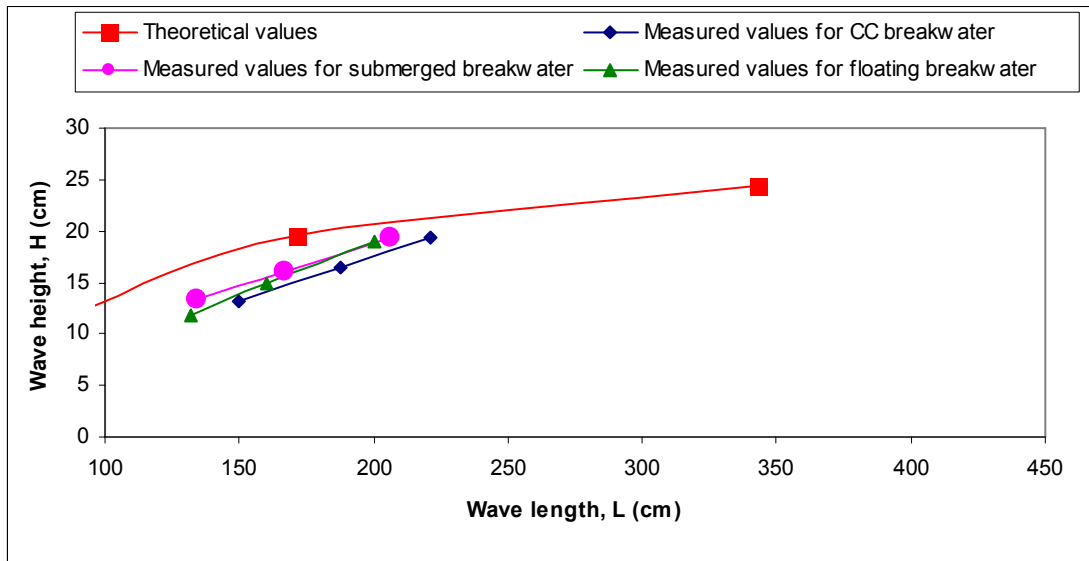


Figure 4.5.4: Relation between wave length and wave height at 1:3 slope and 30 cm water depth.

From the analysis of the four figures the results came out that, wave height values came to less in magnitude with wave length reduction. The floating and submerged breakwater condition made the values smaller than that of normal CC block condition. Among the two breakwater condition, floating breakwater condition made the values smaller than that of submerged. When water depth fall down, the values of wave length and wave height also fall down in magnitude (Figure 4.5.5 to Figure 4.5.7). These figures also showed that milder slope (1:3) made the parameters smaller than steeper slope (1:2).

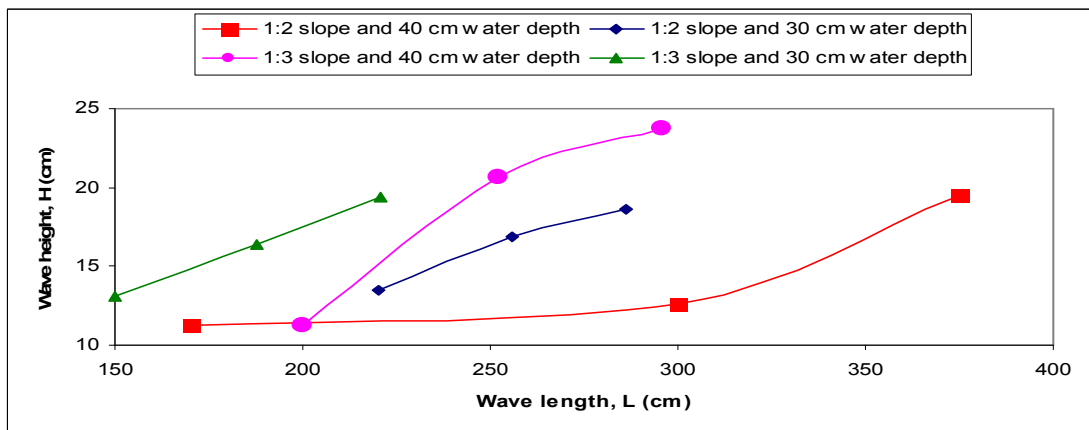


Figure 4.5.5: Comparison of wave parameters for CC block in various slope and water depth.

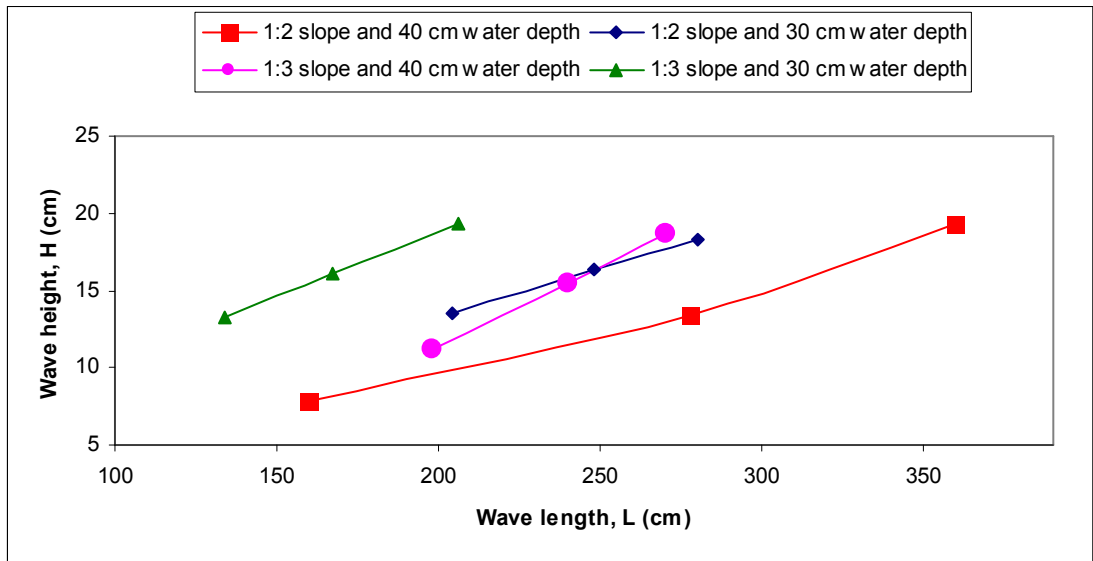


Figure 4.5.6: Comparison of wave parameters for submerged breakwater in various slope and water depth.

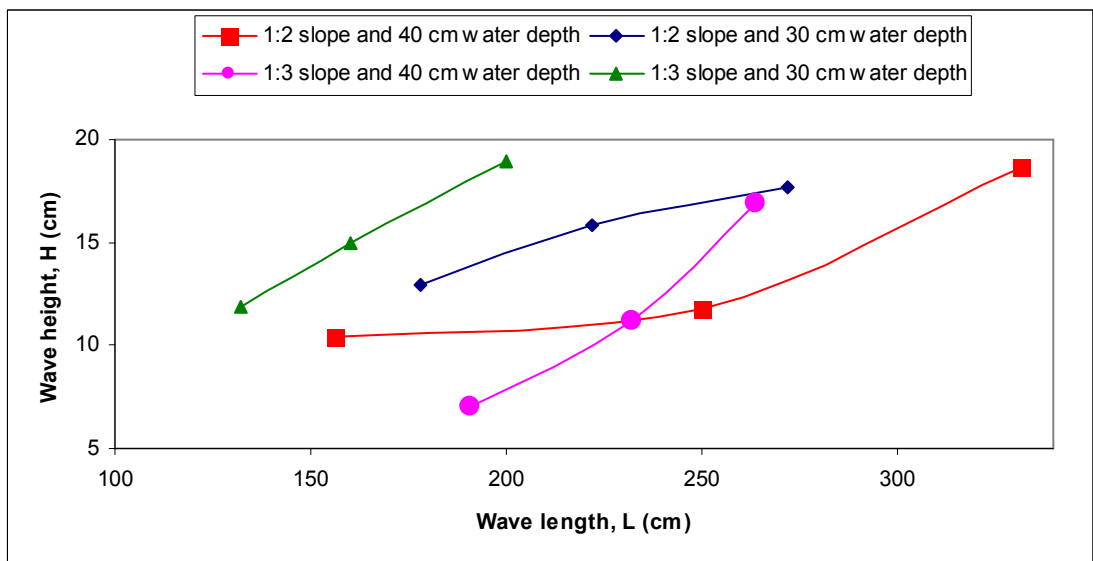


Figure 4.5.7: Comparison of wave parameters for Floating breakwater in various slope and water depth.

4.6 Relation graph between run-up height (R) and Wave period (T)

Wave run-up depends on the structural shape and roughness, water depth at structure toe, bottom slope in front of a structure and incident wave characteristics (Navera and Nandi, 2007). Experimental values of wave run-up and wave period were plotted

on the graph. Figure 4.6.1 to Figure 4.6.4 represents the run-up height changes for different loading condition and slope.

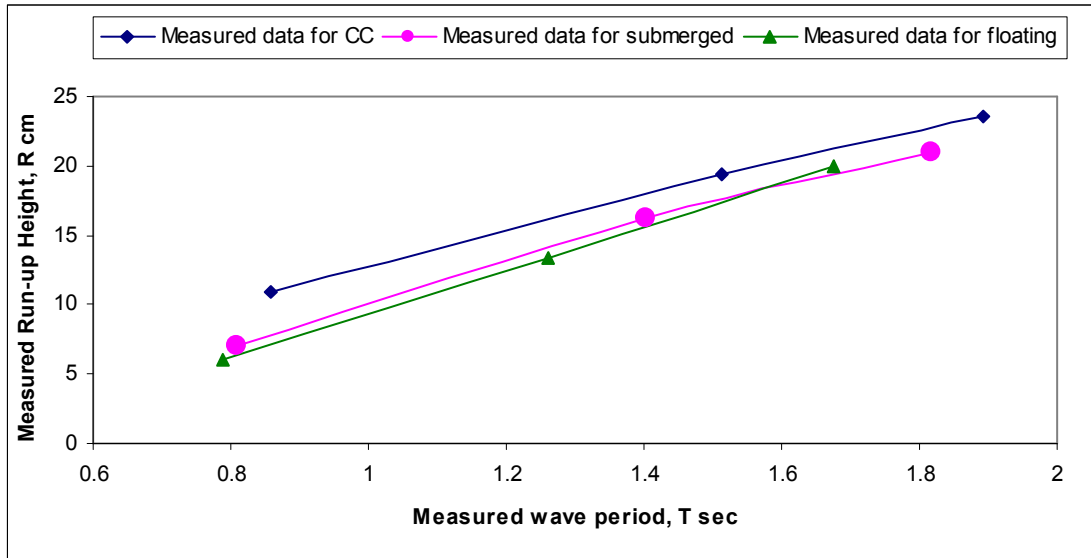


Figure 4.6.1: Run-up height changes with wave period for 1:2 slope and 40 cm water depth.

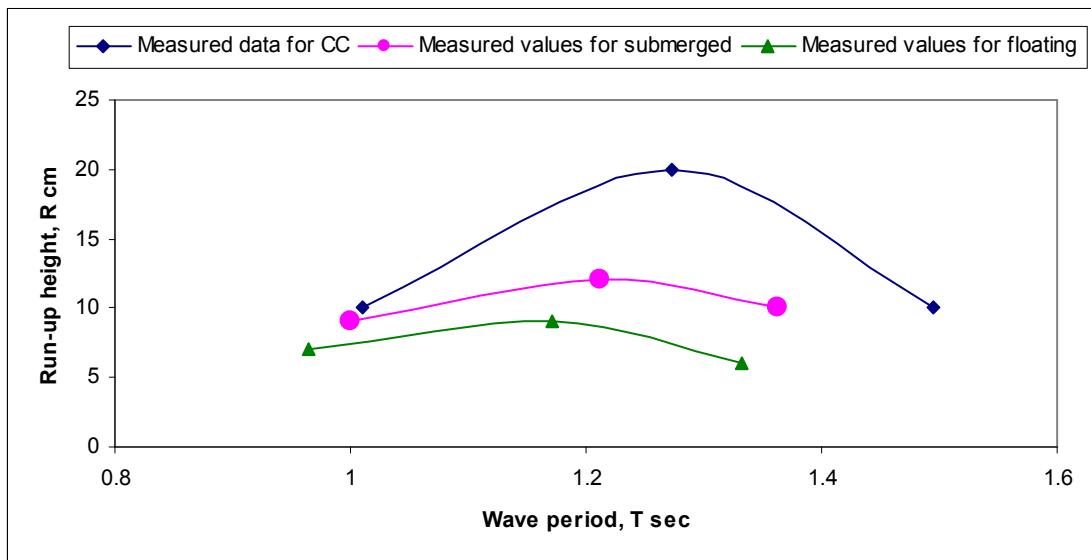


Figure 4.6.2: Run-up height changes with wave period for 1:3 slope and 40 cm water depth.

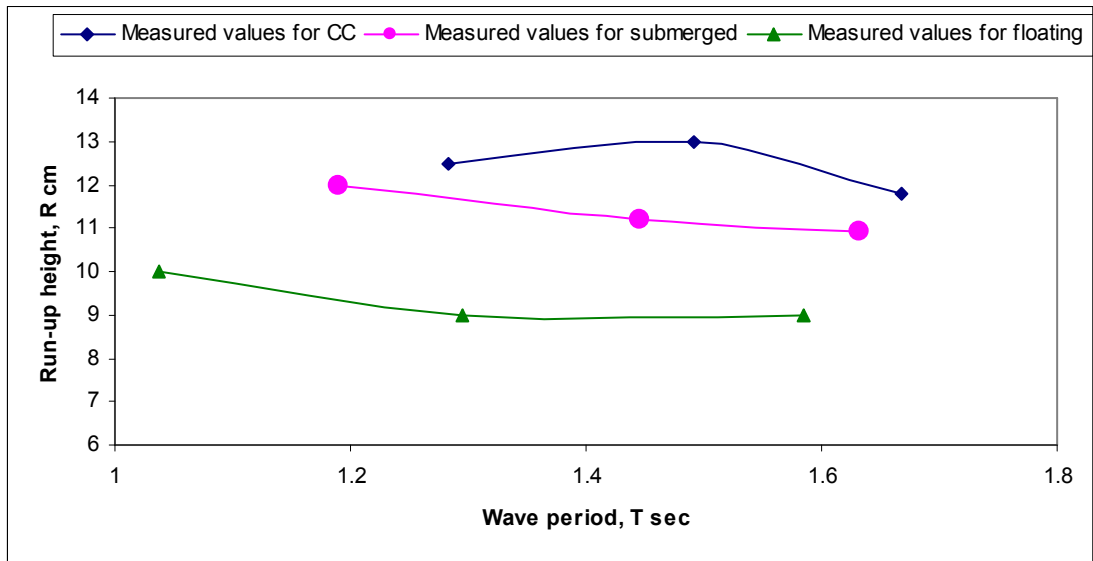


Figure 4.6.3: Run-up height changes with wave period for 1:2 slope and 30 cm water depth.

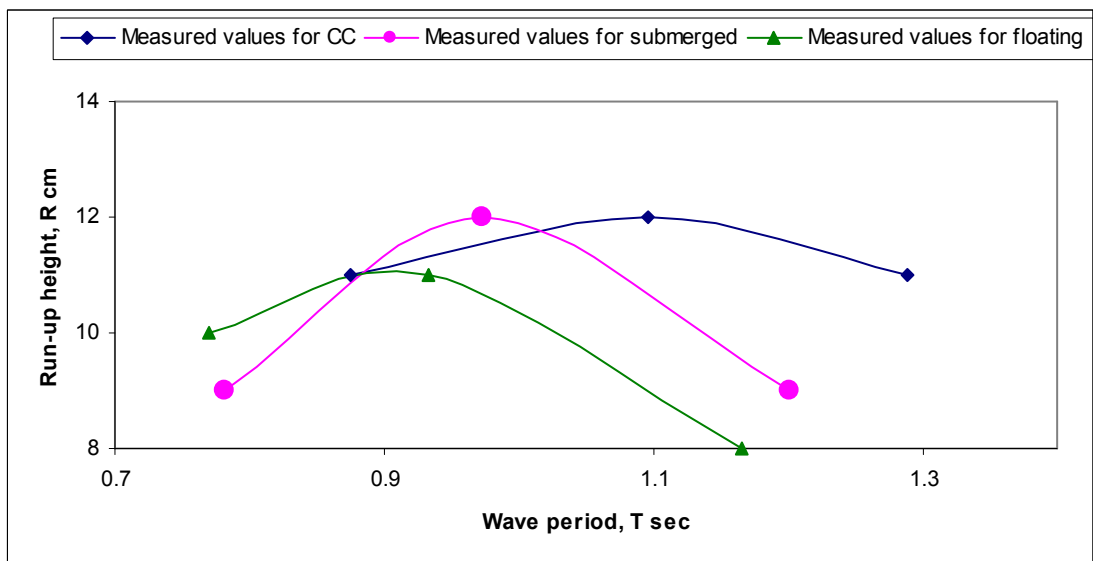


Figure 4.6.4: Run-up height changes with wave period for 1:3 slope and 30 cm water depth.

When slope and water depth is fixed, run-up height values changes with wave period. Figure 4.6.1 to Figure 4.6.4 showed that, run-up heights were reduced with the use of breakwater. And run-up height was least in floating breakwater condition. For the submerged breakwater condition it is less than normal CC block condition. For same water depth but different slope the values of run-up height for all loading condition

had decreased with reduction of embankment slope. From those figures it is also clear that, if water depth was less, values were small. Here the values for the water depth 30 cm are smaller than 40 cm water depth.

Figure 4.6.5, Figure 4.6.6 and Figure 4.6.7 showed the run-up height change with wave period change in same loading condition. Each figure showed that run-up heights were reduced with slope and water depth reduction that is milder slope (1:3) is more suitable for run-up height reduction.

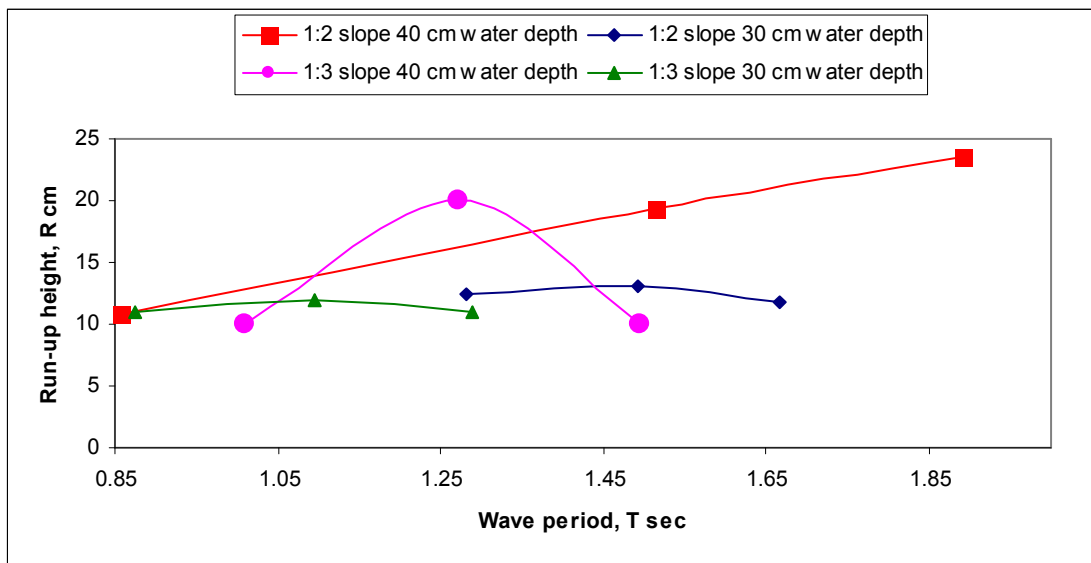


Figure 4.6.5: Run-up height changes with wave period for CC block at different slope and water depth.

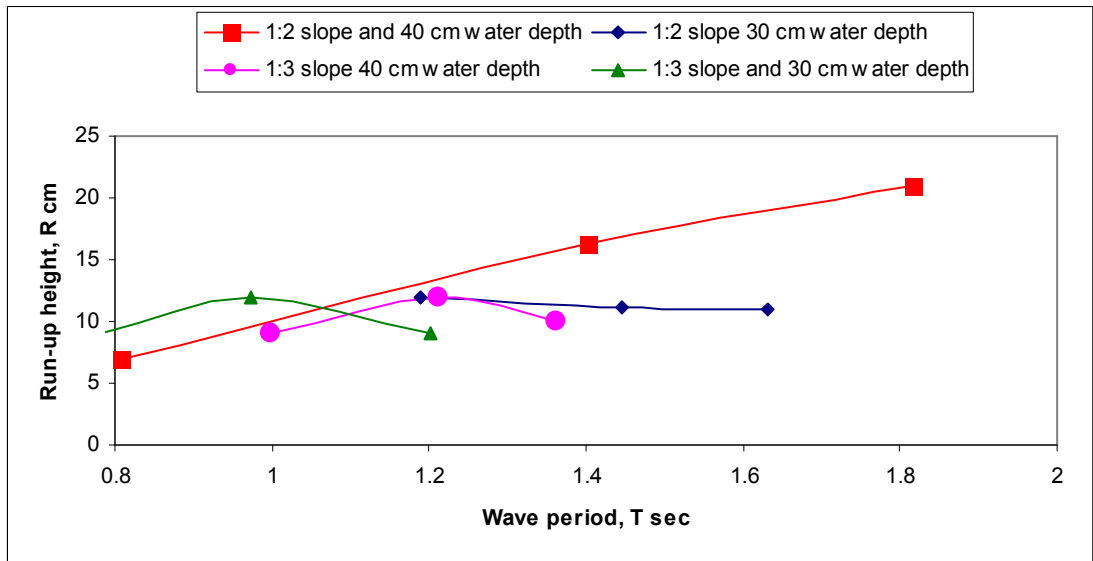


Figure 4.6.6: Run-up height changes with wave period for submerged breakwater condition at different slope and water depth.

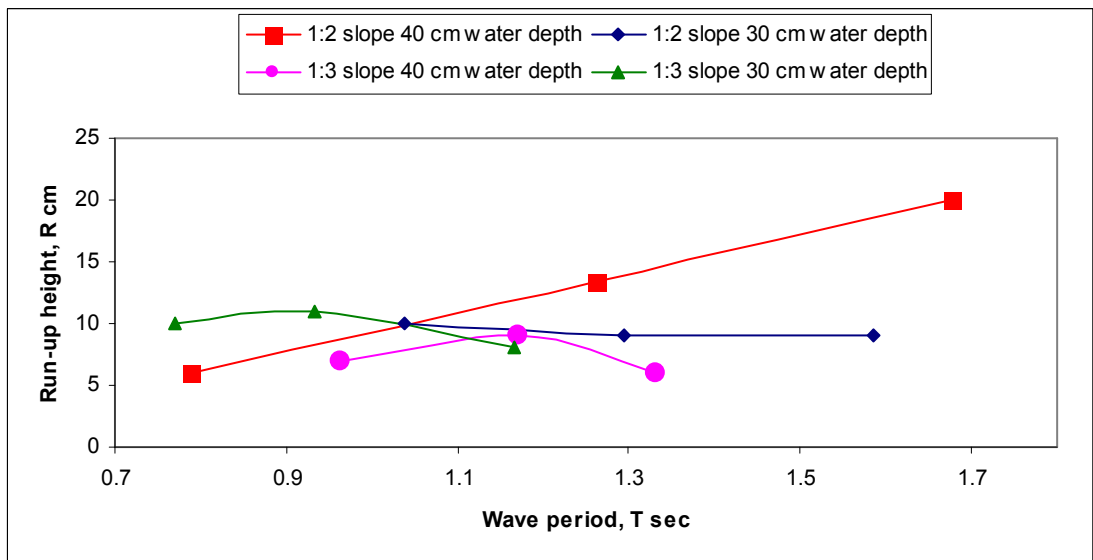


Figure 4.6.7: Run-up height changes with wave period for floating breakwater condition at different slope and water depth

Wave run-up was changed with changing type of breakwater. In all cases it had been found that the run-up decreases when there was a breakwater in front of the protection work. Rate of change of run-up height are presented in the Table 4.6.1.

Table 4.6.1: Changes of run-up height due to breakwater with respect to CC condition

Parameters			Change in wave Run-up height (%)		
Theoretical wave period, T sec			1	2	2.5
1:02	40	Submerged breakwater	35.48	16.34	10.64
		Floating breakwater	44.70	31.03	14.89
	30	Submerged breakwater	4.00	13.85	7.63
		Floating breakwater	20.00	30.77	23.73
1:03	40	Submerged breakwater	10.00	40.00	0.00
		Floating breakwater	30.00	55.00	40.00
	30	Submerged breakwater	18.18	0.00	18.18
		Floating breakwater	9.09	8.33	27.27

Note: Positive (+ve) sign indicate reduction and Negative (-ve) sign indicate increment.

4.7 Run-up height (R) and Wave Length (L) relationship

Figure 4.7.1 to Figure 4.7.4 illustrated that, run-up height changes with wave length change. They showed, run-up height changes with wave length are not uniform. But the figures proved that floating breakwater condition reduced the run-up height much more than submerged and CC block condition. In general, wave length reduction and Run-up height reduction should be a straight line. Here the plots were not showing the lines. It might be due to the limitations of the experiment. From the analysis of these figures, it came to clear that smaller wave length reduced the run-up height.

This run-up height reduction is very much important in the design of embankment height. Higher the run-up height makes the higher design height of embankment and lower the run-up height makes the lower design height of embankment which is cost effective.

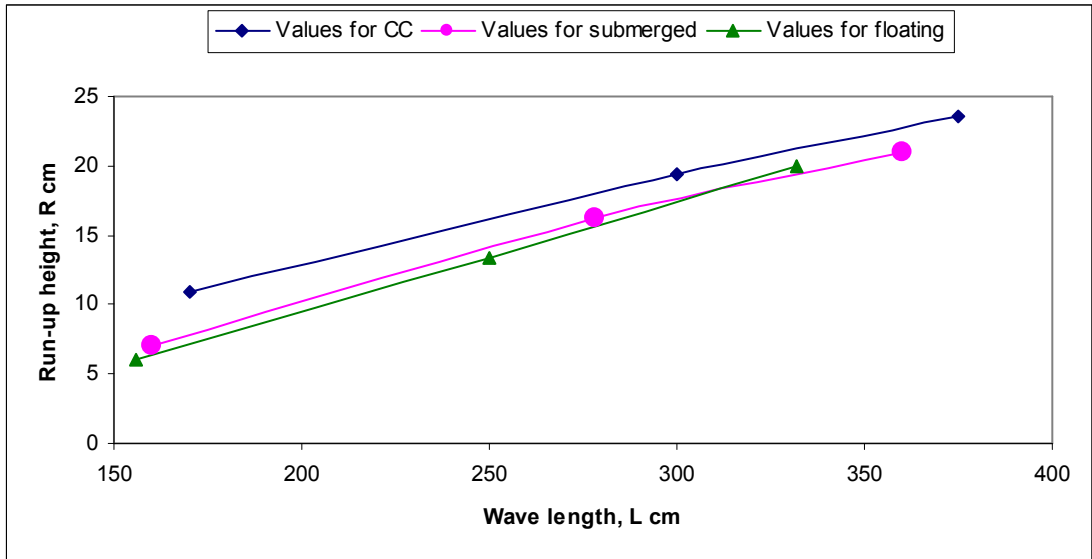


Figure 4.7.1: Wave length and run-up height relationship for 1:2 slope and 40 cm water depth.

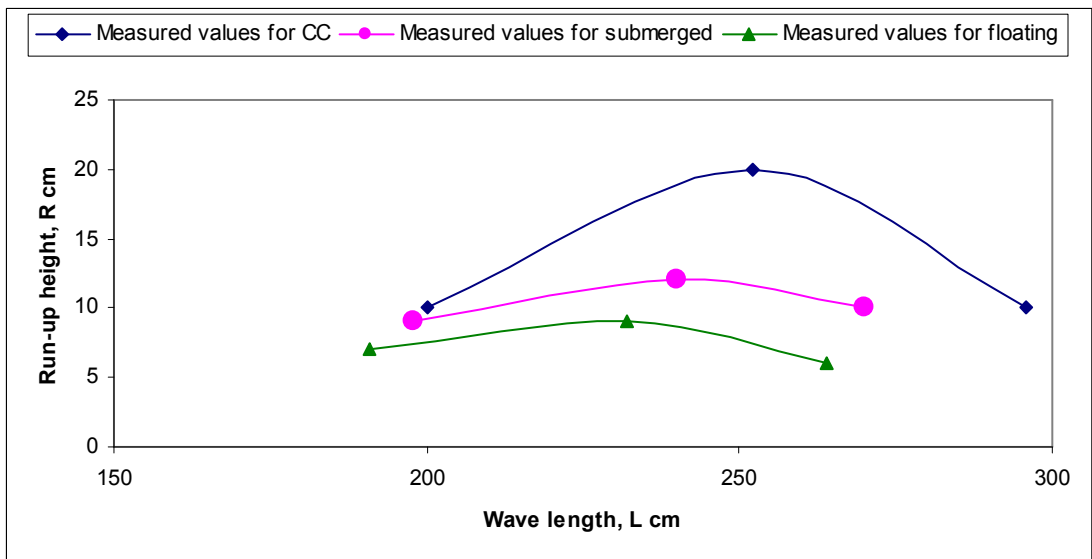


Figure 4.7.2: Wave length and run-up height relationship for 1:3 slope and 40 cm water depth.

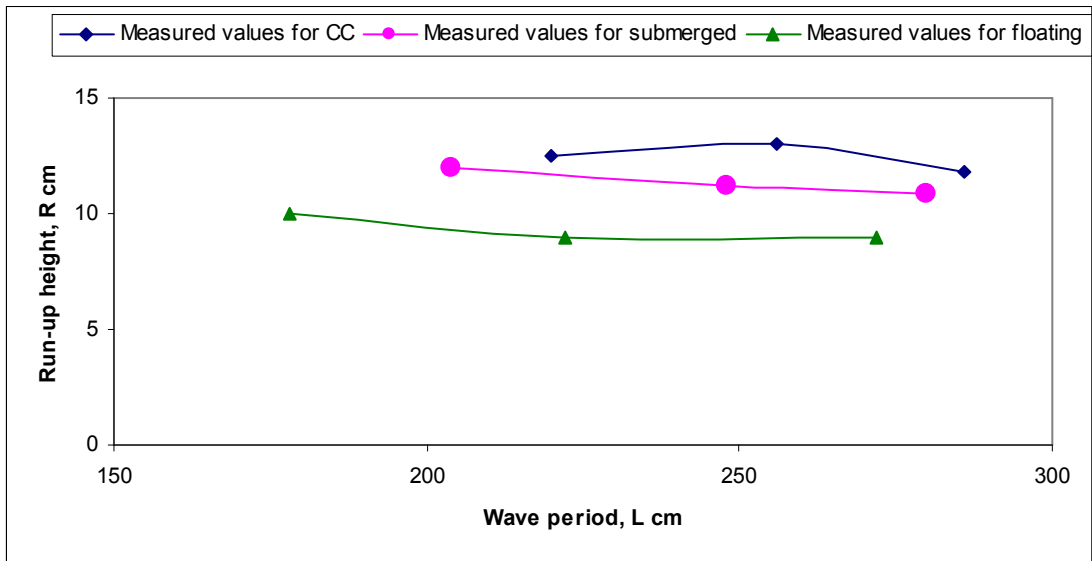


Figure 4.7.3: Wave length and run-up height relationship for 1:2 slope and 30 cm water depth.

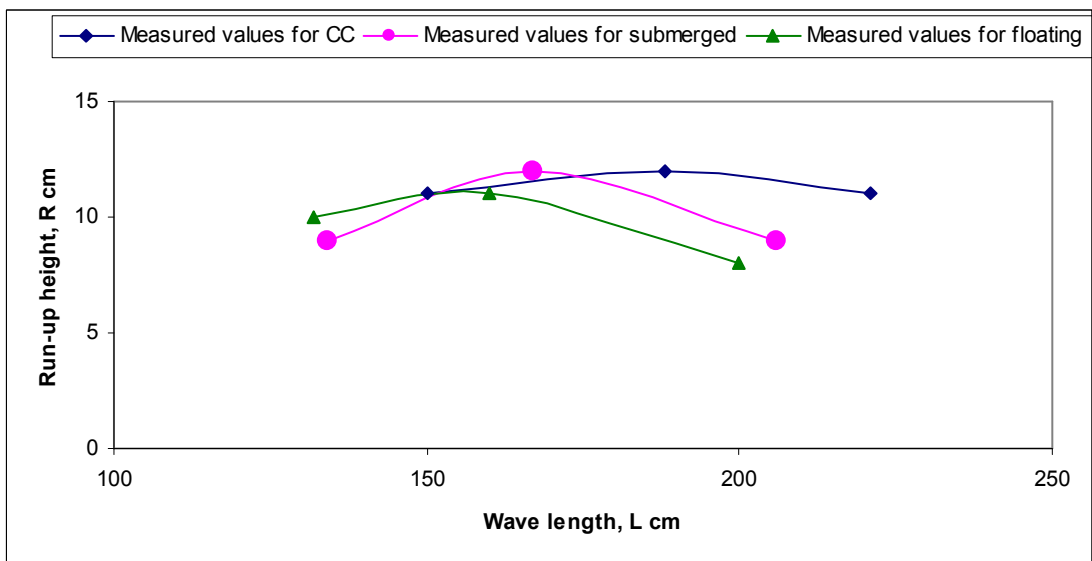


Figure 4.7.4: Wave length and run-up height relationship for 1:3 slope and 30 cm water depth.

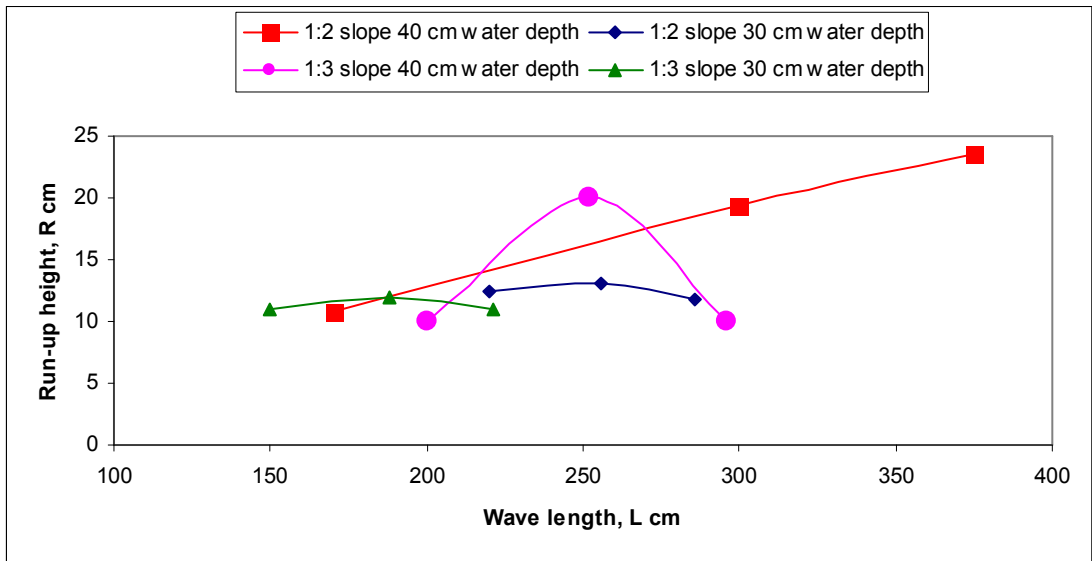


Figure 4.7.5: Variation in run-up height for CC block condition at different slope and water depth.

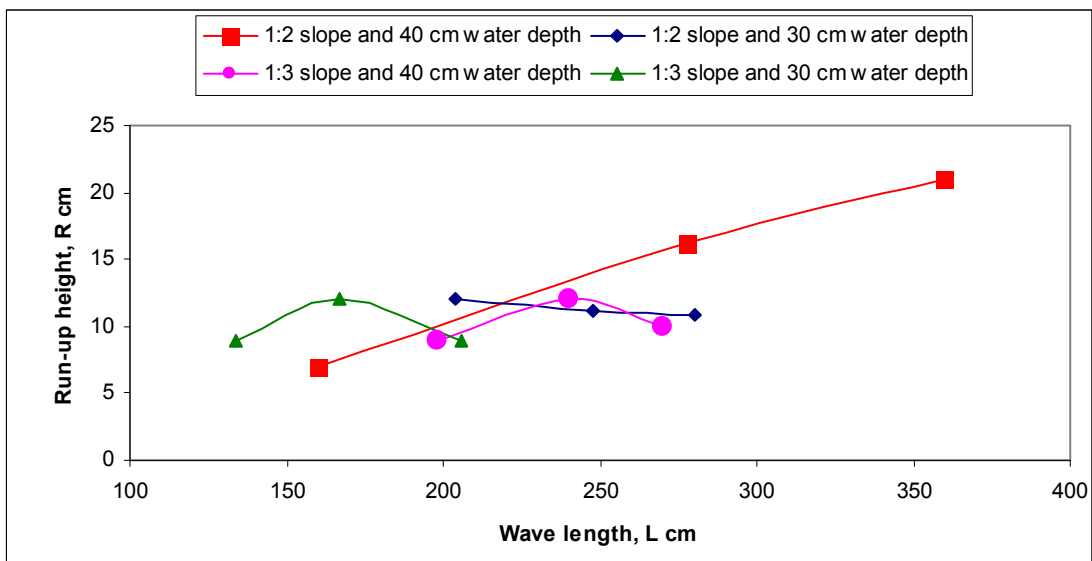


Figure 4.7.6: Variation in run-up height for submerged breakwater condition at different slope and water depth.

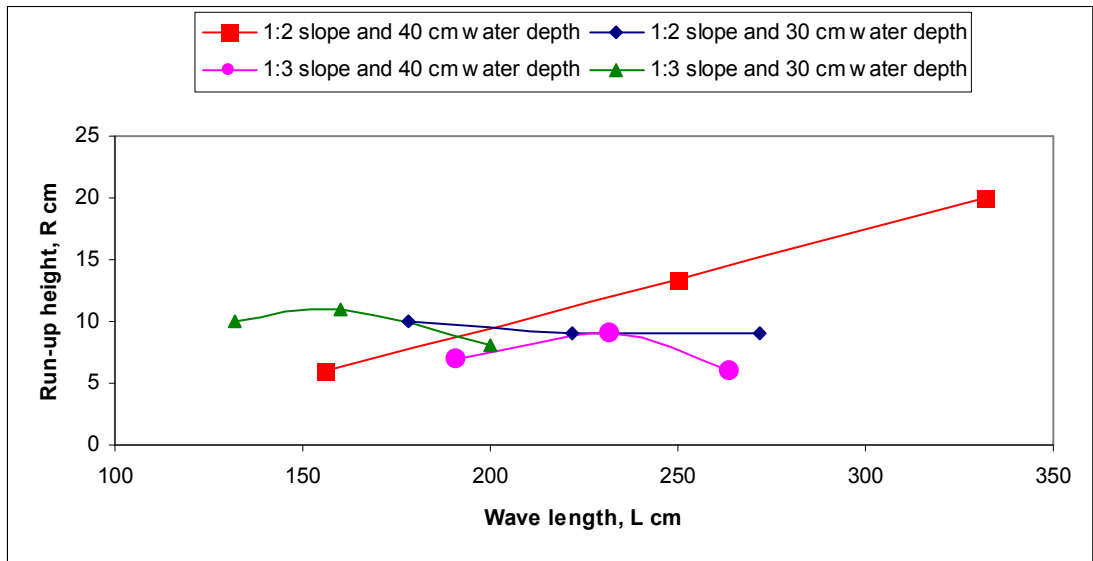


Figure 4.7.7: Variation in run-up height for submerged breakwater condition at different slope and water depth.

4.8 Run-up height (R) and Wave height (H) relationship

Figure 4.8.1 to Figure 4.8.4 show the run-up heights change with changing of wave heights for various slopes and water depth.

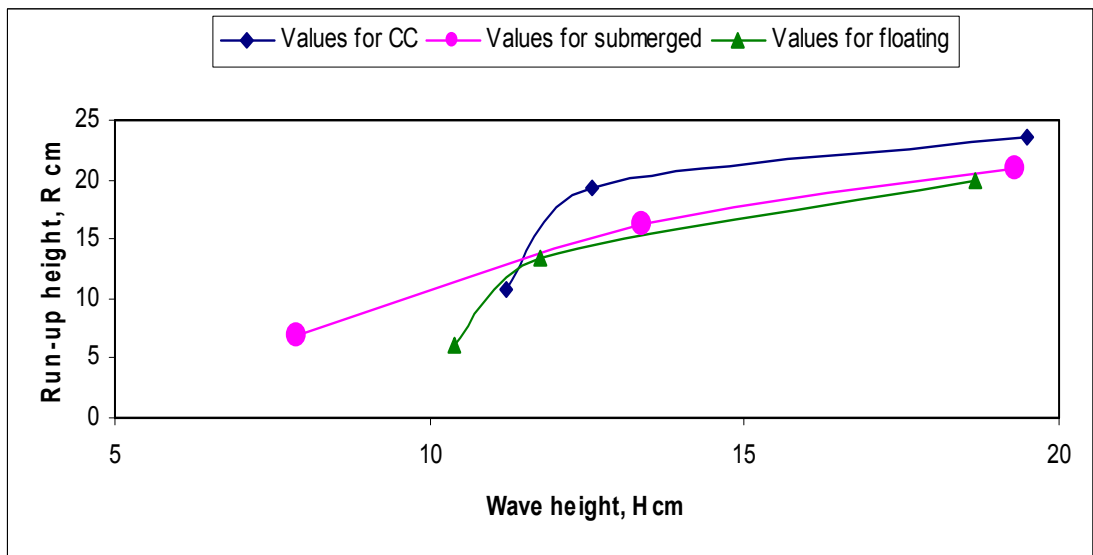


Figure 4.8.1: Comparisons between wave height and run-up height for 1:2 slope and 40 cm water depth

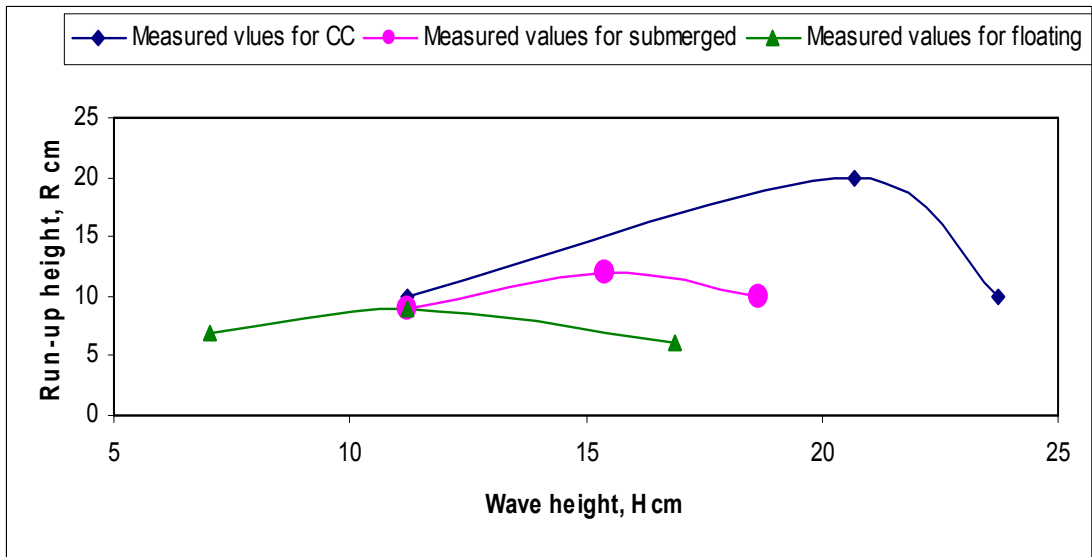


Figure 4.8.2: Comparisons between wave height and run-up height for 1:3 slope and 40 cm water depth

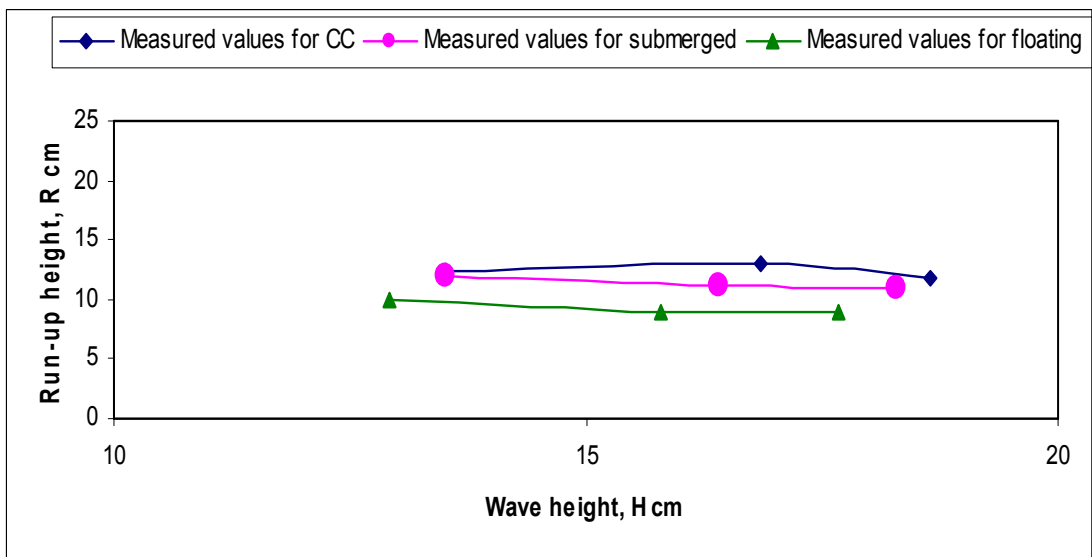


Figure 4.8.3: Comparisons between wave height and run-up height for 1:2 slope and 30 cm water depth

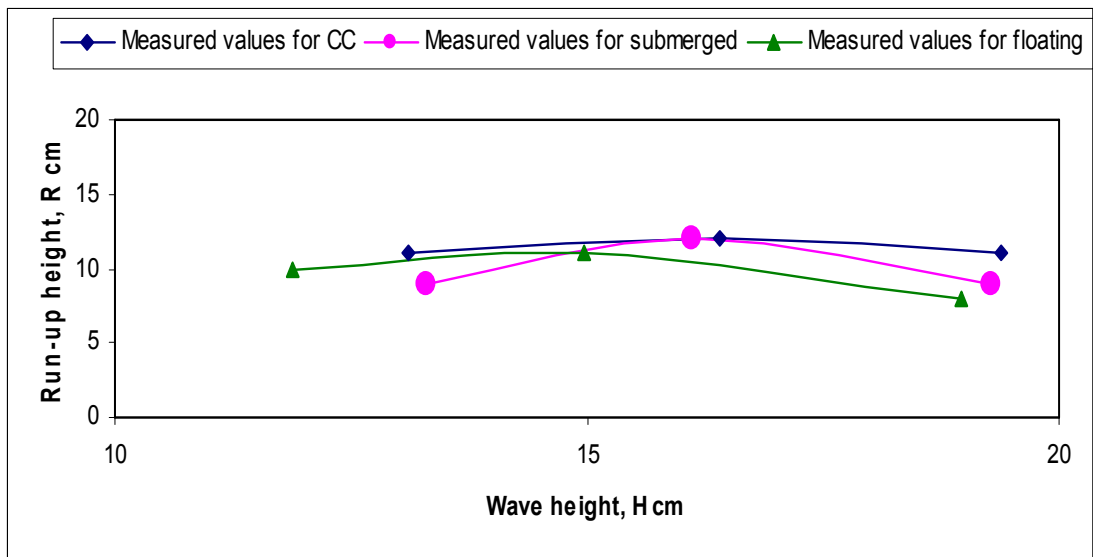


Figure 4.8.4: Comparisons between wave height and run-up height for 1:3 slope and 30 cm water depth

There is no uniform shape of run-up height change with respect to wave height but those figures show that run-up height changes have been affected by breakwater use. When the floating breakwater was used, it reduces the run-up height more than submerged breakwater and CC block. Again, submerged breakwater used decreased the run-up height than that of CC blocks condition.

To show the run up height changes with wave height change in individual loading effect, Figure 4.85, Figure 4.86 and Figure 4.8.7 were plotted. The figures showed that, for every loading condition (CC block, submerged breakwater and floating breakwater) run-up values have been reduced with reduction of slope and water depth. When slope was same the values were reduced at small water depth (30 cm) than the larger depth (40 cm). When water depth was constant, run-up values had reduced at milder slope (1:3) than steeper slope (1:2).

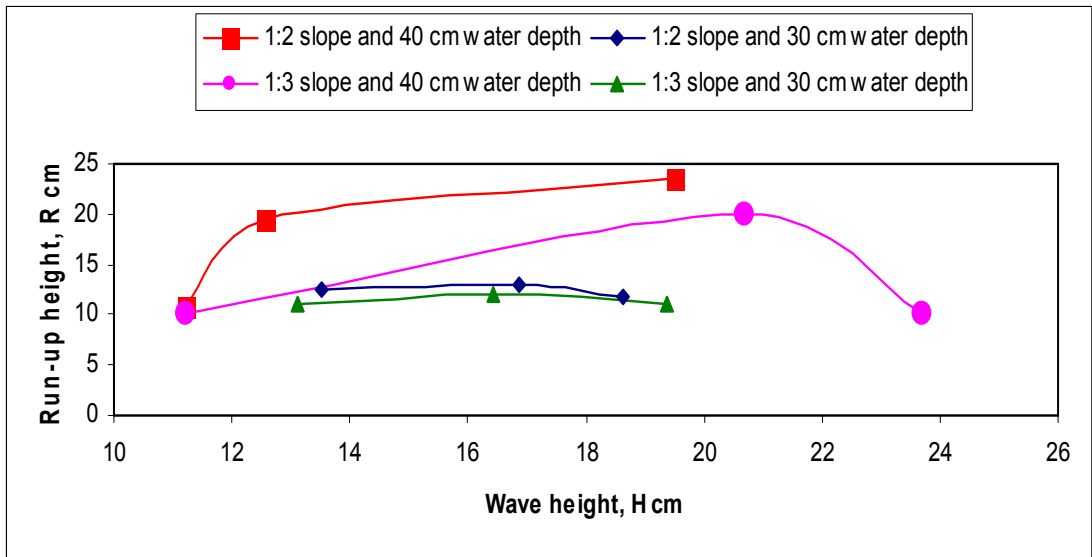


Figure 4.8.5: Comparisons between wave height and run-up height for CC block condition at various slope and water depth.

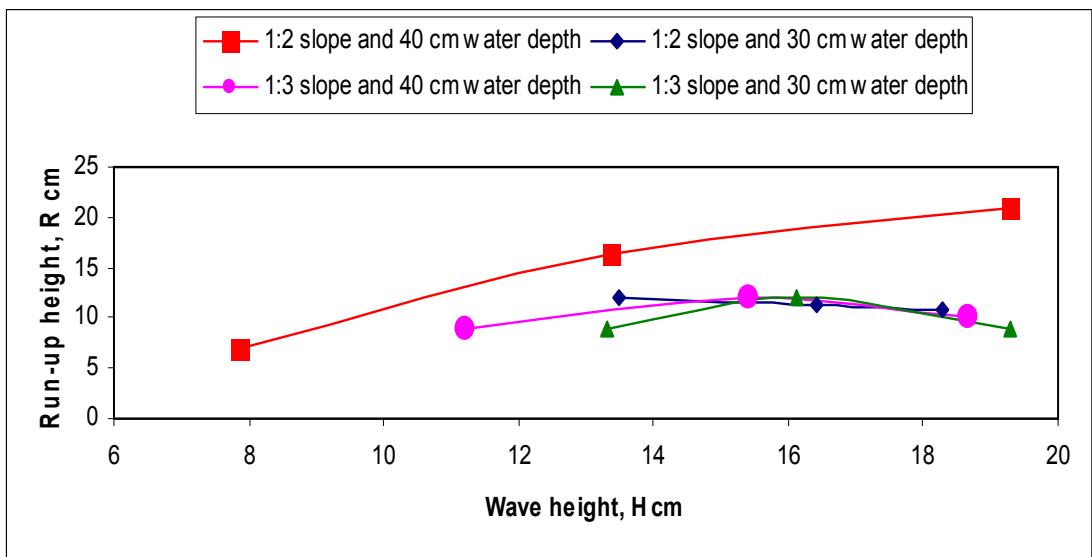


Figure 4.8.6: Comparisons between wave height and run-up height for submerged breakwater condition at various slope and water depth.

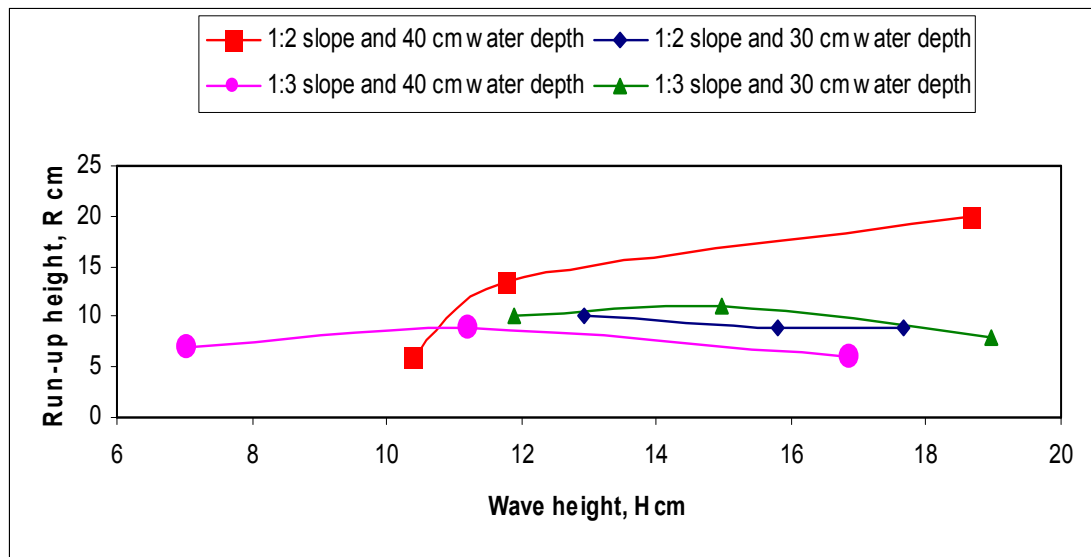


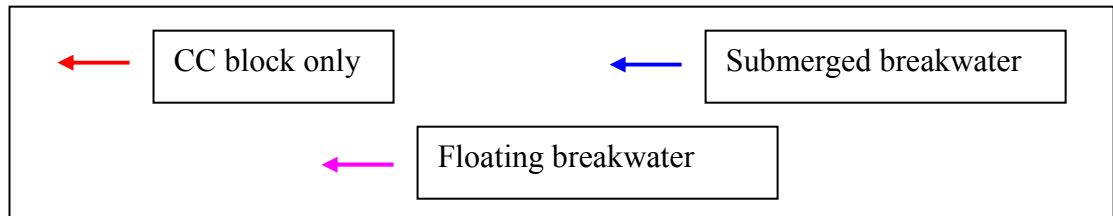
Figure 4.8.7: Comparisons between wave height and run-up height for floating breakwater condition at various slope and water depth.

4.9 Change in Velocity for different loading condition

Two velocity components, namely stream wise velocity (V_x) and transverse velocity (V_y) have been measured at pre-defined point and selected depths with a programmable electromagnetic velocity meter (P-EMS) before the bank slope apart from three distances of toe. To evaluate changes in flow field for variable water depths, bank slope and length-width ratio in three different distance point from toe, comparison has been shown in longitudinal and lateral directions respectively. For longitudinal direction, velocity data at 3R (3*Run-up Height) (cm away from toe), 6R and 9R were considered. Beside these, velocity vector diagrams (produced by Stanford Graphics software) have been presented to examine velocity changes in different loading condition.

In these diagrams it has been found that, velocities on CC blocks only are largest which were decreased by dissipating wave energy through breakwater condition. Floating breakwater has dissipated maximum energy resulting lowest velocity of water particle. Figure 4.9.1 to Figure 4.9.3, Figure 4.9.4 to Figure 4.9.6, Figure 4.9.7 to Figure 4.9.9 and Figure 4.9.10 to Figure 4.9.12 show velocity vectors for two bank slopes (1:2 and 1:3), three wave periods (1, 2, 2.5) and two water depths (40 cm and

30 cm for each) condition. Each diagram illustrates three velocity vectors for three conditions; CC block only, submerged and floating breakwater condition; which are expressed through three different colours. The colors representing three loading conditions are shown in the following diagram.



Comparing with the magnitude of velocity vectors in diagrams, it is observed that larger magnitude are for CC blocks condition, less for submerged condition and lowest for floating condition. So it is clear to say floating breakwater dissipated more energy than others and decreased the wave velocities.

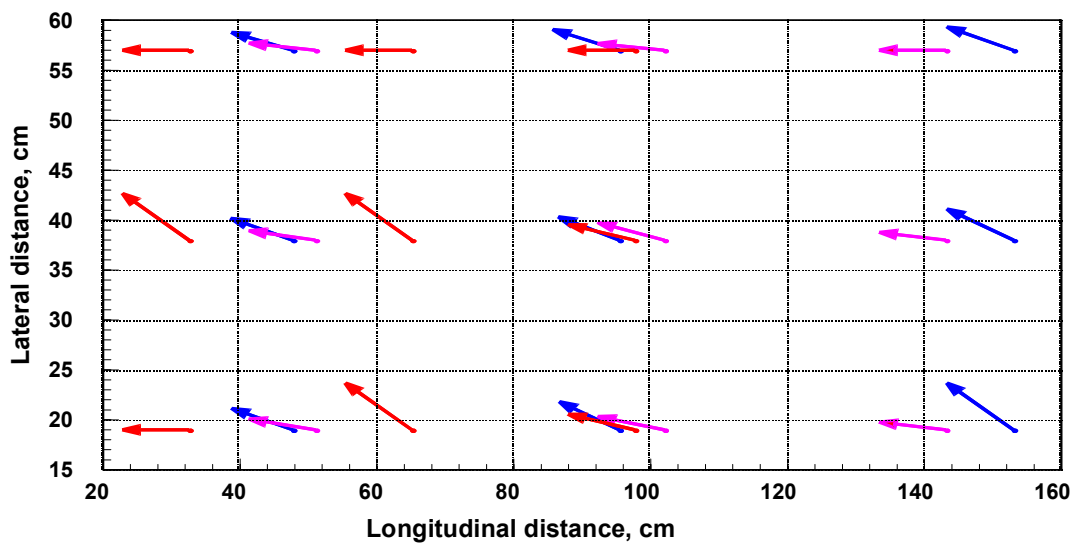


Figure 4.9.1: Velocity vector for 1:2 slope, 1 sec wave period and 40 cm water depth at 3R, 6R and 9R distance from the toe.

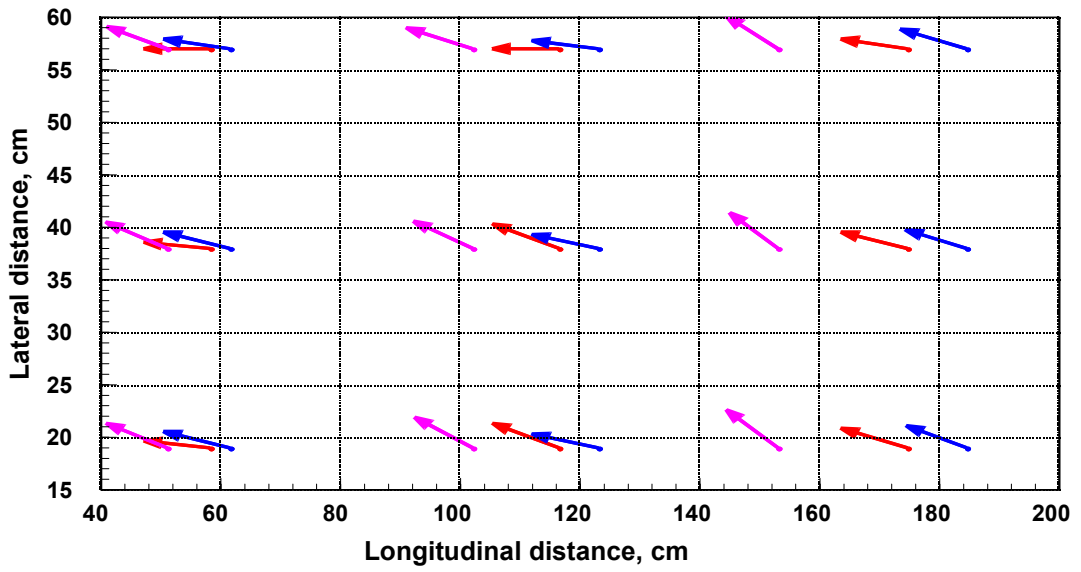


Figure 4.9.2: Velocity vector for 1:2 slope, 2 sec wave period and 40 cm water depth at 3R, 6R and 9R distance from the toe.

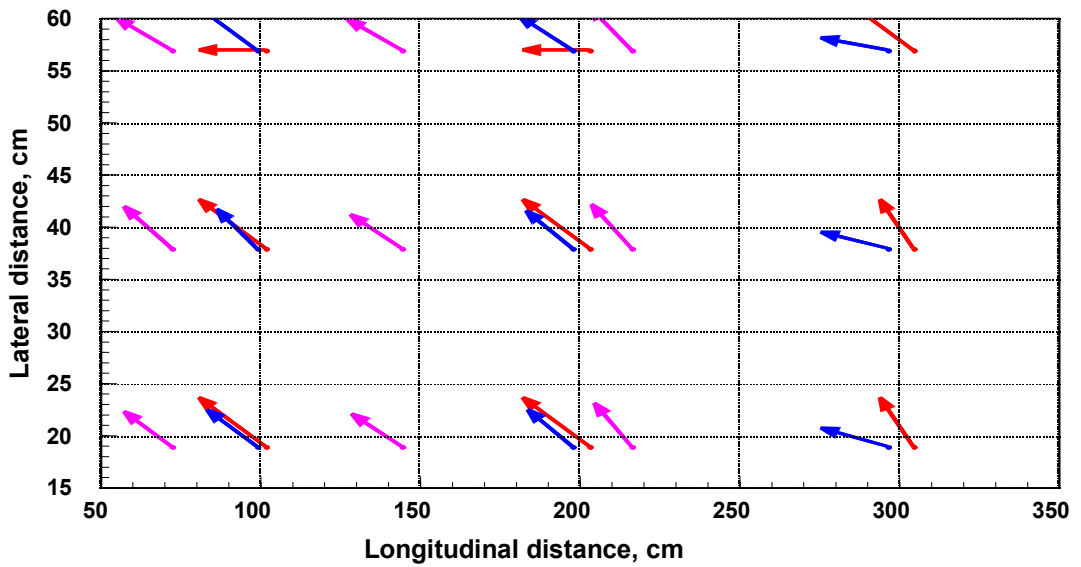


Figure 4.9.3: Velocity vector for 1:2 slope, 2.5 sec wave period and 40 cm water depth at 3R, 6R and 9R distance from the toe.

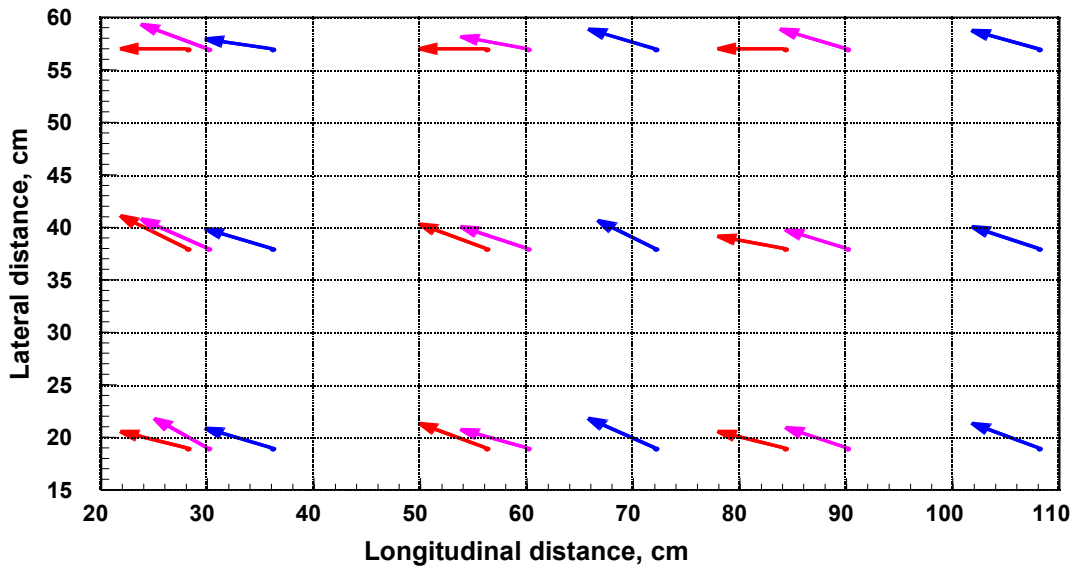


Figure 4.9.4: Velocity vector for 1:2 slope, 1 sec wave period and 30 cm water depth at 3R, 6R and 9R distance from the toe.

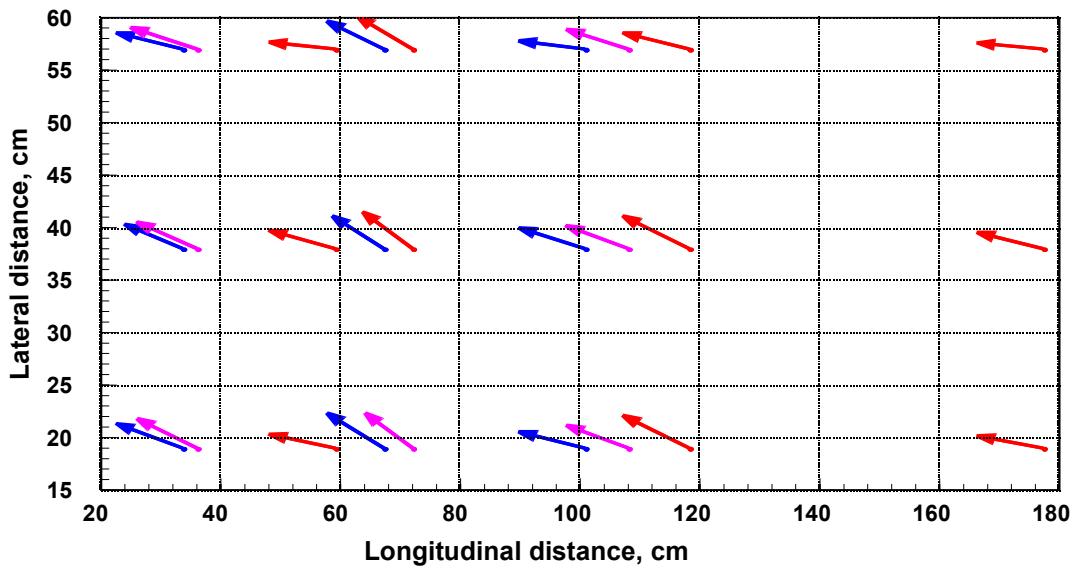


Figure 4.9.5: Velocity vector for 1:2 slope, 2 sec wave period and 30 cm water depth at 3R, 6R and 9R distance from the toe.

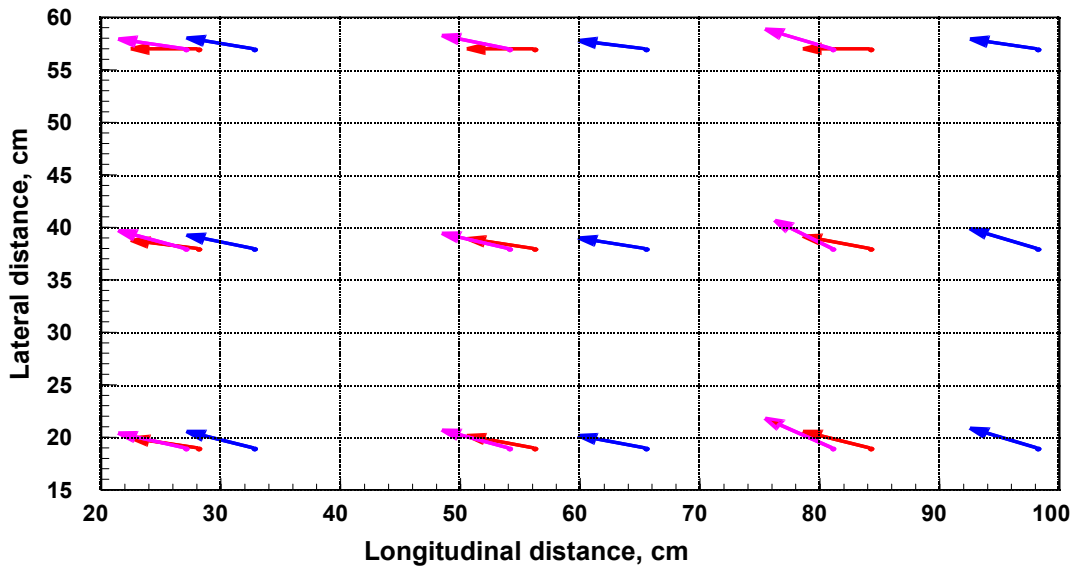


Figure 4.9.6: Velocity vector for 1:2 slope, 2.5 sec wave period and 30 cm water depth at 3R, 6R and 9R distance from the toe.

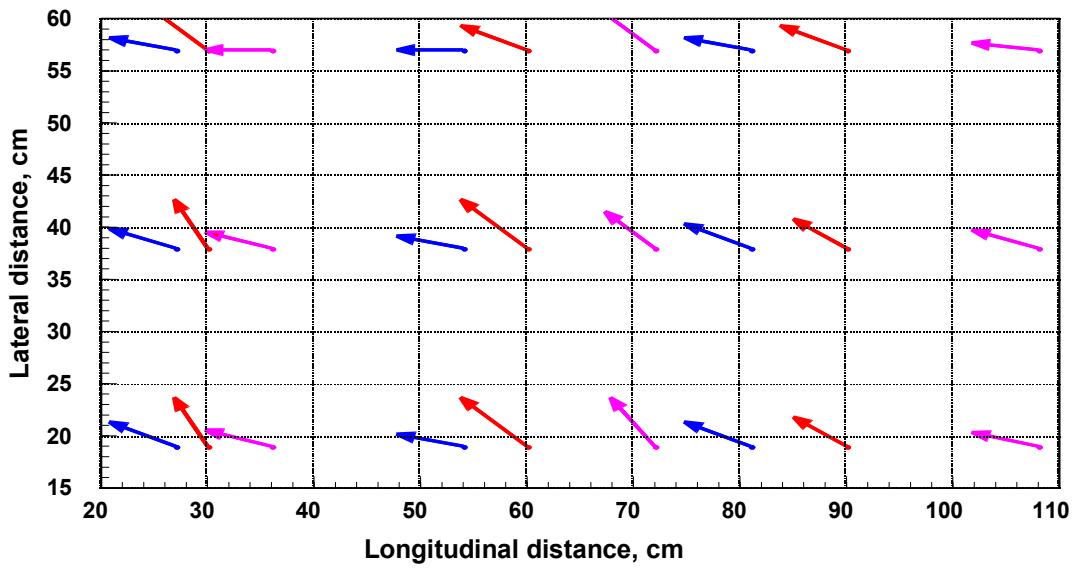


Figure 4.9.7: Velocity vector for 1:3 slope, 1 sec wave period and 40 cm water depth at 3R, 6R and 9R distance from the toe.

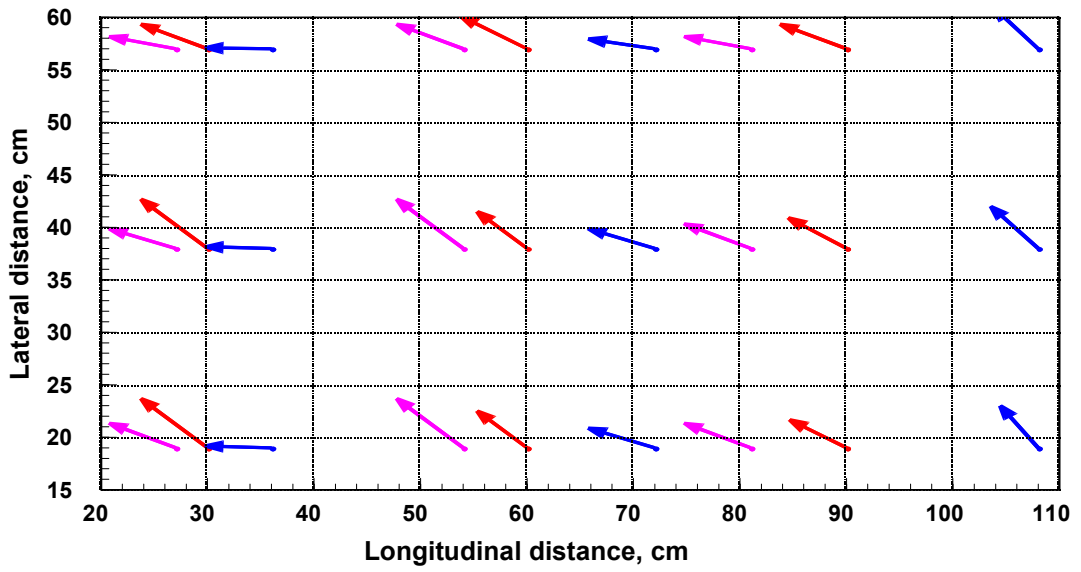


Figure 4.9.8: Velocity vector for 1:3 slope, 2 sec wave period and 40 cm water depth at 3R, 6R and 9R distance from the toe.

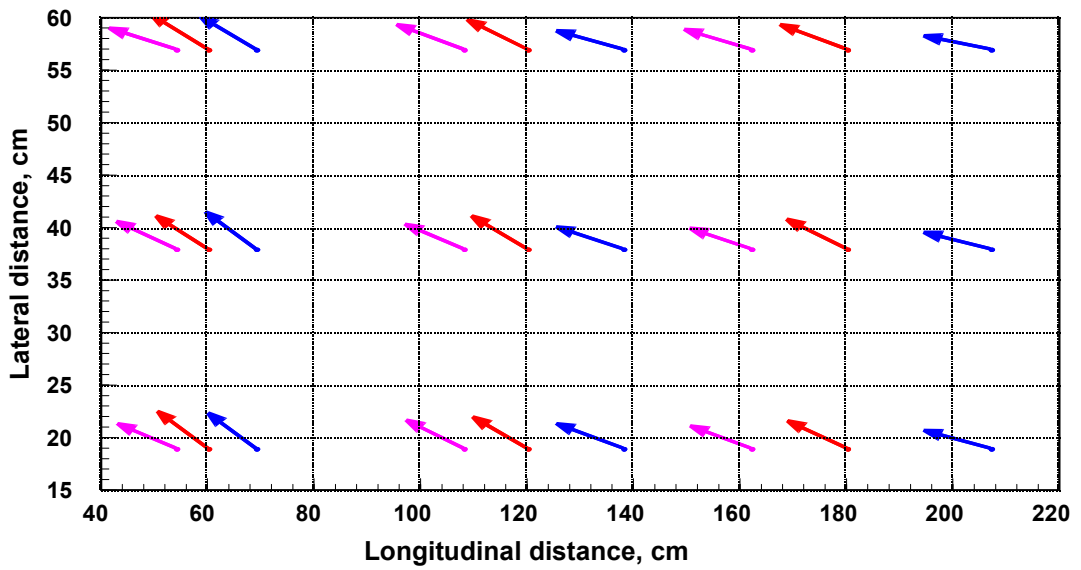


Figure 4.9.9: Velocity vector for 1:3 slope, 2.5 sec wave period and 40 cm water depth at 3R, 6R and 9R distance from the toe.

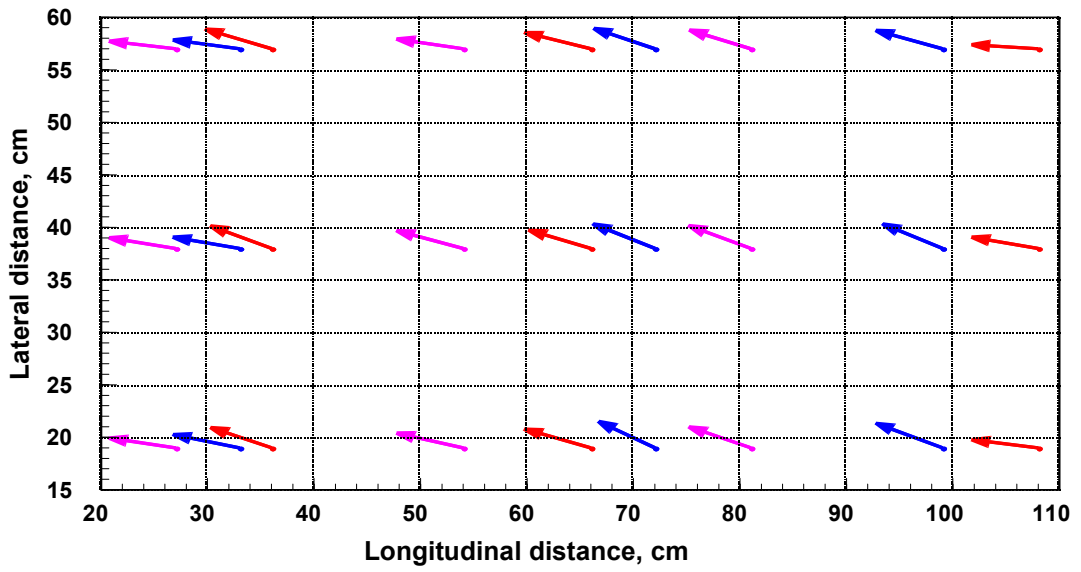


Figure 4.9.10: Velocity vector for 1:3 slope, 1 sec wave period and 30 cm water depth at 3R, 6R and 9R distance from the toe.

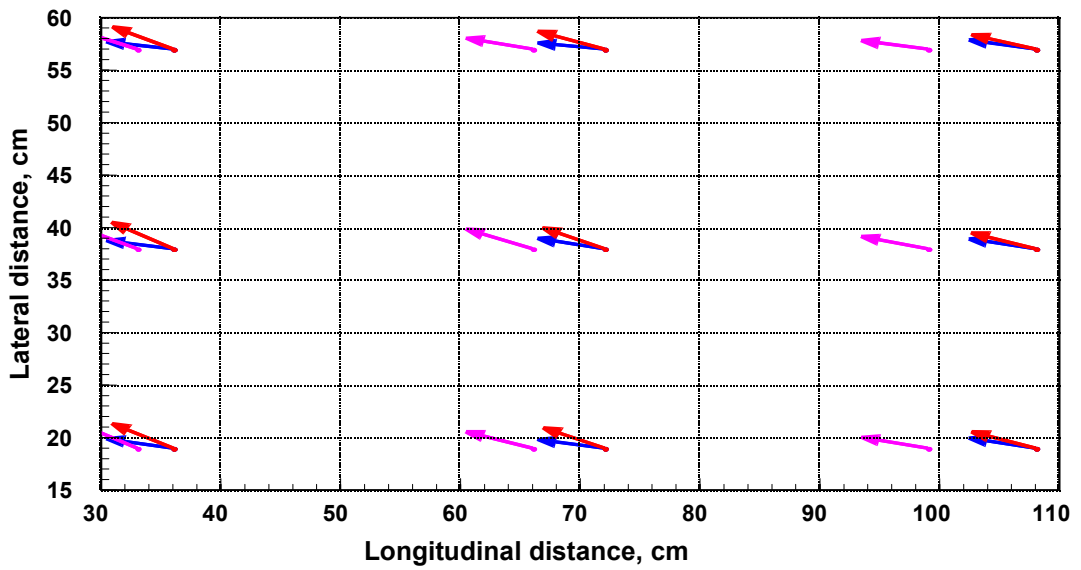


Figure 4.9.11: Velocity vector for 1:3 slope, 2 sec wave period and 30 cm water depth at 3R, 6R and 9R distance from the toe.

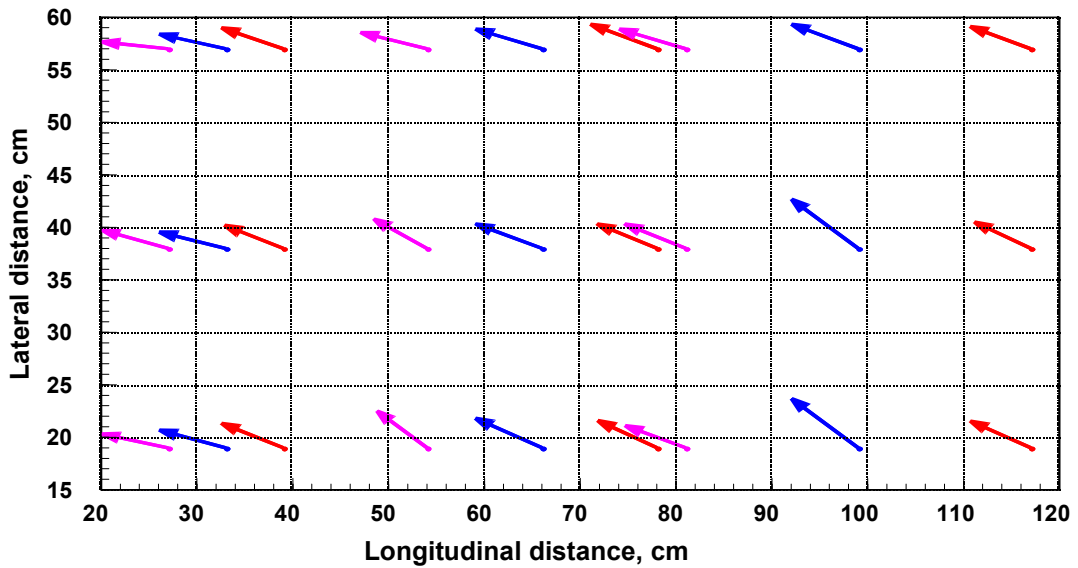


Figure 4.9.12: Velocity vector for 1:3 slope, 2.5 sec wave period and 30 cm water depth at 3R, 6R and 9R distance from the toe.

In the figure 4.9.1 to 4.9.12 the velocity values used are average values. Velocity was measured at three lateral positions of the flume. The positions were, 19 cm from each side wall and at the centre. Two ends velocity vectors shown in the figures were small in magnitude than the centrally shown vectors. This was due to the friction of side wall which had reduced the values.

Measured velocities data at 3R (3*run-up height), 6R and 9R points for various loading conditions have been plotted which is shown in Appendix B (central position data were shown only). At each point 20 actual velocity data were taken. The figures shown in Appendix B illustrate that the magnitude of velocities were decreased at the nearest distance from toe. That is, at 3R distance the velocities were small in magnitude, at 6R distance they were more and at 9R distance they were larger than others two. When breakwater was used, these values were reduced further more. Floating position of breakwater was reduced the values more than the other two.

The actual velocity data measured at the centre of the flume were shown in the Table 4.9.1 to Table 4.9.4 for different sloping and water depth conditions.

Table 4.9.1: The velocities (m/s) measured for various conditions for 1:2 slope and 40 cm water depth.

Slope	Water depth, d (cm)	Conditions	Wave periods, T (sec)	Point of velocity measurement	Velocity, V (m/sec)
1:2	40	CC block only	1	3R	0.015129
				6R	0.018319
				9R	0.040723
			2	3R	0.161852
				6R	0.042458
				9R	0.102995
			2.5	3R	0.031596
				6R	0.055663
				9R	0.051442
		Submerged breakwater	1	3R	0.238599
				6R	0.13657
				9R	0.056204
			2	3R	0.129077
				6R	0.129603
				9R	0.232459
			2.5	3R	0.106281
				6R	0.314283
				9R	0.326005
		Floating breakwater	1	3R	0.230035
				6R	0.178373
				9R	0.106468
			2	3R	0.242605
				6R	0.144904
				9R	0.160918
			2.5	3R	0.193331
				6R	0.352311
				9R	0.236588

Table 4.9.2: The velocities (m/s) measured for various conditions for 1:2 slope and 30 cm water depth.

Slope	Water depth, d (cm)	Conditions	Wave periods, T (sec)	Point of velocity measurement	Velocity, V (m/sec)
1:2	30	CC block only	1	3R	0.038741
				6R	0.026035
				9R	0.038683
			2	3R	0.141328
				6R	0.06356
				9R	0.171293
			2.5	3R	0.054694
				6R	0.048165
				9R	0.031091
		Submerged breakwater	1	3R	0.052467
				6R	0.072176
				9R	0.093067
			2	3R	0.134558
				6R	0.142927
				9R	0.120722
			2.5	3R	0.103303
				6R	0.128366
				9R	0.054557
		Floating breakwater	1	3R	0.061727
				6R	0.104759
				9R	0.12621
			2	3R	0.21655
				6R	0.128682
				9R	0.296219
2.5	3R		0.115557		
	6R		0.129461		
	9R		0.069741		

Table 4.9.3: The velocities (m/s) measured for various conditions for 1:3 slope and 40 cm water depth.

Slope	Water depth, d (cm)	Conditions	Wave periods, T (sec)	Point of velocity measurement	Velocity, V (m/sec)
1:3	40	CC block only	1	3R	0.021374
				6R	0.032027
				9R	0.046553
			2	3R	0.027714
				6R	0.044523
				9R	0.073791
			2.5	3R	0.173694
				6R	0.237642
				9R	0.192888
		Submerged breakwater	1	3R	0.055923
				6R	0.051469
				9R	0.042649
			2	3R	0.062024
				6R	0.065828
				9R	0.501275
			2.5	3R	0.142635
				6R	0.209559
				9R	0.240339
		Floating breakwater	1	3R	0.028239
				6R	0.040328
				9R	0.07646
			2	3R	0.055119
				6R	0.033305
				9R	0.040062
2.5	3R		0.172032		
	6R		0.158298		
	9R		0.222278		

Table 4.9.4: The velocities (m/s) measured for various conditions for 1:3 slope and 30 cm water depth.

Slope	Water depth, d (cm)	Conditions	Wave periods, T (sec)	Point of velocity measurement	Velocity, V (m/sec)
1:3	30	CC block only	1	3R	0.128435
				6R	0.151455
				9R	0.135462
			2	3R	0.226264
				6R	0.173977
				9R	0.465516
			2.5	3R	0.189132
				6R	0.11044
				9R	0.144471
		Submerged breakwater	1	3R	0.244702
				6R	0.126153
				9R	0.152
			2	3R	0.131865
				6R	0.126821
				9R	0.296271
			2.5	3R	0.101489
				6R	0.04762
				9R	0.139441
		Floating breakwater	1	3R	0.140058
				6R	0.164198
				9R	0.099615
			2	3R	0.089204
				6R	0.094366
				9R	0.185844
2.5	3R		0.140409		
	6R		0.067798		
	9R		-		

4.10 Analysis of Force on embankment

In this research work, static loads were calculated from Equation 3.2.2 and total loads were calculated by using Equation 3.2.5 stated earlier at the section 3.2.9. So, the dynamic load is the difference between total load and static load. Table 4.10.1 and Table 4.10.2 present static load, total load and dynamic load values for different conditions like slope, wave periods and depths; when reflection coefficient $\chi = 1$.

Table 4.10.1: Magnitude of loads for 1:2 bank slope, when $\chi = 1$

Condition	Slope	Wave period, T (sec)	Depth, d (cm)	Static load, F_s (kN/m)	Total load, F (kN/m)	Dynamic load, F_d (kN/m)	
CC	1:2	0.858192	40	0.8	1.162019	0.464	
		1.514456		0.8	1.436654	0.816	
		1.89307		0.8	1.898541	1.408	
Submerged breakwater		0.80771		0.8	0.954794	0.1984	
		1.403396		0.8	1.424171	0.8	
		1.817348		0.8	1.798673	1.28	
Floating breakwater		0.787517		0.8	0.999735	0.256	
		1.262047		0.8	1.286853	0.624	
		1.675998		0.8	1.761223	1.232	
CC		1:2	1.282412	30	0.45	0.976644	0.675
			1.492261		0.45	1.14517	0.891
			1.667136		0.45	1.257521	1.035
Submerged breakwater	1.189146		0.45		0.99771	0.702	
	1.445628		0.45		1.131126	0.873	
	1.632161		0.45		1.236455	1.008	
Floating breakwater	1.037588		0.45		0.836206	0.495	
	1.29407		0.45		1.011754	0.72	
	1.585527		0.45		1.194324	0.954	

Table 4.10.2: Magnitude of loads for 1:3 bank slope when, $\chi = 1$

Condition	Slope	Wave period, T (sec)	Depth, d (cm)	Static load, F_s (kN/m)	Total load, F (kN/m)	Dynamic load, F_d (kN/m)
CC	1:3	1.009638	40	0.8	0.855553	0.096
		1.272143		0.8	1.429595	1.088
		1.494264		0.8	1.707358	1.568
Submerged breakwater		0.999541		0.8	1.077763	0.48
		1.211565		0.8	1.253679	0.784
		1.363011		0.8	1.438854	1.104
Floating breakwater		0.964204		0.8	1.003693	0.352
		1.17118		0.8	1.074059	0.4736
		1.332722		0.8	1.374043	0.992
CC		0.874372	30	0.45	0.658322	0.36
		1.095879		0.45	0.824979	0.648
		1.288241		0.45	0.976013	0.909
Submerged breakwater	0.781105	0.45		0.611449	0.279	
	0.973467	0.45		0.741651	0.504	
	1.200804	0.45		0.908308	0.792	
Floating breakwater	0.769447	0.45		0.595825	0.252	
	0.932663	0.45		0.68957	0.414	
	1.165829	0.45		0.887476	0.756	

The reflection co-efficient depends on the geometry and roughness of the reflecting wall and possible wave steepness and the “wave height to water depth” ratio. Domzig, Greslou (1955) and Mahe (1954) have shown that the reflection coefficient decrease with both increasing wave steepness and “wave height to water depth” ratio. Goda and Abe (1968) indicate that for reflection from smooth vertical wall this effect may be due to measurement techniques and could be only an apparel effect. Until additional research is available, it should be assumed that smooth walls completely

reflect incident wave and $\chi = 1$. A lower value of λ may be assumed when the embankment is built on a rubble base but any value of χ less than 0.9 should not be used for design purpose. (SPM, 1984)

As χ can not be less than 0.9, the loads were also calculated for the minimum value of $\chi = 0.9$, which were shown in Table 4.10.3 for 1:2 slope and Table 4.10.4 for 1:3 slope.

Table 4.10.3: Magnitude of loads for 1:2 bank slope, when $\chi = 0.9$

Condition	Slope	Wave period, T (sec)	Depth, d (cm)	Static load, F_s (kN/m)	Total load, F (kN/m)	Dynamic load, F_d (kN/m)
CC	1:2	0.858192	40	0.8	1.099602	0.384
		1.514456		0.8	1.399204	0.768
		1.89307		0.8	1.886057	1.392
Submerged breakwater		0.80771		0.8	0.939814	0.1792
		1.403396		0.8	1.399204	0.768
		1.817348		0.8	1.873574	1.376
Floating breakwater		0.787517		0.8	1.024702	0.288
		1.262047		0.8	1.23692	0.56
		1.675998		0.8	1.74874	1.216
CC		1.282412	30	0.45	0.941535	0.63
		1.492261		0.45	1.152192	0.9
		1.667136		0.45	1.264543	1.044
Submerged breakwater	1.189146	0.45		0.885359	0.558	
	1.445628	0.45		1.081973	0.81	
	1.632161	0.45		1.257521	1.035	
Floating breakwater	1.037588	0.45		0.801096	0.45	
	1.29407	0.45		1.018776	0.729	
	1.585527	0.45		1.194324	0.954	

Table 4.10.4: Magnitude of loads for 1:3 bank slope, when $\chi = 0.9$

Condition	Slope	Wave period, T (sec)	Depth, d (cm)	Static load, F_s (kN/m)	Total load, F (kN/m)	Dynamic load, F_d (kN/m)	
CC	1:3	1.009638	40	0.8	1.290714	0.848	
		1.272143		0.8	1.411078	1.056	
		1.494264		0.8	1.605511	1.392	
Submerged breakwater		0.999541		0.8	1.040728	0.416	
		1.211565		0.8	1.225903	0.736	
		1.363011		0.8	1.383301	1.008	
Floating breakwater		0.964204		0.8	0.901846	0.176	
		1.17118		0.8	1.09628	0.512	
		1.332722		0.8	1.374043	0.992	
CC		30	0.874372	30	0.45	0.653114	0.351
			1.095879		0.45	0.798939	0.603
			1.288241		0.45	0.939556	0.846
Submerged breakwater	0.781105		0.45		0.611449	0.279	
	0.973467		0.45		0.741651	0.504	
	1.200804		0.45		0.9031	0.783	
Floating breakwater	0.769447		0.45		0.606241	0.27	
	0.932663		0.45		0.697382	0.4275	
	1.165829		0.45		0.866644	0.72	

The total loads which pressed the embankment slope wall should be as less as possible. To reduce these loads, a breakwater was used at two positions (submerged and floating) in this experiment. The values of load in the tables shown that, the magnitudes of loads were small when the breakwater was used. From the tables it is also clear that loads were reduced more at floating breakwater condition than that of submerged. To ensure this statement value of total load were plotted on the graph with respect to the run number. Figure 4.10.1 to Figure 4.10.4 were representing the different loading conditions when reflection co-efficient was 1.

These figures showed that, wave loads were reduced for breakwater use. Floating breakwater condition had reduced the load more than submerged breakwater and CC block condition.

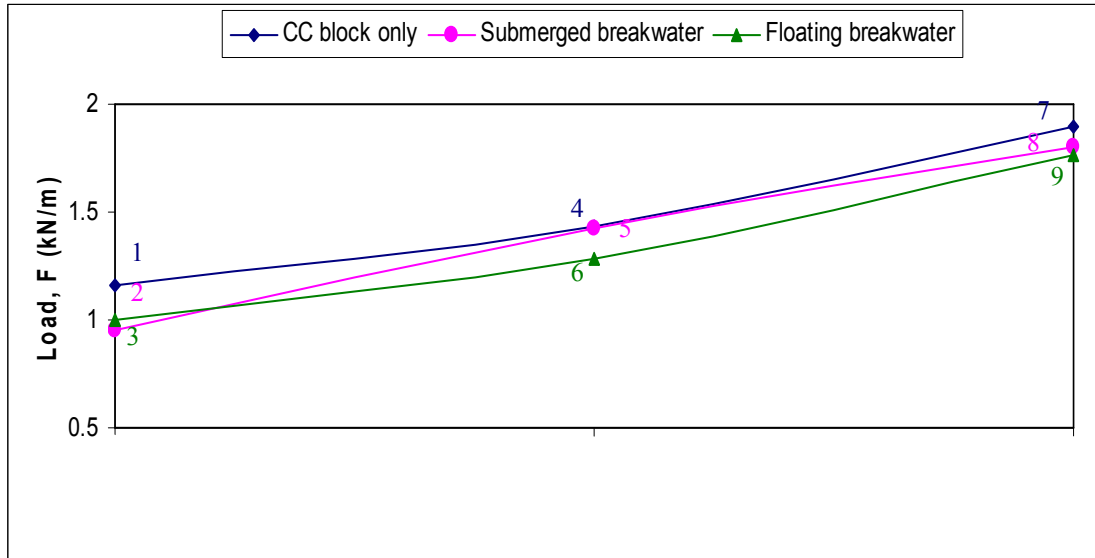


Figure 4.10.1: Variation of loads for 1:2 slope and 40 cm water depth, when $\chi = 1$.

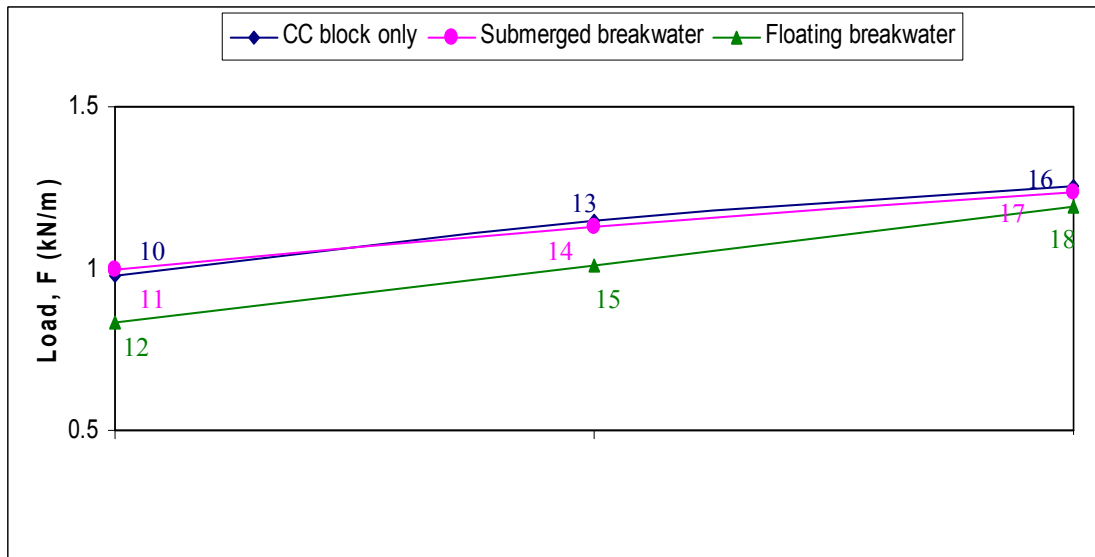


Figure 4.10.2: Variation of loads for 1:2 slope and 30 cm water depth, when $\chi = 1$.

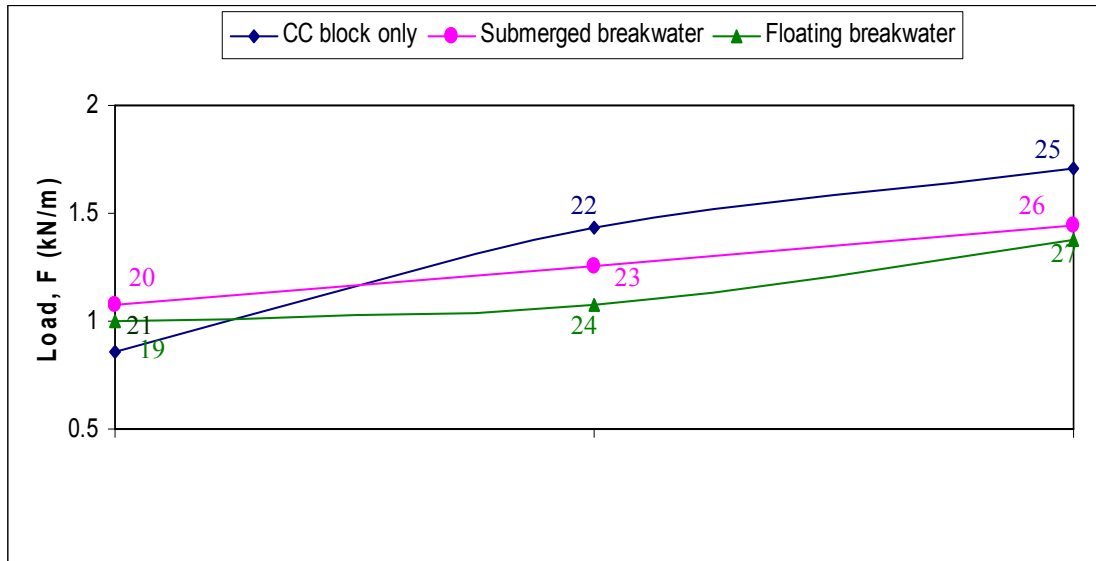


Figure 4.10.3: Variation of loads for 1:3 slope and 40 cm water depth, when $\chi = 1$.

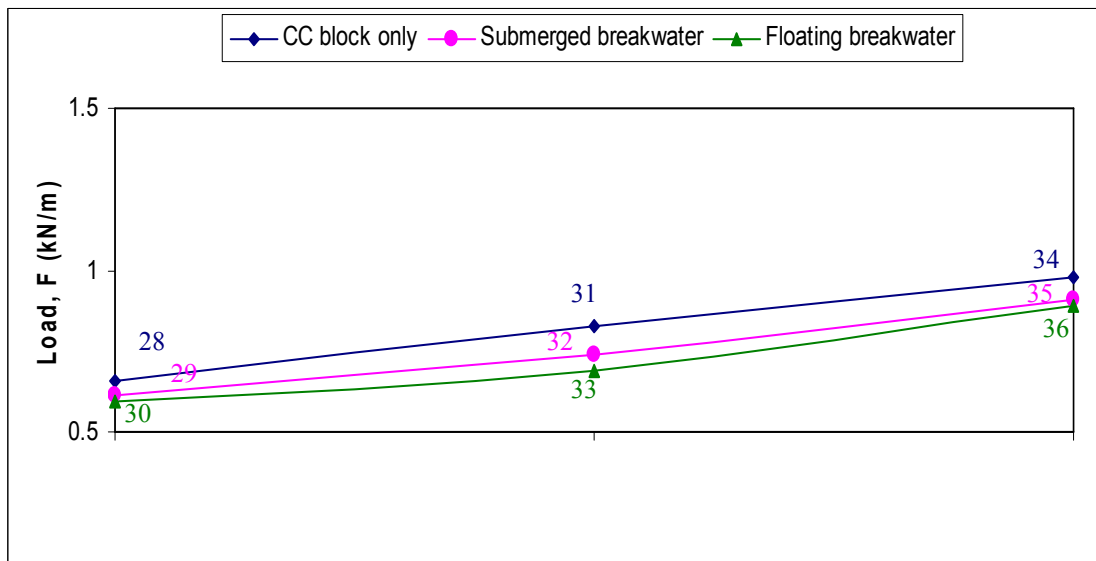


Figure 4.10.4: Variation of loads for 1:3 slope and 30 cm water depth, when $\chi = 1$.

Figure 4.10.5 to Figure 4.10.8 also conformed that, floating breakwater had reduced the wave load more successfully than that of other loading conditions when reflection co-efficient was 0.9.

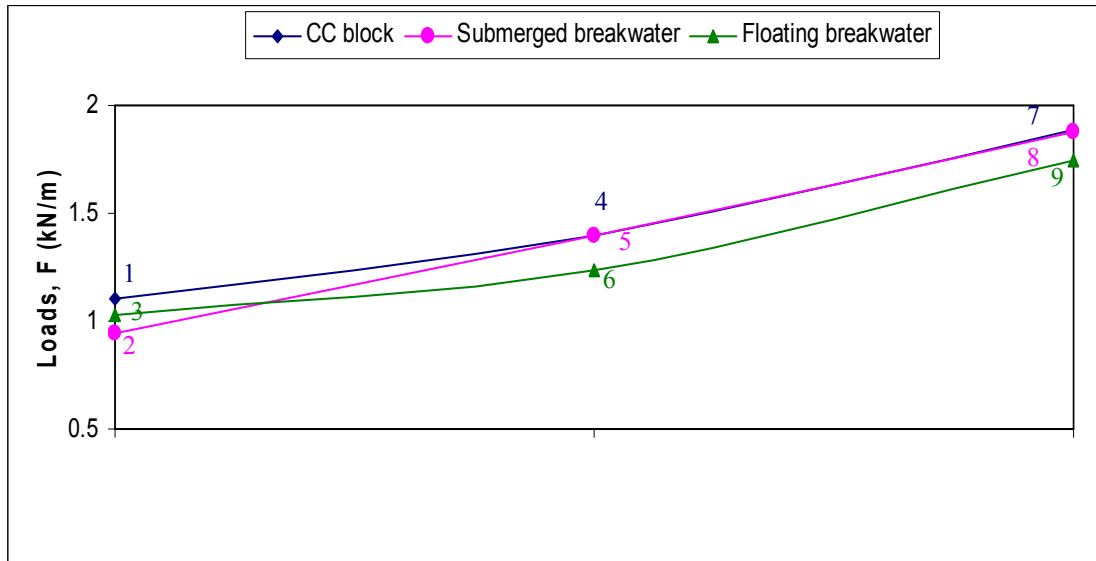


Figure 4.10.5: Variation of loads for 1:2 slope and 40 cm water depth, when $\chi = 0.9$.

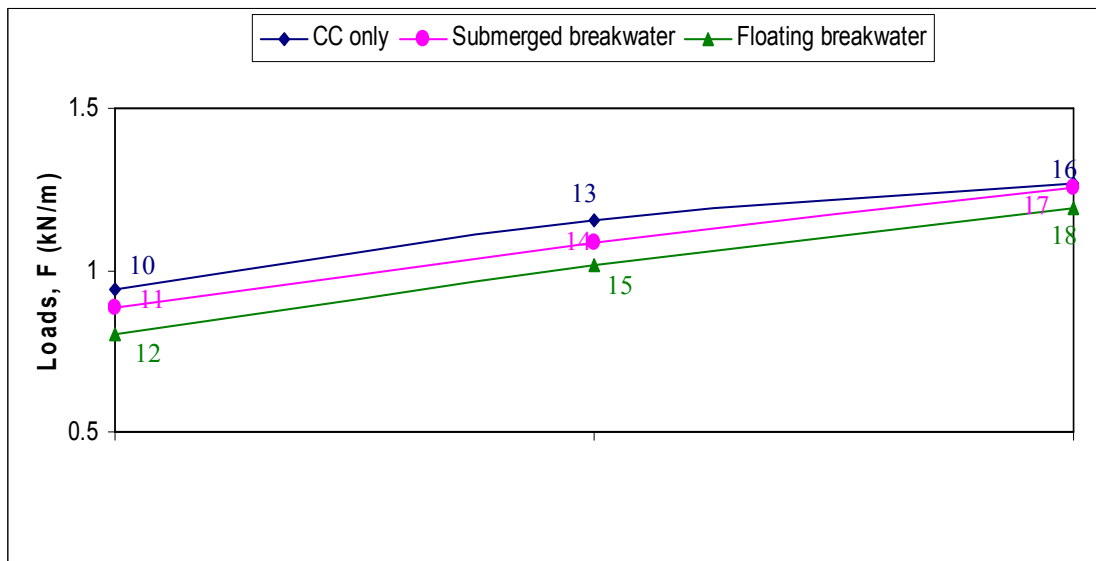


Figure 4.10.6: Variation of loads for 1:2 slope and 30 cm water depth, when $\chi = 0.9$.

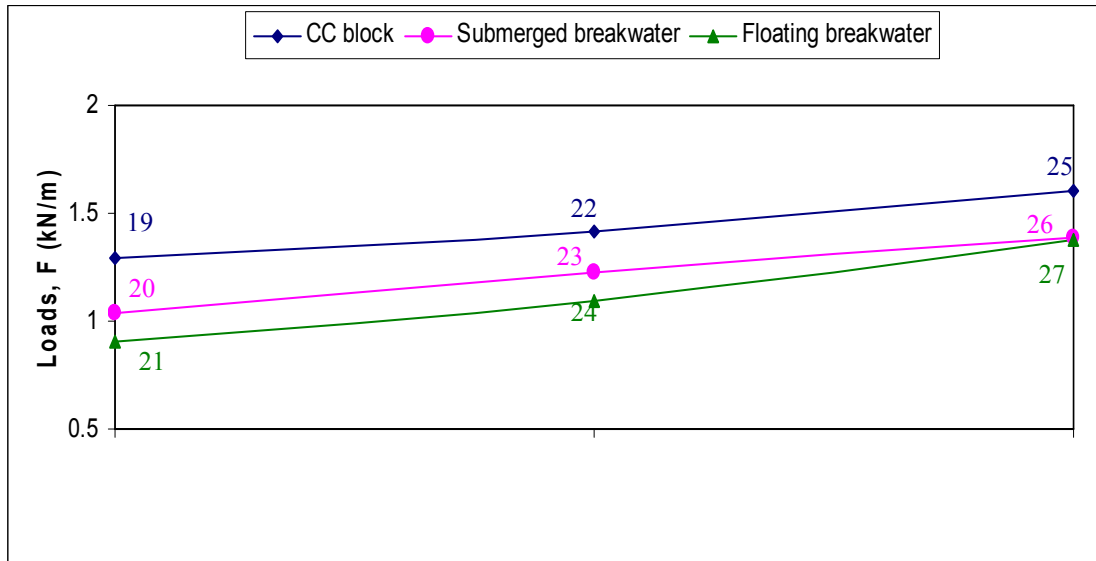


Figure 4.10.7: Variation of loads for 1:3 slope and 40 cm water depth, when $\chi = 0.9$.

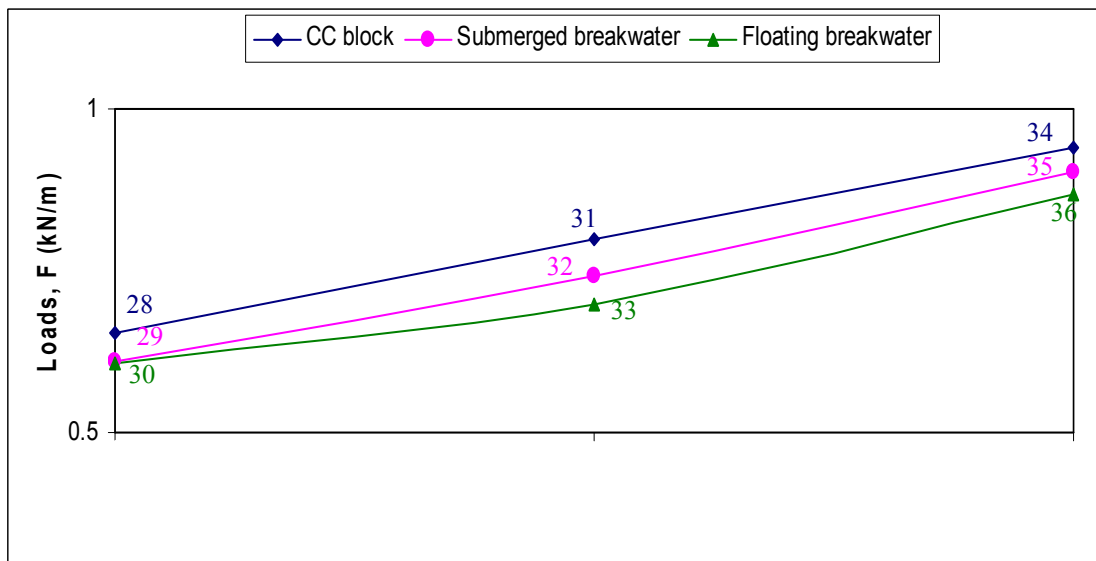


Figure 4.10.8: Variation of loads for 1:3 slope and 30 cm water depth, when $\chi = 0.9$.

So, both for $\chi = 1$ and $\chi = 0.9$ cases, it is clear that, floating breakwater is more effective than submerged breakwater condition and submerged breakwater is more effective than normal CC block condition in reducing wave loads.

Load values for three different loading conditions were plotted to observe the slope and water depth effect on the loads. Figure 4.10.9 to Figure 4.10.14 are showing different loading conditions for $\chi = 1$ & $\chi = 0.9$.

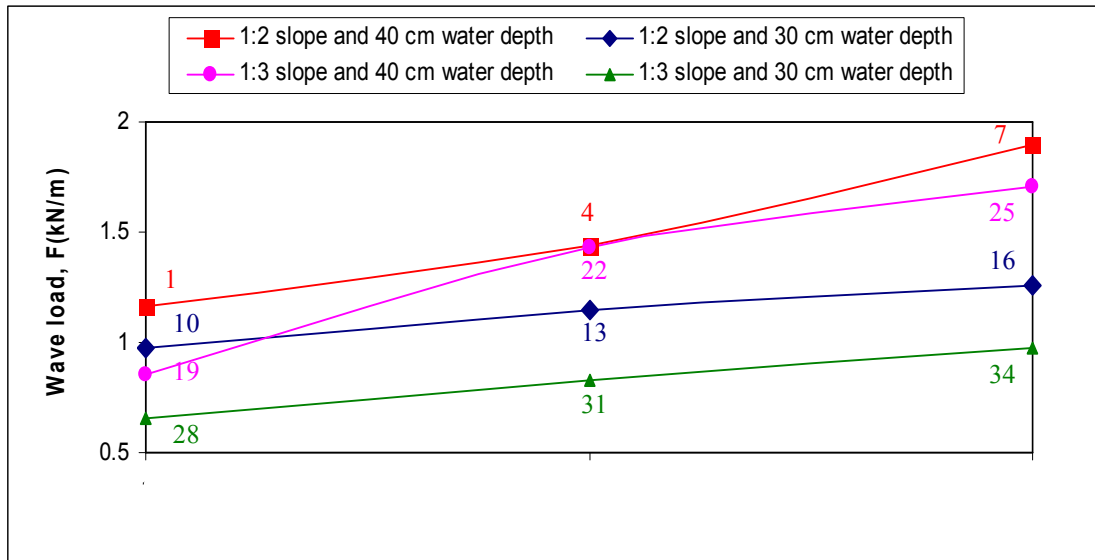


Figure 4.10.9: Comparison of wave load reduction for CC block with various slope and water depth condition, when $\chi = 1$.

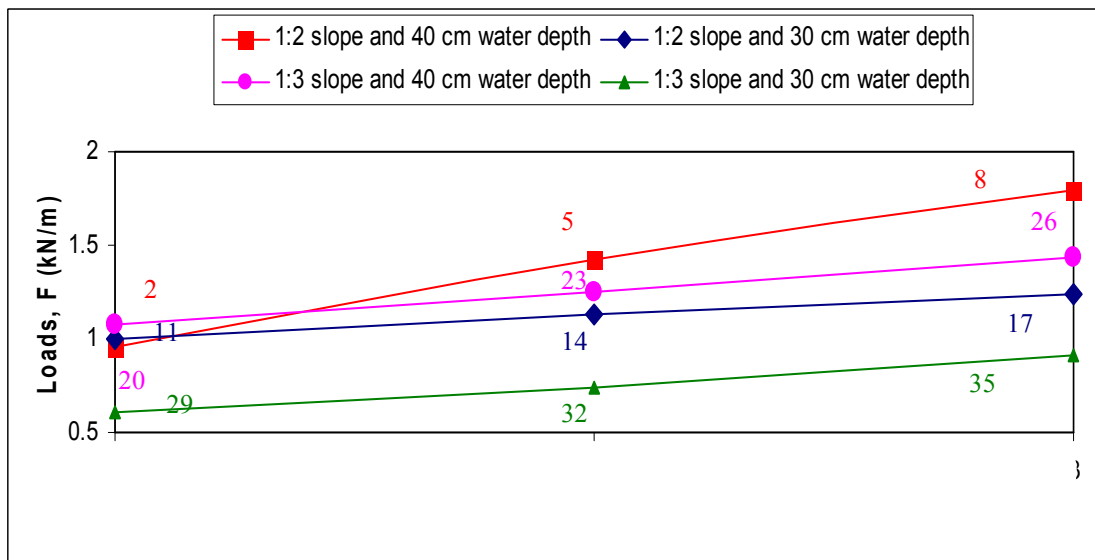


Figure 4.10.10: Comparison of wave load reduction for submerged breakwater with various slope and water depth condition, when $\chi = 1$.

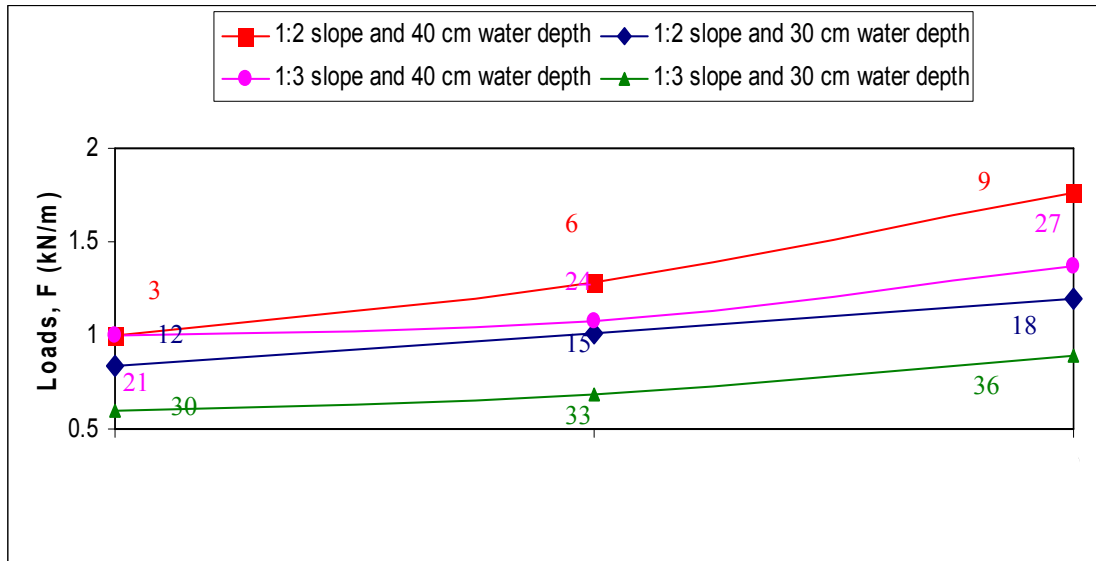


Figure 4.10.11: Comparison of wave load reduction for floating breakwater with various slope and water depth condition, when $\chi = 1$.

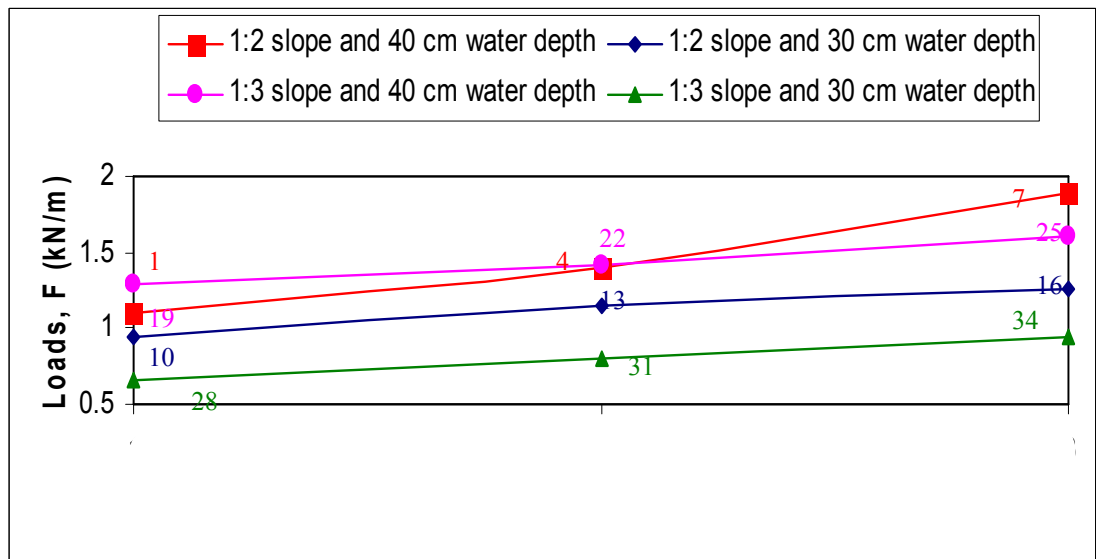


Figure 4.10.12: Comparison of wave load reduction for CC block with various slope and water depth condition, when $\chi = 0.9$.

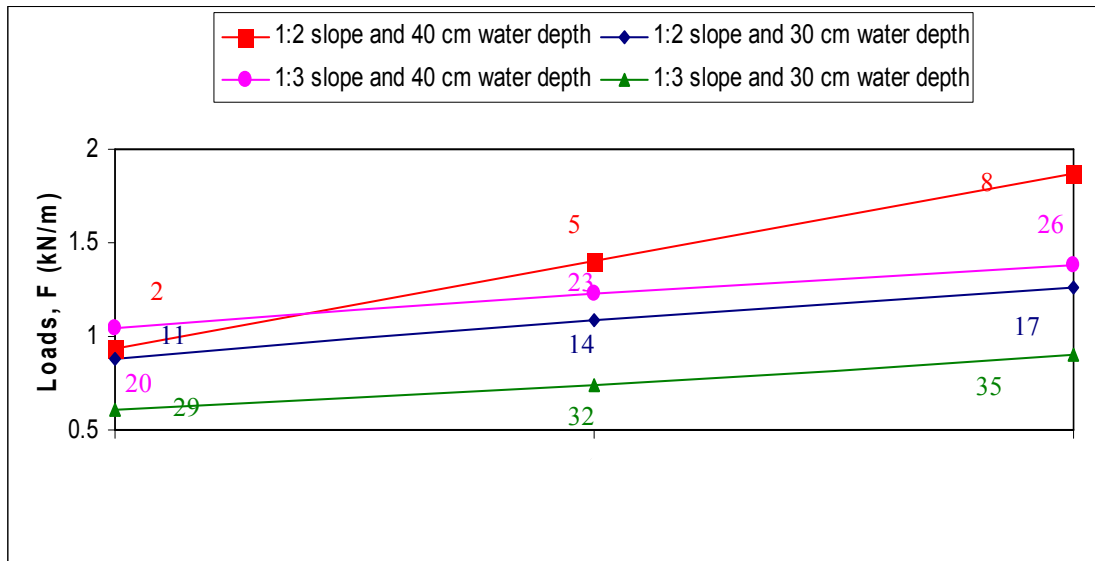


Figure 4.10.13: Comparison of wave load reduction for submerged breakwater with various slope and water depth condition, when $\chi = 0.9$.

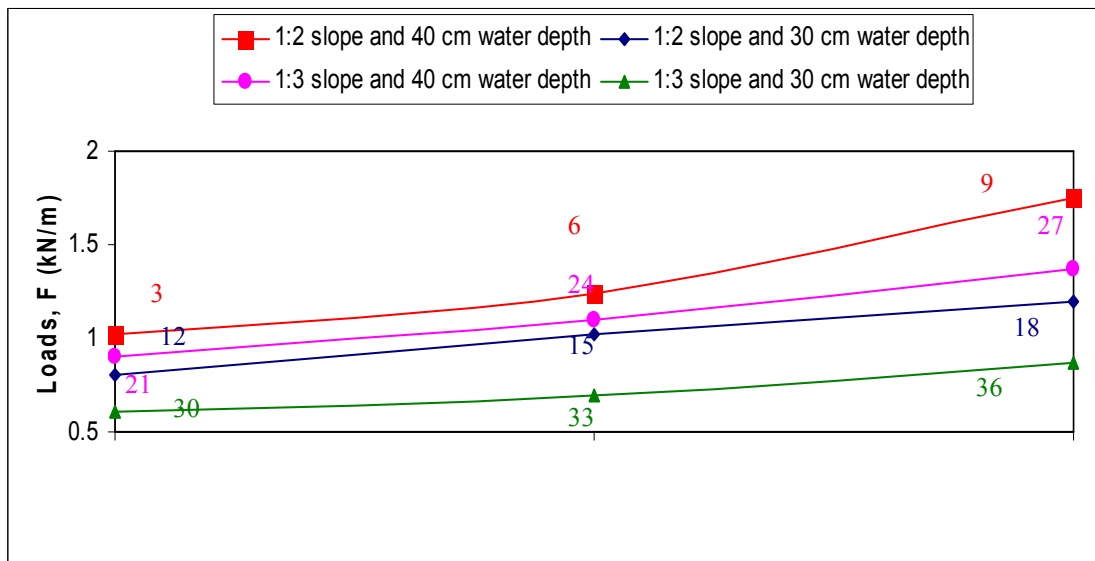


Figure 4.10.14: Comparison of wave load reduction for floating breakwater with various slope and water depth condition, when $\chi = 0.9$.

These figures showed that the loads were reduced due to embankment slope and water depth. Milder slope (1:3) have been reduced the loads than steeper (1:2) slope. Also, small water depth (30 cm) had reduced the values than that of larger water depth (40 cm).

4.11 Relation to Dynamic and Static load

Coastal structure must be designed to satisfy a number of sometimes conflicting criteria, including structural stability, functional performance, environmental impact, life cycle cost which adds challenges to any designers' task. It has been observed some embankments have catastrophic failure under wave loading (Navera and Nandi, 2007). Total wave load that interact with embankment wall includes static and dynamic loads. For coastal structure design, both static and dynamic loads should be considered.

So, Total wave load, $F = \text{Static load } (F_s) + \text{Dynamic load } (F_d)$.

There are some relation with total load and dynamic load; dynamic load and static load; total load and static load for different conditions are given in the tabular form below.

Table 4.11.1: Relation with Total force, static force and dynamic force, when $\chi = 1$

Condition	Slope	Depth, d (cm)	Ratio F_s/F	Ratio F_d/F	Ratio F_d/F_s
CC	1:2	40	0.688457	0.399305	0.58
			0.556849	0.567986	1.02
			0.421376	0.741622	1.76
Submerged breakwater			0.837877	0.207793	0.248
			0.56173	0.56173	1
			0.444772	0.711636	1.6
Floating breakwater			0.800212	0.256068	0.32
			0.621672	0.484904	0.78
			0.45423	0.699514	1.54
CC		30	0.460761	0.691142	1.5
			0.392955	0.77805	1.98
			0.357847	0.823048	2.3
Submerged breakwater	0.451033		0.703611	1.56	
	0.397834		0.771797	1.94	
	0.363944		0.815234	2.24	
Floating breakwater	0.538145		0.59196	1.1	
	0.444772		0.711636	1.6	
	0.376782		0.798778	2.12	

Table 4.11.2: Relation with Total force, static force and dynamic force, when $\chi = 1$

Condition	Slope	Depth, d (cm)	Ratio F_s/F	Ratio F_d/F	Ratio F_d/F_s
CC	1:3	40	0.935068	0.112208	0.12
			0.559599	0.761055	1.36
			0.46856	0.918378	1.96
Submerged breakwater			0.742279	0.445367	0.6
			0.638122	0.62536	0.98
			0.555998	0.767277	1.38
Floating breakwater			0.797057	0.350705	0.44
			0.744838	0.440944	0.592
			0.582224	0.721957	1.24
CC		30	0.683556	0.546845	0.8
			0.545468	0.785474	1.44
			0.46106	0.93134	2.02
Submerged breakwater	0.735956		0.456293	0.62	
	0.606755		0.679565	1.12	
	0.495427		0.871951	1.76	
Floating breakwater	0.755255		0.422943	0.56	
	0.65258		0.600374	0.92	
	0.507056		0.851854	1.68	

To relate with the wave height and dynamic load, values were plotted. Figure 4.11.1 to Figure 4.11.4 showed that, floating breakwater condition is the best suited to reduce dynamic loads and wave height as well. These figures were plotted using the values when reflection co-efficient was 1.

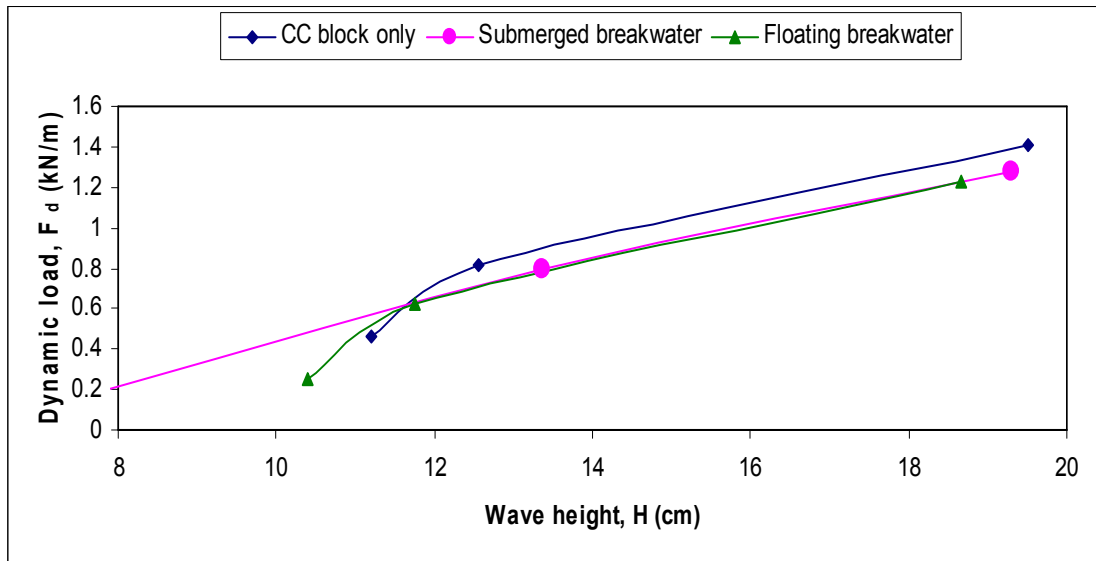


Figure 4.11.1: Dynamic load change with wave height for 1:2 slope and 40 cm water depth, when $\chi = 1$.

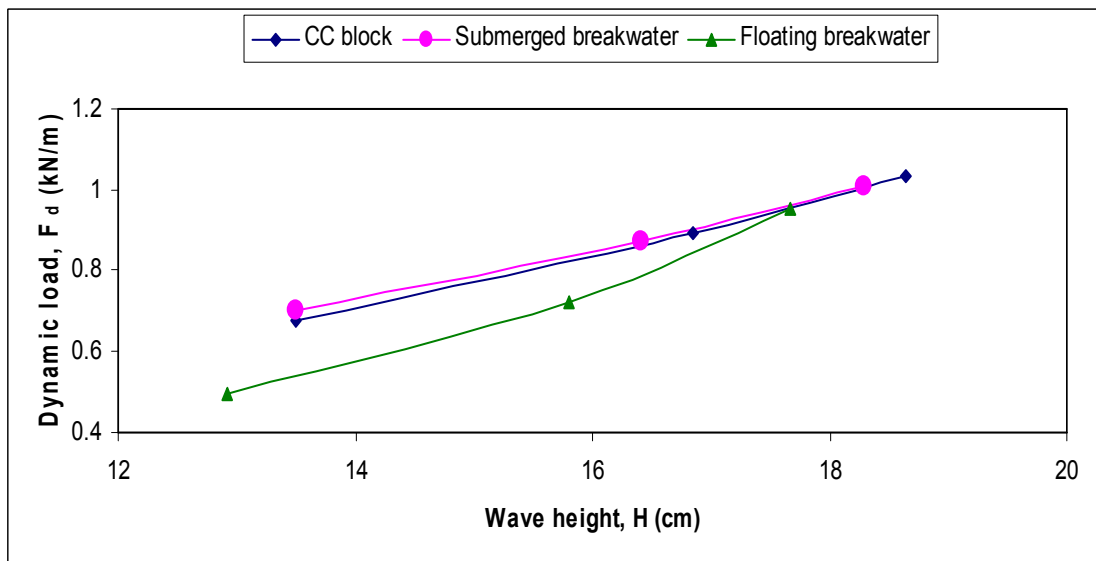


Figure 4.11.2: Dynamic load change with wave height for 1:2 slope and 30 cm water depth, when $\chi = 1$.

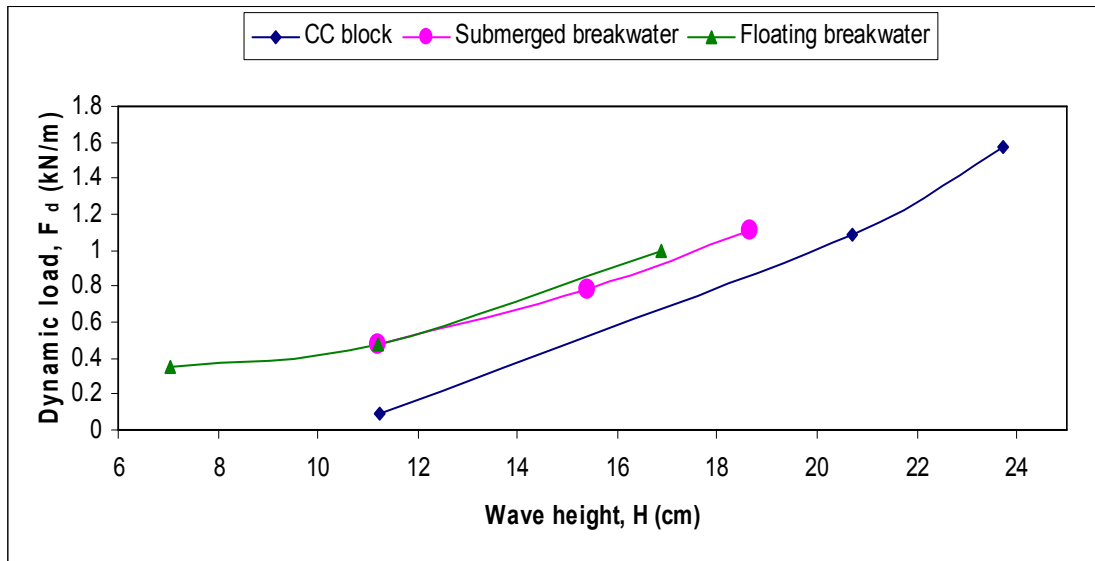


Figure 4.11.3: Dynamic load change with wave height for 1:3 slope and 40 cm water depth, when $\chi = 1$.

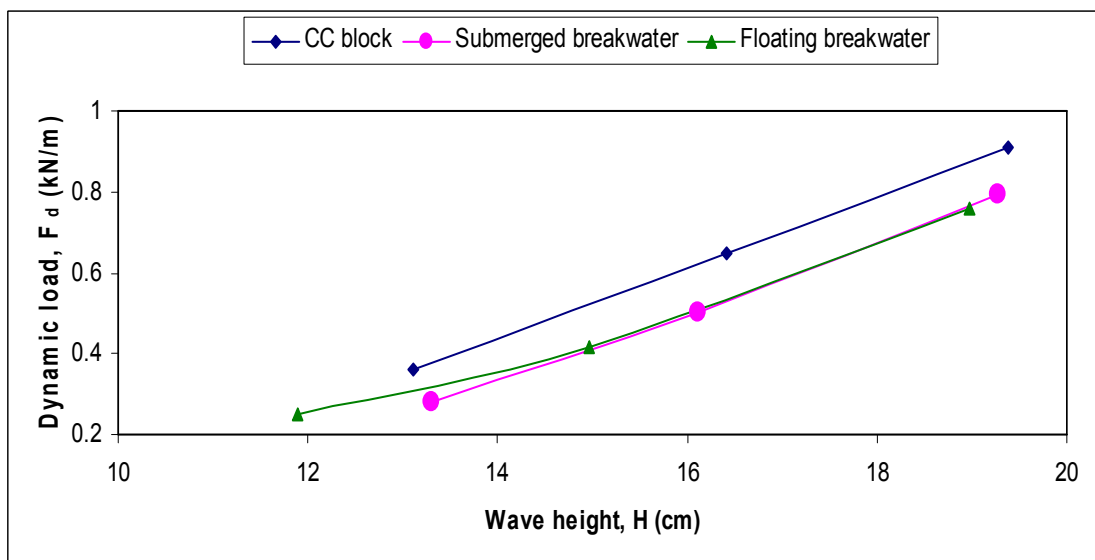


Figure 4.11.4: Dynamic load change with wave height for 1:3 slope and 30 cm water depth, when $\chi = 1$.

Table 4.11.3: Relation with Total force, static force and dynamic force, when

$$\chi = 0.9$$

Condition	Slope	Depth, d (cm)	Ratio F_s/F	Ratio F_d/F	Ratio F_d/F_s
CC	1:2	40	0.727536	0.349217	0.48
			0.571754	0.548884	0.96
			0.424165	0.738048	1.74
Submerged breakwater			0.851232	0.190676	0.224
			0.571754	0.548884	0.96
			0.426991	0.734425	1.72
Floating breakwater		0.780715	0.281057	0.36	
		0.646768	0.452738	0.7	
		0.457472	0.695358	1.52	
CC		30	0.477943	0.66912	1.4
			0.39056	0.78112	2
			0.35586	0.825595	2.32
Submerged breakwater	0.508268		0.630253	1.24	
	0.415907		0.748632	1.8	
	0.357847		0.823048	2.3	
Floating breakwater	0.56173		0.56173	1	
	0.441707		0.715565	1.62	
	0.376782		0.798778	2.12	

Table 4.11.4: Relation with Total force, static force and dynamic force, when

$$\chi = 0.9$$

Condition	Slope	Depth, d (cm)	Ratio F_s/F	Ratio F_d/F	Ratio F_d/F_s
CC	1:3	40	0.619812	0.657001	1.06
			0.566943	0.748364	1.32
			0.498284	0.867013	1.74
Submerged breakwater			0.768693	0.39972	0.52
			0.65258	0.600374	0.92
			0.578327	0.728692	1.26
Floating breakwater		0.887069	0.195155	0.22	
		0.729741	0.467034	0.64	
		0.582224	0.721957	1.24	
CC		30	0.689007	0.537425	0.78
			0.563247	0.754751	1.34
			0.478949	0.900425	1.88
Submerged breakwater	0.735956		0.456293	0.62	
	0.606755		0.679565	1.12	
	0.498284		0.867013	1.74	
Floating breakwater	0.742279		0.445367	0.6	
	0.64527		0.613007	0.95	
	0.519244		0.830791	1.24	

Figure 4.11.5 to Figure 4.11.8 showed the relations of dynamic load and wave height for reflection co-efficient 0.9. Figures also agreed with the pre statement that, floating breakwater condition is the best suited to reduce dynamic loads and wave height as well.

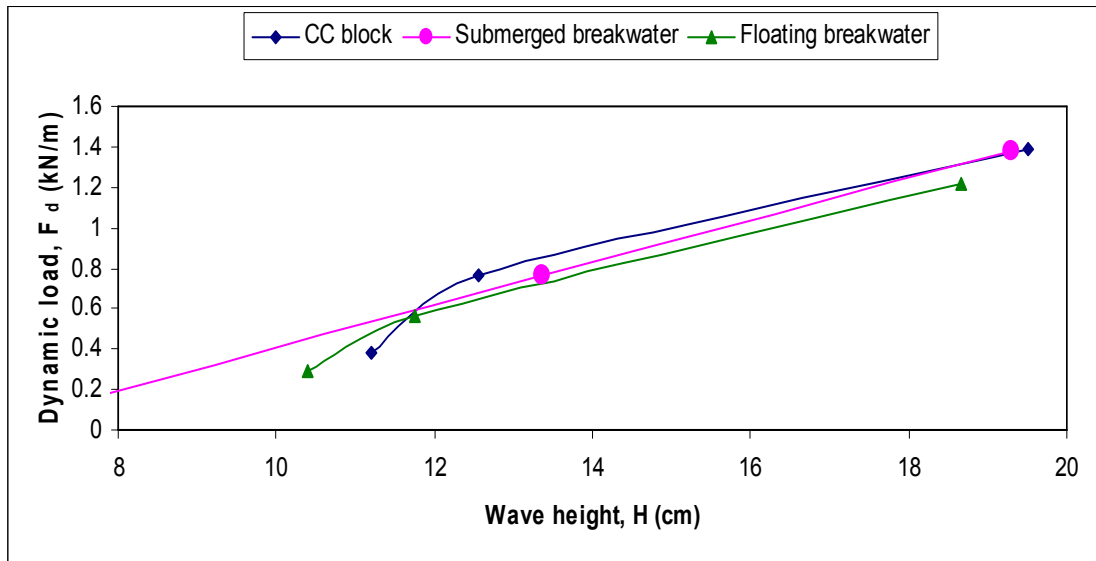


Figure 4.11.5: Dynamic load change with wave height for 1:2 slope and 40 cm water depth, when $\chi = 0.9$.

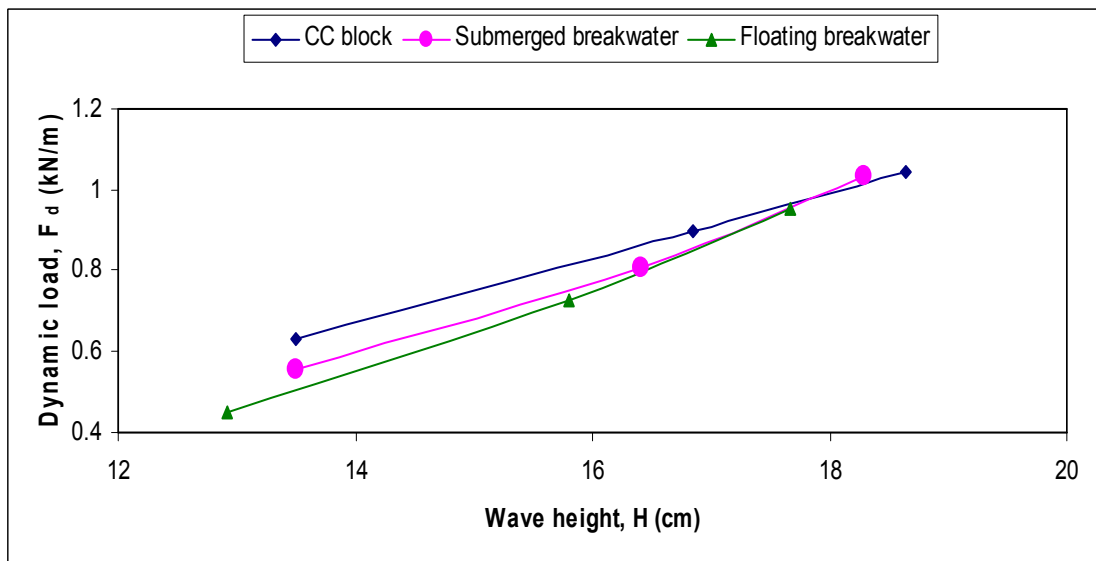


Figure 4.11.6: Dynamic load change with wave height for 1:2 slope and 30 cm water depth, when $\chi = 0.9$.

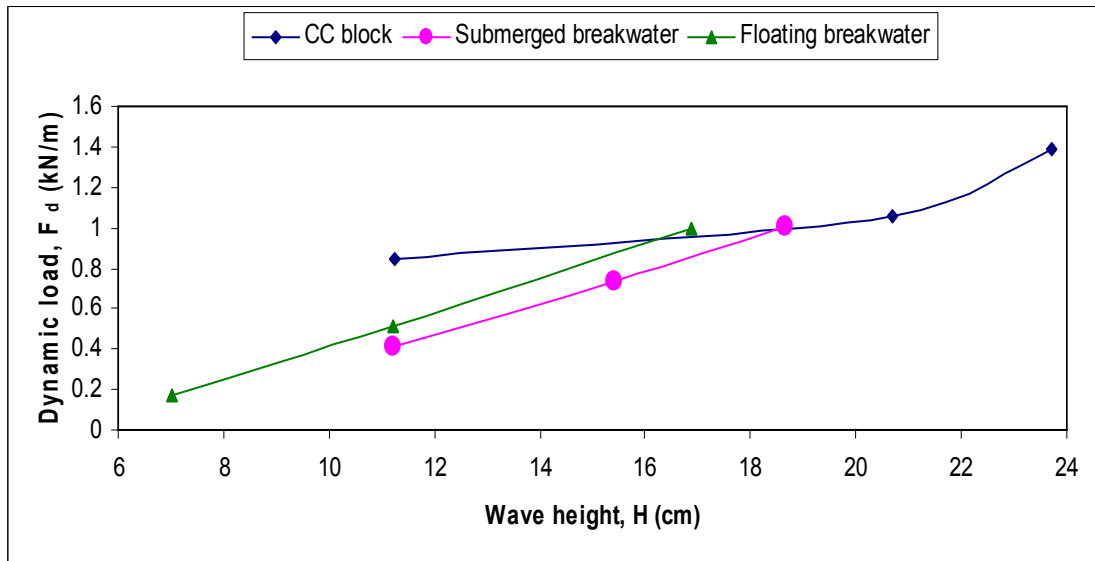


Figure 4.11.7: Dynamic load change with wave height for 1:3 slope and 40 cm water depth, when $\chi = 0.9$.

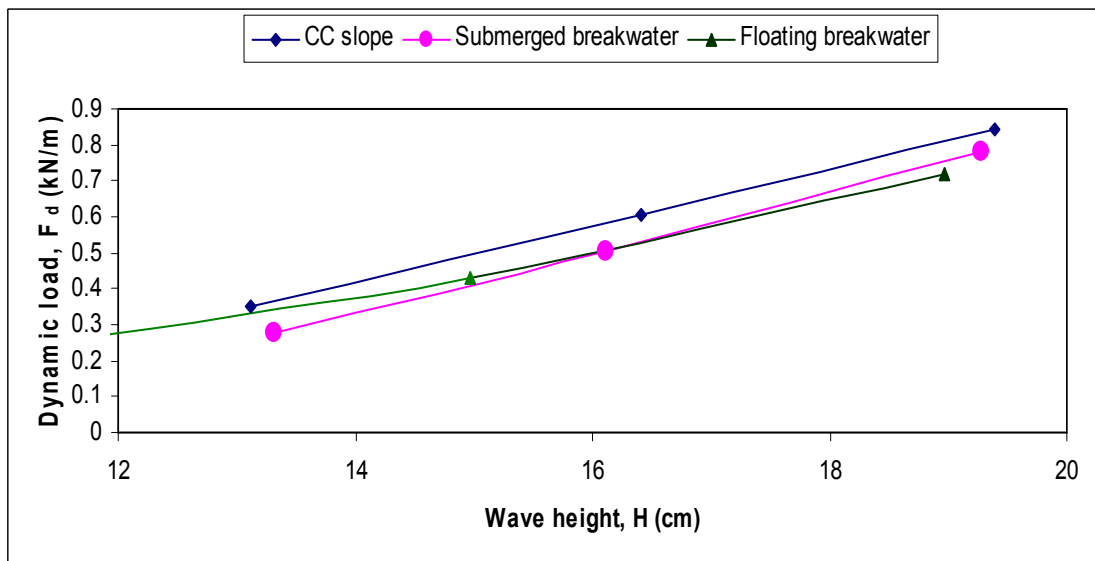


Figure 4.11.8: Dynamic load change with wave height for 1:3 slope and 30 cm water depth, when $\chi = 0.9$.

4.12 Dynamic load Effect on embankment Height

The height of an embankment or other coastal structure for many centuries has been on the highest known flood level that could be remembered. It is evident that in this way the real risk of damage or the probability of flooding was unknown. In the

twentieth century it was found that the occurrence of extremely high water levels and wave heights could adequately be described by probability distribution. However, the extreme distributions, often based on relatively short periods of observations, mostly have to be extrapolated into regions for beyond the field of observations. Besides, the design flood level several other elements also play a role in determining the design crest level.

- Wave run-up or over topping height depends on wave height and period, wave angle of approach, roughness and permeability of the slope and the profile shape.
- An extra margin to the embankment height must be taken into account are seiches (oscillation) and gust bumps (single waves resulting form a sudden violent rush of wind) depending on the location.
- A change in bottom level or a rise of the mean sea level (the forecast for the estimated life time to the structure).
- Settlement of the subsoil and the embankment body during its life time (Figure 4.12.1).

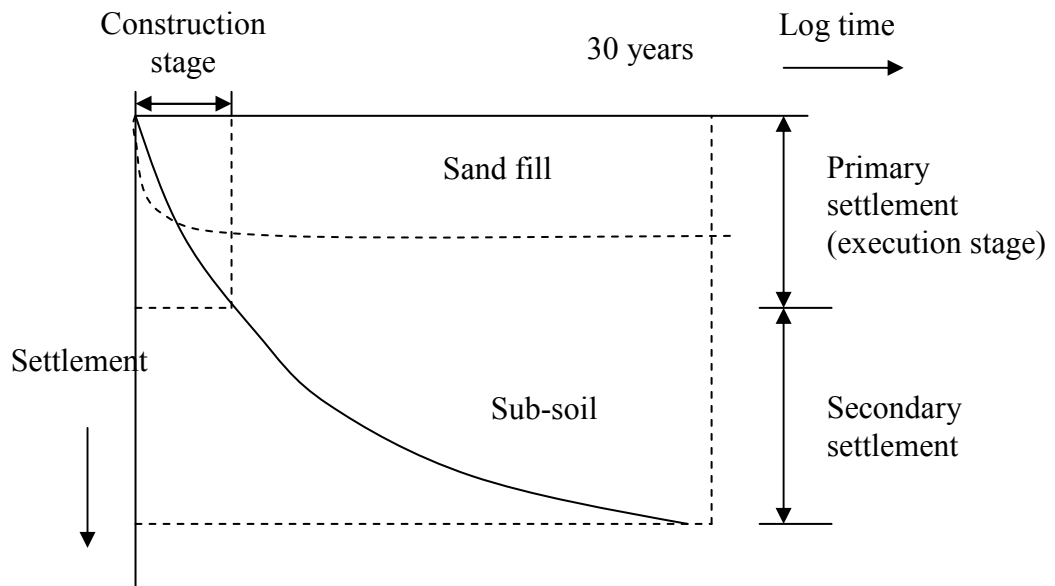


Figure 4.12.1: Settlement as function of time (Source: Van-der-meer, 2002)

The combination of all these factors mentioned above defines the crest freeboard of the embankment and embankment height for the construction (<http://www.scribd.com/doc/7332876/Van-Der-Meer>). The recommended minimum freeboard is 0.5 m (Pilarezyk, 1990). In many areas in the world wave-heights and

foundation conditions are such that no gravity-structures or sheet-piles can be used. Sloping structures are a solution then, as wave loads on these structures are more easily accounted for. Moreover, foundation-loads are more evenly distributed and differential settlements can, to a certain extent, be accepted.

Height of embankment is the different between the design crest level of the embankment and the average ground level on which the embankment is constructed. Again, the design crest level is composed of design flood level (H_{DFS}), height of wind set up (H_W), height of wave run-up height (R) and freeboard. Upon contact with the face of the embankment, the waves move up the inclined plane and extend part of their energy in raising the water level will dissipate due to embankment slope. Also, when the breakwater is used, it dissipated the energy and reduces the load impact on the embankment. Less load makes less run-up height which minimize the design crest level finally minimize the embankment height. Figure 4.12.2 to Figure 4.12.5 illustrate that wave run-up height is reducing with wave loads reduction for different breakwater effect. For slope reduction reduced load also deduct the run-up height. Figure 4.12.6, 4.12.7 and 4.12.8 shows run-up height reduction with slope reduction for three different loading conditions. Figure 4.12.6 is for CC block only; Figure 4.12.7 is for submerged breakwater condition and Figure 4.12.8 is for floating breakwater condition.

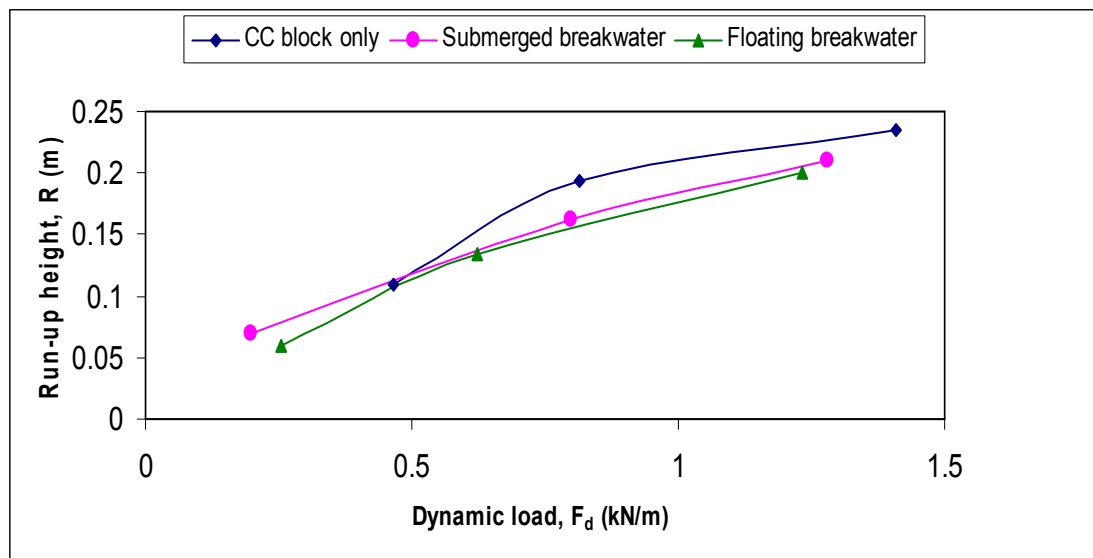


Figure 4.12.2: Run-up height reduction for different load condition on 1:2 slope and 40 cm water depth.

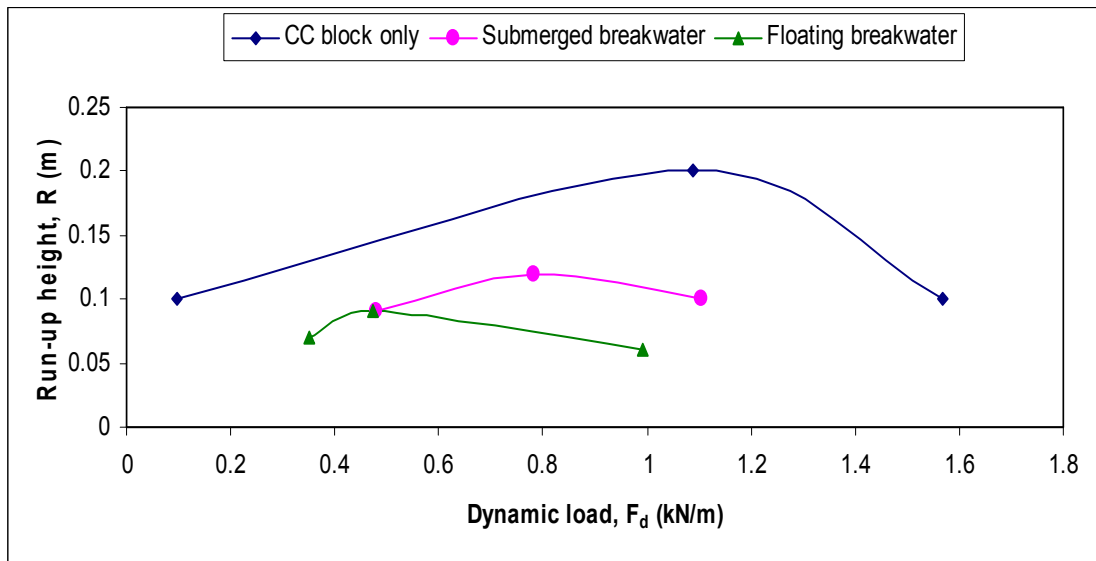


Figure 4.12.3: Run-up height reduction for different load condition on 1:2 slope and 30 cm water depth.

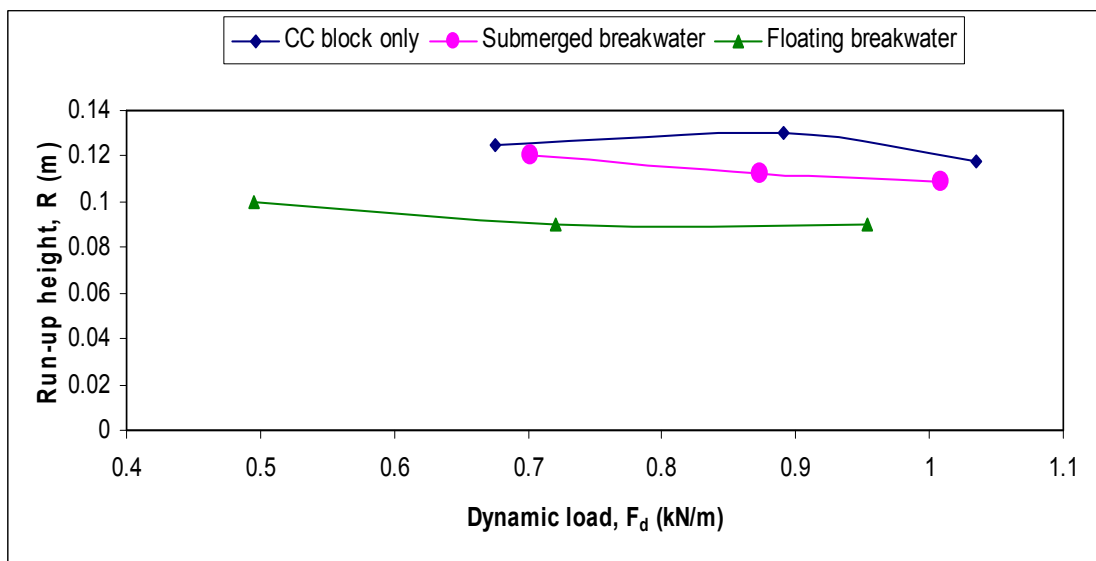


Figure 4.12.4: Run-up height reduction for different load condition on 1:3 slope and 40 cm water depth.

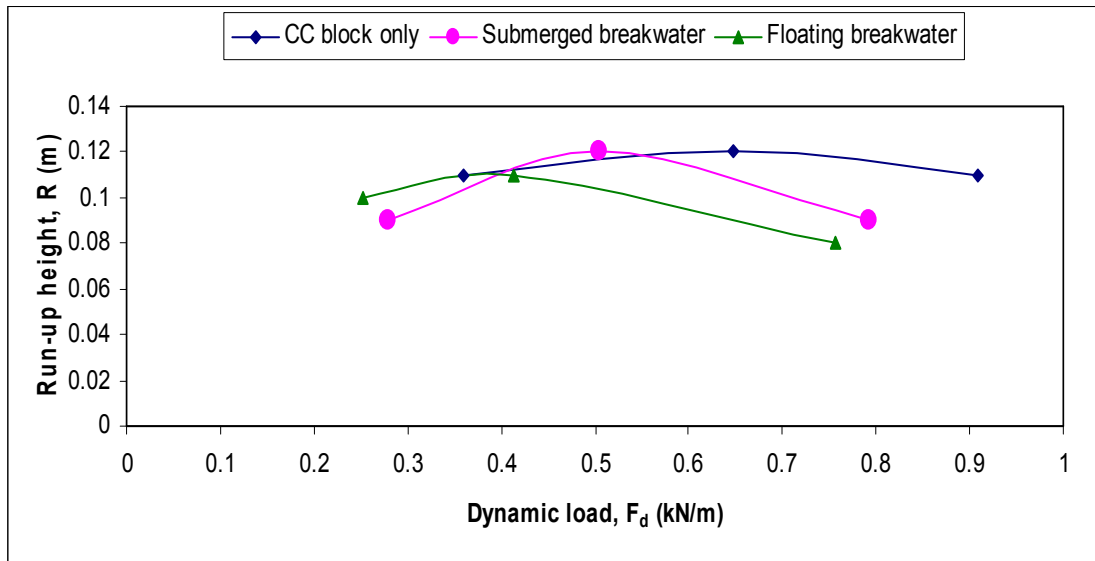


Figure 4.12.5: Run-up height reduction for different load condition on 1:3 slope and 30 cm water depth.

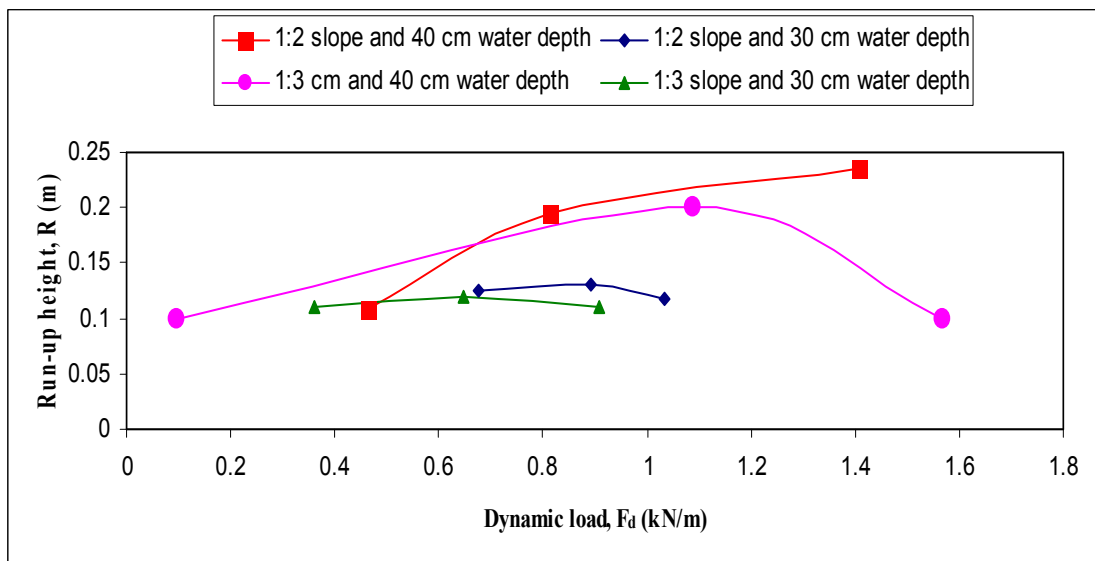


Figure 4.12.6: Run-up height reduction for CC block condition on different slope and water depth.

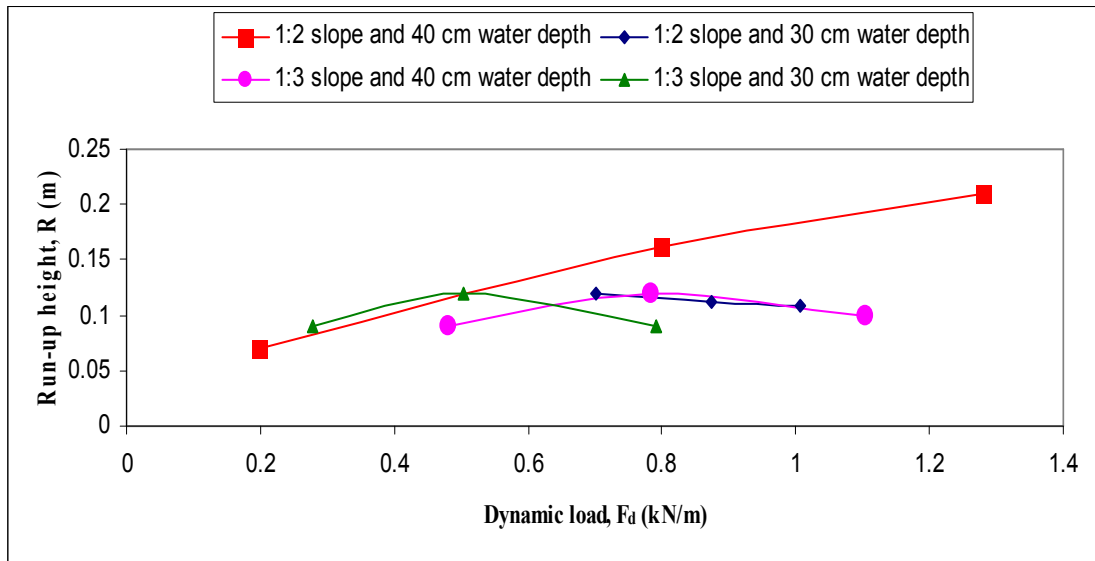


Figure 4.12.7: Run-up height reduction for submerged breakwater condition on different slope and water depth.

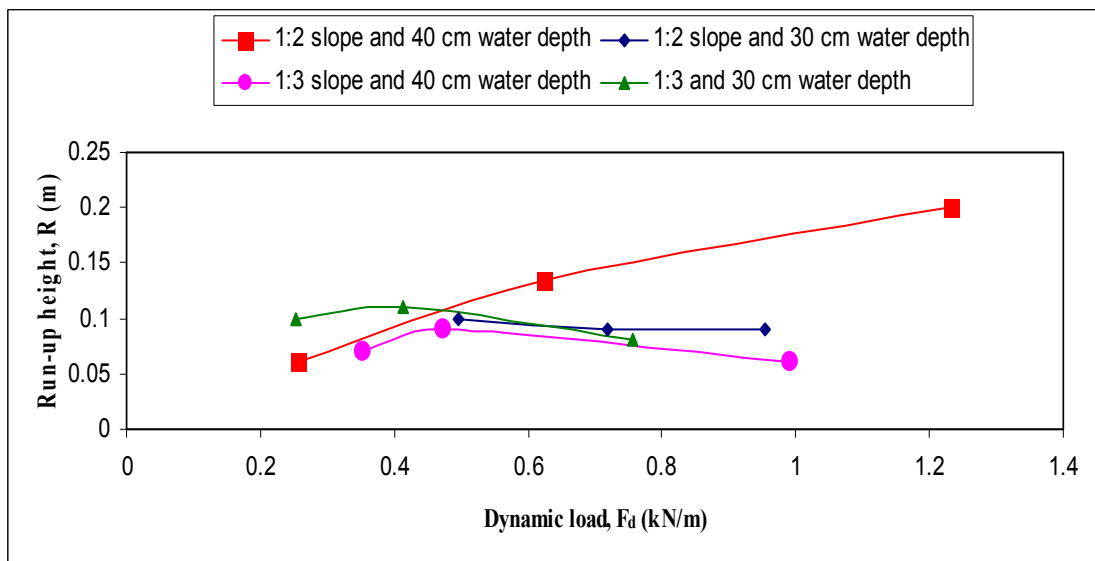


Figure 4.12.8: Run-up height reduction for floating breakwater condition on different slope and water depth.

4.13 Comparison with Miche-Rundgren curve

Considering the wave reflection co-efficient Miche (1944) has given the higher order theory which was modified by Rundgren (1958). The experimentally measured forces were calculated on vertical walls for steep slope. But this research work was

performed for sloping side on 1:2 and 1:3 slopes. These experimental values were super imposed on Miches' graph converting it for vertical wall (shown in the figures 4.13.1 and 4.13.2).

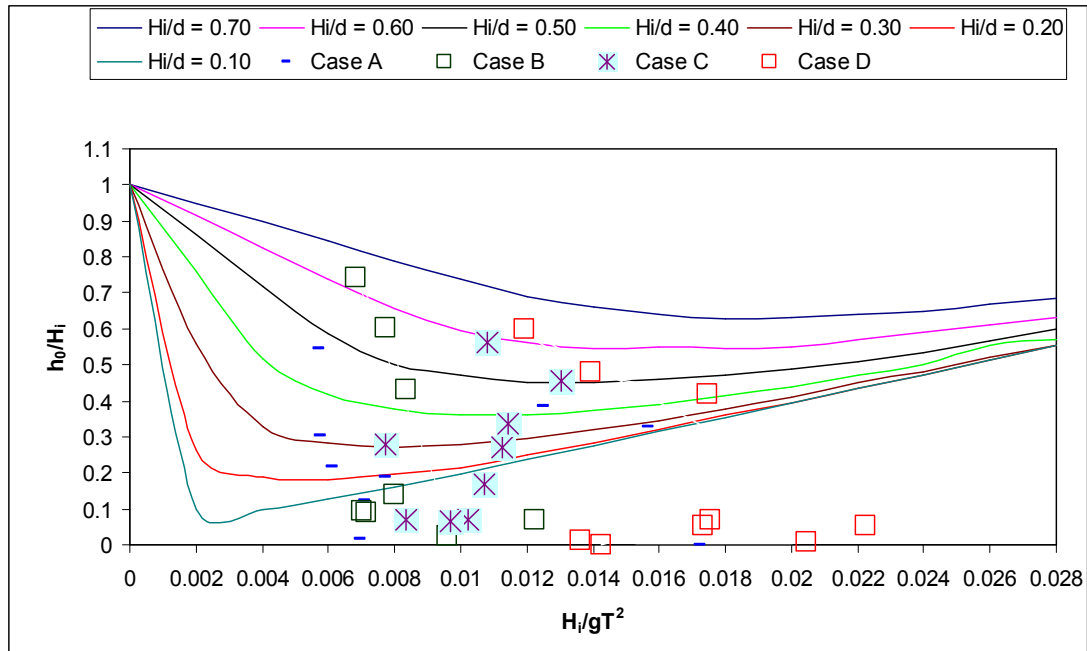


Figure 4.13.1: Comparison with Miche-Rundgren curve for $\chi = 1$.

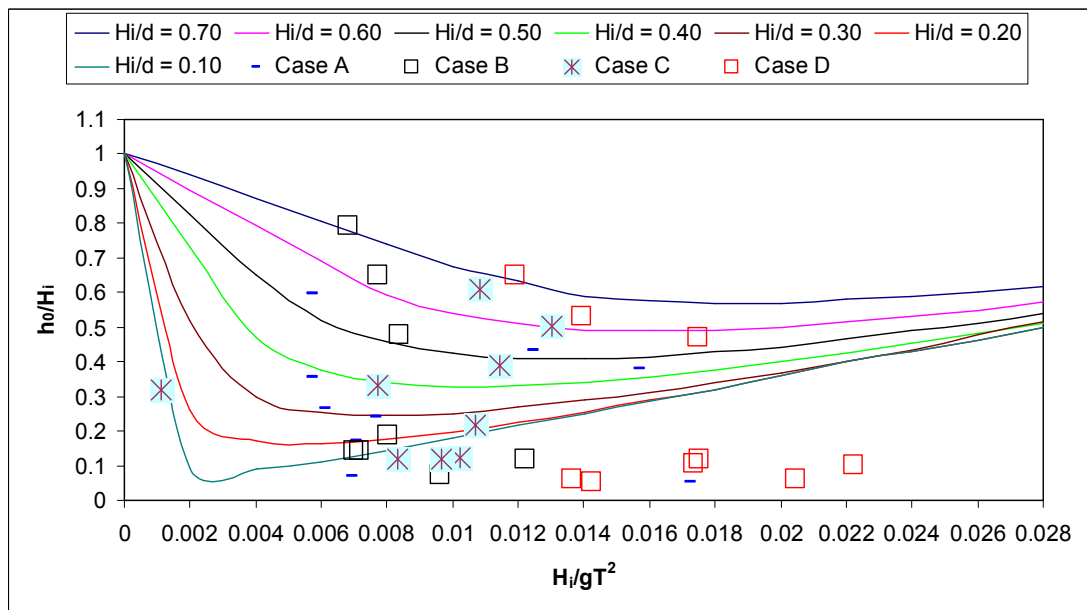


Figure 4.13.2: Comparison with Miche-Rundgren curve for $\chi = 0.9$.

In these two figures the lines are plotted based on Miche-Rundgren experimental graph (SPM, 1984) and the points are showing the present experimental values. Four cases (Case A, Case B, Case C and Case D) represent the behaviour of different loading condition (Table 4.13.1). The values of CC blocks for different conditions were shown well arranged which were agreed with Miche-Rundgren conditions. More data on same condition might produce a pattern.

Table 4.13.1: Meaning of four cases

Topics	Descriptions
Case A	Bank slope = 1: 2 Water depth = 40 cm. Three conditions = CC, Submerged breakwater & Floating breakwater
Case B	Bank slope = 1: 2 Water depth = 30 cm. Three conditions = CC, Submerged breakwater & Floating breakwater
Case C	Bank slope = 1: 3 Water depth = 40 cm. Three conditions = CC, Submerged breakwater & Floating breakwater
Case D	Bank slope = 1: 3 Water depth = 30 cm. Three conditions = CC, Submerged breakwater & Floating breakwater

At the present study the performance of the structures is observed under the effect of waves only. Experiments were conducted in a flume of 2.5 ft. in width, where the effects of sidewall cannot be avoided. Experiments are conducted with regular waves. But in nature waves in the sea are irregular. The laboratory setup does not allow for the use of vibratory compaction device. Limitations for wave reflections

should be minimize through more effective process. This reflection of the waves increases the magnitude of the incident wave height by some percentage and also causes difficulty in the measurement of the actual wave height.

4.14 Summary

In this chapter, firstly the experimental values of wave parameters are compared with the theoretical values which showed good agreement between theory and experiments. Small dissimilarities are for the limitations of the study stated at section 3.8. Afterwise the experimental values of wave parameters are related to each other.

Velocity vectors of different points also illustrate the validities of measured data. Calculated wave loads (showed on the tables) and their changes for different conditions have the significant importance on embankment stability and height reduction. Finally, all the analysis will help to find out the embankment design considerations at coastal region.

CHAPTER 5

CONCLUSIONS AND RECOMMENDATIONS

5.1 General

Dynamic loads due to wave can be reduced by the two main phenomenon reflection and absorption. In this study, a breakwater (submerged and floating) has been used in the sea side of the embankment to observe the effect of dynamic loading on the embankment. The breakwater has been used as submerged and floating condition. Again, energy dissipation has been done by two different slopes. In this study, total 36 experimental runs have been conducted for two variable water depths (40 cm and 30 cm); two variable sea side bank slope 1:2 and 1:3; and three different loading conditions, normal condition (CC block), submerged breakwater condition and floating breakwater condition which are stated detail in art 3.5. General changed behaviour of wave parameters has been analyzed with respect to the slope, depth and loading conditions. Observation and findings made from experimental results are compared with the theoretical value (stated in art 3.5). A comparison of dynamic wave loads and static wave loads was shown from present experimental data set.

5.2 Conclusions

Based on the detail experimental investigation, analysis and discussion presented in foregoing chapters, the summary and conclusion of the present research work can be stated as follows:

1. The experimental values of wave length, wave period and wave height were found to be less than the theoretical values with the decrease of water depth. The reduction percentage of wave parameter were higher for floating breakwater condition compare to submerged breakwater condition and CC block condition.
2. The study shows that, the limit of the reduction rate of wave length is 2% to 10% for submerged breakwater condition, 4% to 19% for floating breakwater condition; wave period is 1% to 30% for submerged breakwater condition and 5% to 50% for floating breakwater condition. Wave height reduction rate

is 1% to 29% for submerged breakwater condition and 4% to 45% for floating breakwater condition.

3. The run-up heights were reduced with wave length, wave period, wave height and sea side embankment slope reduction. The study shows the reduction rate 4% to 35% for submerged breakwater condition and 8% to 55% for floating breakwater.
4. The velocities of propagative waves were reduced more by the floating breakwater condition comparing with submerged breakwater condition and CC block condition.
5. The velocities of water particle are less near the toe of the embankment slope and more near the breakwater.
6. Magnitudes of loads are large for large wave period, wave length and small for small wave period and wave length.
7. The study shows the ratio of dynamic and static loads greater than 1 as the dynamic wave loads were more than the static wave loads in maximum case.
8. It can be concluded from the study that the embankment height is reduced by using breakwater. It has been found that, floating breakwater is more effective comparing submerged breakwater.

5.3 Recommendations for further Study

Based on present research work, some recommendations can be suggested for further study on coastal embankment. They are as follows,

- In current study, two prepared bank slope structure have been used (1:2 and 1:3). Recommendation can be made to undertake other slope structure in consideration.
- Similar types of study can be conducted for widely varied depth of water.
- In this study floating breakwater have been used in fully floated condition. Further experiment can be done by making it partly floating and partly submersed.
- Research can be conducted to find out the suitable location for breakwater construction.

- Measurements were taken in three different distance from toe relating with run-up height (R) which were 3R, 6R and 9R. Different distances can be used in further experiment to adjust most appropriate point to construct breakwater.
- Comparison between dynamic and static load is based on present experimental data set only. It can be verified with available practical field data set to evaluate its significance. This developed relationship will be modified as a new equation can be proposed to predict load (dynamic or static) more accurately.
- Cost analysis of this experiment or it's extend can be done to make it more economical.
- Research on wave dynamics and its effects on various protective measures can be conducted using Numerical modeling technique focusing on field application.

REFERENCES

- Ali, A., 1997, "A Review on Coastal Embankment Project," Undergraduate thesis, Department of Water Resources Engineering, BUET, Dhaka.
- Anthoni, J. F., 2000, "Theory and principles of waves, how they work and what causes them", from: www.seafriends.org.nz/oceano/waves.htm
- BANGLAPEDIA: National Encyclopedia of Bangladesh, 2006. Asiatic society of Bangladesh. 5, Old secretariat road Nimtali, Dhaka, Bangladesh. From www.banglapedia.org
- CEM, 2003, "Coastal Engineering Manual", Department of the Army, U.S. Army Corps of Engineers, Washington, DC 20314-1000, Part-II, Chapter I.
- ESCAP, 1988, "Coastal Environmental Management Plan for Bangladesh", Vol. 2: Final Report, Economic and Social Commission for Asia and the Pacific, Bangkok, Thailand.
- Horikawa, K., 1978, "Coastal Engineering", University of Tokyo press, Japan, Chap2, pp. 5-108.
- Horikawa, K., 1988, "Nearshore Dynamics and Coastal Processes", University of Tokyo press.
- Haque, M. E., 2010, "An experimental study on flow behaviour around launching apron", M. Sc. Thesis, Department of Water Resources Engineering, BUET, Dhaka.
- IUCN, 1993, "Marine Protected Area Needs in the South Asian Seas Region", Vol. 1: Bangladesh, a Marine Conservation and Development Report. IUCN, Gland, Switzerland.
- IPCC, 2001a. Climate Change 2001: Mitigation, Contribution of Working Group III to the Third Assessment Report of the Intergovernmental Panel on Climate Change (IPCC), Cambridge University Press, UK.
- IPCC, 2001b, Climate Change 2001: Synthesis Report, Contribution of Working Group III to the Third Assessment Report of the Intergovernmental Panel on Climate Change (IPCC), Cambridge University Press, UK.
- Islam, M. N. 2004, "Embankment Erosion Control: Towards Cheap and Simple Practical Solutions for Bangladesh", Coastal Embankment Rehabilitation Project South Khulshi, Chittagong, Bangladesh, from: http://www.vetiver.org/TVN_IVC2/CP-3-1.PDF
- Kausher, A., Kay, R.C., Asaduzzaman, M., Paul, S., 1993. Climate Change and Sea-level Rise: the Case of the Coast. Briefing Document No. 6, Bangladesh Unnayan Parishad (BUP), Dhaka.

Masoom, S., 2002, "Experimental Study on the Effectiveness of Riprap Protection Structure with soil Reinforcement under Wave Action", M. Sc. Thesis, Department of Water Resources Engineering, BUET, Dhaka.

Muttray, M., Oumeraci, H., Oever, E. T., "Reflection and Wave Run-up at Rubble Mound Breakwaters", a coastal engineering research paper from <http://www.xbloc.com/htm/downloads.php>.

Massie, W.W. P.E., 1976, "Coastal Engineering", Vol-III.

Murthy, V. N. S., 1989, "Soil Mechanics and Foundation Engineering", vol 1, Third edition, Chapter 6.

Mitwally, H. and Novak, M., 1989, "Wave Forces on Fixed Offshore Structures in Short Crested seas" journal of Engineering Mechanics, Vol-115, No. 3, Paper no. 23303.

Navera, U. K. and Nandi, B., 2007, "Effect of Dynamic forces in Designing Embankment near Coastline in Bangladesh", Proceedings of the International Conference on Water and Management, 12-14 March, Dhaka, Bangladesh, pp. 269-278.

Nandi, B., 2002, "A Study on the Stability of C.C blocks as revetment Material against wave attack", M. Sc. Thesis, Department of Water Resources Engineering, BUET.

Neelamani, S., Schuttrumpf, H., Muttray, M. and Oumeraci, H., 1999, " Prediction of wave pressures on smooth impermeable sea walls", Journal of Ocean Engineering, Vol. 26, pp. 739–765.

Niedzwecki, J. M. and Duggal, A. S., 1992, "Wave Run-up and Forces on Cylinders in Regular and Random Waves", Journal of Water way, Port, Coastal and Ocean engineering, Vol. 118, No. 6, Paper No. 522.

Oumeraci, H., Klammer, P., Kortenhaus, A., 1994, "Impact loading and Dynamic response of vertical breakwaters-review of experimental results", In: PHRI (Ed.), Proceedings Int. Workshop Wave Barriers in Deep Waters, Yokosuka, Japan, pp. 347–361.

Pilarczyk, K. W., 1990, "Design of seawalls and dikes-Including overview of revetments", coastal protection, Pilarczyk (ed.), Balkema, Rotterdam, Delft University of Technology, Netherlands, pp.211-216.

Pilarczyk, K. W., Breteler, M. K., and Bezuijen, A., 1995, "Wave Forces and Structural Response of Placed Block Revetments on Inclined Structure", Ch-6, pp-25-31, from: <http://books.google.com.bd>.

SPM, 1984, "Shore Protection Manual", Department of the Army Waterways Experiment Station, U.S. Government Printing Office Washington D.C. 20402, Fourth edition, Volume-I, chap2, pp. 1-50.

SPM, 1984, “Shore Protection Manual”, Department of the Army Waterways Experiment Station, U.S. Government Printing Office Washington D.C. 20402, Fourth edition, Volume-II, chap 7, pp. 155-202.

Sarwar, M., G., M., 2005, “Impacts of Sea Level Rise on the Coastal Zone of Bangladesh”, Masters thesis, Lund University International Masters Program in Environmental Science, Lund University, Sweden.

Takahashi, S., Tanimoto, K., Simosako, K., 1993, “Experimental study of impulsive pressures on composite breakwaters—fundamental feature of impulsive pressure and impulsive pressure coefficient”, Rept. Port and Harbour Res. Inst. 31 (5), 33–72.

Van der Meer, J. W., “Geometrical Design of Coastal Structure”, From: <http://www.scribd.com/doc/7332876/Van-Der-Meer>.

Van der Meer, J. W., 1990, “Static and dynamic stability of loose materials”, coastal protection, Pilarczyk (ed.), Balkema, Rotterdam, pp. 159-161.

Van der Meer, J. W., 2002, “Wave Run-up and Wave Overtopping at Dikes”, Technical report, technical advisory committee on flood defence, delft, Natherland.

Wigley, T.M.L., Raper, S.C.B., 1987. Thermal expansion of sea water associated with global warming, Nature 357, pp.293-300.

Wickramanayala, M., 2002, “The engineer’s role in coastal Ecosystem Management”, Proceedings of Workshop on coastal zone management, 29-30 October, BUET, Dhaka, pp. 145-148.

Wikipedia, the free encyclopedia, from: http://en.wikipedia.org/wiki/Wind_wave.

Yong, I. R., 1999, “Wind generated ocean waves”, Elsevier Ocean Engineering Book series volume 2, pp 1-8.

Zaman, M. S. and Bhuiyan, M. H., 2007, “Observation of Basic Parameters of near Shore Wave Hydrodynamics and Floating Breakwater effect”, Undergraduate thesis, Department of Water Resources Engineering, BUET, Dhaka.

APPENDIX-A

Step wise procedure of wave generator operation:

► Desk Works:

1. From wind speed and fetch length wave height can be obtained by following wave forecasting formula or using nomograms (SPM, 1984). Then model T and h has been fixed.
2. Find ω by following the formula $\omega = \frac{2\pi}{T}$ from T and determine a dimensionless wave parameter $\frac{\omega^2 h}{g}$.
3. Set e and f from figure A.2 and find $\frac{f+e}{f}$.

► Setting Wave Generator:

4. Mark h on the side glass of flume.
5. Empty the flume if there is water.
6. Turn on the switch of wave generator.
7. Fix frequency of wave generator as slow as possible by rotating dial (don't change frequency while it is at rest).
8. Make the vertical arms perfectly vertical (see Figure A.1) for pure translation.
9. Keep the vertical arms apart from each other as possible for pure rotation.
10. Measure f at bottom and f+e on marked line (desired water level).
11. Find $\frac{f+e}{f}$ and compare with the value obtained in step 3. If it does not satisfy adjust vertical arms to alter translation and rotation of paddle.

12. Turn the switch off.

► Start runs:

13. Pour water in the flume up to desired water level.

14. Turn the switch on and quickly increase frequency of wave generator by rotating dial.

15. Measure frequency of wave generator. If it is not satisfied then adjust frequency by rotating dial.

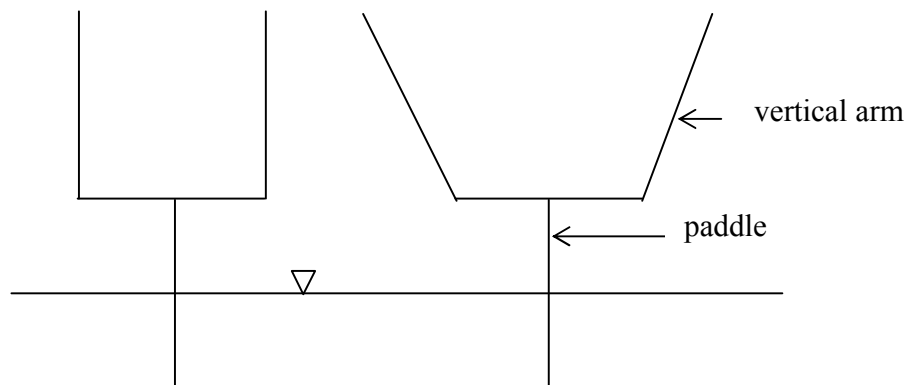


Figure A.1: Line sketch of wave generator (pure translation is shown in left sketch)

Parameters:

T = wave period

h = water depth

ω = angular frequency

f = translation of paddle of wave generator

e = rotation of paddle of wave generator

Example:

Model wave period, T is 1.0 sec and depth of water, h is 40 cm. Then dimension less parameter becomes 1.61. From figure A.2, e and f have been obtained as 0.74 and 0.21 respectively.

The ratio $\frac{f+e}{f}$ is then obtained as 4.52. In the laboratory wave generator has been adjusted by trial and error such that $e+f$ has been obtained as $(0.74+0.21) = 0.95$ and f as 0.21. Then $\frac{f+e}{f}$ has been obtained as 4.52.

Thus the setup has been completed.

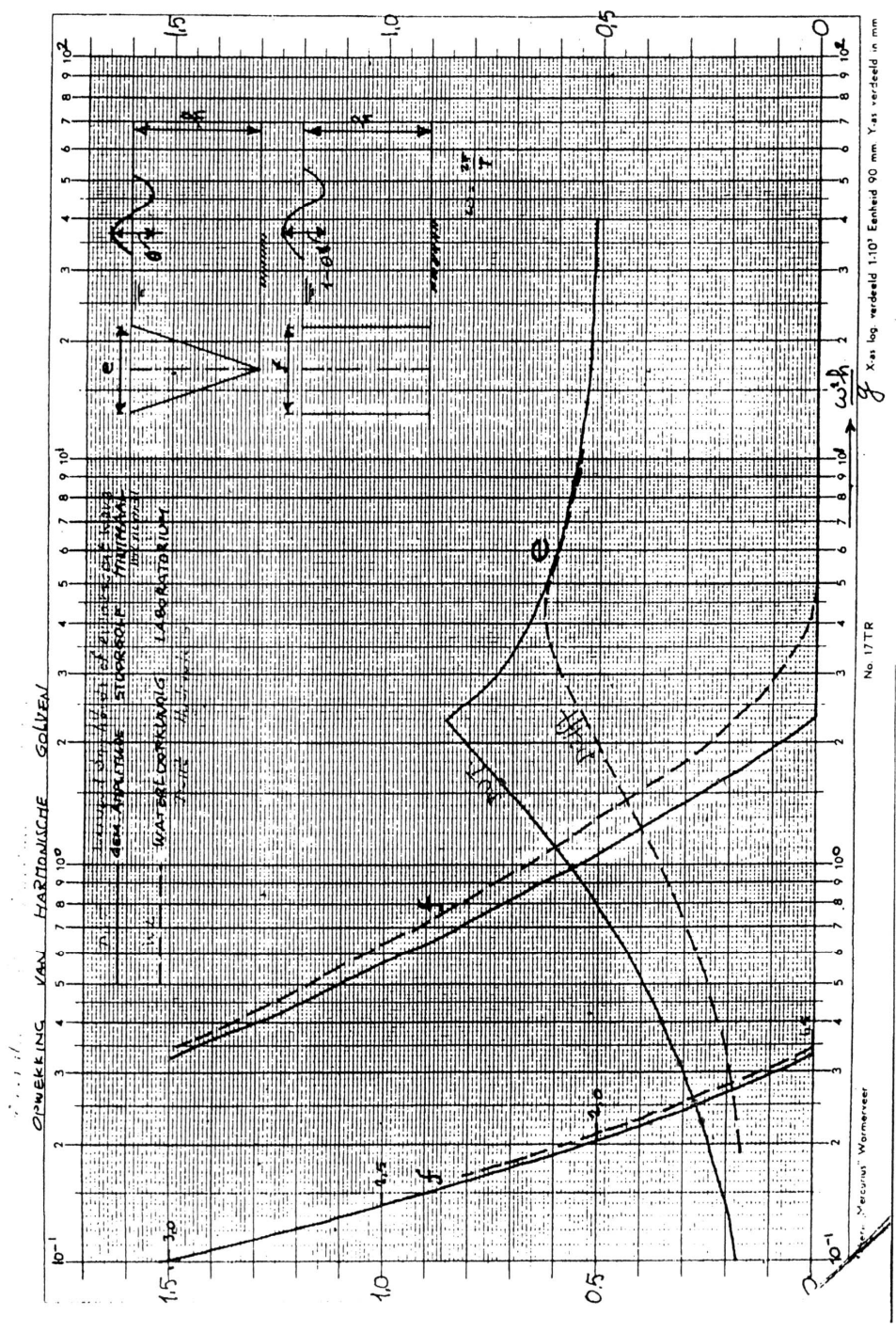


Figure A.2: Graph to get value of e and f

Pictorial presentation of experimental set-up



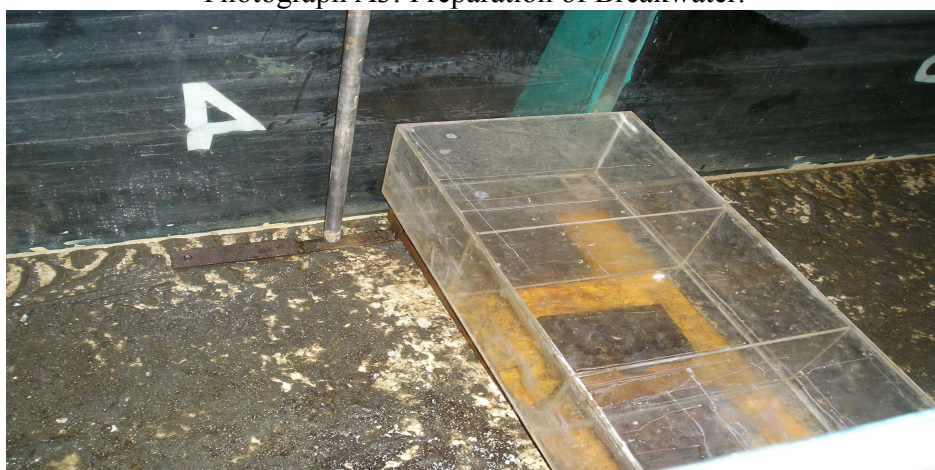
Photograph A1: Velocity meter



Photograph A2: Velocity meter



Photograph A3: Preparation of Breakwater.



Photograph A4: Submerged breakwater installation



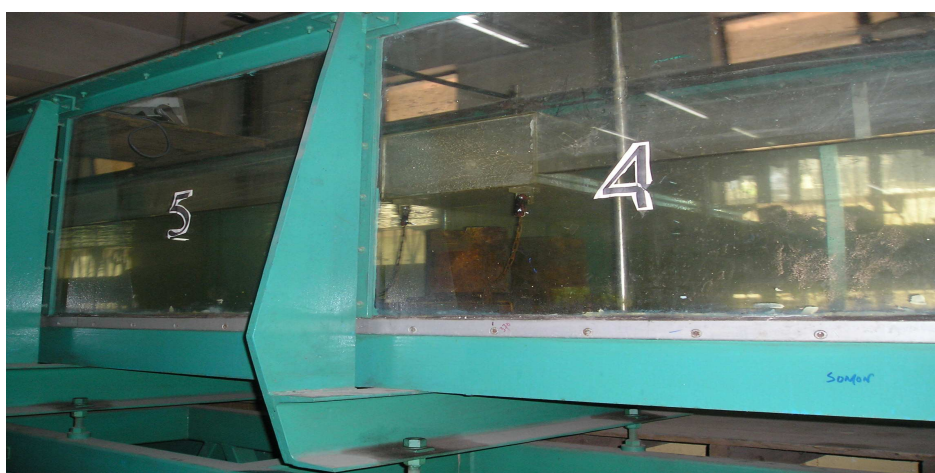
Photograph A5: Breakwater in submerged condition



Photograph A6: Breakwater in submerged condition



Photograph A7: Breakwater in floating condition



Photograph A8: Breakwater in floating condition

APPENDIX-B
Velocity changes for various test scenarios

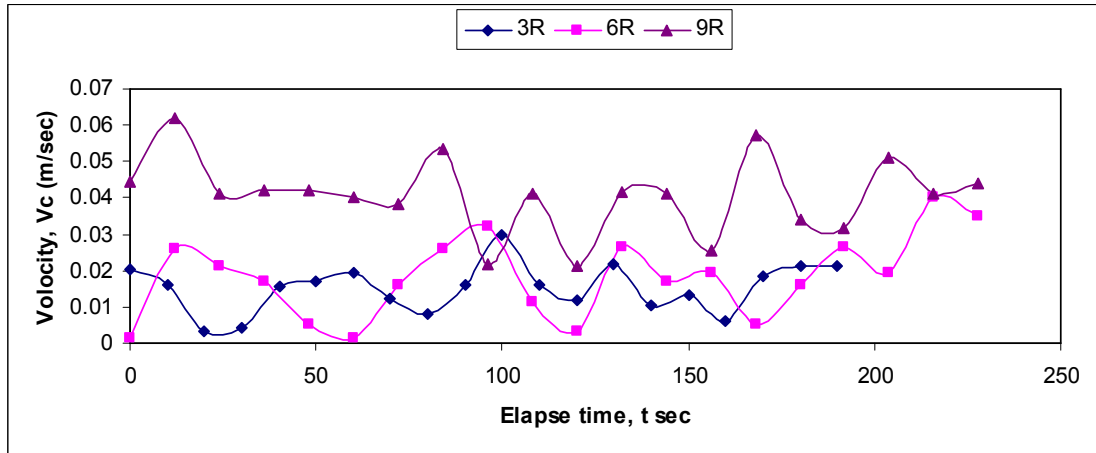


Figure B1: Velocity changes at 1:2 slope, 40 cm water depth and 1 sec wave period for CC blocks only.

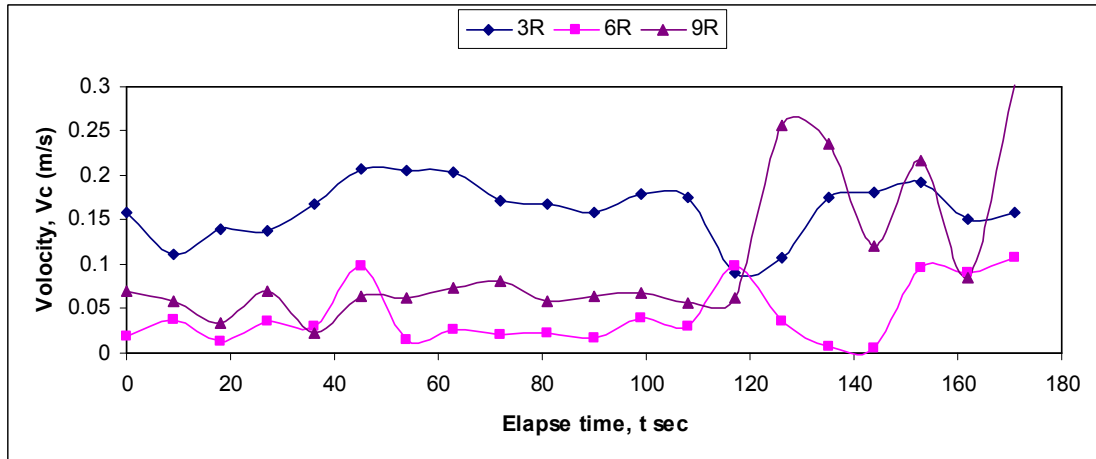


Figure B2: Velocity changes at 1:2 slope, 40 cm water depth and 2 sec wave period for CC blocks only.

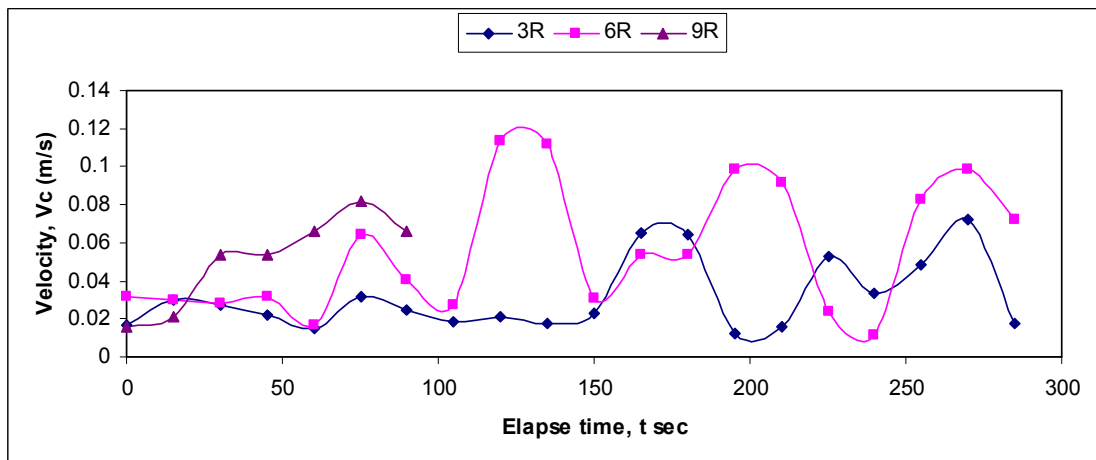


Figure B3: Velocity changes at 1:2 slope, 40 cm water depth and 2.5 sec wave period for CC blocks only.

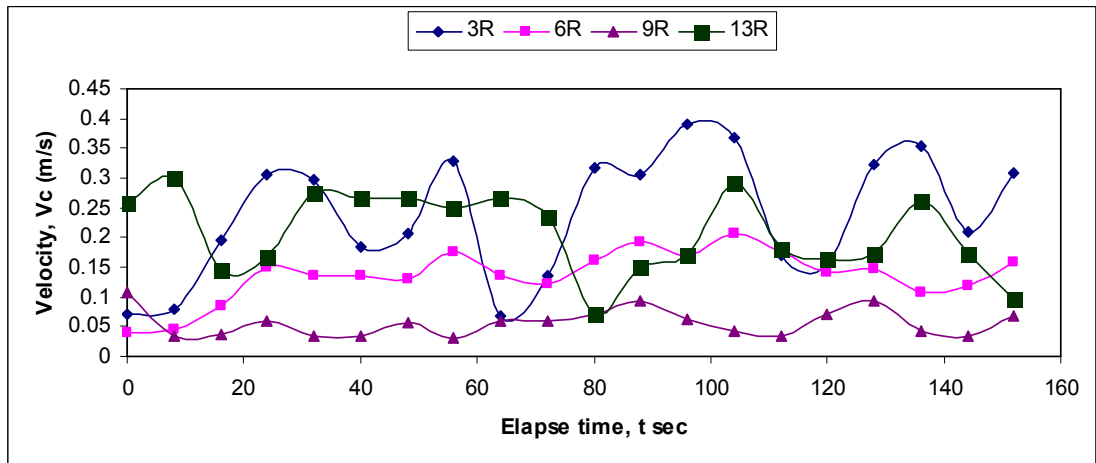


Figure B4: Velocity changes at 1:2 slope, 40 cm water depth and 1 sec wave period for submerged breakwater.

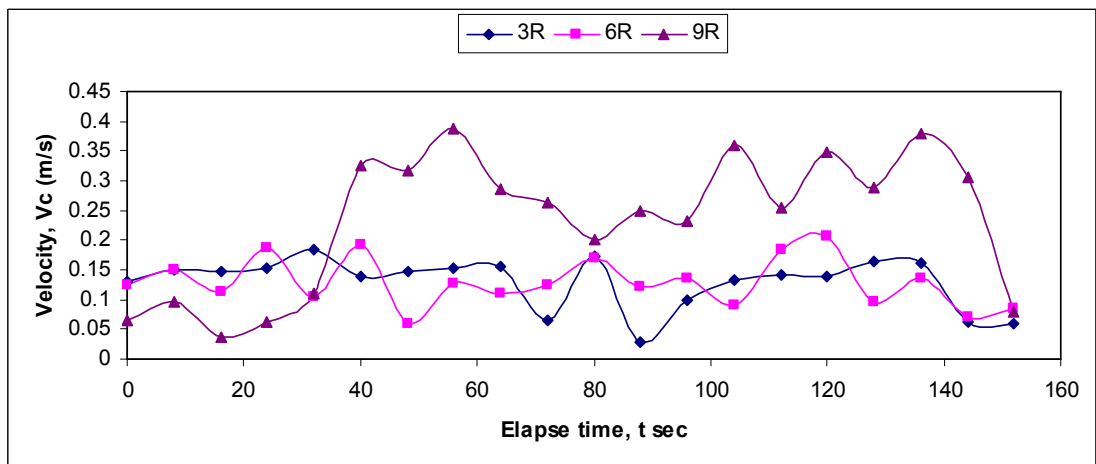


Figure B5: Velocity changes at 1:2 slope, 40 cm water depth and 2 sec wave period for submerged breakwater.

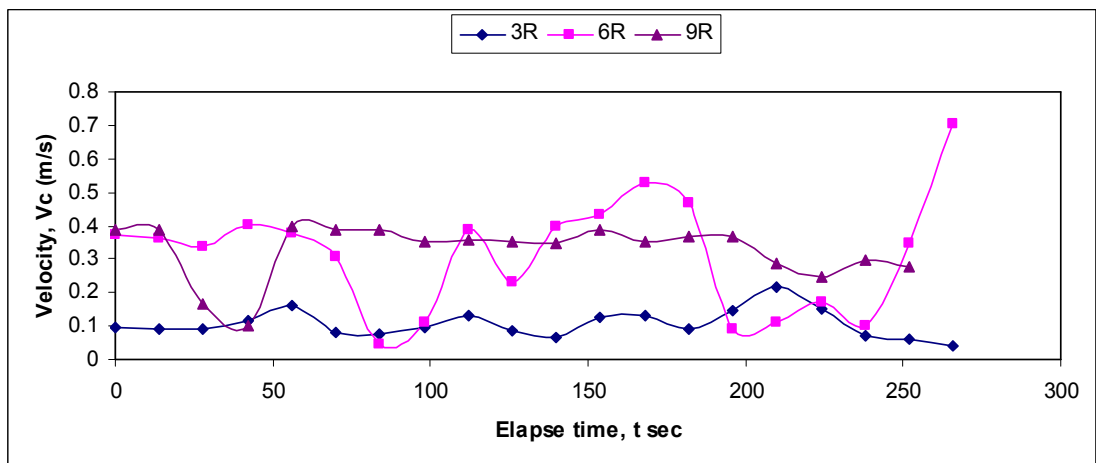


Figure B6: Velocity changes at 1:2 slope, 40 cm water depth and 2.5 sec wave period for submerged breakwater.

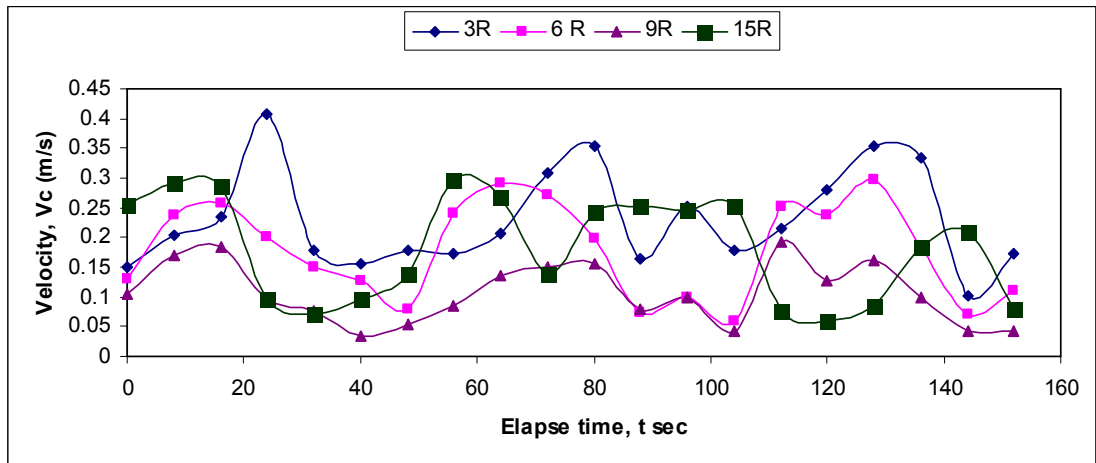


Figure B7: Velocity changes at 1:2 slope, 40 cm water depth and 1 sec wave period for floating breakwater.

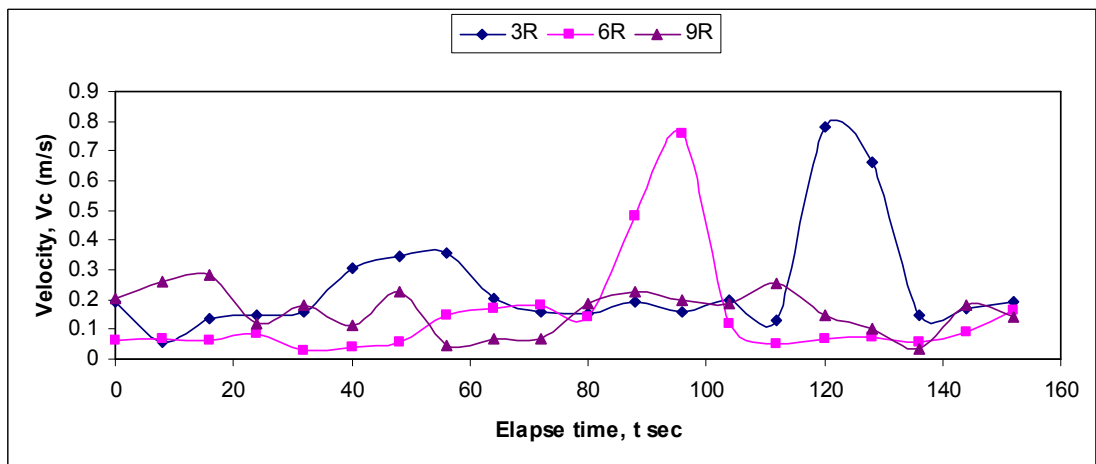


Figure B8: Velocity changes at 1:2 slope, 40 cm water depth and 2 sec wave period for floating breakwater.

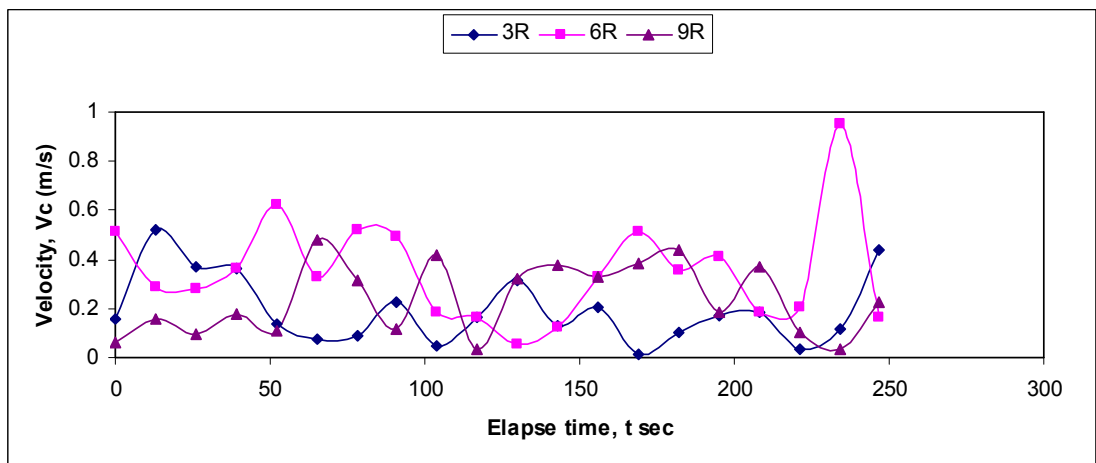


Figure B9: Velocity changes at 1:2 slope, 40 cm water depth and 2.5 sec wave period for floating breakwater.

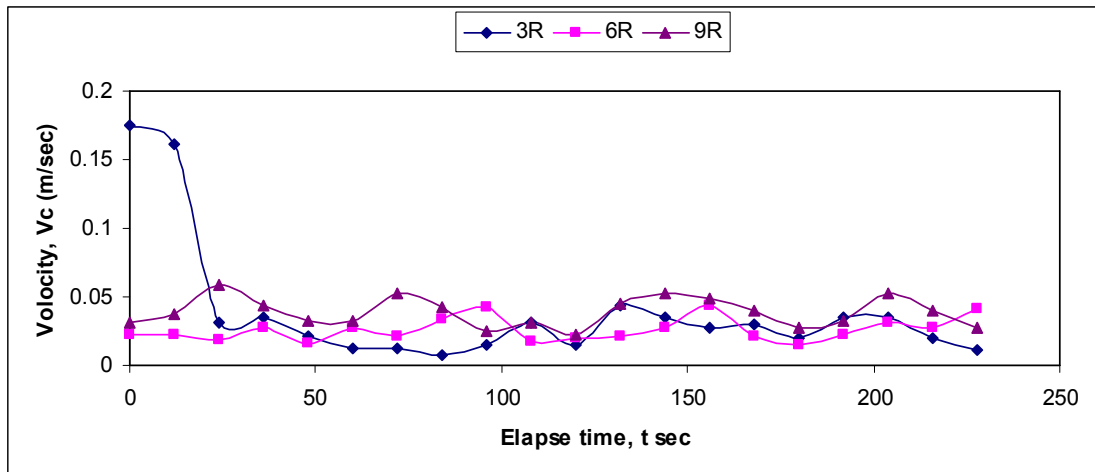


Figure B10: Velocity changes at 1:2 slope, 30 cm water depth and 1 sec wave period for CC blocks only.

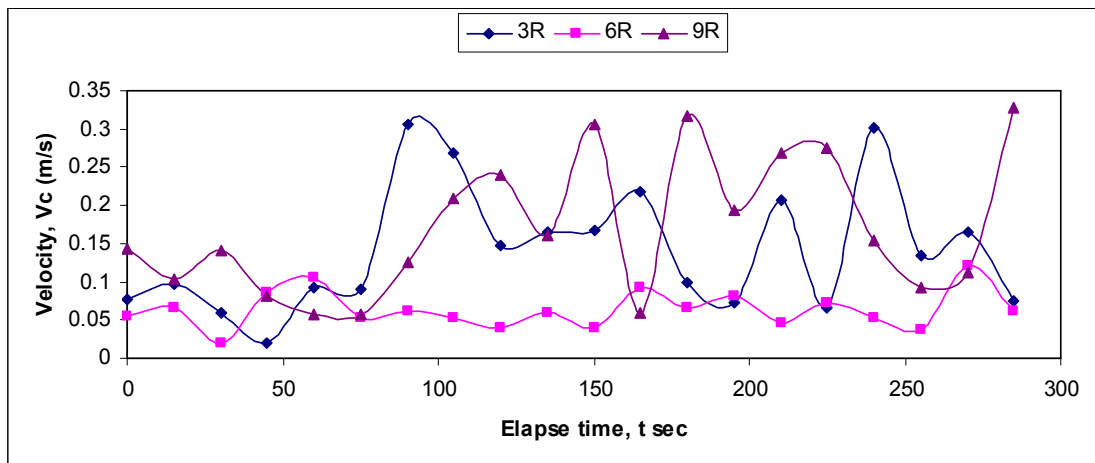


Figure B11: Velocity changes at 1:2 slope, 30 cm water depth and 2 sec wave period for CC blocks only.

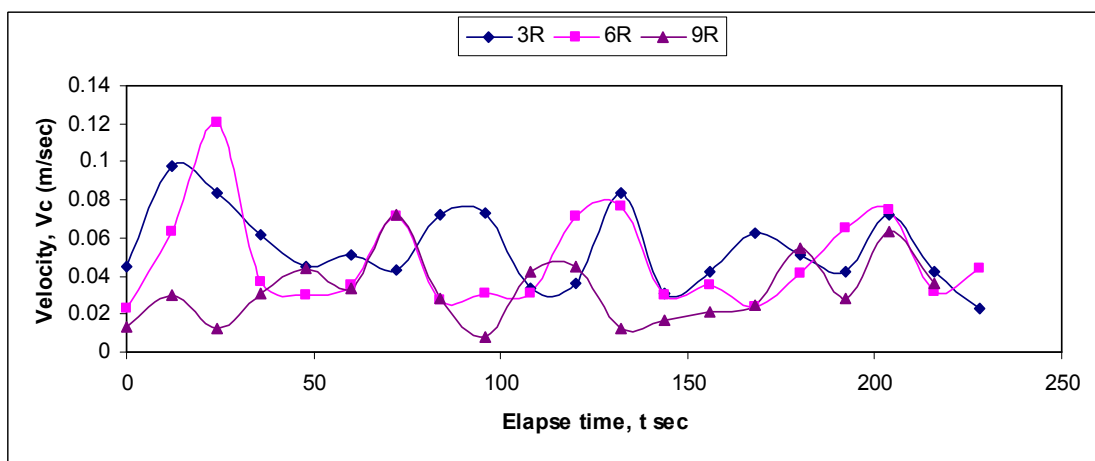


Figure B12: Velocity changes at 1:2 slope, 30 cm water depth and 2.5 sec wave period for CC blocks only.

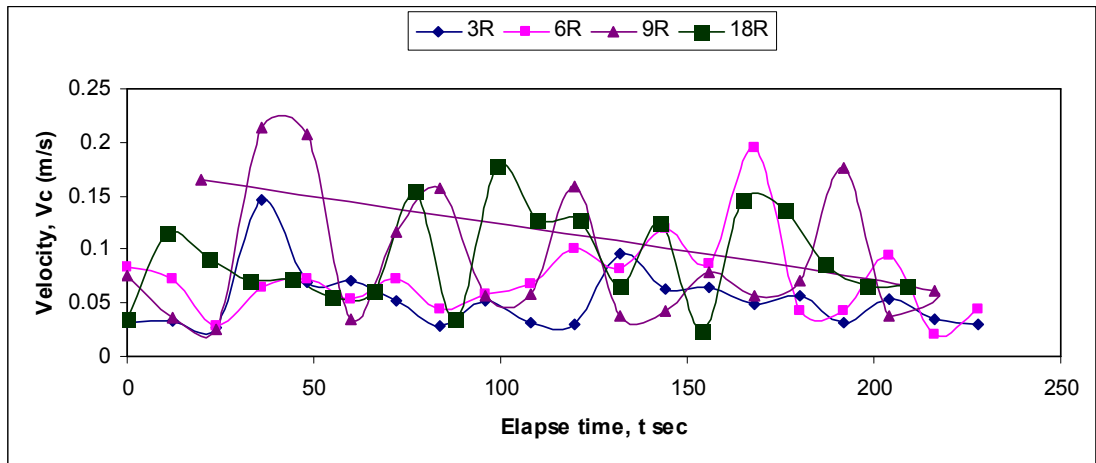


Figure B13: Velocity changes at 1:2 slope, 30 cm water depth and 1 sec wave period for submerged breakwater.

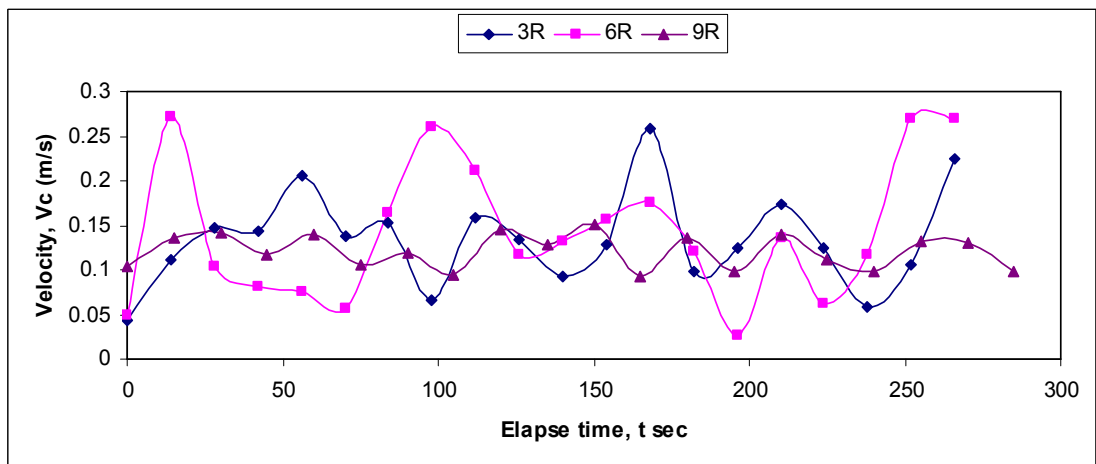


Figure B14: Velocity changes at 1:2 slope, 30 cm water depth and 2 sec wave period for submerged breakwater.

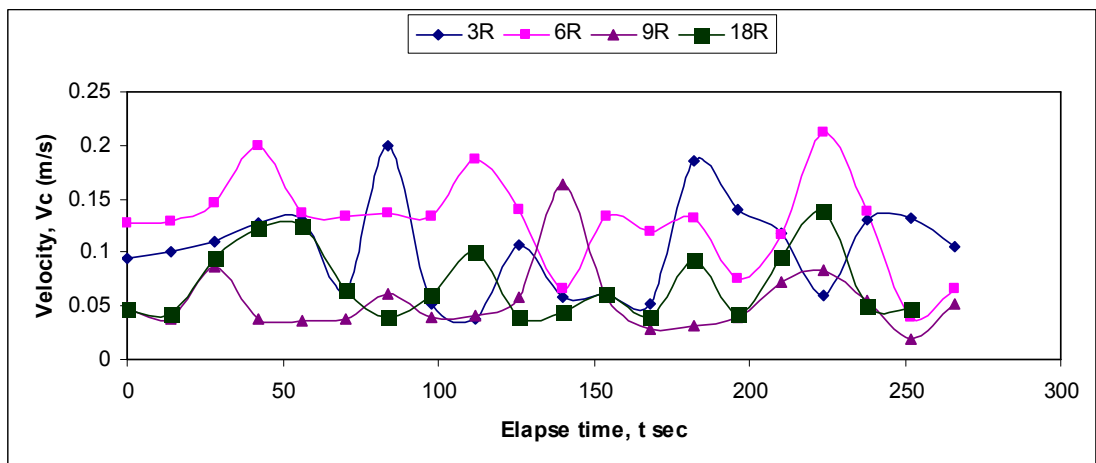


Figure B15: Velocity changes at 1:2 slope, 30 cm water depth and 2.5 sec wave period for submerged breakwater.

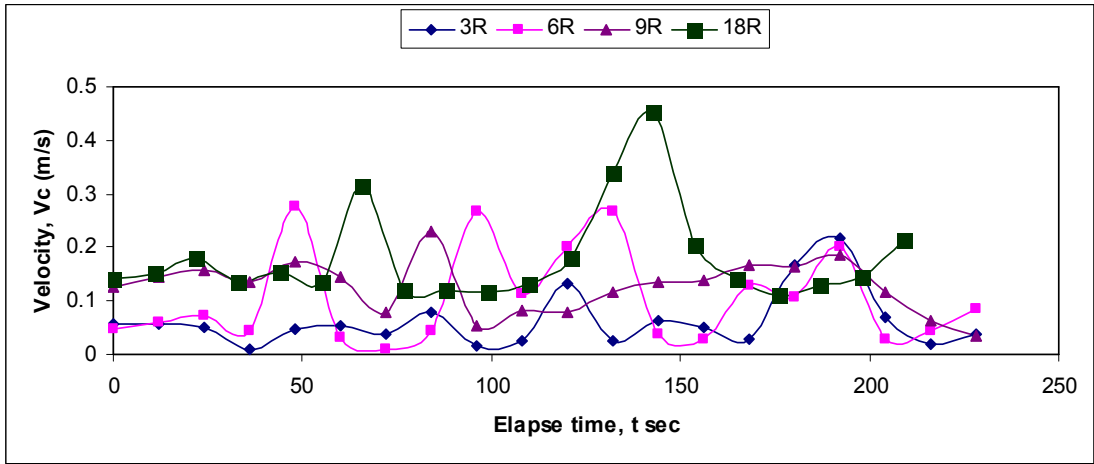


Figure B16: Velocity changes at 1:2 slope, 30 cm water depth and 1 sec wave period for floating breakwater.

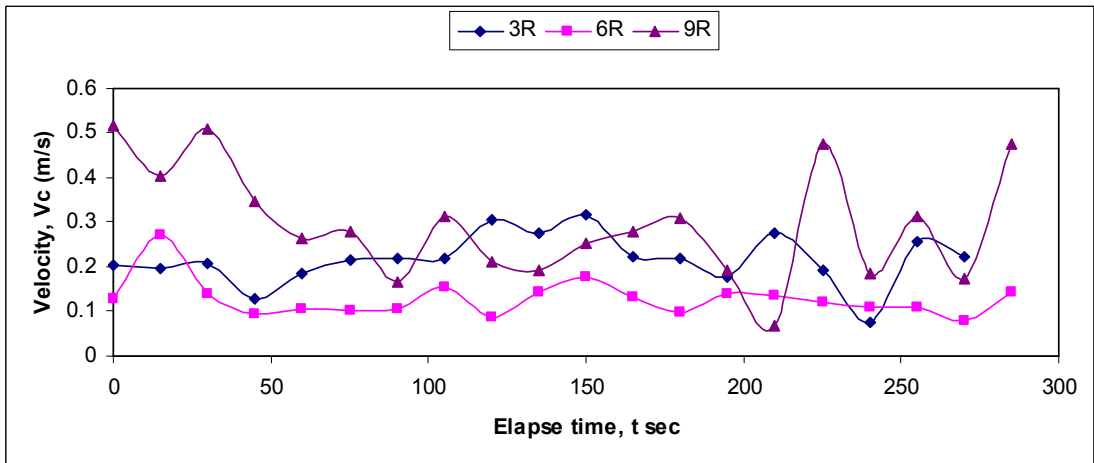


Figure B17: Velocity changes at 1:2 slope, 30 cm water depth and 2 sec wave period for floating breakwater.

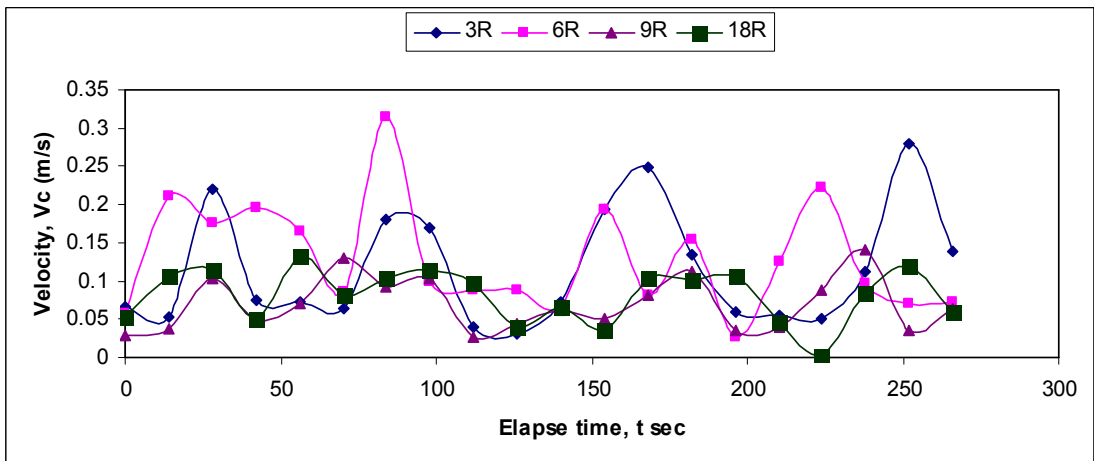


Figure B18: Velocity changes at 1:2 slope, 30 cm water depth and 2.5 sec wave period for floating breakwater.

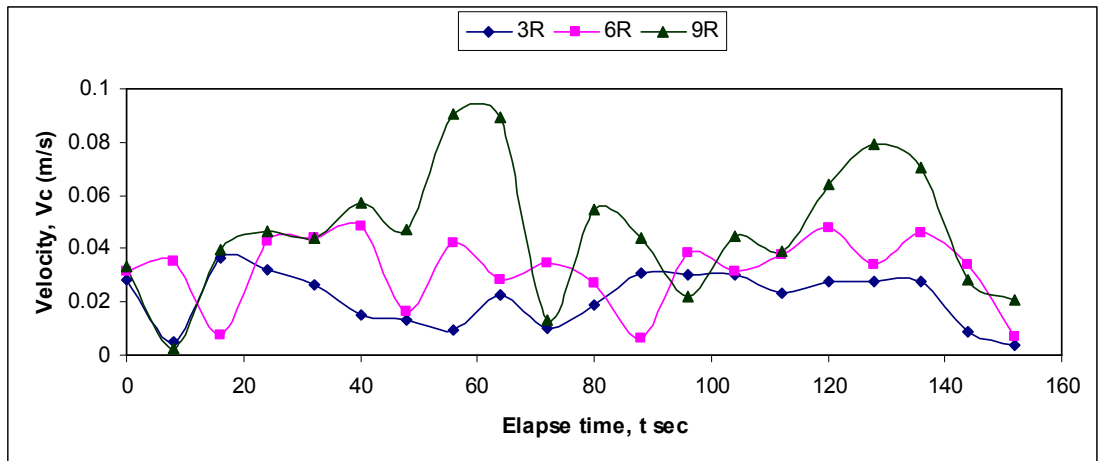


Figure B19: Velocity changes at 1:3 slope, 40 cm water depth and 1 sec wave period for CC blocks only.

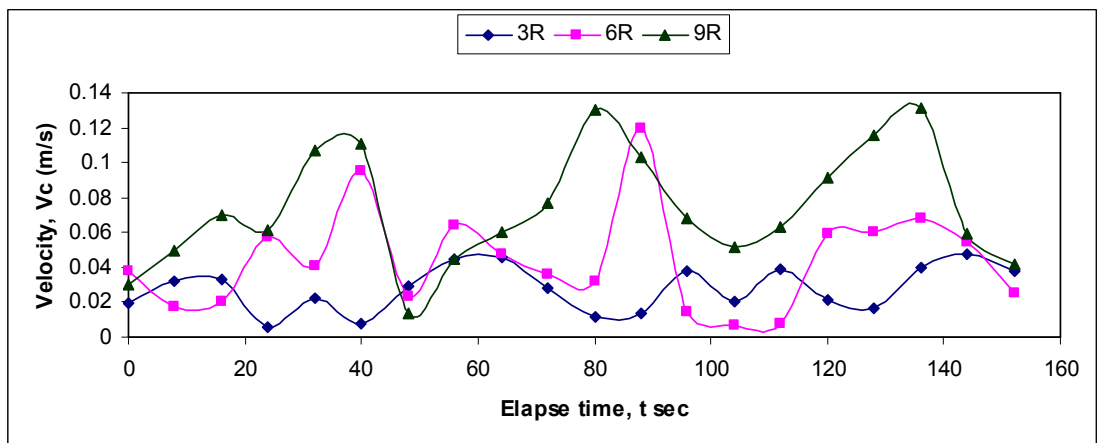


Figure B20: Velocity changes at 1:3 slope, 40 cm water depth and 2 sec wave period for CC blocks only.

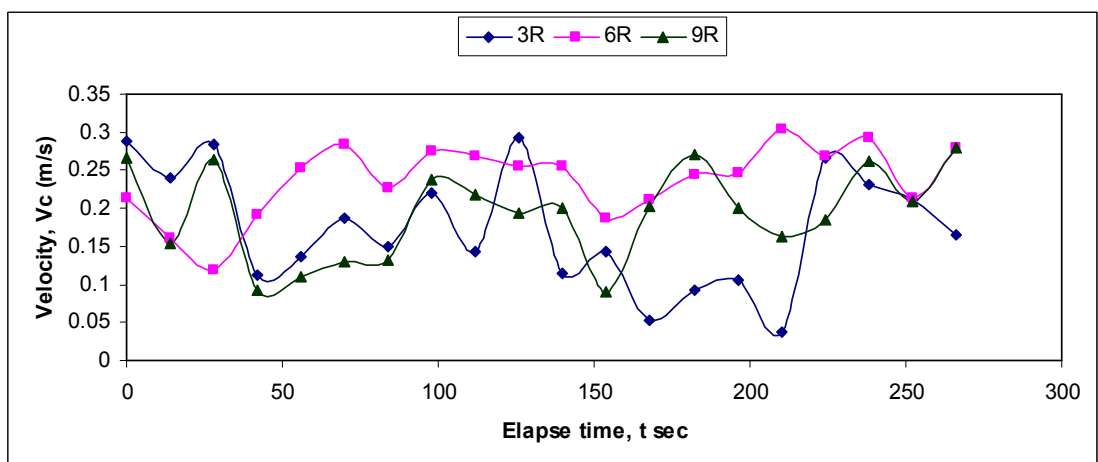


Figure B21: Velocity changes at 1:3 slope, 40 cm water depth and 2.5 sec wave period for CC blocks only.

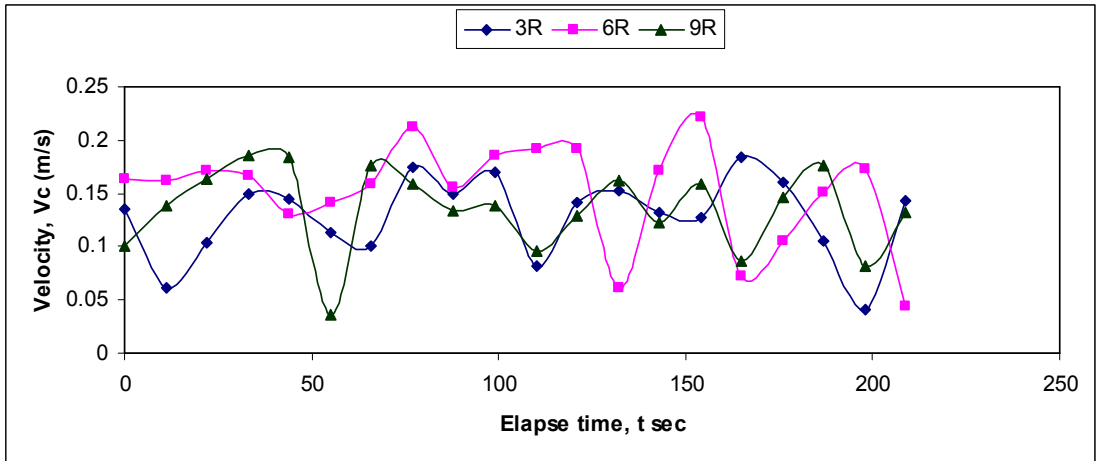


Figure B22: Velocity changes at 1:3 slope, 30 cm water depth and 1 sec wave period for CC blocks only.

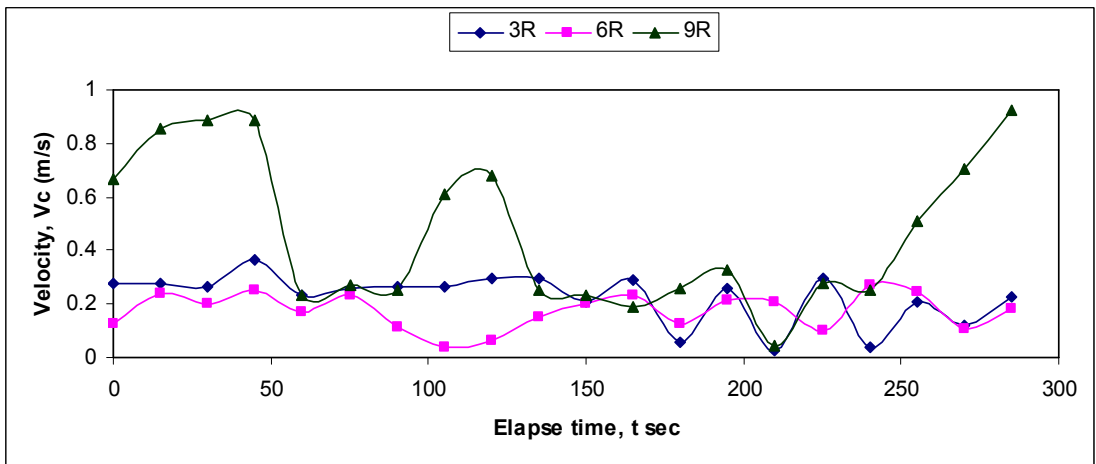


Figure B23: Velocity changes at 1:3 slope, 30 cm water depth and 2 sec wave period for CC blocks only.

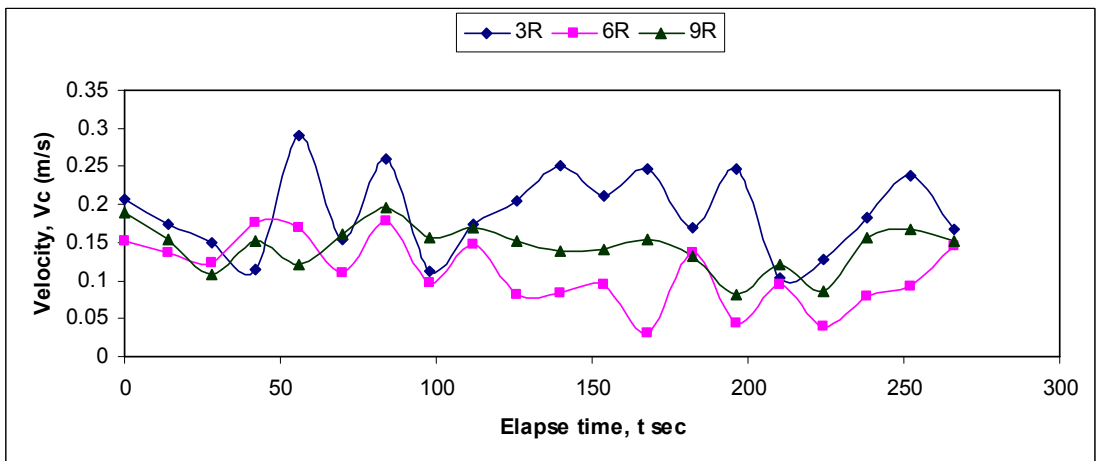


Figure B24: Velocity changes at 1:3 slope, 30 cm water depth and 2.5 sec wave period for CC blocks only.

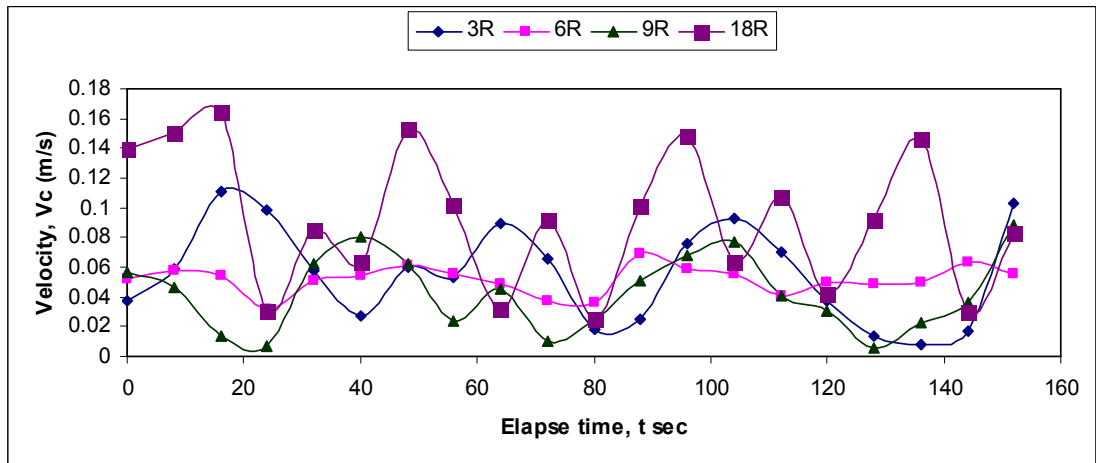


Figure B25: Velocity changes at 1:3 slope, 40 cm water depth and 1 sec wave period for submerged breakwater.

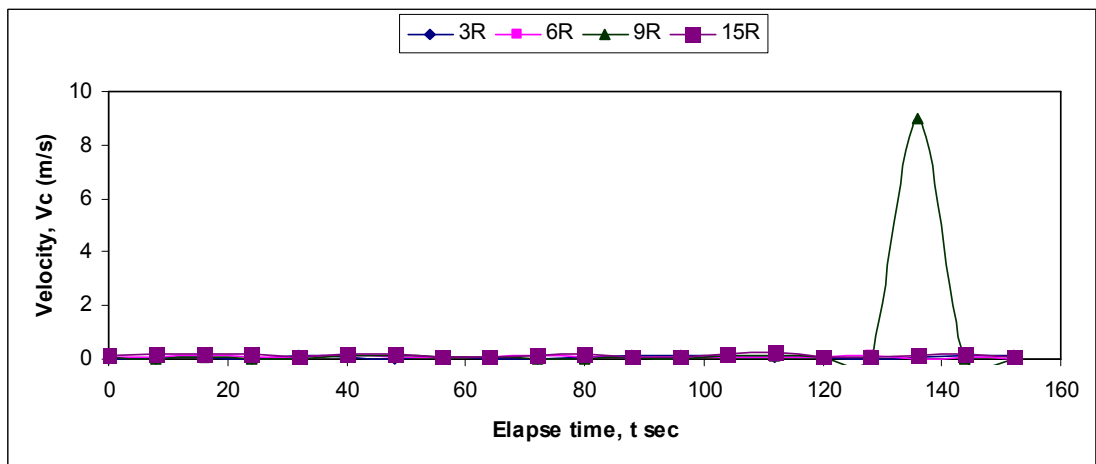


Figure B26: Velocity changes at 1:3 slope, 40 cm water depth and 2 sec wave period for submerged breakwater.

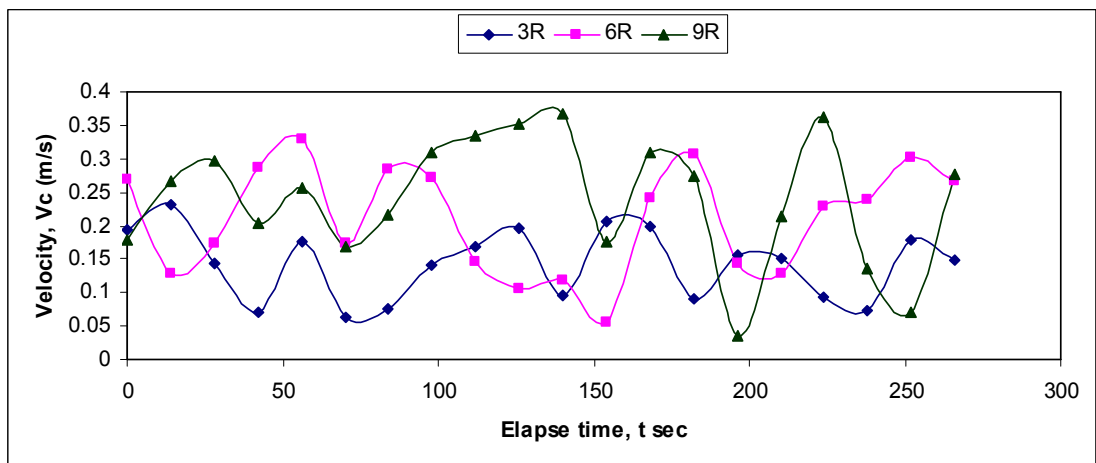


Figure B27: Velocity changes at 1:3 slope, 40 cm water depth and 2.5 sec wave period for submerged breakwater.

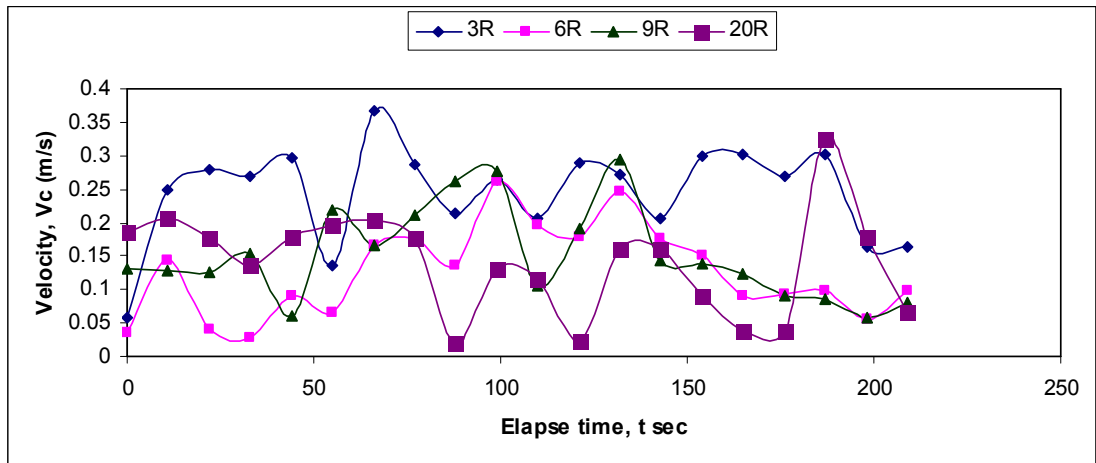


Figure B28: Velocity changes at 1:3 slope, 30 cm water depth and 1 sec wave period for submerged breakwater.

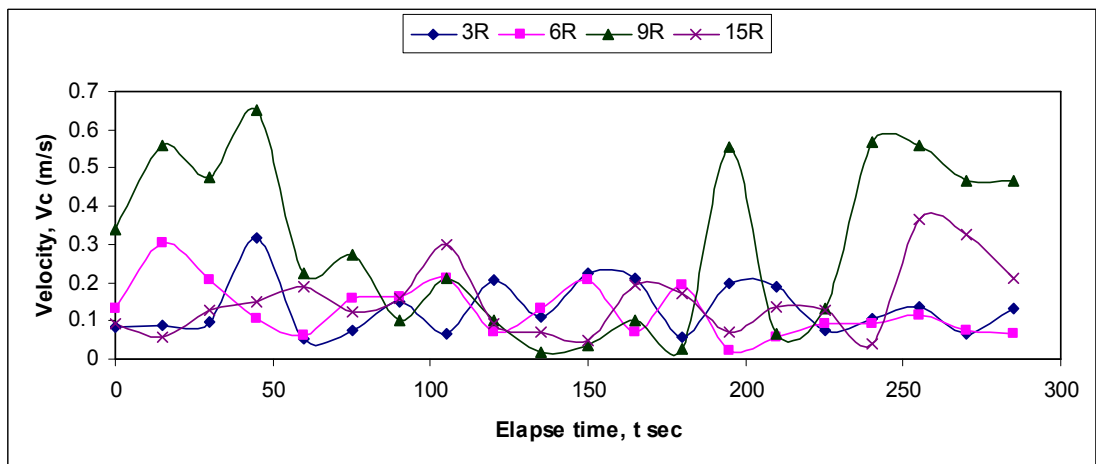


Figure B29: Velocity changes at 1:3 slope, 30 cm water depth and 2 sec wave period for submerged breakwater.

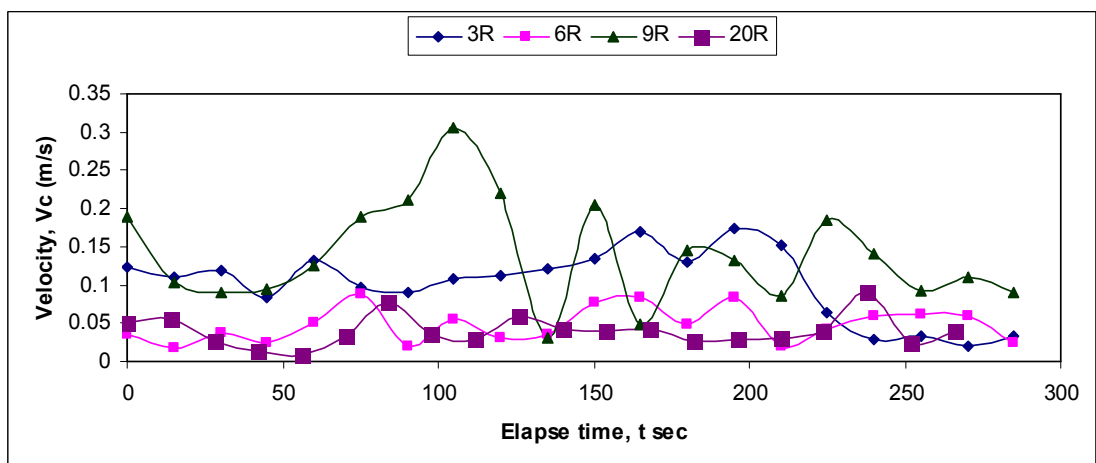


Figure B30: Velocity changes at 1:3 slope, 30 cm water depth and 2.5 sec wave period for submerged breakwater.

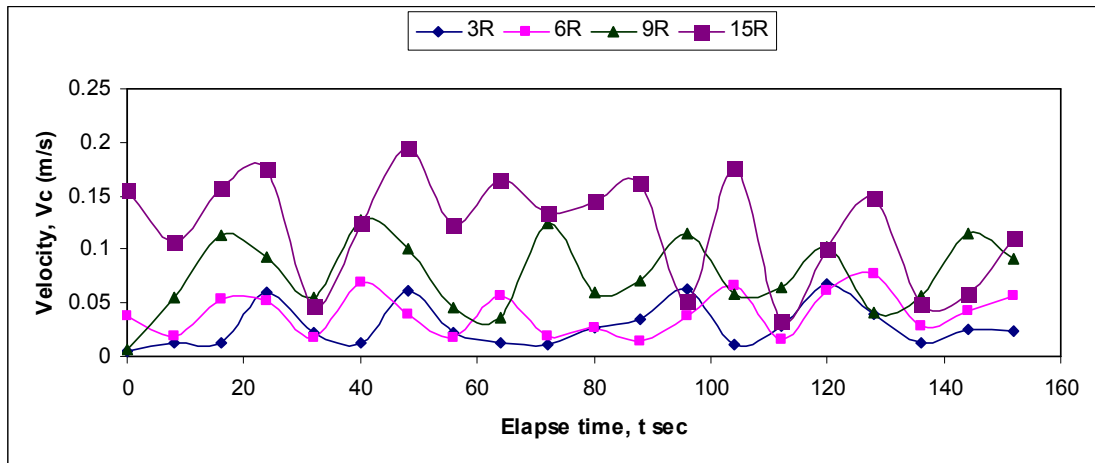


Figure B31: Velocity changes at 1:3 slope, 40 cm water depth and 1 sec wave period for Floating breakwater.

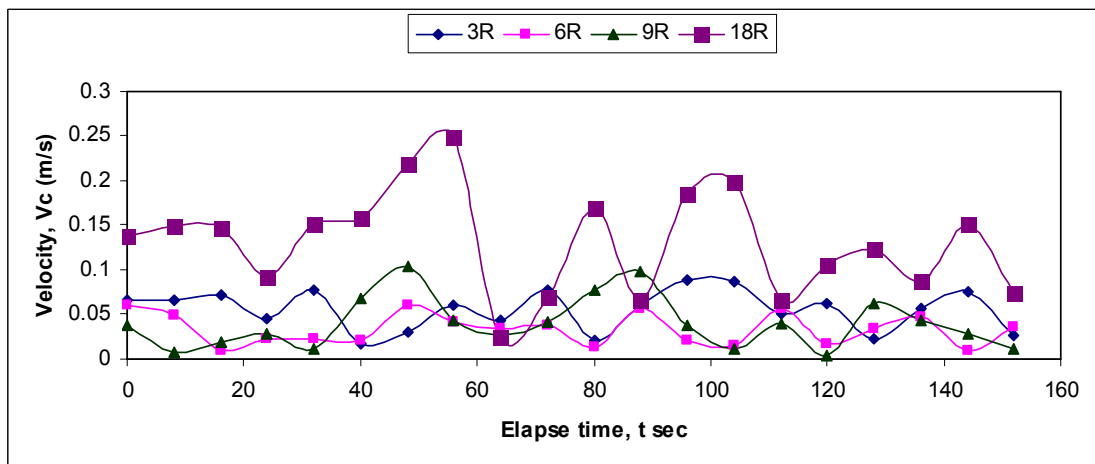


Figure B32: Velocity changes at 1:3 slope, 40 cm water depth and 2 sec wave period for Floating breakwater.

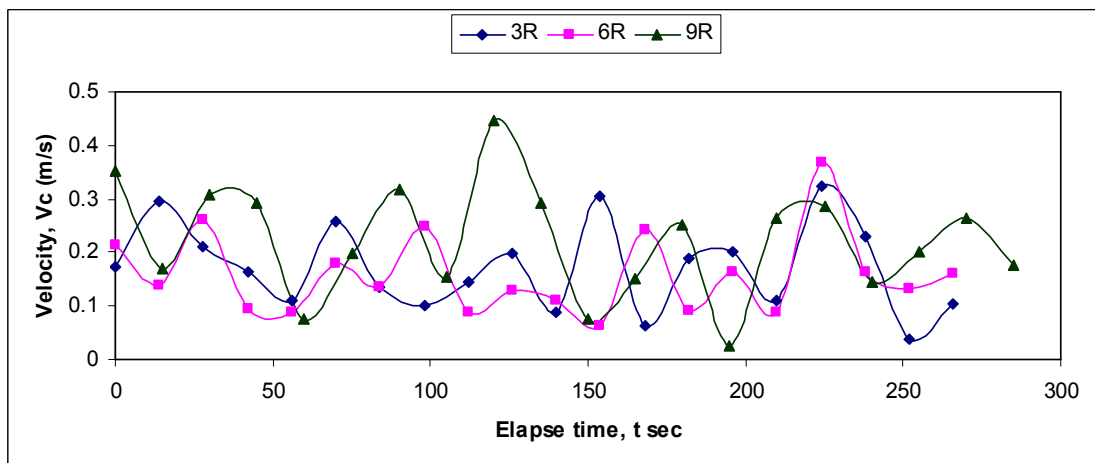


Figure B33: Velocity changes at 1:3 slope, 40 cm water depth and 2.5 sec wave period for Floating breakwater.

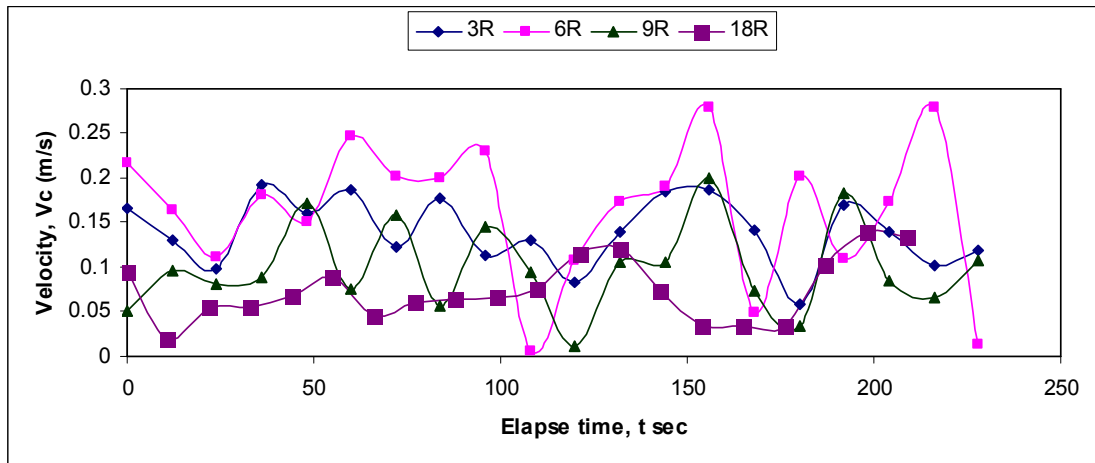


Figure B34: Velocity changes at 1:3 slope, 30 cm water depth and 1 sec wave period for Floating breakwater.

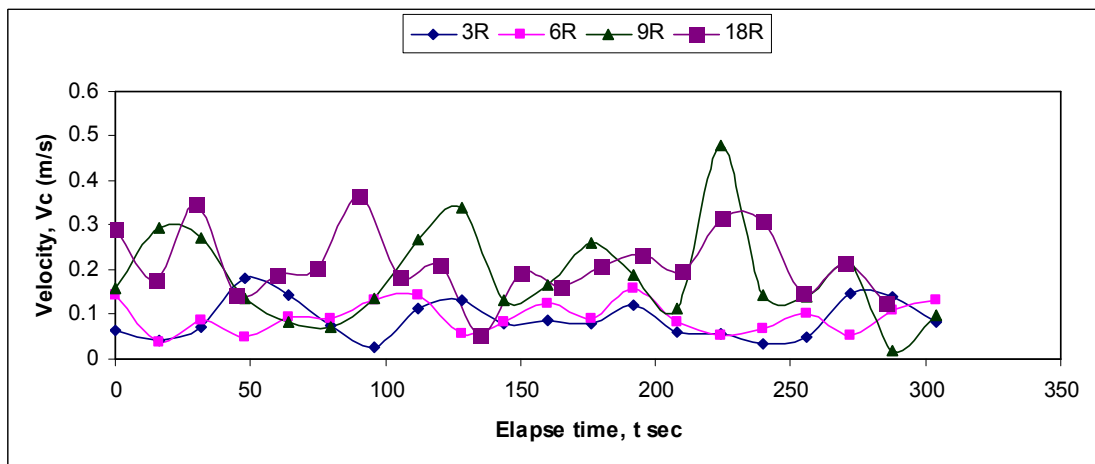


Figure B35: Velocity changes at 1:3 slope, 30 cm water depth and 2 sec wave period for Floating breakwater.

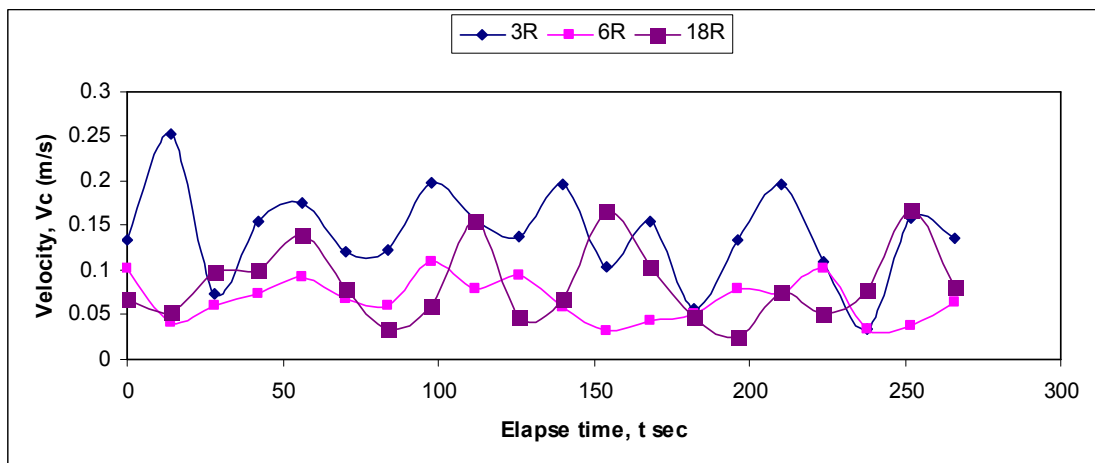


Figure B36: Velocity changes at 1:3 slope, 30 cm water depth and 2.5 sec wave period for Floating breakwater.

APPENDIX-C

Pictorial representation of Marine drive at various locations



Figure C1: Protections made by general people at Kalatoli, Cox's bazar



Figure C2: Washed out portion of Marine drive at Kalatoli, Cox's bazar



Figure C3: Washed out portion of Marine drive during tidal wave



Figure C4: Protection work constructed by Modern Hatchary



Figure C5: Protection work constructed local businessman



Figure C6: Wave action on the Protection work



Figure C7: Damaged portion near Brac centre, kalatoly, Cox's bazar



Figure C8: Wave attack at the Damaged portion of the embankment



Figure C9: Protection work at Sonarpara, Cox's bazar

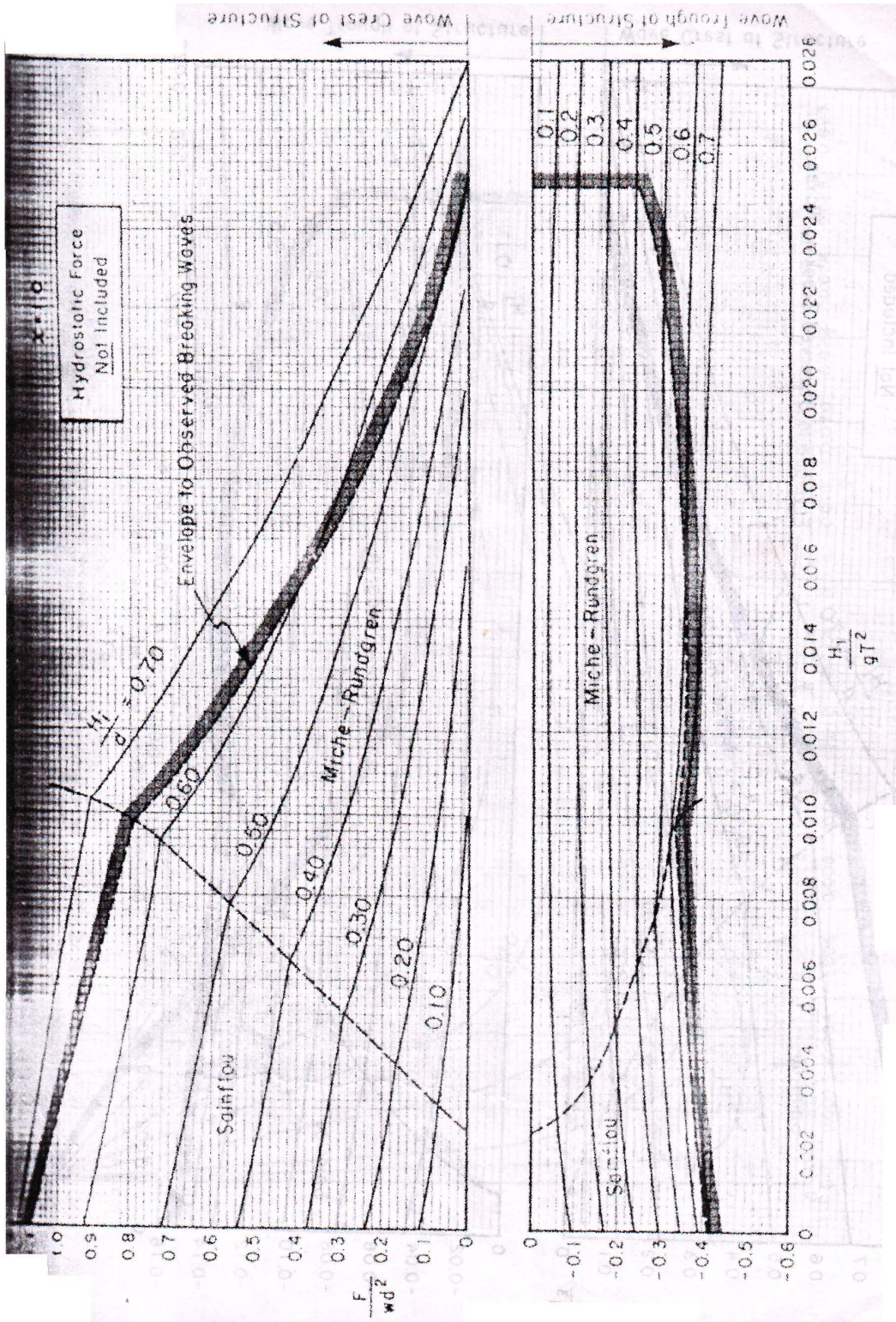


Figure C10: Drainage system of Marine drive



Figure C11: Destroying part of the Marine drive at Himchari, Cox's bazar

APPENDIX-D



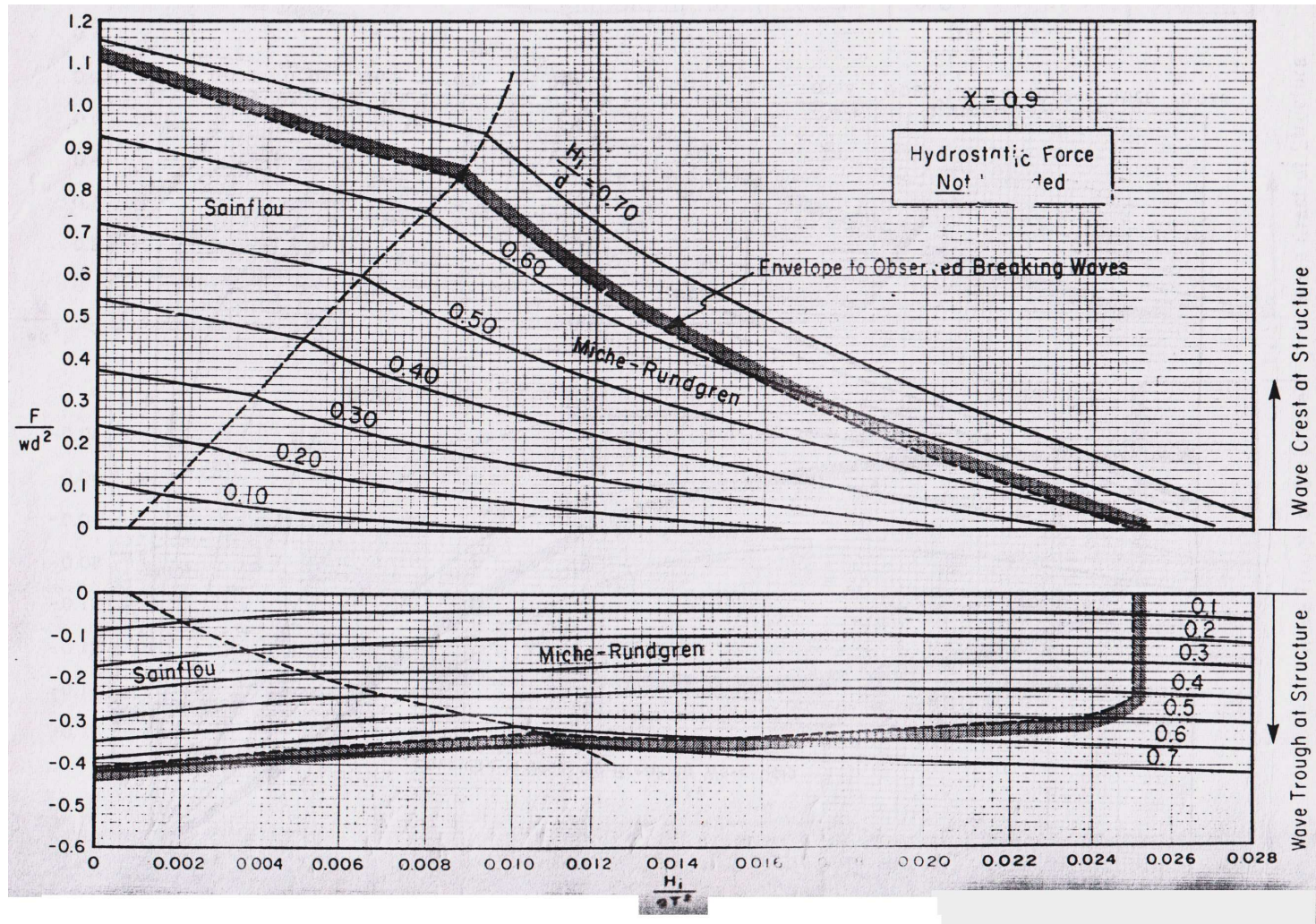


Figure D2: Nonbreaking wave forces, $\chi = 0.9$